ANALYSIS OF AIR AND WATER SPRAY INTERACTION

Thesis Submitted in fulfilment of the requirements for the Degree of

DOCTOR OF PHILOSOPHY

IN

MECHANICAL ENGINEERING

Submitted By

MOHAMMAD ZUNAID

(2K10/PHDME/14)

Under the Supervision of

PROF. QASIM MURTAZA **(Professor)**

PROF. SAMSHER **(Professor)**

Department of Mechanical Engineering
Delhi Technological University

(Formerly Delhi College of Engineering)

Bawana Road, Delhi- 110042, INDIA.

November 2017

DECLARATION

I hereby declare that the research work presented in this thesis entitled **"Analysis of Air and Water Spray Interaction"** is original and carried out by me under the supervision of Prof. Qasim Murtaza and Prof. Samsher, Professor, Department of Mechanical Engineering, Delhi Technological University, Delhi, and being submitted for the award of Ph.D. degree to Delhi Technological University, Delhi, India. The content of this thesis has not been submitted either in part or whole to any other university or institute for the award of any degree or diploma.

MOHAMMAD ZUNAID

CERTIFICATE

This is to certify that the thesis entitled **"Analysis of Air and Water Spray Interaction"** being submitted by **Mohammad Zunaid (2K10/PHDME/14)** to the Delhi Technological University, Delhi for the award of the degree of **Doctor of Philosophy** is a bonafide record of original research work carried out by him. He has worked under our guidance and supervision and has fulfilled the requirements for the submission of this thesis, which has reached the requisite standard. The results contained in this thesis have not been submitted, in part or full, to any other University or Institute for the award of any degree or diploma.

PROF. QASIM MURTAZA
SUPERVISOR,
Professor,
Department of Mechanical Engineering,
Delhi Technological University,
Delhi-110042,
INDIA.

PROF. SAMSHER
SUPERVISOR,
Professor,
Department of Mechanical Engineering,
Delhi Technological University,
Delhi-110042,
INDIA.

ACKNOWLEDGEMENTS

I want to express my gratitude to my supervisors Prof. Samsher and Prof. Qasim Murtaza for their valuable guidance, support, and encouragement throughout my Ph.D. program. This thesis could not have attained its present form without their supervision, direction, and interest in the research work. I express my gratitude to Prof. R. S. Mishra, Chairman of DRC, and SRC members, Prof. Avdhesh K. Sharma, Dr. Suresh Lal, Dr. Awadhesh Kumar, Dr. K. Manjunath for providing valuable comments and suggestions. I am thankful to all faculty and staff members of Mechanical, Production & Industrial and Automobile Engineering Department for their continued valuable support. I am grateful to Prof. S. K. Garg, Prof. S.S. Kachhwaha, Prof. Naveen Kumar, Prof. Abdul Khaliq, Prof. Raj Kumar Singh, and Prof. Amit Pal for their encouragement and help. I appreciate reviewers of research papers, industry people for sparing their valuable time and constructive comments.

I wish to thank my parents, brother, sister, family members and friends whose blessings made this work reality. I sincerely thank to my wife Nashreen Fatima, and my son Mohd. Faraz Khan for their patience, support and loving participation in accomplishing this research work. I would like to acknowledge Prof. Faisal Baig, my mentor in AMU, Aligarh for his support and guidance. At last, I am thankful to the God for giving me the mental and physical strength to work sincerely, diligently, and honestly.

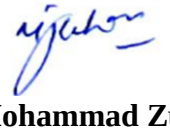

Mohammad Zunaid

ABSTRACT

In this study, we present energy and exergy analysis of mono and multi droplets shower cooling tower (SCT) for two-dimension (2-D) MATLAB mathematical model and three dimensional (3-D) Computational Fluid Dynamics (CFD) model for parallel flow and counter flow arrangements. SCT operated without fill because salt decomposition on the fill performance of conventional cooling tower leads to deteriorate. In MATLAB model mass, momentum, energy, exergy and droplet trajectory equations are solved simultaneously for predicting the exit conditions of water and air. 3-D CFD model has also been used for predicting the exit condition of water and air. The low temperature exit water is required for industrial application to cool condenser in industries, and low temperature exit air can be used for air cooling application for producing comfortable atmosphere indoors in India and other parts of the world. Mono and multi droplet diameters model were used to study 2-D MATLAB model and 3-D CFD model. Experimental data obtained from SCT are used to validate mono and multi droplets MATLAB and CFD models. Mono droplet model has uniform Sauter mean diameter (SMD), and multi droplet model has ten different diameters water droplets for the study. Rosin Rammler distribution is used to distribute ten different diameter droplets in multi droplet model.

Parametric study of industrial and air cooling application of SCT are based on the variation of Inlet droplet diameters, water temperature, air DBT, air relative humidity, and water to air mass flow ratio (RLG). The variation in inlet parameters shows significant changes in exit air DBT, air specific humidity, water temperature,

thermal efficiency, air convective exergy, evaporative air exergy, total exergy of air, water exergy, total exergy of the system, exergy destruction and second law efficiency (SLE). The results show the thermal efficiency of parallel and counter flow mono and multi droplet SCT decreases with increase in the inlet droplet diameters and RLG, and SCT thermal efficiency increases with increase in the inlet air DBT and air relative humidity. The results also show the model of cooling tower system produces the entropy. Therefore the amount of total exergy absorbed by air is less than exergy supplied by water. SLE of parallel and counter flow mono and multi droplet SCT decreases with increase in the inlet water temperature and air relative humidity, and SLE of SCT increases with increase in the inlet droplet diameter, air DBT and RLG. Parameters of air and water become asymptotic up to 0.5 m height of the parallel flow SCT, so the optimum height of tower should be 0.5 m for same operating conditions. Thus by reducing tower height investment cost can also be reduced.

TABLE OF CONTENTS

LIST OF FIGURES

LIST OF TABLES

NOMENCLATURE

A	Cross section area of test section, m^2
A_s	Surface area of droplet, m^2
C	Specific heat, kJ/kg K
C_d	Coefficient of drag
D	Droplet diameter, m
D_c	Cross-sectional diameter of SCT, m
g	Gravitational acceleration, m/s^2
h	Specific enthalpy, kJ/kg
h_f	Specific enthalpy of saturated water, kJ/kg
h_{fg}	Specific enthalpy of evaporation, kJ/kg
$h_{fg,0}$	Specific enthalpy of evaporation at 0°C, kJ/kg
h_g	Specific enthalpy of saturated vapour, kJ/kg
h_m	Mass transfer coefficient, kg/m^2 s
I	Exergy destruction of system, W
Le_f	Lewis factor
m_a	Mass flow rate of air, kg/s
m_d	Mass flow rate of water from the nozzle, kg/s
M_d	Mass of a drop, kg
N	Number of droplets
q	Heat transfer, kJ/kg
R_a	Gas constant for per unit molecular weight of dry air, J/kg K
R_v	Gas constant per unit molecular weight of water vapour, J/kg K
S_f	Specific entropy of saturated water, kJ/kg K
S_g	Specific entropy of saturated vapour, kJ/kg K
T	Temperature, °C

u_a	Air velocity, m/s
U	Drop velocity, m/s
W	Droplet relative velocity w.r.t. air, m/s
X	Exergy, W

Subscripts

0	Restricted dead state
a	Air
av	Average condition
c	Convective
d	Droplet
e	Evaporative
in	Inlet
l	Evaporative loss
m	Mean
out	Outlet
p	Constant pressure
s	Saturated
t	Total
v	Vapor
w	Water
x	Horizontal coordinate
y	Vertical coordinate

Greek Symbols

ϕ_0	Ambient humidity, kg_w/kg_a
ρ	Density, kg/m^3
ϕ	Relative humidity of air, %
η_{II}	Second law efficiency, %

ω	Specific humidity, kg_w/kg_a
η_{th}	Thermal efficiency, %

Abbreviations

DBT	Dry bulb temperature
RLG	Water to air mass flow ratio
SCT	Shower cooling tower
SMD	Sauter mean diameter
SLE	Second law efficiency
HPOM	Two-dimensional parallel flow mono droplet SCT for industrial application
HPUM	Two-dimensional parallel flow multi droplets SCT for industrial application
HPOC	Three-dimensional parallel flow mono droplet SCT for industrial application
HPUC	Three-dimensional parallel flow multi droplets SCT for industrial application
HCOM	Two-dimensional counter flow mono droplet SCT for industrial application
HCUM	Two-dimensional counter flow multi droplets SCT for industrial application
HCOC	Three-dimensional counter flow mono droplet SCT for industrial application
HCUC	Three-dimensional counter flow multi droplets SCT for industrial application
NPOM	Two-dimensional parallel flow mono droplet SCT for air cooling application
NPUM	Two-dimensional parallel flow multi droplets SCT for air cooling application
NPOC	Three-dimensional parallel flow mono droplet SCT for air cooling application
NPUC	Three-dimensional parallel flow multi droplets SCT for air cooling application
NCOM	Two-dimensional counter flow mono droplet SCT for air cooling application

NCUM	Two-dimensional counter flow multi droplets SCT for air cooling application
NCOC	Three-dimensional counter flow mono droplet SCT for air cooling application
NCUC	Three-dimensional counter flow multi droplets SCT for air cooling application

Chapter 1 INTRODUCTION

1.1 Introduction

Water spray extensively used in several engineering applications, such as combustion systems, agricultural and industrial processes, dust control, firefighting, spray drying, transport systems, nuclear reactor core cooling and evaporative cooling. In hot and dry climates, such as the summer season in India and other parts of the world, evaporative cooling of air is an attractive energy-efficient technique for producing a comfortable indoor environment.

Cooling towers widely used in industry for cooling circulating water and for evaporative cooling of air. The aim of cooling towers is to release the heat from the condenser of the refrigeration system to the atmosphere via an evaporative cooling process of hot water. Cooling towers include two types, viz. direct and indirect cooling towers. Indirect cooling towers hot water spray on packing which is used to spread out the water to film and thus increase its contact surface with air which increased heat and mass transfer (Nasrabadi and Finn 2014; Hernandez-Calderon et al. (2014). Indirect cooling towers, hot water goes through coils arranged in rows, while the air flows over the external side of the coil, and an additional circuit sprays water to cool the coils via evaporation (Gao et al. 2014; Zheng et al. 2012). In the conventional cooling tower, fill acts as the medium of heat and mass transfer, using which the air entrains thermal energy by absorbing heat and humidity. However, the fills are subjected to fouling during the operation, which reduces the efficiency of the tower with time. Fouling of cooling tower fills are one of the most important factors affecting its thermal performance which reduces the cooling tower's efficiency and

capability, other general disadvantages of the conventional cooling tower include: fill blockage, the difficulty of replacing or cleaning the fills and so on (Qureshi and Zubair 2004). Given these disadvantages of the conventional packed cooling towers, a new type of shower cooling tower (SCT) has been proposed in which fills eliminated entirely. In SCTs, circulated water is sprayed with high pressure and converted into small droplets in the spray distribution water zone, and the drenching zone in which normal heat transfer accomplished without fill and the circulating water and air cooled to the anticipated temperature.

Figure 1.1 and Figure 1.2 show the diagrams of parallel flow and counter flow SCT; these SCT can be used in industries for cooling of hot water by direct contact with air. Because of heat and mass transfer between the water and air, the water temperature reduced, while the air enthalpy increased. The parallel and counter flow SCT (Figure 1.1 and Figure 1.2) also used for cooling of air for human comfort.

In parallel flow air cooling application of SCT (Figure 1.1), the ambient air enters from the top of the SCT by a mechanical fan, and is cooled by the evaporation of water, and leaves the tower at the bottom. The exit air, with a lower dry-bulb temperature and a higher relative humidity than that of the ambient, is supplied to the lowest part of a building complex, thus providing cooling of hot climate zone for the occupants of the open or semi-open spaces. The thermal force driving the air through a direct down draft evaporative SCT created by the introduction of water at the top of the tower. The evaporation of water may cause initial cooling. The water droplet falls through the tower, so that the air inside it remains moist and close to saturation if sufficient amount water provided. In parallel flow industrial application of SCT (Figure 1.1), where the primary objective is to cool the circulating hot water, air and

water come in contact at the top of SCT, water is cooled down and collected in the sump and supplied to industrial application.

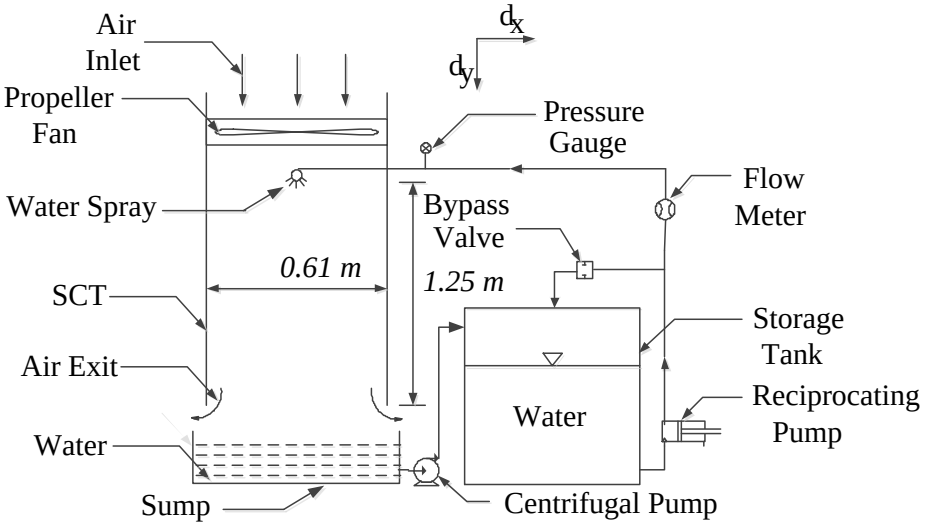

Figure 1.1 Parallel flow downdraft evaporative SCT

In counter flow industrial application of SCT (Figure 1.2) the water is sprayed through pressurized nozzles and flows downward, opposite to the air flow which enters from the bottom and flows upward. The heat exchange takes place between the water droplets and the air. The cold water collected at the bottom from where it pumped to the desired location. The warm and humid air expelled from the tower. In counter flow air cooling application of SCT (Figure 1.2) air enter from the bottom of the tower and come in contact with downward flow water spray. The air temperature reduced due to heat and mass transfer between hot air and water and this low-temperature air supplied to provide cooling hot climate zone.

Heat transfer between air and water take place due to convection and evaporation. In convection heat is transferred due to the temperature gradient that exists between the water drops and the air. In evaporation, Spray water drop absorbs latent heat partly from the air and partly from water thereby reducing air temperature and hence gets converted into vapour form.

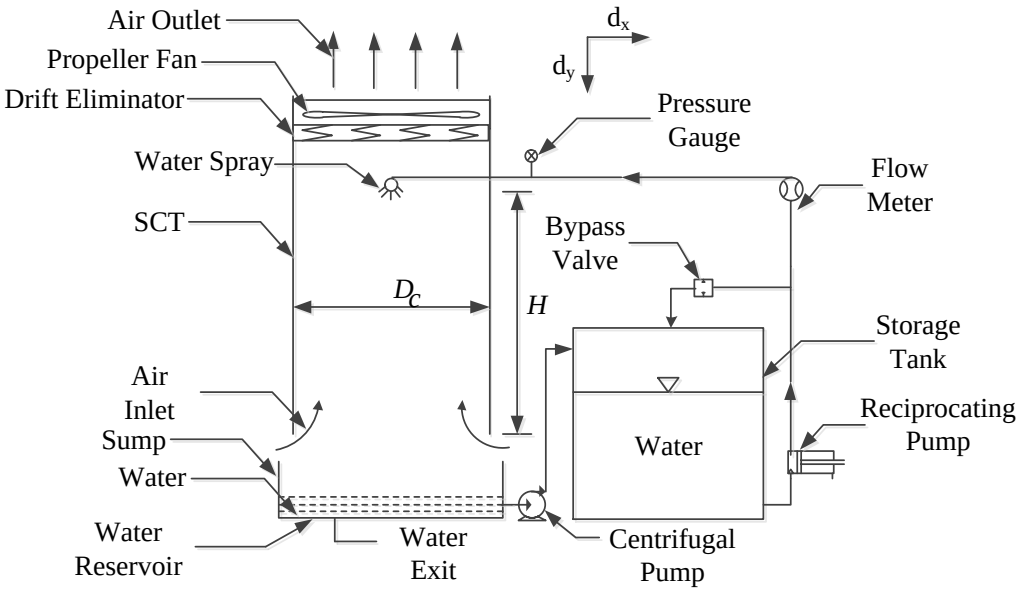

Figure 1.2 Parallel flow downdraft evaporative SCT

The principle of evaporative cooling based on the relatively large amount of energy required to convert water from its liquid form into its gaseous form vapour. While the heat energy required to raise the temperature of water by 1 °C is 4.18 kJ/kg, the specific latent heat of vaporization is 2257 kJ/kg. In the case of an evaporative cooling system, this energy is supplied primarily by the intake air, whose heat content and capacity to hold vapour indicated by its dry bulb temperature and relative humidity. The combined high temperature and low humidity typical of daytime summer air in hot climate provide promising conditions for the efficient, large-scale utilization of the evaporative process for cooling of inhabited spaces. In counter flow SCT (Figure 1.2) air entre from the bottom of the tower with the help of an induced draft fan and come in contact with spray water droplet. Counterflow SCT also used for industrial and air cooling application.

Chapter 2 LITERATURE REVIEW

2.1 Literature Review

A few studies have presented in open literature related to the performance analysis of SCT. The literature review has classified into spray characterization, heat and mass transfer analysis and exergy analysis.

2.1.1 Spray Characterization

The spray characteristics include droplet size and droplet velocity, the droplet size of spray is a very important variable. Droplet size was measured using a Malvern Laser Particle Analyzer. Inlet pressure of nozzle is varied for find different sizes of droplets. Terblanche et al. (2009) measured drop size distribution photographically below three different counter-flow wet-cooling tower fills. It observed that an increase in water mass velocity results in slightly larger Sauter mean drop diameters. Nuyttens et al. (2007) developed a test rig and protocol for the characterization of spray nozzles using a phase Doppler particle analyzer (PDPA). This test rig was able to measure droplet sizes and velocities based on light-scattering principles. It has observed that nozzle type, as well as nozzle size, have an important effect on droplet size as well as on velocity spectra. Simmons and Hanratty (2001) and Santangelo (2010) said a laser-diffraction-based instrument (Malvern Spraytec) had been used to evaluate drop size. Santangelo et al. (2008 and 2009) characterized the high-pressure spray produced by a water mist injector. The engineering application field is mainly fire suppression, where water mist systems seem to represent one of the most promising technologies,

suggest a light-diffraction-based instrument (Malvern Spraytec) has been used to determine the characteristic drop size of the spray.

2.1.2 Heat and Mass Transfer Analysis

Merkel (1925) was the first to develop a one-dimensional model to predict the heat and mass transfer in the cooling tower. To simplify the model, Merkel combined the partial differential equations, describing the rate of change in properties of the water and air, into one simplified equation. The equation is commonly known as the Merkel equation, and it describes simultaneous heat and mass transfer from a surface in terms of the coefficient, area, and enthalpy driving potential. Zivi and Brand (1956) developed and solved the Merkel model for a cross-flow cooling tower. This cross-flow model is 2-D and is solved mathematically using a computer program. The more common model used for cross-flow towers is an effectiveness-NTU (Number of Transfer Units) method. Jaber and Webb (1989) adopted the e-NTU method and applied to cross and counter flow wet-cooling towers. The method can be solved one-dimensionally for both cross-flow and counter flow with equal effort. All of these models make simplifying assumptions regarding heat and mass transfer which allows them to be solved more easily; these models are not accurate. Poppe and Rogener (1991) developed a model that does not make the same simplifying assumptions as Merkel and can use for prediction of air outlet conditions. The model consists of four partial differential equations which are functions of each other and solved simultaneously. The differential equations describe water temperature, water flow rate, air enthalpy and humidity. In comparison with the Merkel and e-NTU models, the Poppe model is complicated to solve and understand. Mohiuddin and Kant (1996a, 1996b) have given the process of selecting a cooling tower includes the determination

of pressure drop, tower characteristic ratio and water to air ratio. Halasz (1999) reported a dimensionless model to estimate the cooling efficiency of cooling towers in terms of two non-dimensional variables. Facao and Oliveira (2004) reported empirical correlations for heat and mass transfer coefficients in indirect contact mechanical draft cooling tower. Apart from these, several studies dealing with performance analysis suggesting different empirical correlations for various cooling towers are also available (Elsarrag 2006; Gharagheizi et al., 2007; Kloppers and Kroger, 2005; Lucas et al., 2009; Klimanek and Białecki 2009). Naik (2017) developed a finite difference model for predicting the characteristics of coupled heat and mass transfer processes occurring in a counter flow forced draft cooling tower and found that evaporation loss of cooling tower increases with increasing the mass flow rate of air and water inlet temperature. Khan et al. (2003) and Zubair (2001) considered the effects of Lewis number and heat transfer resistance at the air-water interface and developed a detailed model on counter flow wet cooling towers. They assumed Lewis factor as 0.9. It has noticed that the majority of heat transfer was due to the latent heat. Ghazani et al. (2017) had investigated the performance of cooling tower and found that as the water temperature decreases along the tower from top to bottom, both the air wet and dry-bulb temperatures increases linearly with the height of the cooling tower from bottom to top. Air wet-bulb temperature approaches its dry-bulb temperature at the tower exit, which is an indication of water evaporation. Smrekar et al. (2006) calculated entropy generation in a cooling tower and showed that when heat transfer in a cross-section of the cooling tower is homogeneous, entropy generation is uniform and at its minimum value. Wang and Li (2011) investigated the effects of RLG and thermal efficiency on cooling tower performance using exergy analysis and showed that the RLG and the thermal efficiency have different effects on the performance. Ram kumar and

Ragupathy (2011) analyzed the performance of a counter-flow wet cooling tower and compared their results with experiments. They studied cooling tower range and tower characteristic variations as a function of air and water flow rates. It concluded that the tower characteristic has an inverse relation with water-to-air mass flow rate. In their results, a reduction in air wet-bulb temperature decreases NTU. Qi et al. (2016) present a local linear wavelet neural network (WNN) model. The model was used to predict various performance parameters of the system, namely the temperature difference of the outlet and inlet water stream and the dry bulb temperature, relative humidity of the outlet air stream, the evaporative water ratio and the cooling efficiency of the system. The performances of the WNN predictions were tested using experimental data; the predictions yielded good agreement with the experimental values. Cui et al. (2016) developed reversibly used cooling tower (RUCT), in this tower water sprayed upward from the bottom. The results showed that droplet diameter had a large impact on the thermal performance and the droplet temperature rise. Mansour et al. (2014), Al-Bassam et al. (2011), Goudarzi et al. (2013), Lemouari et al. (2011), Asvapoositkul et al. (2014), Jiang et al. (2011) investigated cooling towers and said it had widely used in large refrigeration systems. Qureshi and Zubair (2004 & 2006) investigated full cooling tower which consists of three zones; namely, spray zone, filling and rain zones. In the cooling tower, a significant portion of the total heat rejected may occur in the spray and rain zones and fouling is a primary source of cooling tower performance deterioration. Stabat and Marchio (2004) investigated corrosion and fouling problems are often encountered in cooling towers, airborne dusts and scale deposit on the packing resulting in a decrease of thermal performance for the cooling towers. Subsequent blockages in coils or packing could induce damage to the draught fan. Qi and Liu (2008a and b) proposed a packing-free

cooling tower, in which the packing is replaced by a set of efficient nozzles. In the packing-free cooling tower, the total contact area between water and air increases because the sprayed droplets become finer. Rotar et al. (2005) present experimental and numerical analyses of the natural-draft cooling tower they sense fill system mainly reduce the air mass flow rate, which results in a lower heat and mass-transfer from the water to the air. Naphon (2005) studied experimentally and theoretically about heat transfer characteristics of the cooling tower with water mass flow 0.01 - 0.07 kg/s, and 0.04 - 0.08 kg/s, respectively. The inlet air and inlet water temperatures were 23 ˚C, and 30-40 ˚C respectively. Kloppers and Kroger (2005c), Lemouari (2009), Klimanek and Białecki (2009) gave a detailed procedure to solve the governing equations with its unique requirements for heat and mass transfer equations of evaporative cooling in wet-cooling towers. Xiaoni et al. (2007), Saffari and Hosseinnia (2009), Muangnoi (2014) conducted the study on the cooling tower without fill packing and found that small Sauter mean droplet diameter is desirable for high performance of SCT. Qi et al. (2008) design tower with no tower packing and observed that equivalent diameter of inlet water droplets and the initial air velocity affects the outlet water temperature. In a study of SCT Yajima and Givoni (1997) observed about 7 ˚C drops in DBT at the maximum ambient temperature. Givoni (1997) developed shower tower and compared its performance and found that system provide effective cooling even in an extreme desert climate. Pearlmutter et al. (1996) develop and monitor small-scale down draft evaporative cool tower in arid Negev Highlands of southern Israel. The result shows a scope for substantial temperature reduction in the order of 10 °C under summer daytime conditions. Farnham et al. (2011) carried out experiments by spraying water from varying heights in a large atrium and found that a single spray nozzle with Sauter mean droplet diameter of 41

microns can provide maximum cooling. Kachhwaha et al. (1998) developed two-dimensional (2-D) straightforward and efficient numerical model and observed that DBT decrease up to 9°C by employing evaporative cooling during dry summer months. Sureshkumar et. al. (2007) develop 1-D parallel flow heat and mass transfer model to solve air and water spray interaction for different combinations of drop diameter, air velocities, DBT and specific humidity. By using an optimum number of categories and velocity sub-classes, reasonably accurate predictions are obtainable with savings in computation time. Sureshkumar et al. (2008) study evaporative cooling of air by water sprays for two ambient conditions, viz., hot-dry and hot-humid, covering DBT from 35 to 47 ˚C, and relative humidity 10 – 60%. Cui et al. (2016) concluded that the droplet diameter had the great impact on the droplet temperature distribution and thermal performance of cooling tower. Sirok et al. (2003) investigated that efficiency of cooling tower decreases with increase the water to air mass flow ratio. Blain et al. (2016) reported that the cooling tower approach are decreasing with increase in the ratio of mass flux of air to liquid. Huan et al. (2015) observed that the heat rejection of cooling tower increases with increase in the crosswind velocity. Nasrabadi et al. (2014) investigated that range of cooling tower decreases with decrease in the inlet water temperature. Sirena et al. (2013) reported that the cooling tower quantitative parameters were increases with increase in the RLG. Jiang et al. (2013) developed a closed wet cooling tower and investigated that the thermal efficiency of cooling tower got remarkably modified with change in the inlet water temperature and inlet air flow rate. Asvapoositkul et al. (2012) developed a cooling tower model and analyzed that cooling tower range increased with increase in the inlet water temperature. Keshtkar (2017), Marmouch et al. (2010) and Yang (2007) optimized cooling tower performance and found that the outlet water

temperature of cooling tower increases with increase in the RLG. Singh and Das (2017) studied mechanical draft cooling tower and found that heat rejection by water increases with increase in the inlet air flow rate. Rosin (1933), Babinsky and Sojka (2002), Gonzalez-Tello et al. (2008), Lefebvre (1989) and Masters (1991) reported that the Rosin–Rammler distribution is most commonly used function for particle size distribution of coal and spray droplets. Zunaid et al. (2013a) reported as air DBT increases its specific humidity also increases. Murtaza et al. (2012) found that the air enhances the break-up of the liquid sheet from an atomizer; air also disperses droplets and prevents its collision. Fisenko et al. (2002) reported as water droplet diameter increases cooling tower outlet water temperature also increases. Gharagheizi et al. (2007), Sirena (2014) experimentally analyzed the performance of cooling tower and investigated as RLG increases thermal efficiency of cooling tower decreases. Osterle (1991) develop mathematical model of the cooling tower and corrects the Merkel equations by including a term in the energy balance which the Merkel equations neglect, thus enabling the state of the exiting air to be determined and providing a more accurate results. Fisenko et al. (2004) investigated as droplet fall height increases drop in droplet temperature also increases. Wang et al. (2017) investigate performance of cooling tower and fund that 7 ˚C drop in water temperature achieved at 20 m/s air velocity. Reuter et al. (2011) use CFD model for determining the effect of cooling tower geometry on the air flow pattern and concluded that the inlet diameter to height ratio has a major impact on inlet losses. Gan et. al (2001) used CFD for performance evaluation and optimum design of cooling towers they found that when the water flow rate lower than the design value the predicted temperature difference between the top and bottom tube rows is much less than the measured temperature drop of chilled water. Al-waked and Behnia (2006) investigated natural

draft wet cooling tower (NDWCT) numerically under different operating and crosswind conditions. They conclude that the droplet diameter has the most significant effect, among the investigated parameters, on the performance of the NDWCT. Williamson et al. (2008) compare the performance of a simple one-dimensional natural draft wet cooling tower (NDWCT) model and a two-dimensional axisymmetric numerical model. The difference between the overall cooling ranges predicted by the two models is generally less than 2%, with no divergence in the agreement between the methods with respect to any design parameter. Rubio-Castro et al. (2011) developed heat and mass transfer equation for cooling tower. They suggested equation developed by Poppe method give more accurate results then Merkel method because Merkel method neglected water loss due to evaporation and consider Lewis factor equal to unity. Yoon and Heister (2004) said results obtained from mathematical model by considering SMD of droplets are agree well with the actual droplet size of Hoyt and Taylor's experiment. Halasz (1999) said humidity ratio of air increases with increase the air DBT and efficiency of cooling tower increases with increase the number of transfer unit. Kang and Strand (2013) studied passive down draft evaporative cooling tower and suggested by increase the air velocity of SCT exit air temperature also increases. Tan and Deng (2002 and 2003) present a method by which the heat and mass transfer characteristics of a counter-flow cooling tower can be evaluated. The method is developed by introducing to the Merkel's equation for standard water cooling towers. Zhang et al. develop analytical model for counter flow cooling tower and found that by increasing the inlet air wet bulb temperature exit water temperature increases. Rahmati et al. (2016) studied wet cooling tower and postulate by increasing the air mass flow rate range of cooling tower increases. Zamora et al. (2011) have numerically simulated cooling tower and

they reported that the droplet turbulent dispersion has a major impact on the collection efficiency. Milosavljevic et al. (2001) have studied a mathematical model for a counter flow wet cooling tower and found that exit air temperature is decreased with decreased the inlet air velocity. Ardekani et. al. (2014) said inlet and outlet water temperature difference for the wind facing sector was about twice that of the peripheral sectors. Kumar and Pant (2008) investigated as Reynolds number increases flow pattern changes. Heidarnejad and Delfani (2000) studied that Reynolds number changed with variation in changes the geometrical and physical perimeters of flow. Reuter (2010) has analyzed cooling tower by using FLUENT, he suggested that the performance of a cooling tower can be improved by reducing droplet size. Viljoen (2006) studied the performance of cooling tower using FLUENT. He reported the collision of water droplets has not major impact on water distribution pattern in the cooling tower. Hawlader and Liu (2002) analyze evaporative cooling tower and said exit water droplet temperature increases with increase the inlet water droplet temperature. Kasaeian et al. (2013) said available energy is always destroyed when a process involves a temperature change; this destruction is proportional to increase in the entropy of the system. Kairouani et al. (2004) developed a mathematical model predict the water loss from cross flow air cooling towers of geothermal waters used in the South of Tunisia. It has been found that the total water loss through evaporation from the six towers over one year period is about 106 m^3. Qureshi and Zubair (2007) present thermodynamic analysis of counter flow wet cooling towers and evaporative heat exchangers using both the first and second laws of thermodynamics. All computations are conducted with an engineering equation solver (EES) program that has built-in functions for thermodynamic and transport properties. They found that an increase in the inlet wet bulb temperature consistently increases the second-law

efficiency of all the systems investigated. Kloppers and Kroger (2005b) investigated the effect of the Lewis factor on the performance prediction of natural draft and mechanical draft wet-cooling towers. The Lewis factor relates the relative rates of heat and mass transfer in wet-cooling towers. For increasing Lewis factors, the heat rejection rate increases, the water outlet temperature decreases and the water evaporation rate decreases. Hajidavalloo and Mehrabian (2010) developed mathematical model to predict the thermal behavior of an existing cross flow tower under variable wet bulb temperature and the results are compared with experimental data in various operating conditions. It is found that when the wet bulb temperature increases, the approach, range and evaporation loss would increase considerably. Kroger and Kloppers (2005) studied cooling tower at different operating and ambient condition and found, If only the water outlet temperature is of importance to the designer, the Merkel and e-NTU approaches can be used, as all the approaches predict practically identical water outlet temperatures for mechanical and natural draft towers. Chen et al. (2010 and 2011) concluded that the coupled heat and mass transfer in evaporative cooling processes, the moisture entransy, consisting of both sensible and latent heat entransy, is an effective physical quantity to evaluate the endothermic ability of a moist air. Lemouari and Boumaza (2010) investigated counter flow wet cooling tower and concluded that effectiveness of cooling tower decrease with increase the RLG. Lucas et al. (2013) studied cooling tower and find that approach of cooling tower increases with increase the RLG. Xiaoni et al. (2013) provides a descriptive mathematical model of energy and exergy for a shower cooling tower (SCT). The model is used to predict the variation in temperature and exergy along the tower length. The results show that the exergy of water decreases as tower height increases. The distribution of the exergy loss is high at the bottom and gradually

decreases moving up to the top of the tower. The exergy analysis shows that exergy destruction increases with increasing water droplet diameter. Belarbi et al. (2006) develop a model for droplets evaporation and water sprays and also used this model to calculate the time needed for full evaporation. The results show If the distance between the drops is larger than 600 μm, the model of a single droplet may be used; when the distance between the drops is smaller than 600 μm, the model of water spray should be used. Pearlmutter et al. (2008) develop down-draft evaporative cool tower (DECT) which incorporates a secondary air inlet and a complex longitudinal section that comprises two partly overlapping cones. The main advantage of the multi-inlet DECT compared with conventional cool towers is in its potential for saving water, since part of the air flowing through the tower is drawn from within the enclosed space, which is assumed to be cooler and more humid than the ambient environment. Application of evaporative cool towers may be a practical means of providing low-cost, low maintenance cooling of large spaces. Erell et al. (2008) investigated multi-stage down-draft evaporative cool tower (DECT) its main significant is that they validate the concept of a multi-inlet of air, which is the basis for a strategy for reducing the quantity of water evaporated to supply a given volume of cooled air. Carew (2006) presents the design and testing results of a prototype passive downdraft evaporative cooling tower (PDEC) installed and tested to guide the design of a permanent tower intended as a cost-effective retrofit to the Miele Showroom at the South African head offices in Johannesburg. Water is vaporized at the top of the tower using micronizer spray nozzles to produce an evaporative cooling effect. The system behaves like a displacement system providing adequate cooling for days up to 28 ˚C. The building seems adequately vapour permeable to use a recirculation system so that the humidity build-up does not impact on the performance of the tower. Ataei

et al. (2008) developed mathematical model of counter flow wet cooling tower to predict water and air properties and validated it with experimental data. The results of the cooling tower modelling illustrated that the amount of exergy supplied by water is larger than that absorbed by air. This is because the entropy is generated by the system. Kachhwaha et al. (1998) carried out heat and mass transfer analysis between water spray drops and air stream in horizontal counter flow configuration. They investigated change in air DBT increases by increases the nozzle pressure.

2.1.3 Exergy Analysis

Bejan (2006) expressed total exergy air is the sum of convective and evaporative exergy of air. Total exergy of the system can split into thermomechanical and chemical components for any system that undergoes a psychometrics process such as in cooling tower operation. Thirapong Muangnoi et al. (2007) developed a mathematical model based on heat and mass transfer principle to find the properties of water and air. The results show that water exergy decreases continuously from top to bottom. On the other hand, air exergy expressed in terms of convective and evaporative heat transfer. It is noted from the results that the amount of exergy supplied by water is larger than that absorbed by air, because the system produces entropy (Ataei et al. 2008). Zunaid et al. (2011, 2013b, 2013c) and Muangnoi (2008) reported total exergy of air controlled by its convective and evaporative exergy, and evaporative exergy of air are major component present in total exergy of air. Qureshi and Zubair (2003) carried out numerical study using EES software that has built-in functions for thermodynamic and transport properties to determine the variation of second-law efficiency as a function of mass flow rate, relative humidity, and temperature. These built-in properties make it possible for a single simplified equation

to be used for all streams (except humid air). It was shown through calculations that an increase in the relative humidity of the incoming air stream increases the second-law efficiency of the processes. In the case of cooling with dehumidification and heating, an interesting exergy destruction contribution noted. Santos et al. (2013) presents a study on the performance of the evaporative cooling process in air washers and conclude that the optimization of the process should involve both energy and exergy analyses to produce the best conditions of thermal comfort at an admissible thermodynamic cost.

2.2 Research Gap

In the conventional pact cooling tower, the heat and mass transfer phenomenon is well understood. Therefore experimental or simulation studies available in the literature are in abundance. On the other hand, SCT is a new field of study, and very less amount of work has found in the literature regarding 2-D and 3-D analysis of mono and multi droplet SCT. Simplicity, size, saving in installation and operational cost of SCT motivate to undergo in-depth study to correlate heat and mass transfer analysis and to determine the factors which govern the performance of SCT, this could be helpful for maximizing the effects of advantages posed by SCT as a replacement for conventional cooling towers. Therefore, there is a need to develop a generalized integrated spray air interaction model suitable for wide range of applications and performance parameters which will help in optimal system design with low operating cost.

2.3 Research Objectives

Keeping given these gaps in the literature, the following objectives have formulated for carrying the present research work.

(i) Development of a mathematical model of heat and mass transfer for water droplet and air interaction in Shower Cooling Tower (SCT) with parallel and counter flow configurations for wide range of parametric studies integrated to different applications.

(ii) Development of an experimental set up for the collection of heat and mass transfer data for wide range of experimental parameters and model validation.

(iii) Drop size distribution studies for different geometrical parameters of a nozzle.

(iv) CFD modelling of the water droplet and air interaction and comparison with mathematical model mentioned at the objective (i).

(v) Application of exergy approach for better understanding of heat and mass interaction of air and water droplets in SCT.

2.4 Research Methodology

Generalized 2-D mathematical models developed and solved in MATLAB for mono and multi water spray droplet and air interaction for heat and mass transfer analysis in vertical parallel and counter flow configurations. The spray air model represents by ordinary differential equations of conservation of mass, momentum, and energy. Runge Kutta method of the fourth order was employed to solve these equations. With the help of developed mathematical model for SCT following applications was studied in detail:

(i) Parametric investigation of SCT for water cooling application for industries (i.e. power plant).

(ii) Parametric investigation of SCT for air cooling application for human comfort.

(iii) An experimental test rig of SCT developed for validation of above mathematical model. Procurement of SCT with water supply tank, exhaust fan, one centrifugal pump, one reciprocating pump, nozzle and so on with instrumentation like pressure gauge, digital thermometer, digital anemometer, digital humidity meter etc. have already been done for parametric study.

(iv) Experimental water droplet size distribution measurement studied was done with the help of Malvern spraytec analyzer.

(v) Development of a three dimensional (3-D) CFD (using Fluent) model and comparison with simplified modelling mentioned in objective (i) and experimental data.

(vi) Exergetic studies of air, water and SCT system was done for better understanding and interpretation of heat and mass transfer mechanism.

Chapter 3 EXPERIMENTAL PROCEDURES

3.1 Experimental Facility

Schematic diagram of downdraft parallel flow and counter flow SCT used for experimental work shown in Figure 3.1 and Figure 3.2, the actual image of SCT also shown in Figure 3.3. The atmospheric air enters at the top of SCT with the help of a fan. Water from the storage tank supplied to the commercially available impaction pin nozzle with the help of a reciprocating pump. Schematic diagram and the actual image of impaction pin nozzle shown in Figure 3.4 and water spray coming out from the nozzle is shown in Figure 3.5. Nozzle disintegrates the water into the small droplets for maximizing the surface area to increase the heat transfer between the droplets and the air. The different size of droplets produces by applying different pressure on the jet. Increasing the water pressure results in an increase in velocity of jet and flow rate of a nozzle, decrease in droplets sizes. Nozzle orifice diameter, pressure, discharge, and velocity were measured, and the results are given in Table 3.1. The inlet spray water droplets and inlet air cool down by convection and evaporation heat transfer and leave the tower from the bottom. The exit air goes to the atmosphere, and exit water used for an industrial application if inlet water temperature is greater than air DBT. The exit air with a lower dry bulb temperature and higher specific humidity as compared to ambient sent into the lowest part of the centrally covered courtyard of the multiuse building in air cooling application if inlet air DBT greater than inlet water temperature, thus supplying cooled air for the occupants of the space.

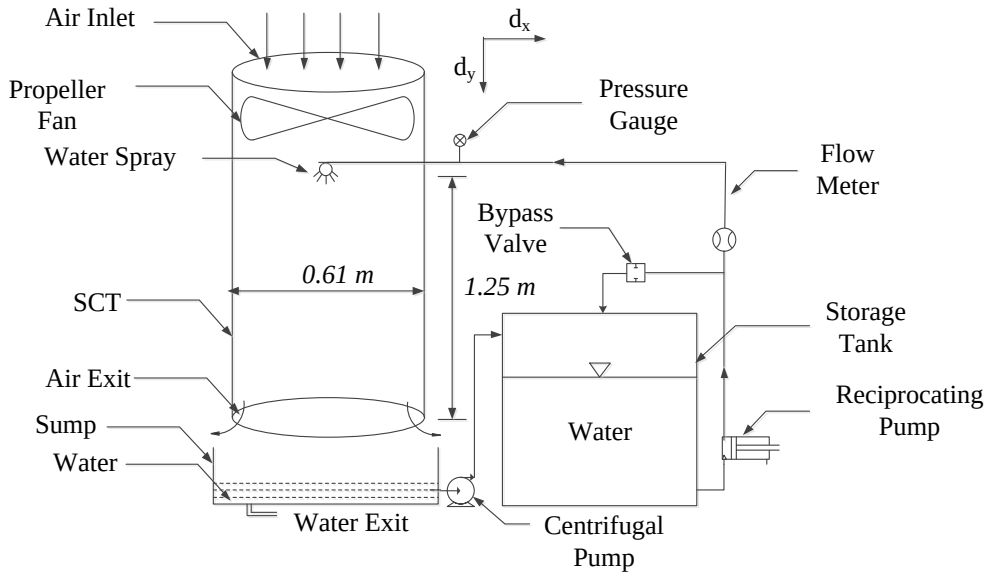

Figure 3.1 Downdraft parallel flow SCT

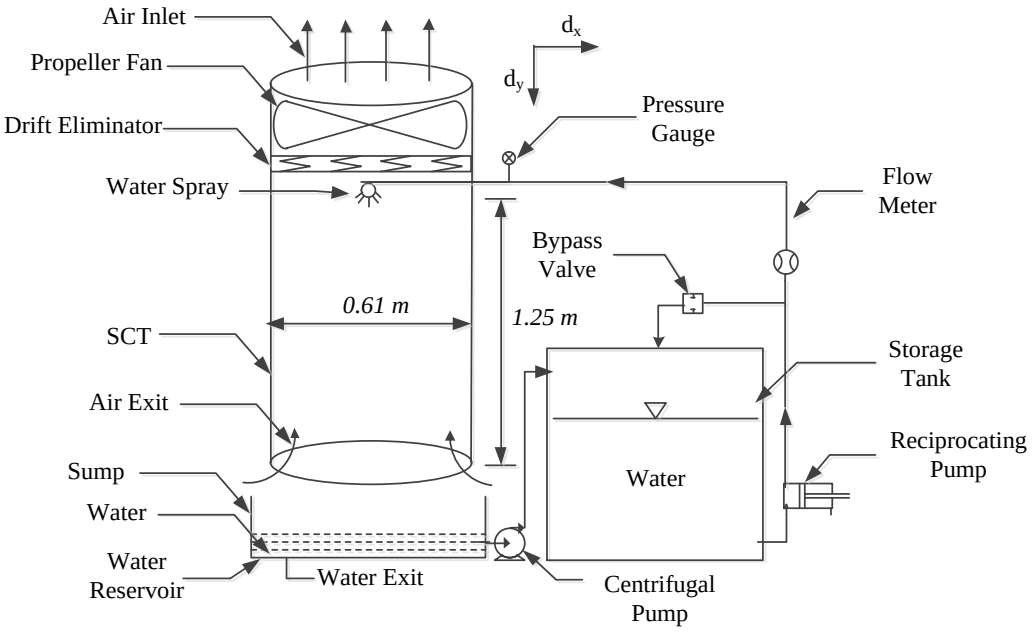

Figure 3.2 Downdraft counter flow SCT

Figure 3.3 Actual shower cooling tower

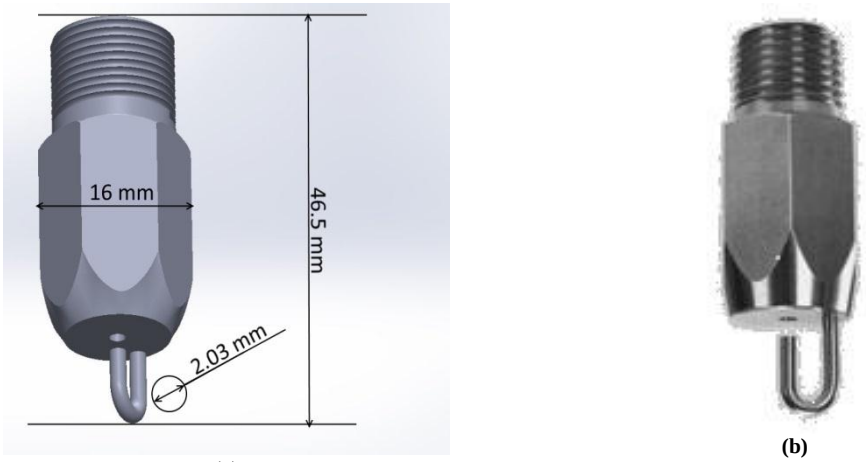

(a)

(b)

Figure 3.4 Impaction pin nozzle (a) schematic diagram, (b) actual image

Figure 3.5 Water spray coming out from impaction pin nozzle

Table 3.1 Discharge characteristic of the nozzle

Nozzle outlet orifice diameter (m)	Nozzle Pressure (bar)	Discharge (l/min)	Nozzle exit water Velocity (m/s)
2.03×10^{-3}	2	3.4	17.7
	3	4.2	21.7
	4	4.9	25.1

3.2 Drop Size Measurement and Modelling

Schematic diagram of Malvern spraytec laser diffraction system shown in Figure 3.6; it used for measure nozzle spray droplets size at the different pressures. Figures 3.7, 3.8 and 3.9 show spray size distribution at 2, 3 and 4 bar pressure. SMD of spray droplets at 2, 3 and 4 bar pressure was 420.75 µm, 311.31 µm, and 204.84 µm respectively. SMD of nozzle spray droplet decreases with increases the nozzle pressure.

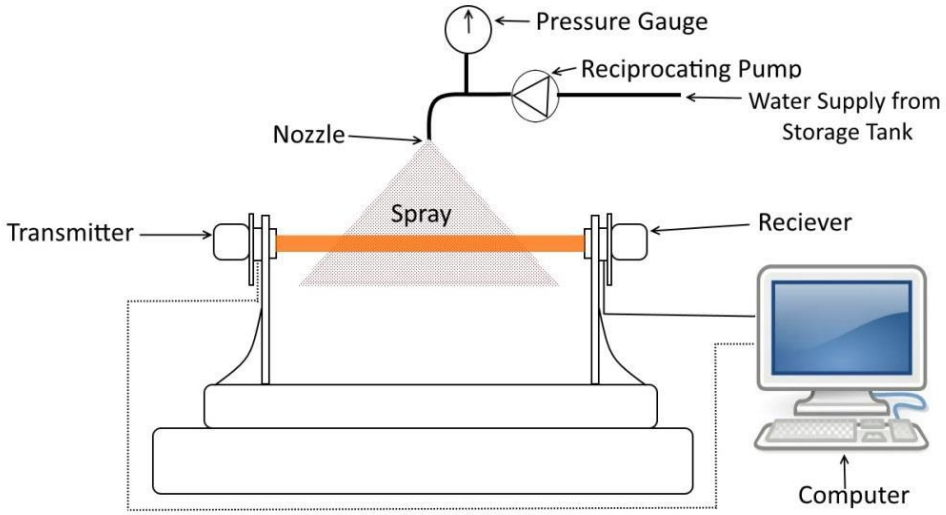

Figure 3.6 Schematic diagram of Malvern spraytec laser diffraction system

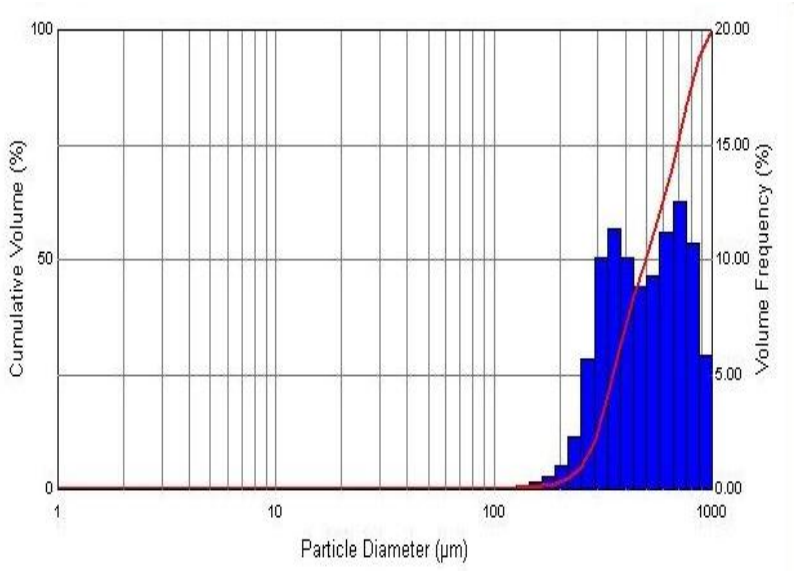

Standard Values:

Transmission = 14.28%	Dv(10) = 286.66 (µm)	Span = 1.09
Cv = 22621.7 (PPM)	Dv(50) = 497.33 (µm)	D[3][2] = 420.75 (µm)
SSA = 0.014 (m^2/cc)	Dv(90) = 826.62 (µm)	D[4][3] = 526.43 (µm)

Figure 3.7 Particle size distribution at pressure 2 bar

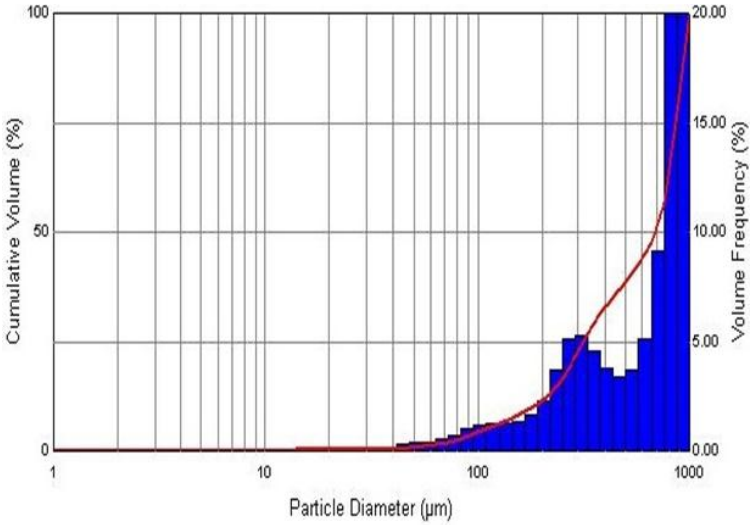

Standard Values:

Transmission = 9.78%	Dv(10) = 182.91 (µm)	Span = 1.11
Cv = 19984.4 (PPM)	Dv(50) = 687.64 (µm)	D[3][2] = 311.31 (µm)
SSA = 0.019 (m^2/cc)	Dv(90) = 943.83 (µm)	D[4][3] = 599.16 (µm)

Figure 3.8 Particle size distribution at pressure 3 bar

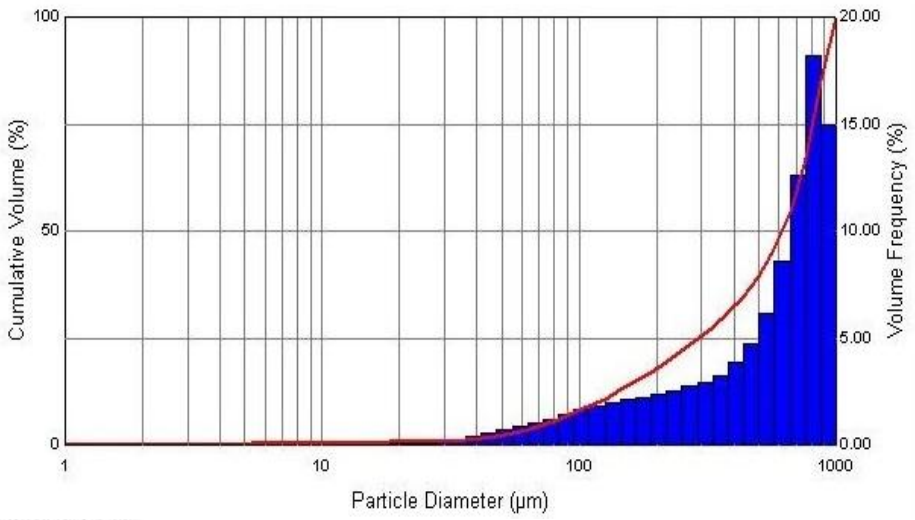

Standard Values:

Transmission = 18.49%	Dv(10) = 118.59 (µm)	Span = 1.29
Cv = 9536.7 (PPM)	Dv(50) = 618.29 (µm)	D[3][2] = 204.84 (µm)
SSA = 0.029 (m^2/cc)	Dv(90) = 913.74 (µm)	D[4][3] = 557.13 (µm)

Figure 3.9 Particle size distribution at pressure 4 bar

3.3 Experimental Uncertainties

For a meaningful comparison of experimental data and model predictions, it is necessary to quantify the uncertainties in the measurement of water temperature, air DBT and relative humidity, and air velocity.

3.3.1 Uncertainties in water temperature measurement

Digital water thermometer full specification has given in Table 3.2; it used to measure inlet and outlet water temperature. The accuracy of the instrument to measure water temperature was ±1 ˚C. Temperature range of instrument varied from -20 °C to +230 °C.

Table 3.2 Measuring device specifications

Device	Range	Accuracy	Resolution	Working fluid
Digital Water Proof Thermometer	-20 °C to +230 °C	±1 ˚C	0.1 ˚C	Water
Digital Anemometer	0 to 10 m/s	±0.1 m/s	0.01 m/s	Air
Digital Thermo-Hygrometer	0 to 100 % & -25 to 50 °C	± 0.5 ˚C & ± 2.5 %	0.1 ˚C & 0.1 %	Air

3.3.2 Uncertainties in air DBT and relative humidity measurement

Digital thermo-hygrometer full specifications are given in Table 3.2; it used for measure inlet and outlet air DBT and relative humidity. The accuracy of the instrument to measure air DBT and relative humidity was ± 0.5 ˚C and ±2.5 %, respectively. Temperature and relative humidity range of instrument varied from -25 to 50 °C and 0 to 100 % respectively.

3.3.3 Uncertainties in air velocity measurement

The digital anemometer is used to measure air velocity; its full specifications are given in Table 3.2. The accuracy of the instrument to measure air velocity was ±0.1 m/s. Range and resolution of the instrument was 0 to 10 m/s and 0.01 m/s respectively.

Chapter 4 HEAT AND MASS TRANSFER MODELS

4.1 Mathematical Models of SCT

To describe the motion characteristics of the mono and multi water droplets in mathematical models some critical assumptions concerning the water droplet was made. It assumed that the water droplet is spherical, and droplet temperatures are uniform. The possibility of collision or scattering of the water droplet during the motion process neglected. In mono droplet model the entire droplet having the same diameter, but in multi droplet model droplets have ten different diameters. Ten different droplets diameter model give better results in comparison to single droplet diameter model. Its results are very much close to the experimental results. The mass, momentum, and energy conservation equations for varying diameter of water droplets and air derived with the help of Kloppers and Kroger (2005), Xiaoni and Zhenyan (2007) and Masters (1991). The thermal efficiency of cooling tower was derived with the help of Fisenko et al. (2002). The equations for air exergy, water exergy, system exergy, exergy destruction and second law efficiency (SLE) derived with the help of Bejan (2006). The mass flow of air is constant at the inlet of tower however velocity of air varying along the length of the tower with varying its density. The following analysis considers the property variations in the vertical direction. The SCT height divided into ‘n' sections of finite thickness and finite volume.

4.2 Mathematical Model for 2-D Mono Droplet Parallel Flow SCT

Mono droplet mathematical model for parallel flow SCT which used for industrial and air cooling application are given below.

4.2.1 Conservation of mass for water droplet

A control volume for air-water droplet for parallel flow SCT is shown in Figure 4.1.

$$(m_d)_{in} = (m_d)_{out} + \frac{dm_d}{dy} dy \tag{1}$$

Where mass flow rate of water $'m_d' = N.M_d$

The water evaporation rate of single droplet associated with the mass transfer at given height:

$$\frac{dM_d}{dt} = -h_m(\omega_s - \omega_a)A_s \tag{2}$$

Where $A_s = \pi D^2$ and $'\omega_s'$ = specific humidity of water vapour at the drop surface.

$$\frac{dM_d}{dy} = -\frac{h_m}{U_y}(\omega_s - \omega_a)A_s \tag{3}$$

Where, $U_y = \frac{dy}{dt}$

Since, $M_d = \frac{1}{6}\pi D^3 \rho_w$, then ,

$$\frac{1}{6}\pi\rho_w \frac{d}{dy}(D^3) = -\frac{h_m}{U_y}(\omega_s - \omega_a)\pi D^2 \tag{4}$$

Here variation in density of water is neglected with respect to height of SCT and the variation of droplet diameter with tower height can be written as:

$$\frac{d(D)}{dy} = -\frac{2h_m}{U_y \rho_w}(\omega_s - \omega_a) \tag{5}$$

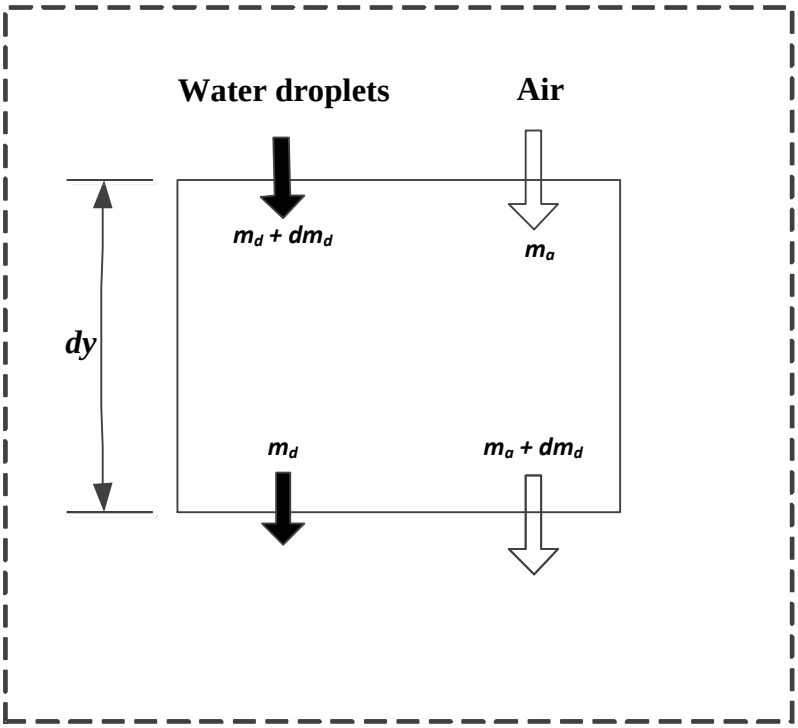

Figure 4.1 Control volume of mass along parallel flow SCT

4.2.2 Conservation of momentum for water droplet

The gravity forces, buoyancy forces and the resistive forces (drag forces) acting on the droplet moving in a downward direction with a velocity 'U' are shown in Figure 4.2. The forces can be expressed as:

$$\text{Gravity, } G = M_d g = \frac{\pi D^3 \rho_w g}{6} \tag{6}$$

$$\text{Buoyancy force, } F = \frac{\pi D^3 \rho_a g}{6} \tag{7}$$

$$\text{Resistance force, } R = \frac{\pi C_d \rho_a W^2 D^2}{8} \tag{8}$$

Velocity of droplet in x and y directions are given as:

$$U_x = U\cos\theta \tag{9}$$

$$U_y = U\sin\theta \tag{10}$$

Resultant velocity of the droplet and its inclination angle 'θ' from horizontal is shown in Figure 4.3 and it is given as:

$$W = \sqrt{(U_y - u_a)^2 + U_x^2} \tag{11}$$

$$\theta = \tan^{-1}\left(\frac{U_y}{U_x}\right) \tag{12}$$

Now the resistive force (drag force) acts in the opposite direction of the relative velocity of the droplet w. r. t. air. Resolving the drag forces in the x and y directions respectively we get

$$R_x = R\frac{U_x}{U} = \frac{1}{8}\pi\rho_a C_d W D^2 U_x \tag{13}$$

$$R_y = R(\frac{U_y - u_a}{U}) = \frac{1}{8}\pi\rho_a C_d W D^2 (U_y - u_a) \tag{14}$$

The momentum of the droplet in vertical direction yield the variation of a vertical component of droplet velocity in the y-direction with height is expressed as:

$$\frac{dU_x}{dy} = -\left[\frac{3(C_d \rho_a W U_x)}{4D\rho_w U_y}\right] - \frac{3U_x}{D}\frac{dD}{dy} \tag{15}$$

Similarly, the momentum of the droplet in the *x*-direction with a variation of height is expressed as:

$$\frac{dU_y}{dy} = \left[g(\rho_w - \rho_a) - \frac{3(C_d \rho_a W (U_y - u_a))}{4D}\right]\frac{1}{\rho_w U_y} - \frac{3U_y}{D}\frac{dD}{dy} \tag{16}$$

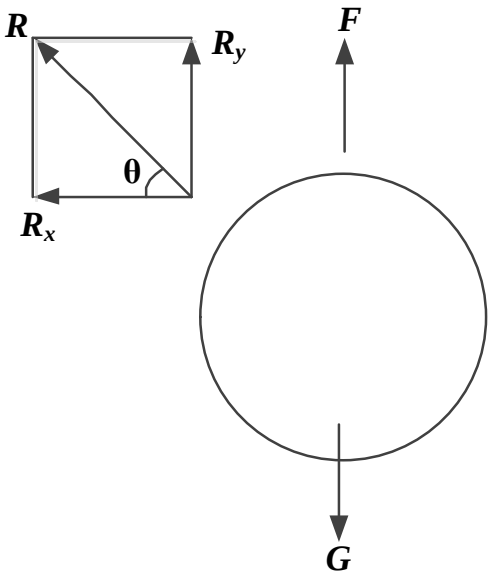

Figure 4.2 Forces acted on a droplet

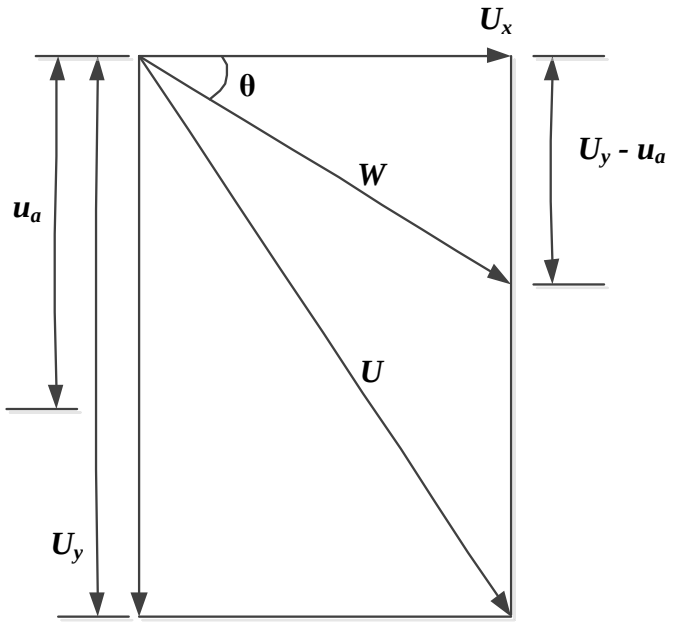

Figure 4.3 Velocity vector diagram of water droplet and air for parallel flow SCT

4.2.3 Conservation of energy for water droplet

The water droplets lose its sensible heat and latent heat to the air at the expense of the internal energy. Figure 4.4 shows convective heat transfer 'q_c' and evaporative heat transfer 'q_e' from drop surface. Energy balance on control surface surrounding the water droplet yields following equations.

$$\frac{dE}{dt} = -(q_c + q_e) \tag{17}$$

Where $E = M_d c_{pd} T_d$ (18)

$$q_c = hA_s(T_d - T_a) \tag{19}$$

$$q_e = h_m A_s(\omega_s - \omega_a) h_{fg} \tag{20}$$

Where $h_{fg} = h_{fg0} + c_{pv}T_d$ (21)

Then $M_d c_{pd} \frac{dT_d}{dt} = -[h(T_d - T_a) + h_m(\omega_s - \omega_a)h_{fg}]A_s$ (22)

$$\frac{dT_d}{dt} = -\frac{6h_m}{\rho_w c_{pd} D}\left[\frac{h}{h_m}(T_d - T_a) + (\omega_s - \omega_a)h_{fg}\right] \quad (23)$$

Where $T_d - T_a = \frac{(h_s - h_{av}) - (\omega_s - \omega_a)h_{fg}]}{c_{pav}}$ (24)

$$Le_f = \frac{h}{h_m c_{pav}} \quad (25)$$

And $c_{pav} = c_{pa} + \omega_a c_{pv}$ (26)

Then, $\frac{dT_d}{dt} = -\frac{6h_m[Le_f(h_s - h_{av}) + (1 - Le_f)(\omega_s - \omega_a)h_{fg}]}{c_{pd} D \rho_w} - \frac{3T_d}{D}\frac{dD}{dt}$ (27)

$$\frac{dT_d}{dt} = \frac{dT_d}{dy}\frac{dy}{dt} = U_y\left[\frac{dT_d}{dy}\right] = -\frac{6h_m[Le_f(h_s - h_{av}) + (1 - Le_f)(\omega_s - \omega_a)h_{fg}]}{c_{pd} D \rho_w} - \frac{3T_d}{D}\frac{dD}{dt} \quad (28)$$

Therefore energy balance of drops is represented by

$$\frac{dT_d}{dy} = -\frac{6h_m[Le_f(h_s - h_{av}) + (1 - Le_f)(\omega_s - \omega_a)h_{fg}]}{U_y c_{pd} D \rho_w} - \frac{3T_d}{D}\frac{dD}{dy} \quad (29)$$

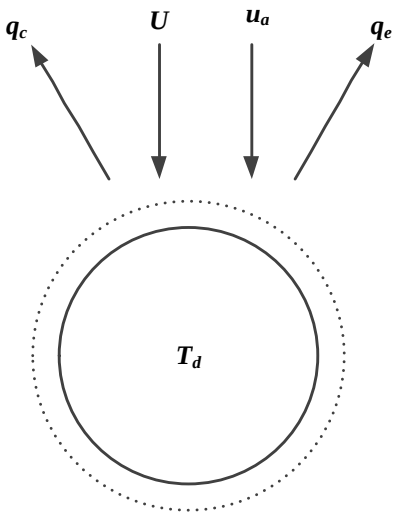

Figure 4.4 Energy exchange at water droplet level

4.2.4 Thermal energy balance equations in the SCT

The total enthalpy transfer at air-water interface consists of an enthalpy transfer associated with the mass transfer due to the difference in vapour concentration between the saturated air and mainstream air. Sensible heat transfer between air and water droplets occurs due to the difference in temperature of water droplets and DBT of air. A mass balance in the control volume is given as:

$$dm_d = m_a d\omega_a \tag{30}$$

The energy balance in the control volume of the SCT

$$m_a dh_{av} = m_d dh_d + h_d dm_d \tag{31}$$

Rearranging using above two equations

$$dT_d = \frac{m_a}{m_d}\left(\frac{dh_{av}}{c_{pd}} - T_d d\omega_a\right) \tag{32}$$

Energy balance at the water and air interface yields

$$dq = dq_c + dq_e \tag{33}$$

$$dq = \left[h\left(T_d - T_a\right) + h_m h_{fg}\left(\omega_s - \omega_a\right)\right] dA \tag{34}$$

$$dq = \left[\frac{h}{C_{pav}}\left(h_s - h_{av}\right) + \left(h_m - \frac{h}{c_{pav}} \right) h_{fg}\left(\omega_s - \omega_a\right) \right] dA \tag{35}$$

The enthalpy transfer to the air stream is $dh_{av} = \frac{dq}{m_a}$

$$dh_{av} = \frac{dq}{m_a} = \frac{h_m}{m_a}\left[Le_f\left(h_s - h_{av}\right) + \left(1 - Le_f\right) h_{fg}\left(\omega_s - \omega_a\right)\right] dA \tag{36}$$

Where, $dA = \frac{m_d dy \pi D^2}{M_d U_y} = \frac{6 m_d dy}{\rho_w D U_y}$

Now change in air temperature due to mass and heat transfer interaction can be expressed as:

$$\frac{dh_{av}}{dy} = \left(\frac{m_d}{m_a} \right) \frac{6 h_m}{\rho_w D U_y}\left[Le_f\left(h_s - h_{av}\right) + \left(1 - Le_f\right) h_{fg}\left(\omega_s - \omega_a\right)\right] \tag{37}$$

4.2.5 Mass balance equation in the SCT

Mass balance equation for the control volume

$$dm_d = m_a d\omega_a = N \frac{dM_d}{dt} \tag{38}$$

Substituting, $N = \frac{m_d dy}{M_d U_y}$ and $M_d = \frac{1}{6}\pi D^3 \rho_w$,

$$dw_a = \left(\frac{m_d}{m_a}\right)\frac{6h_m}{\rho_w U_y D}\left(\omega_s - \omega_a\right)dy \tag{39}$$

The mass transfer associated with the control volume expressed as:

$$\frac{dw_a}{dy} = \frac{m_d h_m A_s}{m_a M_d U_y}\left(\omega_s - \omega_a\right) \tag{40}$$

4.2.6 Equation for Thermal Efficiency

The thermal efficiency of SCT gives as:

$$\eta_{th} = \frac{\left(T_{d,in} - T_{d,m,i}\right)100}{T_{d,in} - T_{wb,in}} \tag{41}$$

$$T_{d,m,i} = \frac{\sum_i m_{d,i} T_{d,i}}{\sum_i m_{d,i}} \tag{42}$$

Where,

4.2.7 Droplet trajectory equation

Droplet trajectory expressed in terms of horizontal and vertical components of velocity.

$$\frac{dx}{dy} = \frac{U_x}{U_y} \tag{43}$$

4.3 Mathematical Model for 2-D Mono Droplet Counter flow SCT

Mono droplet mathematical model for counter flow SCT used for industrial and air cooling application is given below.

4.3.1 Conservation of mass for water droplet

A control volume for air-water droplet for counter flow SCT shown in Figure 4.5 and, conservation of mass for water droplet can be written as:

$$\frac{d(D)}{dy} = -\frac{2h_m}{U_y \rho_w}(\omega_s - \omega_a) \tag{44}$$

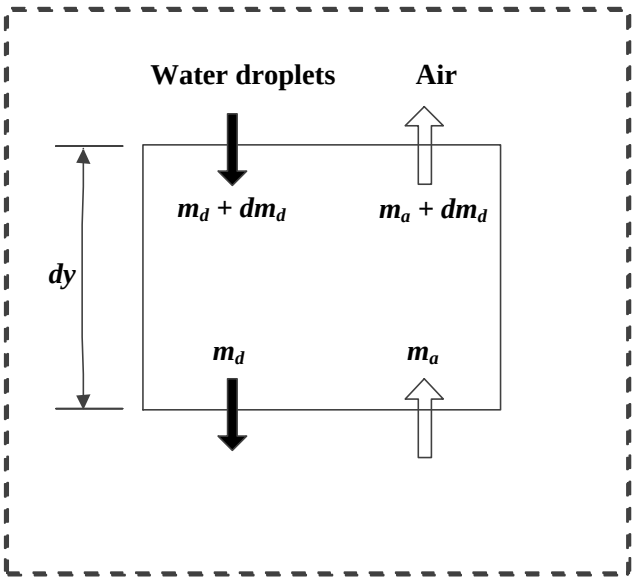

Figure 4.5 Control volume of mass along counter flow SCT

4.3.2 Conservation of momentum for water droplet

The gravity forces, buoyancy forces and the resistive forces (drag forces) acting on the droplet moving in a downward direction with a velocity $'U'$. Resultant

velocity 'W' of droplet and its inclination angle 'θ' from horizontal is shown in Figure 4.6 and it is give as:

$$W = \sqrt{(U_y + u_a)^2 + U_x^2} \tag{45}$$

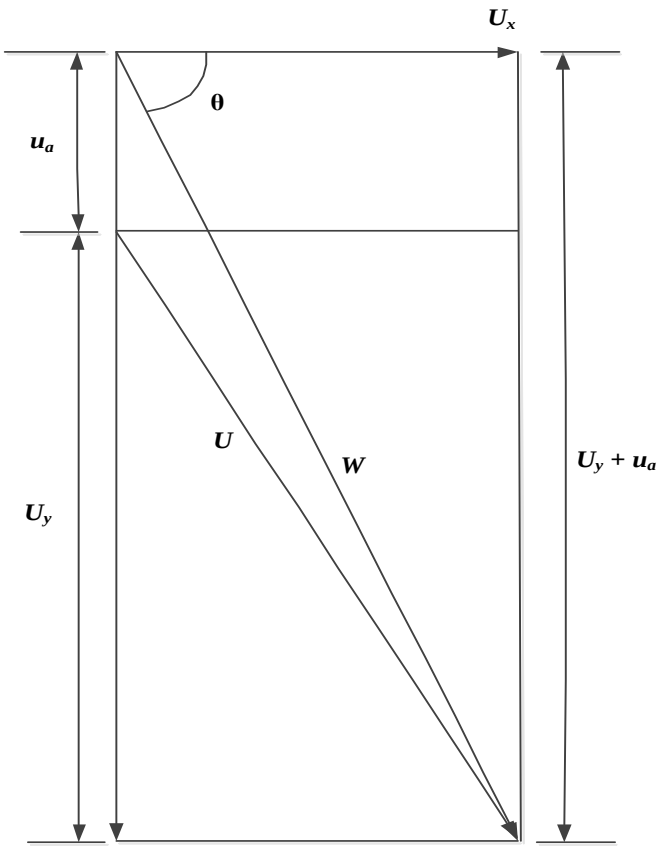

Figure 4.6 Velocity vector diagram of water droplet and air for counter flow SCT

The variation in the momentum of the droplet in horizontal and vertical direction with tower height expressed as:

$$\frac{dU_x}{dy} = -\left[\frac{3(C_d \rho_a W U_x)}{4D\rho_w U_y}\right] - \frac{3U_x}{D}\frac{dD}{dy} \tag{46}$$

Similarly, variation in the momentum of the droplet in the vertical direction with tower height expressed as:

$$\frac{dU_y}{dy} = \left[g(\rho_w - \rho_a) - \frac{3(C_d \rho_a W(U_y + u_a))}{4D} \right] \frac{1}{\rho_w U_y} - \frac{3U_y}{D} \frac{dD}{dy} \tag{47}$$

4.3.3 Conservation of energy for water droplet

The water droplets lose its sensible heat and latent heat to the air. Figure 4.7 shows convective heat transfer 'q_c' and evaporative heat transfer 'q_e' from droplet surface. The energy balance of the droplet shown below:

$$\frac{dT_d}{dy} = -\frac{6h_m[Le_f(h_s - h_{av}) + (1 - Le_f)(\omega_s - \omega_a)h_{fg}]}{U_y c_{pd} D \rho_w} - \frac{3T_d}{D} \frac{dD}{dy} \tag{48}$$

4.3.4 Thermal energy balance equations in the SCT

Variation in air temperature due to mass and heat transfer interaction can be given as:

$$\frac{dT_a}{dy} = \left(\frac{m_d}{m_a} \right) \frac{6h_m}{\rho_w D\, U_y C_{pav}} \left[Le_f \left(h_s - h_{av} \right) + \left(1 - Le_f \right) h_{fg} \left(\omega_s - \omega_a \right) \right] - \frac{h_{fg,0}}{C_{pav}} \frac{dw_a}{dy} \tag{49}$$

4.3.5 Mass balance equation in the SCT

The mass transfer associated with the control volume expressed as:

$$\frac{dw_a}{dy} = \frac{m_d h_m A_s}{m_a M_d U_y} \left(\omega_s - \omega_a \right) \tag{50}$$

4.3.6 Equation for thermal efficiency

The thermal efficiency of SCT gives as:

$$\eta_{th} = \frac{\left(T_{d,in} - T_{d,out}\right)100}{T_{d,in} - T_{wb,in}} \tag{51}$$

4.3.7 Droplet trajectory equation

Droplet trajectory expressed in terms of the horizontal and vertical components of velocity.

$$\frac{dx}{dy} = \frac{U_x}{U_y} \tag{52}$$

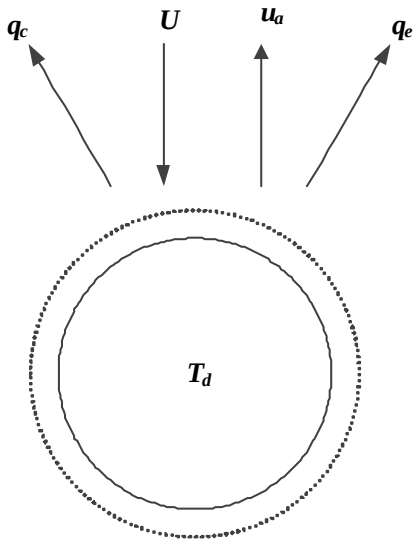

Figure 4.7 Energy exchange at water droplet level for counter flow SCT

4.4 Mathematical Model for 2-D Multi Droplet Parallel Flow SCT

4.4.1 Conservation of mass for water droplet

For droplet of the category $'i'$, a control volume for air and water droplet shown in Figure 4.8.

$$(m_{d,i})_{in} = (m_{d,i})_{out} + \frac{dm_{d,i}}{dy} dy \tag{53}$$

Where mass flow rate of water is given as $'m_{d,i}' = N_i.M_{d,i}$, here $'M_{d,i}'$ is a mass of single droplet.

$$\frac{dM_{d,i}}{dt} = -h_{m,i}(\omega_{s,i} - \omega_a)A_{s,i} \tag{54}$$

Where $A_{s,i} = \pi D_i^2$ and $'\omega_{s,i}'$= specific humidity of water vapour at the droplet surface.

$$\frac{dM_{d,i}}{dy} = -\frac{h_{m,i}}{U_{y,i}}(\omega_{s,i} - \omega_a)A_{s,i} \tag{55}$$

Since, $M_{d,i} = \frac{1}{6}\pi D_i^3 \rho_w$, then ,

$$\frac{1}{6}\pi\rho_w \frac{d}{dy}(D_i^3) = -\frac{h_{m,i}}{U_{y,i}}(\omega_{s,i} - \omega_a)\pi D_i^2 \tag{56}$$

Variation of droplet diameter with tower height can be written as:

$$\frac{d(D_i)}{dy} = -\frac{2h_{m,i}}{U_{y,i}\rho_w}(\omega_{s,i} - \omega_a) \tag{57}$$

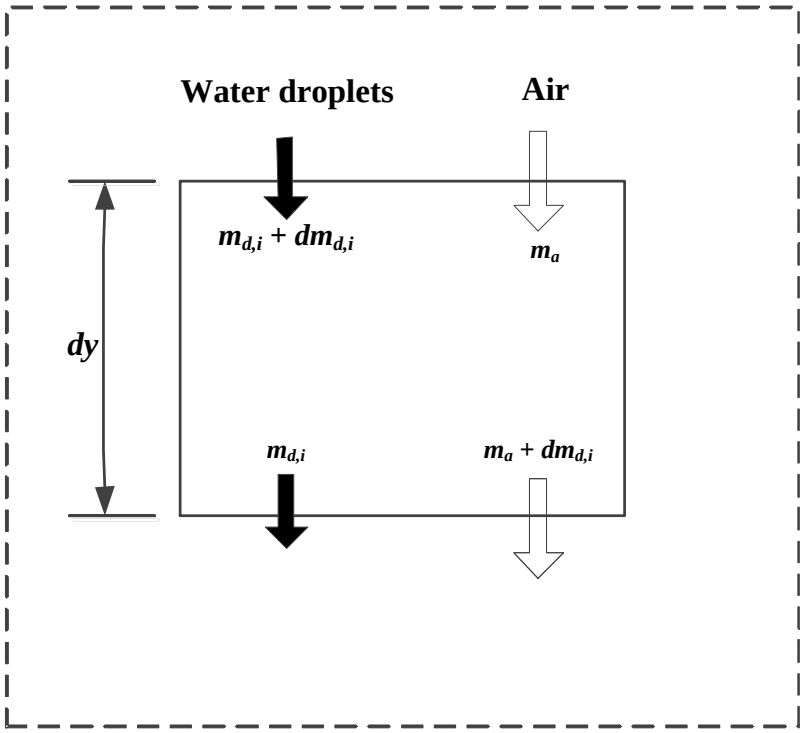

Figure 4.8 Control volume of mass for $'i$ th$'$ category of water droplet and air along parallel flow SCT

4.4.2 Conservation of momentum for water droplet

Distribution of multi-diameter water droplets are based on Rosin Rammler function.

Rosin Rammler function,

$$RR = 1 - \exp\left(-\left(\frac{D}{D_m}\right)^{uc}\right) \tag{58}$$

Where, $'D_m'$ is characteristic droplet size and $'uc'$ is uniformity constant.

The gravity forces, buoyancy forces and the resistive forces (drag forces) acting on the droplet moving in a downward direction with a velocity 'U_i' are shown in Figure 4.9. For droplet of the category 'i', forces can be expressed as:

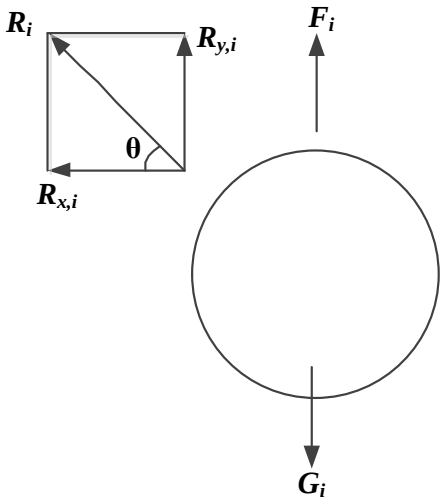

Figure 4.9 Forces acted on 'i th' category of water droplet

$$\text{Gravitational force, } G_i = M_{d,i}g = \frac{\pi D_i^3 \rho_w g}{6} \tag{59}$$

$$\text{Buoyancy force, } F_i = \frac{\pi D_i^3 \rho_a g}{6} \tag{60}$$

$$\text{Drag force, } R_i = \frac{\pi C_{d,i} \rho_a W_i^2 D_i^2}{8} \tag{61}$$

Velocities of the droplet in x and y directions are given as:

$$W_{x,i} = W_i \cos\theta \tag{62}$$

$$W_{y,i} = W_i \sin\theta \tag{63}$$

Resultant velocity of droplet and its inclination 'θ' from horizontal is shown in Figure 4.10 and it is given as:

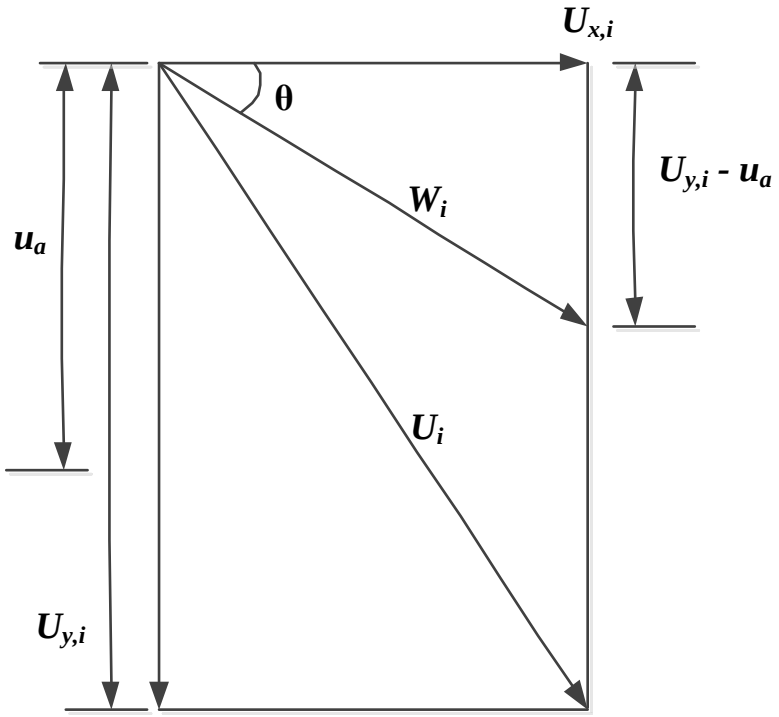

Figure 4.10 Velocity vector diagram of '*i* th' category of water droplet and air for parallel flow SCT

$$W_i = \sqrt{(U_{y,i} - u_a)^2 + U_{x,i}^2} \tag{64}$$

$$\theta = \tan^{-1}(\frac{W_{y,i}}{W_{x,i}}) = \tan^{-1}(\frac{U_{y,i} - u_a}{U_{x,i}}) \tag{65}$$

Now the drag force in the x and y directions respectively we get:

$$R_{x,i} = R_i \frac{W_{x,i}}{W_i} = \frac{1}{8}\pi\rho_a C_{d,i} W_i D_i^2 W_{x,i} \tag{66}$$

$$R_{y,i} = R_i(\frac{W_{y,i}}{W_i}) = \frac{1}{8}\pi\rho_a C_{d,i} W_i D_i^2 W_{y,i} \tag{67}$$

For droplet of the category $'i'$, the variation in the momentum of the droplet in the horizontal direction with tower height is expressed as:

$$\frac{d(M_{d,i}U_{x,i})}{dt}+\frac{\pi C_{d,i}\rho_a W_i D_i^2 W_{x,i}}{8}=0 \tag{68}$$

Multiply and divide LHS of above equation by dy

$$\frac{d(M_{d,i}U_{x,i})}{dt}\times\frac{dy}{dy}+\frac{\pi C_{d,i}\rho_a W_i D_i^2 W_{x,i}}{8}=0 \tag{69}$$

$$\frac{d(M_{d,i}U_{x,i})}{dy}+\frac{\pi C_{d,i}\rho_a W_i D_i^2 W_{x,i}}{8U_y}=0 \tag{70}$$

Differentiate above equation with respect to y

$$M_{d,i}\frac{dU_{x,i}}{dy}+U_{x,i}\frac{dM_{d,i}}{dy}=-\frac{\pi C_{d,i}\rho_a W_i D_i^2 W_{x,i}}{8U_{y,i}} \tag{71}$$

$$\frac{\pi\rho_w D_i^3}{6}\frac{dU_{x,i}}{dy}+U_{x,i}\frac{\pi\rho_w}{6}\frac{dD_i^3}{dy}=-\frac{\pi C_{d,i}\rho_a W_i D_i^2 W_{x,i}}{8U_y} \tag{72}$$

$$\frac{\pi\rho_w D_i^3}{6}\frac{dU_{x,i}}{dy}=-\frac{\pi C_{d,i}\rho_a W_i D_i^2 W_{x,i}}{8U_y}-U_{x,i}\frac{\pi\rho_w}{6}\frac{dD_i^3}{dy} \tag{73}$$

$$\frac{dU_{x,i}}{dy}=-\frac{6}{\pi\rho_w D_i^3}\left[\frac{\pi C_{d,i}\rho_a W_i D_i^2 W_{x,i}}{8U_y}+U_{x,i}\frac{\pi\rho_w}{6}\frac{dD_i^3}{dy}\right] \tag{74}$$

Now conserving momentum for a droplet in horizontal direction yield the variation of a horizontal component of droplet velocity in *x*-direction with height is.

$$\frac{dU_{x,i}}{dy} = -\frac{3\rho_a C_{d,i} W_i W_{x,i}}{4\rho_w D_i U_{y,i}} - \frac{3U_{x,i}}{D_i}\frac{dD_i}{dy} \tag{75}$$

For droplet of the category 'i', variation in the momentum of the droplet in the vertical direction with tower height is expressed as:

$$\frac{d(M_{d,i}U_{y,i})}{dt} = M_{d,i}g - \frac{\pi\rho_a g D_i^3}{6} - \frac{\pi C_{d,i}\rho_a W_i^2 D_i^2}{8}\frac{W_{y,i}}{W_i} \tag{76}$$

Multiply and divide LHS of above equation by dy

$$\frac{d(M_{d,i}U_{y,i})}{dt}\times\frac{dy}{dy} = M_{d,i}g - \frac{\pi\rho_a g D_i^3}{6} - \frac{\pi C_{d,i}\rho_a W_i^2 D_i^2}{8}\frac{W_{y,i}}{W_i} \tag{77}$$

$$\frac{d(M_{d,i}U_{y,i})}{dy} = \frac{M_{d,i}g}{U_{y,i}} - \frac{\pi\rho_a g D_i^3}{6U_{y,i}} - \frac{\pi C_{d,i}\rho_a W_i\ D_i^2 W_{y,i}}{8U_{y,i}} \tag{78}$$

Differentiate above equation with respect to y

$$M_{d,i}\frac{dU_{y,i}}{dy} + U_{y,i}\frac{dM_{d,i}}{dy} = \frac{M_{d,i}g}{U_{y,i}} - \frac{\pi\rho_a g D_i^3}{6U_{y,i}} - \frac{\pi C_{d,i}\rho_a W_i\ D_i^2 W_{y,i}}{8U_{y,i}} \tag{79}$$

$$\frac{\pi\rho_w D_i^3}{6}\times\frac{dU_{y,i}}{dy} + U_{y,i}\frac{\pi\rho_w}{6}\frac{dD_i^3}{dy} = \frac{\pi\rho_w D_i^3 g}{6U_{y,i}} - \frac{\pi\rho_a g D_i^3}{6U_{y,i}} - \frac{\pi C_{d,i}\rho_a W_i\ D_i^2 W_{y,i}}{8U_{y,i}} \tag{80}$$

$$\frac{\pi\rho_w D_i^3}{6}\times\frac{dU_{y,i}}{dy} = \frac{\pi\rho_w D_i^3 g}{6U_{y,i}} - \frac{\pi\rho_a g D_i^3}{6U_{y,i}} - \frac{\pi C_{d,i}\rho_a W_i\ D_i^2 W_{y,i}}{8U_{y,i}} - \frac{3\pi\rho_w U_{y,i} D_i^2}{6}\frac{dD_i}{dy} \tag{81}$$

$$\frac{dU_{y,i}}{dy} = \left[g(\rho_w - \rho_a) - \frac{3C_{d,i}\rho_a W W_{y,i}}{4D_i} \right] \frac{1}{\rho_w U_{y,i}} - \frac{3U_{y,i}}{D_i} \frac{dD_i}{dy} \quad (82)$$

4.4.3 Conservation of energy for water droplet

Figure 4.11 shows convective heat transfer 'q_c' and evaporative heat transfer 'q_e' from droplet surface. For 'i th' category of droplet, Energy balance on control surface surrounding the water droplet yields following equations.

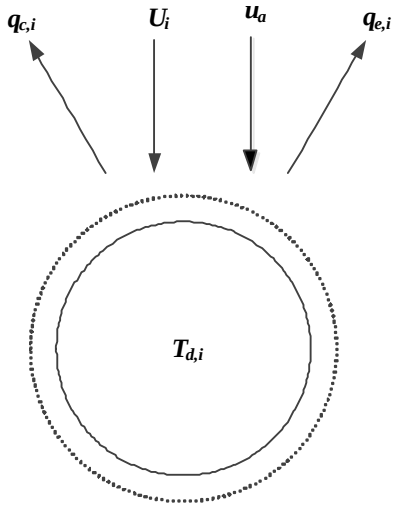

Figure 4.11 Energy exchange in 'i th' category of water droplet for parallel flow SCT

$$\frac{dE_i}{dt} = -(q_{c,i} + q_{e,i}) \quad (83)$$

Where, $E_i = M_{d,i} c_{pd,i} T_{d,i}$ (84)

$$q_{c,i} = h_i A_{s,i} (T_{d,i} - T_a) \quad (85)$$

$$q_{e,i} = h_{m,i} A_{s,i} (\omega_{s,i} - \omega_a) h_{fg,i} \tag{86}$$

Where, $h_{fg,i} = h_{fg0,i} + c_{pv,i} T_{d,i}$ (87)

Then, $M_{d,i} c_{pd,i} \frac{dT_{d,i}}{dt} = -[h_i (T_{d,i} - T_a) + h_{m,i} (\omega_{s,i} - \omega_a) h_{fg,i}] A_{s,i}$ (88)

$$\frac{dT_{d,i}}{dt} = -\frac{6h_{m,i}}{\rho_w c_{pd,i} D_i} \left[\frac{h_i}{h_{m,i}} (T_{d,i} - T_a) + (\omega_{s,i} - \omega_a) h_{fg,i} \right] - \frac{3T_{d,i}}{D_i} \frac{dD_i}{dt} \tag{89}$$

Where, $T_{d,i} - T_a = \frac{(h_{s,i} - h_{av,i}) - (\omega_{s,i} - \omega_a) h_{fg,i}}{c_{pav,i}}$ (90)

$$Le_{f,i} = \frac{h_i}{h_{m,i} c_{pav,i}} \tag{91}$$

And, $c_{pav,i} = c_{pa} + \omega_a c_{pv,i}$

Here 'c_{pav}' is the specific heat of air vapour mixture at constant pressure. (92)

Then,

$$\frac{dT_{d,i}}{dt} = -\frac{6h_{m,i}[Le_{f,i}(h_{s,i} - h_{av}) + (1 - Le_{f,i})(\omega_{s,i} - \omega_a) h_{fg,i}]}{c_{pd,i} D_i \rho_w} - \frac{3T_{d,i}}{D_i} \frac{dD_i}{dt} \tag{93}$$

$$\frac{dT_{d,i}}{dt} = \frac{dT_{d,i}}{dy} \frac{dy}{dt} = U_{y,i} \left[\frac{dT_{d,i}}{dy} \right]$$
$$= -\frac{6h_{m,i}[Le_{f,i}(h_{s,i} - h_{av}) + (1 - Le_{f,i})(\omega_{s,i} - \omega_a) h_{fg,i}]}{c_{pd,i} D_i \rho_w} - \frac{3T_{d,i}}{D_i} \frac{dD_i}{dt} \tag{94}$$

Therefore, energy balance of droplets is represented by

$$\frac{dT_{d,i}}{dy} = -\frac{6h_{m,i}[Le_{f,i}(h_{s,i} - h_{av}) + (1 - Le_{f,i})(\omega_{s,i} - \omega_a)h_{fg,i}]}{U_{y,i}c_{pd,i}D_i\rho_w} - \frac{3T_{d,i}}{D_i}\frac{dD_i}{dy} \quad (95)$$

4.4.4 Thermal energy balance equations in the SCT

A mass balance in the control volume is given as:

$$\sum_i dm_{d,i} = m_a d\omega_a \quad (96)$$

The energy balance in the control volume of the SCT

$$m_a dh_{av,i} = \sum_i m_d dh_{d,i} + h_{d,i} dm_{d,i} \quad (97)$$

Rearranging using above two equations

$$dT_{d,i} = \sum_i \frac{m_a}{m_{d,i}} \left(\frac{dh_{av,i}}{c_{pd,i}} - T_{d,i} d\omega_a \right) \quad (98)$$

Energy balance at water and air interface yields

$$dq_i = \sum_i dq_{c,i} + dq_{e,i} \quad (99)$$

$$dq_i = \sum_i \left[h_i \left(T_{d,i} - T_a \right) + h_{m,i} h_{fg,i} \left(\omega_{s,i} - \omega_a \right) \right] dA_i \quad (100)$$

$$dq_i = \sum_i \left[\frac{h_i}{C_{pav,i}} \left(h_{s,i} - h_{av,i} \right) + \left(h_{m,i} - \frac{h_i}{c_{pav,i}} \right) h_{fg,i} \left(\omega_{s,i} - \omega_a \right) \right] dA_i \quad (101)$$

The enthalpy transfer to air stream is $dh_{av} = \frac{dq}{m_a}$

$$dh_{av,i} = \sum_i \frac{dq_i}{m_a} = \sum_i \frac{h_{m,i}}{m_a}\left[Le_{f,i}\left(h_{s,i} - h_{av,i}\right) + \left(1 - Le_{f,i}\right) h_{fg,i}\left(\omega_{s,i} - \omega_a\right)\right] dA_i \quad (102)$$

Where, $dA_i = \frac{m_{d,i}\pi D_i^2 dy}{M_{d,i} U_{y,i}} = \frac{6 m_{d,i} dy}{\rho_w D_i U_{y,i}}$

Now change in air temperature due to mass and heat transfer interaction can be expressed as:

$$\frac{dh_{av,i}}{dy} = \sum_i \left(\frac{m_{d,i}}{m_a}\right) \frac{6 h_{m,i}}{\rho_w D_i U_{y,i}}\left[Le_{f,i}\left(h_{s,i} - h_{av,i}\right) + \left(1 - Le_{f,i}\right) h_{fg,i}\left(\omega_{s,i} - \omega_a\right)\right] \quad (103)$$

$$\frac{dT_a}{dy} = \sum_i \left(\frac{m_{d,i}}{m_a}\right) \frac{6 h_{m,i}}{\rho_w D_i U_{y,i} C_{pav,i}} \left[\begin{array}{l} Le_{f,i}\left(h_{s,i} - h_{av,i}\right) + \\ \left(1 - Le_{f,i}\right) h_{fg,i}\left(\omega_{s,i} - \omega_a\right) \end{array}\right] - \frac{h_{fg,0}}{C_{pav,i}} \frac{dw_a}{dy} \quad (104)$$

4.4.5 Mass balance equation in the SCT

Mass balance equation for the control volume

$$\sum_i dm_{d,i} = m_a d\omega_a = \sum_i N_i \frac{dM_{d,i}}{dt} \quad (105)$$

Substituting, $N_i = \frac{m_{d,i} dy}{M_{d,i} U_{y,i}}$ and $M_{d,i} = \frac{1}{6}\pi D_i^3 \rho_w$,

$$dw_a = \sum_i \left(\frac{m_{d,i}}{m_a}\right) \frac{6 h_{m,i}}{\rho_w U_{y,i} D_i}\left(\omega_{s,i} - \omega_a\right) dy \quad (106)$$

The mass transfer associated with the control volume expressed as:

$$\frac{dw_a}{dy} = \sum_i \frac{m_{d,i} h_{m,i} A_{s,i}}{m_a M_{d,i} U_{y,i}} \left(\omega_{s,i} - \omega_a \right) \tag{107}$$

4.4.6 Equation for thermal efficiency

The thermal efficiency of SCT gives as:

$$\eta_{th} = \frac{\left(T_{d,in} - T_{d,m,i} \right) 100}{T_{d,in} - T_{wb,in}} \tag{108}$$

$$T_{d,m,i} = \frac{\sum_i m_{d,i} T_{d,i}}{\sum_i m_{d,i}} \tag{109}$$

Where,

4.4.7 Droplet trajectory equation

Droplet trajectory expressed in terms of the horizontal and vertical components of velocity.

$$\frac{dx}{dy} = \frac{U_{x,i}}{U_{y,i}} \tag{110}$$

4.5 Mathematical Model for 2-D Multi Droplet Counter flow SCT

Mono and multi droplet mathematical model for counter flow SCT which used for industrial and air cooling application is given below.

4.5.1 Conservation of mass for water droplet

A control volume for air-water droplet for counter flow SCT is shown in Figure 4.12. Conservation of mass for $'i^{th}'$ category of water droplet can be written as:

$$\frac{d(D_i)}{dy} = -\frac{2h_{m,i}}{U_{y,i}\rho_w}(\omega_{s,i} - \omega_a) \tag{111}$$

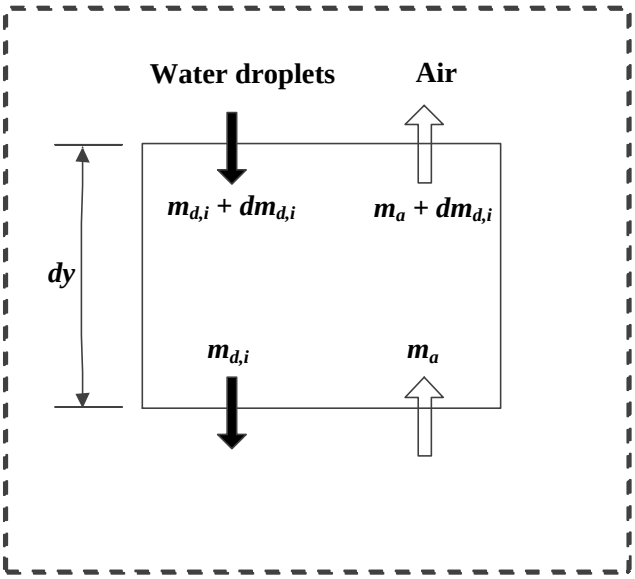

Figure 4.12 Control volume of $'i$ th$'$ category of water droplet and air for counter flow SCT

4.5.2 Conservation of momentum for water droplet

Distribution of multi-diameter water droplets are based on Rosin Rammler function.

Rosin Rammler function, $$RR = 1 - \exp\left(-\left(\frac{D}{D_m}\right)^{uc}\right) \tag{112}$$

Where $'D_m'$ is the characteristic droplet size and $'uc'$ is uniformity constant.

The gravity forces, buoyancy forces and the resistive forces (drag forces) acting on the droplet moving in a downward direction with a velocity 'U_i'. Resultant velocity 'W_i' of the category 'i', droplet and its inclination angle 'θ' from horizontal is shown in Figure 4.13, and it is given as:

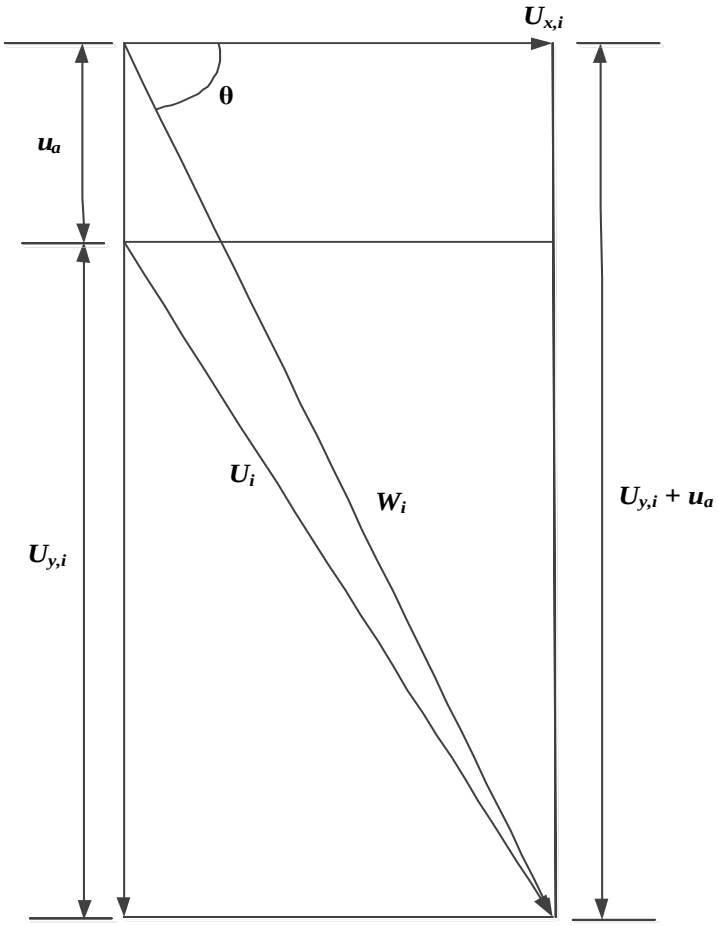

Figure 4.13 Velocity vector diagram of 'i th' category of water droplet and air for counter flow SCT

$$W_i = \sqrt{(U_{y,i} + u_a)^2 + U_{x,i}^2} \tag{113}$$

For a droplet of the category 'i', Variation in the momentum of the droplet in horizontal and vertical direction with tower height expressed as:

$$\frac{dU_{x,i}}{dy} = -\left[\frac{3(C_{d,i}\rho_a W_i U_{x,i})}{4D_i \rho_w U_{y,i}}\right] - \frac{3U_{x,i}}{D_i}\frac{dD_i}{dy} \tag{114}$$

$$\frac{dU_{y,i}}{dy} = \left[g(\rho_w - \rho_a) - \frac{3(C_{d,i}\rho_a W_i (U_{y,i} + u_a))}{4D_i}\right]\frac{1}{\rho_w U_{y,i}} - \frac{3U_{y,i}}{D_i}\frac{dD_i}{dy} \tag{115}$$

4.5.3 Conservation of energy for water droplet

The water droplets lose its sensible heat and latent heat to the air. Energy balance equation for the 'i th' category of droplet shown in Figure 4.14.

$$\frac{dT_{d,i}}{dy} = -\frac{6h_{m,i}[Le_{f,i}(h_{s,i} - h_{av}) + (1 - Le_{f,i})(\omega_{s,i} - \omega_a)h_{fg,i}]}{U_{y,i}c_{pd,i}D_i\rho_w} - \frac{3T_{d,i}}{D_i}\frac{dD_i}{dy} \tag{116}$$

$$T_{d,m} = \frac{\sum_i \left(m_{d,i}\right)T_{d,i}}{\sum_i m_{d,i}} \tag{117}$$

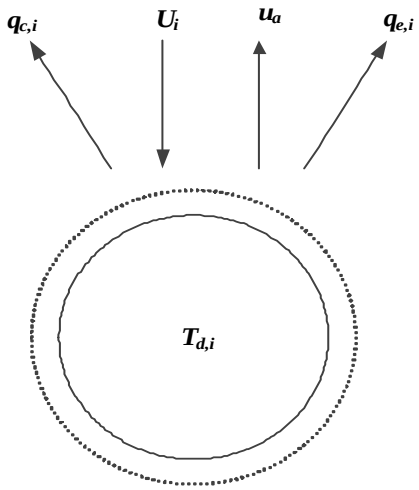

Figure 4.14 Energy exchange of 'i th' category of water droplet and air for counter flow SCT

4.5.4 Thermal energy balance equations in the SCT

Variation in air temperature due to mass and heat transfer interaction for the 'i^{th}' droplet can be given as:

$$\frac{dT_a}{dy} = \sum_i \left(\frac{m_{d,i}}{m_a} \right) \frac{6h_{m,i}}{\rho_w D_i U_{y,i} C_{pav,i}} \left[Le_{f,i} \left(h_{s,i} - h_{av,i} \right) + \left(1 - Le_{f,i} \right) h_{fg,i} \left(\omega_{s,i} - \omega_a \right) \right] - \frac{h_{fg,0}}{C_{pav,i}} \frac{dw_a}{dy} \tag{118}$$

4.5.5 Mass balance equation in the SCT

The mass transfer associated with the control volume expressed as:

$$\frac{dw_a}{dy} = \sum_i \frac{m_{d,i} h_{m,i} A_{s,i}}{m_a M_{d,i} U_{y,i}} \left(\omega_{s,i} - \omega_a \right) \tag{119}$$

4.5.6 Equation for thermal efficiency

The thermal efficiency of SCT gives as:

$$\eta_{th} = \frac{\left(T_{d,in} - T_{d,m,out} \right) 100}{T_{d,in} - T_{wb,in}} \tag{120}$$

Where, $T_{d,m,i} = \dfrac{\sum_i m_{d,i} T_{d,i}}{\sum_i m_{d,i}}$ (121)

4.5.7 Droplet Trajectory Equation

Droplet trajectory expressed in terms of the horizontal and vertical components of velocity.

$$\frac{dx}{dy} = \frac{U_{x,i}}{U_{y,i}} \tag{122}$$

4.6 Exergy Formulation of SCT

Exergy of water is given as:

$$X_{d,i} = m_{d,i}\left((h_{fd,i} - h_{g0}) - T_0(s_{fd,i} - s_{g0}) - R_v \ln(\phi_0)\right) \tag{123}$$

Exergy of air due to the convective heat transfer

$$X_c = \sum_i m_a \left[\begin{array}{l} c_{pa}\left(T_a - T_0\right) - T_0\, c_{pa} \ln\left(\frac{T_a}{T_0}\right) + \\ \omega_a \left\{ c_{pv}\left(T_a - T_0\right) - T_0\, c_{pv} \ln\left(\frac{T_a}{T_0}\right) \right\} \end{array} \right] \tag{124}$$

Exergy of air due to evaporative heat transfer

$$X_e = \sum_i m_a \left[\begin{array}{l} R_a T_0 \ln\left(\frac{1+1.608\omega_{a0}}{1+1.608\omega_a}\right) + \\ \omega_a R_v T_0 \ln\left(\frac{\omega_a(1+1.608\omega_{a0})}{\omega_{a0}(1+1.608\omega_a)}\right) \end{array} \right] \tag{125}$$

Total exergy of a system is given as:

$$X_t = \sum_i (X_{d,i} + X_c + X_e) \tag{126}$$

The total exergy destruction 'I' for discrete height of the tower is given as:

$$I = X_{t,y(j)} - X_{t,y(j+1)} \tag{127}$$

Where, $y(j+1) - y(j) = dy$

4.6.1 Second law efficiency of the SCT

The SLE of SCT is given as:

$$\eta_{II} = \frac{X_{t,out} \times 100}{X_{t,in}} \tag{128}$$

4.7 Boundary Conditions

The boundary conditions required for the solution of above formulation include tower geometry, spray characteristics, inlet air and multi droplets diameters. Tower geometry includes height, cross-section area, and shape of the tower. Spray characteristics are droplet velocity and temperature, the angle of projection, ten different droplets diameters, characteristic droplet size and uniformity constant. The initial air conditions required are air velocity, flow rate, relative humidity and different DBT.

Chapter 5 RESULTS AND DISCUSSION

5.1 Model Validation

The experimental data of a downdraft SCT was used for model validation. The model prediction with test data and test conditions is given in Table 5.1. Figures 5.1 - 5.4 show the comparison between the total data points of the outlet DBT of air and outlet specific humidity of air obtained from the experiment and those obtained from the MATLAB and CFD model for mono and multi droplet. It can be seen that the majority of mathematical and CFD data fall within ±10% of the experimental model.

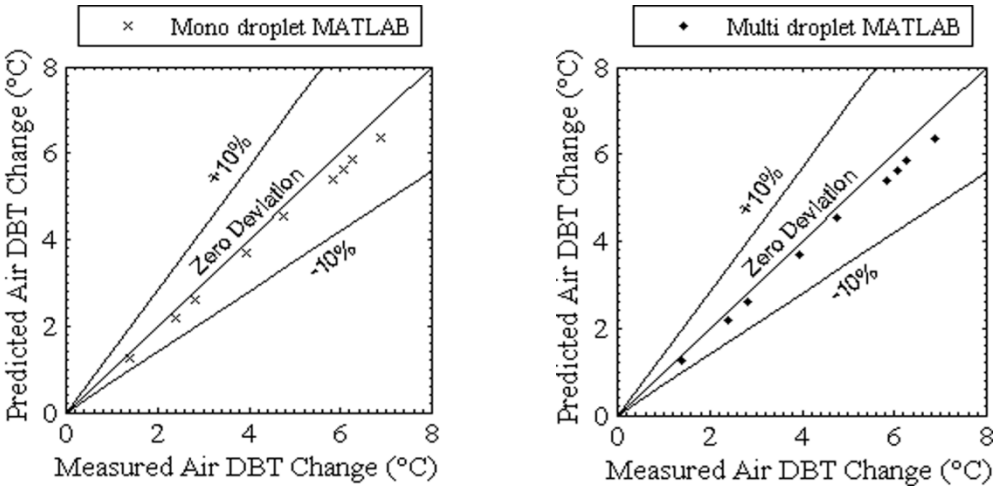

(a) (b)

Figure 5.1 Comparison of experimental and MATLAB data for air DBT (a) mono droplet diameter, (b) multi droplet diameter

Table 5.1 Comparison of experimental results with results of model predictions, (a) 2-D mono droplet model MATLAB results, (b) 2-D multi droplet model MATLAB results, (c) 3-D mono droplet model CFD results, (d) 3-D multi droplet model CFD results for different test conditions

Test No.	1	2	3	4	5	6	7	8	9
Experimental Inlet Parameters									
Inlet air DBT, (˚C)	35.50	35.50	35.30	35.50	35.50	35.30	35.50	35.50	35.30
Inlet air relative humidity, (%)	46.30	46.30	46.00	46.30	46.30	46.00	46.30	46.30	46.00
Inlet air velocity, (m/s)	0.35	0.35	0.35	0.66	0.66	0.66	1.21	1.21	1.21
Inlet air volume flow rate, (m^3/s)	0.10	0.10	0.10	0.19	0.19	0.19	0.35	0.35	0.35
Nozzle pressure, bar	2	3	4	2	3	4	2	3	4
Inlet water droplet temp., (˚C)	31.50	31.50	31.90	31.50	31.50	31.90	31.50	31.50	31.90
Inlet diameter of water droplet, (m)	420.75	311.31	204.84	420.75	311.31	204.84	420.75	311.31	204.84
Inlet water droplet velocity, (m/s)	17.70	21.73	25.07	17.70	21.73	25.08	17.70	21.73	25.08
water to air mass flow ratio, (kg/kg)	0.46	0.57	0.66	0.24	0.30	0.34	0.13	0.16	0.19
Nozzle spray angle	89˚	90˚	91˚	89˚	90˚	91˚	89˚	90˚	91˚
Experimental results									
Outlet air DBT (˚C)	31.81	29.87	29.43	33.30	30.96	28.96	34.23	32.89	29.91
Outlet air sp. humidity (kg/kg of dry air)	0.023103	0.025171	0.026379	0.020878	0.022533	0.025185	0.019503	0.020836	0.022981
2-D mono droplet model predicted MATLAB results									
Outlet DBT, (˚C)	31.55	29.43	29.03	33.11	30.74	28.96	34.12	32.67	29.65
Error in outlet air DBT (%)	7.05	7.82	6.81	8.64	4.85	8.20	8.66	8.43	8.53
Outlet air sp. humidity (kg/kg of dry air)	0.022732	0.024684	0.025777	0.020637	0.022828	0.024476	0.019356	0.020601	0.022643
Error in outlet air specific humidity (%)	6.64	6.36	6.56	7.17	5.88	8.88	7.38	7.08	5,85
2-D multi droplet model predicted MATLAB results									
Outlet DBT, (˚C)	31.60	29.54	29.14	33.18	31.11	28.96	34.16	32.71	29.79
Error in outlet air DBT (%)	5.69	5.86	4.94	5.45	3.30	6.47	5.51	6.90	5.94
Outlet air sp. humidity (kg/kg of dry air)	0.022865	0.024850	0.025900	0.020691	0.022734	0.024630	0.019396	0.020669	0.022754
Error in outlet air sp. humidity (%)	4.26	4.20	5.22	5.56	4.01	6.96	5.37	5.03	3.93
3-D mono droplet model predicted CFD results									
Outlet DBT, (˚C)	31.65	29.64	29.22	33.21	30.85	28.96	34.18	32.76	29.89
Error in outlet air DBT (%)	4.34	4.09	3.58	4.09	2.42	3.94	3.94	4.98	4.08
Outlet air sp. humidity (kg/kg of dry air)	0.022934	0.024942	0.026072	0.0200771	0.022727	0.024893	0.019433	0.020730	0.022814
Error in outlet air sp. humidity (%)	3.02	2.99	3.34	3.18	3.87	3.66	3.50	3.19	2.89
3-D multi droplet model predicted CFD results									
Outlet DBT, (˚C)	31.71	29.74	29.31	33.25	30.88	28.96	34.20	32.81	29.98
Error in outlet air DBT (%)	2.71	2.31	2.04	2.27	1.76	2.37	2.36	3.07	2.41
Outlet air sp. humidity (kg/kg of dry air)	0.022954	0.025066	0.026176	0.020806	0.022611	0.025067	0.019476	0.020768	0.022874
Error in outlet air sp. humidity (%)	2.67	1.37	2.21	2.14	1.55	1.48	1.34	2.05	1.85

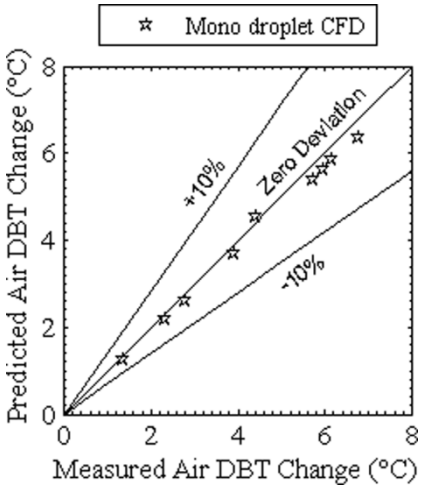

(c)

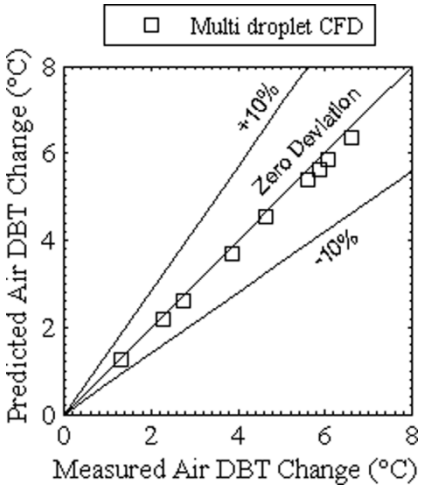

(d)

Figure 5.2 Comparison of experimental and CFD data for air DBT (a) mono droplet diameter, (b) multi droplet diameter

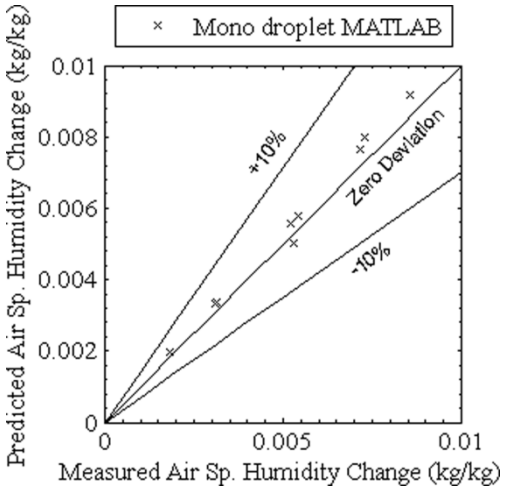

(a)

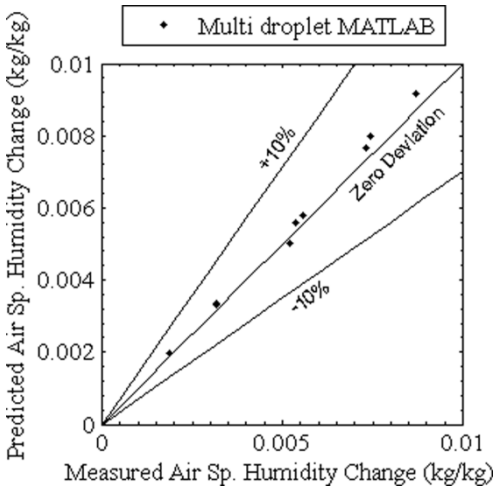

(b)

Figure 5.3 Comparison of experimental and MATLAB data for Sp. Humidity of air (a) mono droplet diameter, (b) multi droplet diameter

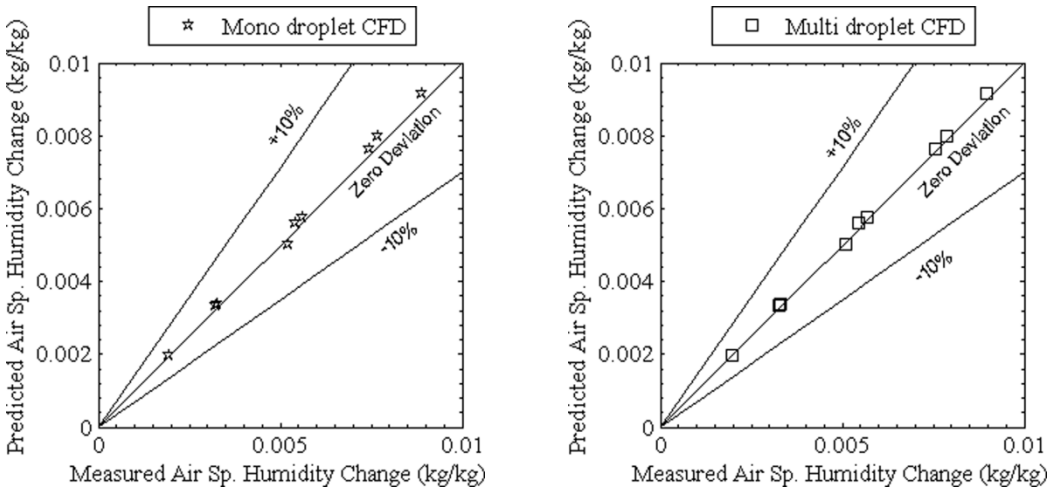

(a) (b)

Figure 5.4 Comparison of experimental and CFD data for Sp. Humidity of air (a) mono droplet diameter, (b) multi droplet diameter

5.2 Parametric Study

5.2.1 SCT for industrial application

SCT can be used for industrial application where water used for cooling of different equipment, is collected in hot condition and after cooling the same using SCT can be reused for cooling purposes. Since the use of SCT in industries remain throughout the year. In 2-D and 3-D modelling, DBT of air was varied from 24-48 ˚C, relative humidity 20-80%, water temperature 52-58 ˚C, air volume flow rate 11.11×10^{-2} m^3/s, droplet velocity 20 m/s, droplet angle of projection at inlet 45˚ and RLG varies from 0.5 to 2 for mono and multi droplet model to represent the real life situation and different weather conditions. In mono droplet model the diameter of droplet taken from 250-2000 µm. However, in multi droplet model droplets of ten different diameters used at a time for the study, and its distribution based on Rosin Rammler function. The inlet diameters of ten different droplets were varied from 31.81-318.18 µm (31.81, 63.63, 95.45, 127.27, 159.09, 190.91, 222.72, 254.54,

286.36, 318.18 µm), 63.63- 636.36 µm (63.63, 127.27, 190.91, 254.54, 318.18, 381.82, 445.45, 509.09, 572.73, 636.36 µm), 127.27- 1272.7 µm (127.27, 254.54, 381.81, 509.08, 636.35, 763.62, 890.89, 1018.16, 1145.43, 1272.70 µm), 190.91-1909.10 µm (190.91, 381.82, 572.73, 763.64, 954.55, 1145.46, 1336.37, 1527.28, 1718. 19, 1909.10 µm), and 254.55-2545.50 µm (254.55, 509.10, 763.65, 1018.20, 1272.75, 1527.30, 1781.85, 2036.40, 2290.95, 2545.50 µm). The distance between the spray water inlets to the bottom of the tower (tower height) was 1.25 m (along with the direction of y-coordinate), and tower diameter was 0.61 m. Effect of variation in inlet water temperature, air DBT, air relative humidity, RLG, and droplet diameter on various performance parameters were studied, and exit conditions were shown as a result. The solution procedure has been outlined in Figure 5.5. Inlet parameters and parametric range for mono and multi droplet SCT are shown in Table 5.2 and 5.3.

Table 5.2 Inlet parameters for mono droplets SCT used for industrial application

Inlet Parameters	**Parameters Range**
Diameter (µm)	250, 500, 1000, 1500, 2000
DBT of Air (˚C)	24, 30, 36, 42, 48
Air Relative Humidity (%)	20, 35, 50, 65, 80
Water Temperature (˚C)	50, 52, 54, 56, 58
RLG	0.5, 1.0, 1.25, 1.5, 2.0

Table 5.3 Inlet parameters for multi droplets SCT used for industrial application

Inlet Parameters	Parameters Range
Diameter (μm)	31.81-318.18, 63.63-636.36, 127.27- 1272.7, 190.91-1909.10, 254.55-2545.5
DBT of Air (˚C)	24, 30, 36, 42, 48
Air Relative Humidity (%)	20, 35, 50, 65, 80
Water Temperature (˚C)	50, 52, 54, 56, 58
RLG	0.5, 1.0, 1.25, 1.5, 2.0

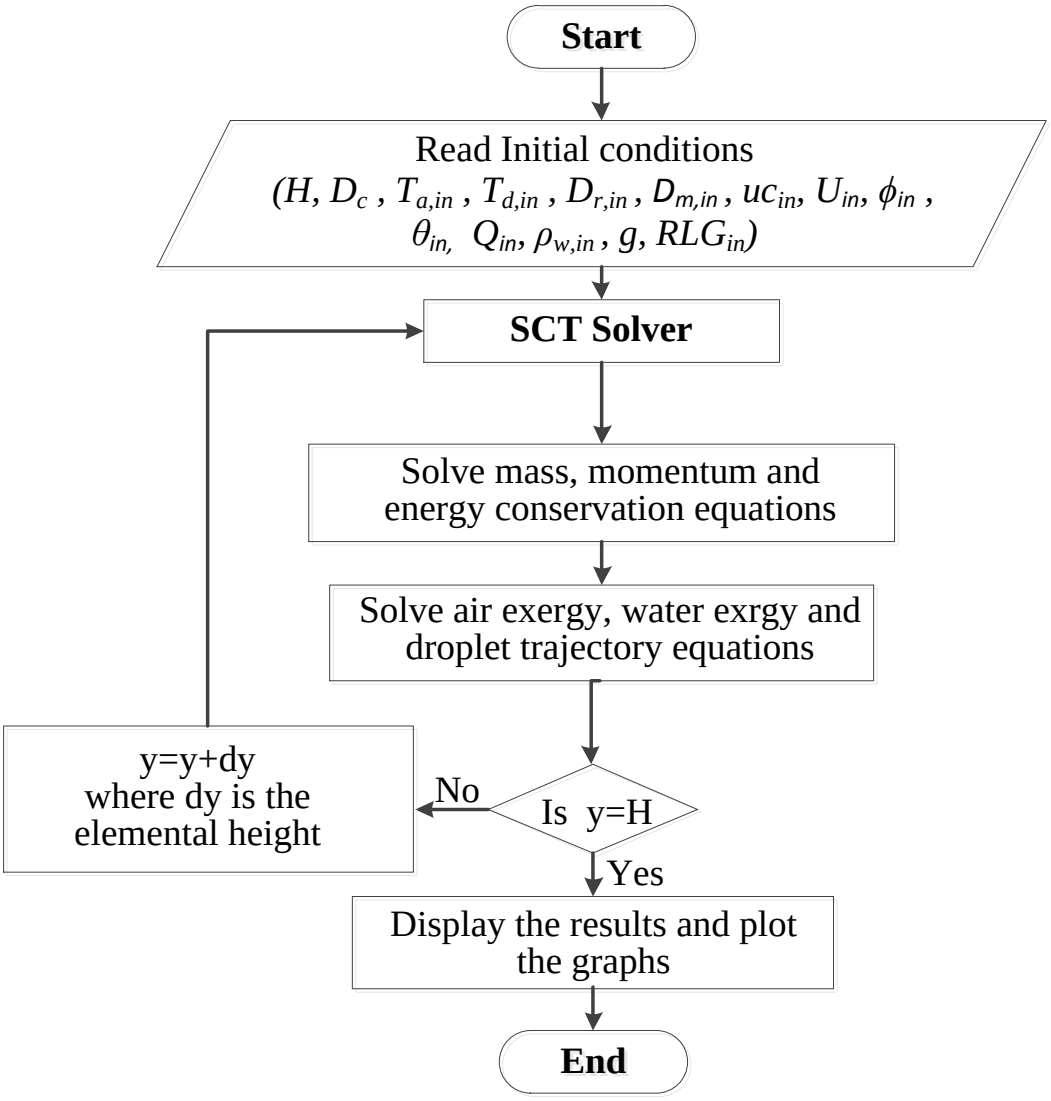

Figure 5.5 Flow chart for the calculation of water and air conditions in SCT

5.2.2 SCT for Air Cooling Application

Use of SCT for space cooling is another application such as cooling of hotels, malls, laboratories etc. In these applications air DBT is higher and need to bring down to human comfort by cooling of air in SCTs. Initial conditions used for the mathematical simulation for air cooling application of 2-D and 3-D SCT are DBT of air varies from 36-44 ˚C, relative humidity 20-40%, water temperature 28-36 ˚C, air volume flow rate 11.11×10^{-2} m^3/s, droplet velocity from 10 m/s, droplet angle of projection at inlet 45˚ and RLG varies from 0.1 to 1.0 for mono and multi droplet model. In mono droplet model the diameter of droplet taken from 200-1000 µm. But in multi droplet model droplets of ten different diameters used at a time for the study, and its distribution based on Rosin Rammler function. Inlet diameters of ten different droplets varies from 25.45 - 254.54 µm (25.45, 50.90, 76.36, 101.81, 127.27, 152.72, 178.18, 203.63, 229.09, 254.54 µm), 50.90 - 509.09 µm (50.90, 101.81, 152.72, 203.63, 254.54, 305.45, 356.36, 407.27, 458.18, 509.09 µm), 76.36 - 763.64 µm (76.36, 152.72, 229.09, 305.45, 381.82, 458.18, 534.54, 610.91, 687.27, 763.64 µm), 101.81 - 1018.18 µm (101.81, 203.63, 305.45, 407.27, 509.09, 610.91, 712.73, 814.54, 916.36, 1018.18 µm), 127.27-1272.73 µm (127.27, 254.54, 381.82, 509.09, 636.36, 763.64, 890.91, 1018.18, 1145.46, 1272.73 µm). The dimension of SCT was same as in section 5.2.1, and similarly the effect of variation in inlet water temperature, air DBT, air relative humidity, RLG, and droplet diameter on various performance parameters were studied, and exit conditions were shown as a result. The solution procedure has been outlined in Figure 5.5. Inlet parameters and parametric range for mono and multi droplet SCT are shown in Tables 5.4 and 5.5.

Table 5.4 Parametric study of mono droplets SCT used for air cooling application

Inlet Parameters	Parameters Range
Diameter (µm)	200, 400, 600, 800, 1000
DBT of Air (˚C)	36, 38, 40, 42, 44
Air Relative Humidity (%)	20, 25, 30, 35, 40
Water Temperature (˚C)	28, 30, 32, 34, 36
RLG	0.5, 0.75, 1.0, 1.25, 1.51.0

Table 5.5 Parametric study of multi droplets SCT used for air cooling application

Inlet Parameters	Parameters Range
Diameter (µm)	25.45 - 254.54, 50.90 - 509.09, 76.36 - 763.64, 101.81 - 1018.18, 127.27-1272.73
DBT of Air (˚C)	36, 38, 40, 42, 44
Air Relative Humidity (%)	20, 25, 30, 35, 40
Water Temperature (˚C)	28, 30, 32, 34, 36
RLG	0.5, 0.75, 1.0, 1.25, 1.5

5.2.3 Cases studied for Industrial and Air Cooling SCT

Two dimensional (2-D) and three dimensional (3-D) parallel flow and counter flow mono and multi droplet SCT was categorized into sixteen cases based on different configurations and applications. Each case is symbolized in letters; first letter indicates application area, i.e. ‘H’ represents industrial application and ‘N’ for air cooling application. The second letter represents types of flow, i.e. ‘P’ for parallel

flow and ‘C’ for counter flow. Similarly the third letter represents a number of drops, i.e. ‘O’ for mono droplet and ‘U’ for multi droplet, and the fifth letter for the type of work, i.e. ‘M’ for the mathematical model and ‘C’ for CFD model. These sixteen cases are:

(i) Two-dimensional parallel flow mono droplet SCT for industrial application (HPOM).

(ii) Two-dimensional parallel flow multi droplets SCT for industrial application (HPUM).

(iii) Three-dimensional parallel flow mono droplet SCT for industrial application (HPOC).

(iv) Three-dimensional parallel flow multi droplets SCT for industrial application (HPUC).

(v) Two-dimensional counter flow mono droplet SCT for industrial application (HCOM).

(vi) Two-dimensional counter flow multi droplets SCT for industrial application (HCUM).

(vii) Three-dimensional counter flow mono droplet SCT for industrial application (HCOC).

(viii) Three-dimensional counter flow multi droplets SCT for industrial application (HCUC).

(ix) Two-dimensional parallel flow mono droplet SCT for air cooling application (NPOM).

(x) Two-dimensional parallel flow multi droplets SCT for air cooling application (NPUM).

(xi) Three-dimensional parallel flow mono droplet SCT for air cooling application (NPOC).

(xii) Three-dimensional parallel flow multi droplets SCT for air cooling application (NPUC).

(xiii) Two-dimensional counter flow mono droplet SCT for air cooling application (NCOM).

(xiv) Two-dimensional counter flow multi droplets SCT for air cooling application (NCUM).

(xv) Three-dimensional counter flow mono droplet SCT for air cooling application (NCOC).

(xvi) Three-dimensional counter flow multi droplets SCT for air cooling application (NCUC).

Five different inlet parameters i.e. inlet water temperature, air DBT, air relative humidity, water to air mass flow ratio and droplet diameters was considered. Summary of parametric studies are shown in Figure 5.6. Out of these sixteen cases, eight cases belong to industrial application and remaining eight cases used for air cooling application, and their comparison is also presented. Mathematical codes used to differentiate different cases are also designated by five letters and one digit. First four letters are denoted above, the last letter is for variation of particular parameters, i.e. ‘D’ for water temperature, ‘A’ for air DBT, ‘H’ for relative humidity, ‘L’ for RLG and ‘R’ for droplet diameter. Digit represent total five variations in particular parameters.

MATLAB and CFD results show variation of exit parameters (i.e. air DBT, air specific humidity, water temperature, makeup water required, thermal efficiency, convective exergy of air, evaporative exergy of air, total exergy of air, water exergy, total exergy of system, exergy destruction and SLE) by varying inlet droplet diameter, air DBT, air relative humidity, water temperature and RLG. Similarly, results of all eight cases of industrial application are compared and plotted. Optimization of tower height has also been done for different performance parameters.

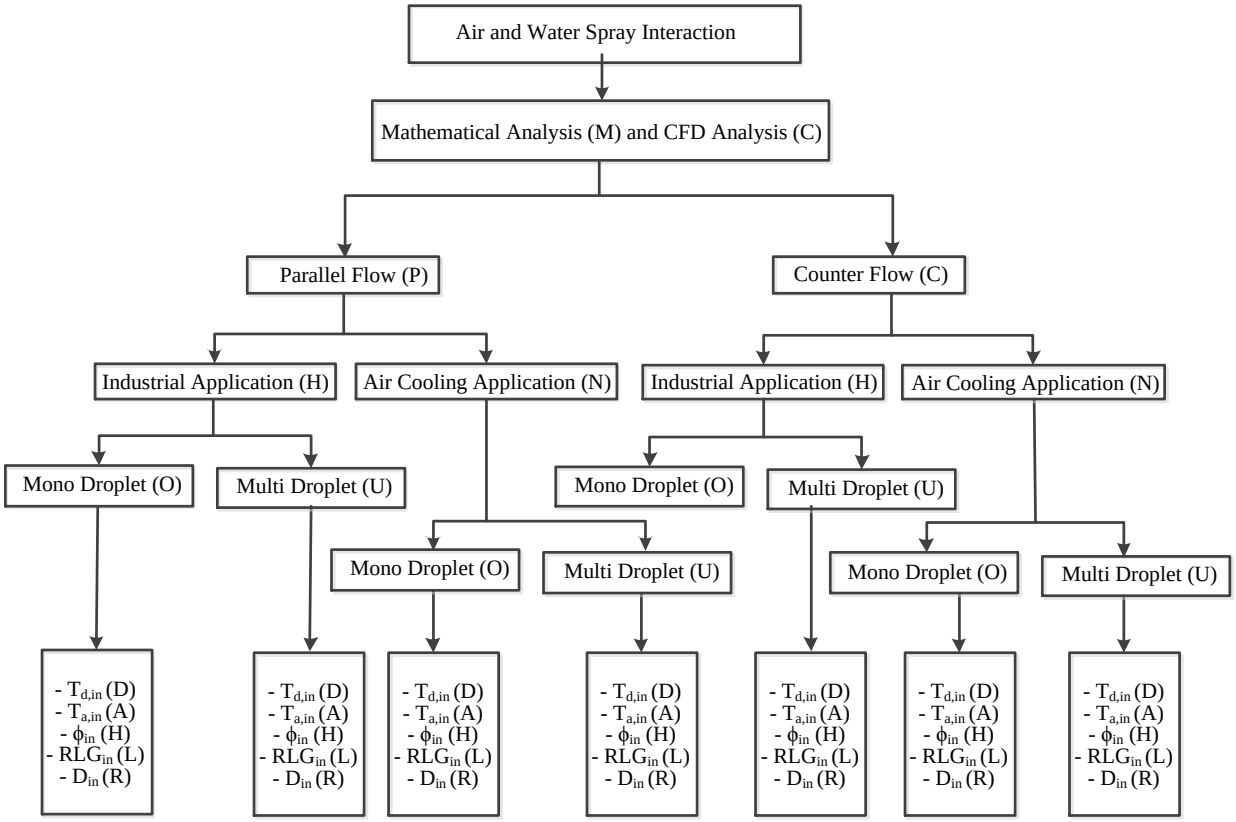

Figure 5.6 Flow chart of sixteen cases of industrial and air cooling application

5.3 Two Dimensional Parallel Flow Mono Droplet SCT for Industrial Application

This study is based on 2-D mono droplet parallel flow MATLAB model to determine the effect of variation in inlet droplet diameters, water temperatures, air DBT, relative humidity of air and RLG on outlet parameters. The schematic diagram of 2-D parallel flow SCT shown is in Figure 1.1. Initial conditions used for computer simulation given in Table 5.2.

5.3.1 Effect of variation in initial droplets diameter (HPOMR)

Table 5.6 shows the effect of change in exit air DBT, air specific humidity, water temperature, makeup water required, thermal efficiency, convective exergy of air, evaporative exergy of air, total exergy of air, water exergy, total exergy of the system, exergy destruction, and SLE at constant inlet air DBT (36 ˚C), air relative humidity (65%), water temperature (56 ˚C), and RLG (0.5). As droplet diameter increased from 250 µm to 2000 µm, exit air DBT and water temperature increased and exited specific humidity, makeup water required and thermal efficiency of SCT decreased because heat and mass transfer between air and water droplet decreased. Total exergy of air is the sum of convective and evaporative exergy of air. This total exergy of air and exergy destruction decreased as inlet droplet diameter increased. Exergy of water, exergy of system and SLE increased with increase in the droplet diameter because as droplet diameter increased heat and mass transfer between air and water decreased.

Table 5.6 Effect of variation in inlet droplet diameter (HPOMR)

1	2	3	4	5	6	7	8	9	10	11	12	13	14
Code	D_{in} (μm)	$T_{a,out}$ (˚C)	$\omega_{a,out}$ (kg_w/kg_a)	$T_{d,out}$ (˚C)	$m_{d,l}$ (kg/s)	η_{th} (%)	$X_{c,out}$ (W)	$X_{e,out}$ (W)	$X_{a,out}$ (W)	$X_{d,out}$ (W)	$X_{t,out}$ (W)	I_t (W)	η_{II} (%)
HPOMR-1	**250**	**38.90**	**0.044**	**38.89**	**0.0023**	**68.19**	**1.52**	**103.72**	**105.24**	**3757.68**	**3862.92**	**871.33**	**81.60**
HPOMR-2	**500**	**44.18**	**0.0373**	**44.17**	**0.0018**	**47.15**	**1.38**	**81.37**	**82.75**	**4006.29**	**4089.04**	**645.21**	**86.37**
HPOMR-3	**1000**	**50.3**	**0.0305**	**50.29**	**0.0014**	**22.76**	**1.21**	**29.08**	**30.29**	**4342.18**	**4372.47**	**361.78**	**92.36**
HPOMR-4	**1500**	**52.66**	**0.0278**	**52.65**	**0.0011**	**13.35**	**1.17**	**11.81**	**12.98**	**4474.31**	**4487.29**	**246.96**	**94.78**
HPOMR-5	**2000**	**53.57**	**0.0269**	**53.56**	**0.0009**	**9.72**	**0.77**	**5.67**	**6.44**	**4536.61**	**4543.05**	**191.20**	**95.96**

5.3.2 Effect of variation in inlet Water Temperature (HPOMD)

The effect of variation of inlet water temperature from 50 to 58 ˚C on outlet air DBT, air specific humidity, water temperature, makeup water required, thermal efficiency, convective exergy of air, evaporative exergy of air, total exergy of air, water exergy, total exergy of system, exergy destruction and SLE at constant inlet air DBT (36 ˚C), air relative humidity (65%), droplet diameter (250 μm), and RLG (0.5) are given in Table 5.7. Table shows as an inlet water temperature increased exit air DBT, air specific humidity, water temperature, thermal efficiency and makeup water required increased. It also shows that when the temperature of inlet water is 58 ˚C, maximum cooling of the droplet achieved (18.88 ˚C) as the high-temperature difference between water and air (keeping air temperature constant), increases sensible cooling as well as evaporative cooling. As inlet water droplet temperature increased, the specific humidity of air increased due to increase in water temperature as more water vapour added to the air. Table 5.7 also shows that due to increased in inlet water temperature more quantity of water vapour mixed with air and increased total exergy of air. The exergy destruction of system increases and SLE decreases by increasing the inlet water droplet temperature. Depicted destruction in total exergy of

a system is more for higher temperature droplet because it transfers water content to air faster than lower temperature droplets.

Table 5.7 Effect of variation in inlet water temperature (HPOMD)

1	2	3	4	5	6	7	8	9	10	11	12	13	14
Code	$T_{d,in}$ (˚C)	$T_{a,out}$ (˚C)	$\omega_{a,out}$ (kg_w/kg_a)	$T_{d,out}$ (˚C)	$m_{d,l}$ (kg/s)	η_{th} (%)	$X_{c,out}$ (W)	$X_{e,out}$ (W)	$X_{a,out}$ (W)	$X_{d,out}$ (W)	$X_{t,out}$ (W)	I_t (W)	η_{II} (%)
HPOMD-1	**50**	**37.10**	**0.0398**	**37.09**	**0.0017**	**67.63**	**0.19**	**66.27**	**66.46**	**3731.85**	**3798.31**	**608.06**	**86.20**
HPOMD-2	**52**	**37.72**	**0.0412**	**37.71**	**0.0019**	**67.76**	**0.50**	**77.80**	**78.30**	**3740.70**	**3819.00**	**691.36**	**84.67**
HPOMD-3	**54**	**38.36**	**0.0426**	**38.35**	**0.0021**	**67.78**	**0.94**	**90.29**	**91.23**	**3749.31**	**3840.54**	**779.14**	**83.13**
HPOMD-4	**56**	**38.90**	**0.044**	**38.89**	**0.0023**	**68.19**	**1.52**	**103.72**	**105.24**	**3757.68**	**3862.92**	**871.33**	**81.60**
HPOMD-5	**58**	**39.47**	**0.0455**	**39.47**	**0.0024**	**68.40**	**2.21**	**118.10**	**120.31**	**3765.84**	**3886.15**	**967.86**	**80.06**

5.3.3 Effect of variation in inlet air DBT (HPOMA)

DBT of air varied from 24 - 48 ˚C. Table 5.8 shows changes in exit parameters at constant inlet air relative humidity (65%), water temperature (56 ˚C), droplet diameter (250 µm) and RLG (0.5). Table shows exit air DBT, specific humidity and droplet temperatures increase relatively as inlet air DBT increases. It also shows 24 ˚C DBT air produced maximum cooling, and it cools down water droplet up to 22.50 ˚C. Table 5.8 also depicts that with increasing inlet air DBT temperature, the thermal efficiency of SCT increases because air wet bulb temperature increase with increasing the inlet air DBT at constant relative humidity. The convective exergy of air, evaporative exergy of air, total exergy of air, exergy of water and total exergy of system decreased with increased the inlet air DBT temperature. The SLE of the system increased with increased in the initial air DBT because exergy destruction of the system was decreased with increasing the inlet air DBT.

Table 5.8 Effect of variation in inlet air DBT (HPOMA)

1	2	3	4	5	6	7	8	9	10	11	12	13	14
Code	$T_{a,in}$ (˚C)	$T_{a,out}$ (˚C)	$\omega_{a,out}$ (kg_w/kg_a)	$T_{d,out}$ (˚C)	$m_{d,l}$ (kg/s)	η_{th} (%)	$X_{c,out}$ (W)	$X_{e,out}$ (W)	$X_{a,out}$ (W)	$X_{d,out}$ (W)	$X_{t,out}$ (W)	I_t (W)	η_{II} (%)
HPOMA-1	**24**	**34.22**	**0.0321**	**34.21**	**0.0028**	**59.39**	**20.55**	**214.54**	**235.09**	**3985.4**	**4220.49**	**1151.47**	**78.57**
HPOMA-2	**30**	**36.40**	**0.0373**	**36.39**	**0.0026**	**62.95**	**7.72**	**154.45**	**162.17**	**3880.8**	**4042.97**	**1005.99**	**80.08**
HPOMA-3	**36**	**38.90**	**0.044**	**38.89**	**0.0023**	**68.19**	**1.52**	**103.72**	**105.24**	**3757.68**	**3862.92**	**871.33**	**81.60**
HPOMA-4	**42**	**41.76**	**0.0528**	**41.75**	**0.0021**	**77.83**	**1.49**	**63.27**	**64.76**	**3660.09**	**3724.85**	**701.56**	**84.15**
HPOMA-5	**48**	**46.83**	**0.0641**	**46.84**	**0.0018**	**86.82**	**1.42**	**33.4**	**34.82**	**3605.65**	**3640.47**	**583.75**	**86.18**

5.3.4 Effect of variation in inlet Air Relative Humidity (HPOMH)

This study based on the variation of inlet relative humidity from 20% to 80%. Table 5.9 shows changes in exit parameters at constant inlet air DBT (36 ˚C), water temperature (56 ˚C), droplet diameter (250 μm) and RLG (0.5). Table also shows exit air DBT, specific humidity, droplet temperature and thermal efficiency of SCT increased with increase in the air relative humidity. Table 5.9 also shows that air with 20% relative humidity produces maximum cooling, i.e. up to 21.97 ˚C and at 80% relative humidity gives maximum efficiency because as the relative humidity of air increased evaporative heat transfer between air and water droplet decreased. It can also see that as the relative humidity of air increases the change in total exergy of air, exergy of water and SLE of SCT decreased. As relative humidity of air increases, the destruction in total exergy of a system is relatively less because low relative humidity air absorbs more amount of water from droplets.

Table 5.9 Effect of variation in inlet air relative humidity (HPOMH)

1	2	3	4	5	6	7	8	9	10	11	12	13	14
Code	ϕ_{in} (%)	$T_{a,out}$ (˚C)	$\omega_{a,out}$ (kg_w/kg_a)	$T_{d,out}$ (˚C)	$m_{d,l}$ (kg/s)	η_{th} (%)	$X_{c,out}$ (W)	$X_{e,out}$ (W)	$X_{a,out}$ (W)	$X_{d,out}$ (W)	$X_{t,out}$ (W)	I_t (W)	η_{II} (%)
HPOMH-1	**20**	**34.72**	**0.0333**	**34.71**	**0.0033**	**58.76**	**0.06**	**431.29**	**431.35**	**13654.43**	**14085.78**	**1303.41**	**91.53**
HPOMH-2	**35**	**36.18**	**0.0368**	**36.17**	**0.003**	**61.66**	**0.11**	**249.65**	**249.76**	**8944.14**	**9193.90**	**1124.67**	**89.10**
HPOMH-3	**50**	**37.58**	**0.0403**	**37.57**	**0.0027**	**64.71**	**0.35**	**157.86**	**158.21**	**5952.05**	**6110.26**	**986.17**	**86.10**
HPOMH-4	**65**	**38.90**	**0.044**	**38.89**	**0.0023**	**68.19**	**1.52**	**103.72**	**105.24**	**3757.68**	**3862.92**	**871.33**	**81.60**
HPOMH-5	**80**	**40.17**	**0.0476**	**40.16**	**0.0021**	**72.20**	**3.36**	**69.25**	**72.61**	**2026.48**	**2099.09**	**778.44**	**72.95**

5.3.5 Effect of variation in inlet RLG (HPOML)

This study based on the variation of RLG from 0.5 to 2.0. Table 5.10 shows changes in outlet parameters at constant inlet air DBT (36 ˚C), air relative humidity (65 %), water temperature (56 ˚C), and droplet diameter (250 µm). Table also shows as RLG increases exit air DBT, air specific humidity and droplet temperature increases because of the mass of water at inlet increases. Maximum and minimum water droplet temperature reduction is 17.44 ˚C and 10.12 ˚C which obtained at 0.5 and 2 RLG respectively. The range of SCT decreased by increased RLG hence the thermal efficiency of SCT also decreased simultaneously increased in the RLG. Total exergy of air, exergy of water increased with increase in the RLG because exit air and water droplet temperature and mass of water increased with increased RLG. As the amount of water in water to air mass flow ratio increased destruction in exergy of the system along tower height increased because the amount of exergy release by water is more than the amount of exergy gain by air. SLE of SCT increased with increase in the RLG.

Table 5.10 Effect of variation in inlet RLG (HPOML)

1	2	3	4	5	6	7	8	9	10	11	12	13	14
Code	**RLG_{in}**	**$T_{a,out}$ (˚C)**	**$\omega_{a,out}$ (kg_w/kg_a)**	**$T_{d,out}$ (˚C)**	**$m_{d,l}$ (kg/s)**	**η_{th} (%)**	**$X_{c,out}$ (W)**	**$X_{e,out}$ (W)**	**$X_{a,out}$ (W)**	**$X_{d,out}$ (W)**	**$X_{t,out}$ (W)**	**I_t (W)**	**η_{II} (%)**
HPOML-1	**0.5**	**38.90**	**0.044**	**38.89**	**0.0023**	**68.19**	**1.52**	**103.72**	**105.24**	**3757.68**	**3862.92**	**871.33**	**81.60**
HPOML-2	**1**	**42.14**	**0.0543**	**42.13**	**0.0035**	**55.28**	**8.16**	**219.75**	**227.91**	**7855.08**	**8082.99**	**1385.35**	**85.37**
HPOML-3	**1.25**	**43.30**	**0.0583**	**43.29**	**0.004**	**50.66**	**11.75**	**273.11**	**284.86**	**9969.48**	**10254.34**	**1581.03**	**86.64**
HPOML-4	**1.5**	**44.27**	**0.0615**	**44.26**	**0.0044**	**46.79**	**15.21**	**322.89**	**338.10**	**12114.93**	**12453.03**	**1749.38**	**87.68**
HPOML-5	**2**	**45.99**	**0.065**	**45.98**	**0.0045**	**39.94**	**21.47**	**412.23**	**433.70**	**12898.49**	**13332.19**	**1817.03**	**88.01**

5.4 Two Dimensional Parallel Flow Multi Droplet SCT for Industrial Application

In this study of 2-D multi droplet parallel flow MATLAB model was used to determine the effect of variation in inlet droplet diameters, water temperatures, air DBT, relative humidity of air and RLG on the performance of outlet parameters of SCT. Schematic diagram of 2-D parallel flow SCT is shown in Figure 1.1. Inlet conditions used for computer simulation are given in Table 5.3.

5.4.1 Effect of variation in initial droplets diameter (HPUMR)

Table 5.11 shows the effect of deviation in exit parameters of SCT at constant inlet air DBT (36 ˚C), air relative humidity (65%), water temperature (56 ˚C), and RLG (0.5) by varying the multi droplet diameters range from 31.81-318.18 µm to 254.55-2545.50 µm. As multi droplet diameters increased exit air DBT and water temperature increased and exit specific humidity, makeup water required and thermal efficiency of SCT decreased because heat and mass transfer between air and water droplet decreased. As inlet droplet diameter decreased, the total exergy of air and

exergy destruction decreases. With the increase in droplet diameters, the heat and mass transfer between air and water decreased. Therefore exergy of water, exergy of the system and SLE increased.

Table 5.11 Effect of variation in inlet droplet diameter (HPUMR)

1	2	3	4	5	6	7	8	9	10	11	12	13	14
Code	D_{in} (μm)	$T_{a,out}$ (˚C)	$\omega_{a,out}$ (kg_w/kg_a)	$T_{d,m,out}$ (˚C)	$m_{d,l}$ (kg/s)	η_{th} (%)	$X_{c,out}$ (W)	$X_{e,out}$ (W)	$X_{a,out}$ (W)	$X_{d,out}$ (W)	$X_{t,out}$ (W)	I_t (W)	η_{II} (%)
HPUMR-1	**31.81-318.18**	**39.24**	**0.0446**	**39.23**	**0.0024**	**66.84**	**1.18**	**98.54**	**99.72**	**3794.4**	**3894.12**	**840.13**	**82.25**
HPUMR-2	**63.63-636.36**	**44.52**	**0.0379**	**44.51**	**0.0019**	**45.80**	**1.12**	**45.08**	**46.20**	**4074.04**	**4120.24**	**614.01**	**87.03**
HPUMR-3	**127.27- 1272.70**	**50.64**	**0.0311**	**50.63**	**0.0015**	**21.40**	**0.85**	**10.05**	**10.90**	**4392.77**	**4403.67**	**330.58**	**93.02**
HPUMR-4	**190.91- 1909.10**	**52.99**	**0.0285**	**52.98**	**0.0012**	**12.04**	**0.62**	**3.14**	**3.76**	**4514.73**	**4518.49**	**215.76**	**95.44**
HPUMR-5	**254.55- 2545.50**	**53.9**	**0.0276**	**53.89**	**0.001**	**8.41**	**0.46**	**1.59**	**2.05**	**4572.2**	**4574.25**	**160.00**	**96.62**

5.4.2 Effect of variation in inlet Water Temperature (HPUMD)

The effect of changes of inlet water temperatures from 50 ˚C to 58 ˚C on various outlet parameters of SCT at constant inlet air DBT (36 ˚C), air relative humidity (65%), droplet diameter range 31.81-318.18 μm, and RLG (0.5) given in Table 5.12. Table 5.12 shows as inlet water temperature increased exit air DBT, air specific humidity, water temperature, makeup water required, and thermal efficiency of SCT increased. It observed that when the temperature of inlet water is 58 ˚C, maximum cooling of the droplet achieved (18.19 ˚C) as the high-temperature difference between water and air (keeping air temperature constant) leads to increase sensible cooling as well as evaporative cooling. When inlet water droplet temperature increased, it adds more water in the air and also increases exit water temperature that results in specific humidity of air increased. Table 5.12 also showed that total exergy of air increased due to increase in inlet water temperature which mixed more quantity of water vapour in the air. It is also observed, with increased the inlet water

temperature heat and mass transfer within SCT decreases hence exergy destruction of the system and SLE decreased.

Table 5.12 Effect of variation in inlet water temperature (HPUMD)

1	2	3	4	5	6	7	8	9	10	11	12	13	14
Code	$T_{d,in}$ (˚C)	$T_{a,out}$ (˚C)	$\omega_{a,out}$ (kg_w/kg_a)	$T_{d,m,out}$ (˚C)	$m_{d,l}$ (kg/s)	η_{th} (%)	$X_{c,out}$ (W)	$X_{e,out}$ (W)	$X_{a,out}$ (W)	$X_{d,out}$ (W)	$X_{t,out}$ (W)	I_t (W)	η_{II} (%)
HPUMD-1	**50**	**37.43**	**0.0404**	**37.42**	**0.0018**	**65.90**	**0.08**	**62.63**	**62.71**	**3766.82**	**3829.53**	**576.84**	**86.91**
HPUMD-2	**52**	**38.05**	**0.0418**	**38.04**	**0.002**	**66.19**	**0.31**	**73.64**	**73.95**	**3776.25**	**3850.2**	**660.16**	**85.36**
HPUMD-3	**54**	**38.69**	**0.0432**	**38.68**	**0.0022**	**66.35**	**0.68**	**85.61**	**86.29**	**3785.45**	**3871.74**	**747.94**	**83.81**
HPUMD-4	**56**	**39.24**	**0.0446**	**39.23**	**0.0024**	**66.84**	**1.18**	**98.54**	**99.72**	**3794.4**	**3894.12**	**840.13**	**82.25**
HPUMD-5	**58**	**39.82**	**0.0461**	**39.81**	**0.0025**	**67.15**	**1.82**	**112.44**	**114.26**	**3803.09**	**3917.35**	**936.66**	**80.70**

5.4.3 Effect of variation in inlet air DBT (HPUMA)

DBT of air varied from 24 - 48 ˚C. The constant inlet parameters of SCT are air relative humidity (65%), droplet diameter range 31.81-318.18 µm, water temperature (56 ˚C), and RLG (0.5). It observed from Table 5.13 that exit air DBT, specific humidity and droplet temperatures increased relatively as inlet air DBT increased; it also shows 24 ˚C DBT air produce maximum cooling and it cools down water droplet up to 21.38 ˚C.

Table 5.13 Effect of variation in inlet air DBT (HPUMA)

1	2	3	4	5	6	7	8	9	10	11	12	13	14
Code	$T_{a,in}$ (˚C)	$T_{a,out}$ (˚C)	$\omega_{a,out}$ (kg_w/kg_a)	$T_{d,m,out}$ (˚C)	$m_{d,l}$ (kg/s)	η_{th} (%)	$X_{c,out}$ (W)	$X_{e,out}$ (W)	$X_{a,out}$ (W)	$X_{d,out}$ (W)	$X_{t,out}$ (W)	I_t (W)	η_{II} (%)
HPUMA-1	**24**	**33.01**	**0.0327**	**34.62**	**0.0026**	**58.28**	**18.54**	**198.80**	**217.34**	**4024.44**	**4241.78**	**1130.18**	**78.96**
HPUMA-2	**30**	**35.51**	**0.0379**	**36.76**	**0.0025**	**61.77**	**11.72**	**144.91**	**156.63**	**3907.58**	**4064.21**	**989.77**	**80.40**
HPUMA-3	**36**	**38.35**	**0.0446**	**39.23**	**0.0024**	**66.83**	**6.71**	**98.54**	**105.25**	**3794.40**	**3899.65**	**840.13**	**82.25**
HPUMA-4	**42**	**41.91**	**0.0534**	**42.06**	**0.0021**	**76.12**	**1.18**	**59.76**	**60.94**	**3686.27**	**3747.21**	**680.37**	**84.63**
HPUMA-5	**48**	**47.91**	**0.0563**	**43.92**	**0.0013**	**91.06**	**0.002**	**20.47**	**20.47**	**3641.22**	**3661.69**	**554.30**	**86.87**

Table 5.13 also represents that increased in inlet air DBT temperature, the thermal efficiency of SCT increased. The convective exergy of air, evaporative

exergy of air, total exergy of air, exergy of water, and total exergy of the system decreased with increasing the inlet air DBT temperature. The SLE of system increases because exergy destruction decreases with increasing the initial air DBT.

5.4.4 Effect of variation in inlet Air Relative Humidity (HPUMH)

For this study inlet relative humidity of air varied from 20% to 80% and inlet constant parameters of SCT are air DBT (36 ˚C), droplet diameter range 31.81-318.18 μm, water temperature (56 ˚C), and RLG (0.5). It observed from Table 5.14 exit air DBT, specific humidity, droplet temperature and thermal efficiency of SCT increased with increasing the air relative humidity.

Table 5.14 Effect of variation in inlet air relative humidity (HPUMH)

1	2	3	4	5	6	7	8	9	10	11	12	13	14
Code	ϕ_{in} (˚C)	$T_{a,out}$ (˚C)	$\omega_{a,out}$ (kg_w/kg_a)	$T_{d,m,out}$ (˚C)	$m_{d,l}$ (kg/s)	η_{th} (%)	$X_{c,out}$ (W)	$X_{e,out}$ (W)	$X_{a,out}$ (W)	$X_{d,out}$ (W)	$X_{t,out}$ (W)	I_t (W)	η_{II} (%)
HPUMH-1	**20**	**35.06**	**0.0339**	**35.05**	**0.0033**	**57.83**	**1.24**	**413.62**	**414.86**	**13702.14**	**14117.00**	**1272.19**	**91.73**
HPUMH-2	**35**	**36.52**	**0.0374**	**36.51**	**0.0029**	**60.60**	**0.11**	**238.67**	**238.78**	**8986.34**	**9225.12**	**1093.45**	**89.40**
HPUMH-3	**50**	**37.92**	**0.0409**	**37.91**	**0.0026**	**63.52**	**0.16**	**150.48**	**150.64**	**5990.83**	**6141.47**	**954.96**	**86.54**
HPUMH-4	**65**	**39.24**	**0.0446**	**39.23**	**0.0024**	**66.84**	**1.18**	**98.54**	**99.72**	**3794.4**	**3894.12**	**840.13**	**82.25**
HPUMH-5	**80**	**40.51**	**0.0483**	**40.5**	**0.0021**	**70.65**	**2.99**	**65.53**	**68.52**	**2061.77**	**2130.29**	**747.24**	**74.03**

Table 5.14 also shows 20% relative humidity air produce maximum cooling, i.e. up to 20.95 ˚C and 80% relative humidity air give maximum efficiency of SCT. Table 5.14 also shows as the relative humidity of air increases the change in total exergy of air, exergy of water, and SLE of SCT is decrease. As relative humidity of air increases, the destruction in total exergy of the system relatively decreases because low relative humidity air absorbs more amount of water from droplets.

5.4.5 Effect of variation in inlet RLG (HPUML)

In this research constant inlet parameters of SCT are air DBT (36 ˚C) relative humidity (65%), droplet diameter range 31.81-318.18 µm, and water temperature (56 ˚C). Table 5.15 shows as RLG increases from 0.5 to 2.0 exit air DBT, air specific humidity and droplet temperature increases because of the mass of water at inlet increases. Maximum and minimum water droplet temperature reduction was 16.77 ˚C and 09.73 ˚C which is obtained at 0.5 and 2 RLG respectively. The range (i.e. $T_{d,in} - T_{d,out}$) of SCT decreases by increases RLG hence the thermal efficiency of SCT also decreases by increases the RLG. Total exergy of air, exergy of water increase with increase the RLG because of the exit air and water droplet temperature and mass of water increases with increases RLG. Exergy destruction increased with increased the RLG because the amount of exergy release by water was more than the amount of exergy gain by air. SLE of SCT also increased with increased the RLG.

Table 5.15 Effect of variation in inlet RLG (HPUML)

1	2	3	4	5	6	7	8	9	10	11	12	13	14
Code	**RLG_{in}**	**$T_{a,out}$ (˚C)**	**$\omega_{a,out}$ (kg_w/kg_a)**	**$T_{d,m,out}$ (˚C)**	**$m_{d,l}$ (kg/s)**	**η_{th} (%)**	**$X_{c,out}$ (W)**	**$X_{e,out}$ (W)**	**$X_{a,out}$ (W)**	**$X_{d,out}$ (W)**	**$X_{t,out}$ (W)**	**I_t (W)**	**η_{II} (%)**
HPUML-1	**0.5**	**39.24**	**0.0446**	**39.23**	**0.0024**	**66.84**	**1.18**	**98.54**	**99.72**	**3794.4**	**3894.12**	**840.13**	**82.25**
HPUML-2	**1**	**42.45**	**0.0549**	**42.44**	**0.0036**	**54.05**	**7.63**	**212.36**	**219.99**	**7893.45**	**8113.44**	**1354.90**	**85.69**
HPUML-3	**1.25**	**43.58**	**0.0589**	**43.57**	**0.0041**	**49.54**	**11.29**	**265.33**	**276.62**	**10006.31**	**10282.93**	**1552.44**	**86.88**
HPUML-4	**1.5**	**44.51**	**0.0622**	**44.5**	**0.0045**	**45.83**	**16.33**	**311.68**	**328.01**	**12150.18**	**12478.19**	**1724.22**	**87.86**
HPUML-5	**2**	**46.27**	**0.0657**	**46.27**	**0.0046**	**38.78**	**23.28**	**319.63**	**342.91**	**13016.44**	**13359.35**	**1789.87**	**88.19**

5.5 Three Dimensional Parallel Flow Mono Droplet SCT for Industrial Application

To determine the effect of variation in inlet droplet diameters, water temperatures, air DBT, relative humidity of air and RLG on outlet parameters on 3-D mono droplet parallel flow CFD model was studied. The schematic diagram of 3-D parallel flow SCT is shown in Figure 3.1. Mesh of 3-D parallel flow SCT is shown in Figure 5.7. Initial conditions used for computer simulation are same as 2-D mono droplets SCT used for industrial application.

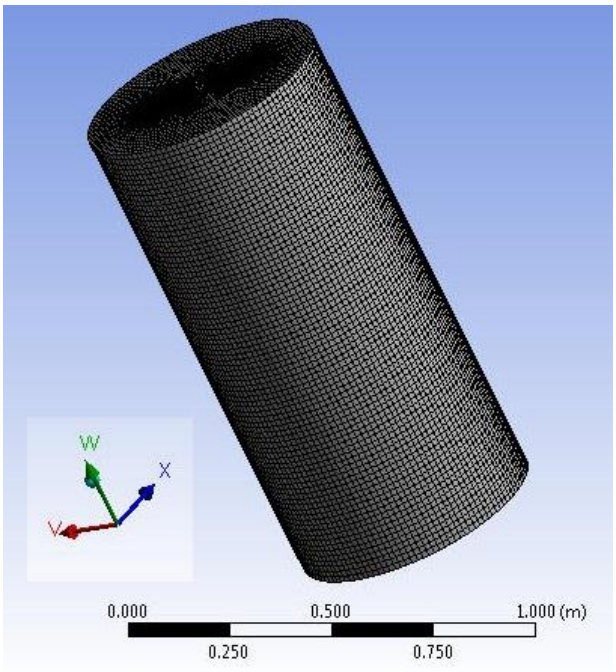

Figure 5.7 Mesh of three dimensional parallel flow SCT

5.5.1 Effect of variation in initial droplets diameter (HPOCR)

The deviation in outlet parameters by varying inlet droplet diameter from 250 µm to 2000 µm and at constant inlet air DBT (36 ˚C), air relative humidity (65%), water temperature (56 ˚C), and RLG (0.5) are shown in Table 5.16. Exit air DBT and

water temperature increases and exit specific humidity, make up water required, and thermal efficiency of SCT decreases as droplet diameter increases from 250 µm to 2000 µm, because heat and mass transfer between air and water droplet decreases. Maximum and minimum water droplet temperature reduction was 16.46 ˚C and 01.81 ˚C which were obtained at 250 µm and 2000 µm respectively. Maximum SCT efficiency was 65.60% achieved at 250 µm droplet diameter, 2000 µm droplet diameter achieved maximum exergy of water and maximum total exergy of the system. SLE of SCT increased, and exergy destruction of system decreased with increased the droplet diameters because heat and mass transfer between air and water decreased.

Table 5.16 Effect of variation in inlet droplet diameter (HPOCR)

1	2	3	4	5	6	7	8	9	10	11	12	13	14
Code	D_{in} (µm)	$T_{a,out}$ (˚C)	$\omega_{a,out}$ (kg_w/kg_a)	$T_{d,out}$ (˚C)	$m_{d,l}$ (kg/s)	η_{th} (%)	$X_{c,out}$ (W)	$X_{e,out}$ (W)	$X_{a,out}$ (W)	$X_{d,out}$ (W)	$X_{t,out}$ (W)	I_t (W)	η_{II} (%)
HPOCR-1	**250**	**39.55**	**0.0452**	**39.54**	**0.0025**	**65.60**	**3.31**	**135.12**	**138.43**	**3787.48**	**3925.91**	**808.34**	**82.93**
HPOCR-2	**500**	**44.83**	**0.0385**	**44.82**	**0.0020**	**44.56**	**1.85**	**88.19**	**90.04**	**4061.99**	**4152.03**	**582.22**	**87.70**
HPOCR-3	**1000**	**50.95**	**0.0317**	**50.94**	**0.0016**	**20.17**	**1.77**	**32.15**	**33.92**	**4401.54**	**4435.46**	**298.79**	**93.69**
HPOCR-4	**1500**	**53.29**	**0.0290**	**53.28**	**0.0013**	**10.84**	**1.65**	**13.74**	**15.39**	**4534.89**	**4550.28**	**183.97**	**96.11**
HPOCR-5	**2000**	**54.20**	**0.0281**	**54.19**	**0.0011**	**7.21**	**0.96**	**7.36**	**8.32**	**4597.72**	**4606.04**	**128.21**	**97.29**

5.5.2 Effect of variation in inlet Water Temperature (HPOCD)

The effects of variation of inlet water droplet temperature from 50 to 58 C on exit parameters at constant inlet air DBT (36 ˚C), air relative humidity (65%), droplet diameter (250 µm), and RLG (0.5) are given in Table 5.17. Table 5.17 shows as inlet water temperature increases exit air DBT, air specific humidity, water temperature, makeup water required, the thermal efficiency of SCT increases. It also shows that when the temperature of inlet water is 58 ˚C, maximum cooling of the droplet is

achieved (17.87 ˚C) as the high temperature difference between water and air (keeping air temperature constant). Maximum SCT efficiency (65.97%) achieved by 58 ˚C inlet droplet temperature due to increase in sensible cooling as well as evaporative cooling. As inlet water droplet temperature increased, the specific humidity of air increases because due to increases in water temperature more water vapour added to the air. Table 5.17 also shows that increase in inlet water temperature, more quantity of water vapour mixed with air and increases total exergy of air. The exergy destruction of system increases and SLE decreases by increases the inlet water droplet temperature. Depicted destruction in total exergy of a system is more for higher temperature droplet because it transfers water content into air faster than lower temperature droplets.

Table 5.17 Effect of variation in inlet water temperature (HPOCD)

1	2	3	4	5	6	7	8	9	10	11	12	13	14
Code	$T_{d,in}$ (˚C)	$T_{a,out}$ (˚C)	$\omega_{a,out}$ (kg_w/kg_a)	$T_{d,out}$ (˚C)	$m_{d,l}$ (kg/s)	η_{th} (%)	$X_{c,out}$ (W)	$X_{e,out}$ (W)	$X_{a,out}$ (W)	$X_{d,out}$ (W)	$X_{t,out}$ (W)	I_t (W)	η_{II} (%)
HPOCD-1	**50**	**37.74**	**0.0411**	**37.73**	**0.0019**	**64.27**	**1.81**	**109.77**	**111.58**	**3749.74**	**3861.32**	**545.05**	**87.63**
HPOCD-2	**52**	**38.36**	**0.0424**	**38.35**	**0.0021**	**64.72**	**2.18**	**117.56**	**119.74**	**3762.25**	**3881.99**	**628.37**	**86.07**
HPOCD-3	**54**	**39.00**	**0.0438**	**38.99**	**0.0023**	**65.01**	**2.43**	**122.75**	**125.18**	**3778.35**	**3903.53**	**716.15**	**84.50**
HPOCD-4	**56**	**39.55**	**0.0452**	**39.54**	**0.0025**	**65.60**	**3.31**	**135.12**	**138.43**	**3787.48**	**3925.91**	**808.34**	**82.93**
HPOCD-5	**58**	**40.14**	**0.0467**	**40.13**	**0.0026**	**65.97**	**3.94**	**153.9**	**157.84**	**3791.31**	**3949.15**	**904.86**	**81.36**

5.5.3 Effect of variation in inlet air DBT (HPOCA)

This research shows changes in outlet parameters of SCT with varying the inlet DBT from 24 – 48 ˚C at constant inlet air relative humidity (65%), water temperature (56 ˚C), droplet diameter (250 μm) and RLG (0.5). Table 5.18 shows exit air DBT, air specific humidity and droplet temperatures increase relatively as inlet air DBT increases because heat and mass transfer between air and water droplet

decreases as inlet air DBT increases. Table 5.18 also shows 24 ˚C DBT air produce maximum cooling, and it cools down water droplet up to 20.99 ˚C. Table 5.18 also represents that increase in inlet air DBT, the thermal efficiency of SCT increases, and maximum thermal efficiency (81.80%) achieved at 48 ˚C. The convective exergy of air, evaporative exergy of air, total exergy of air, exergy of water, total exergy of system and exergy destruction decreasing with increase the inlet air DBT temperature. The SLE of the system increases with increasing the initial air DBT.

Table 5.18 Effect of variation in inlet air DBT (HPOCA)

1	2	3	4	5	6	7	8	9	10	11	12	13	14
Code	$T_{a,in}$ (˚C)	$T_{a,out}$ (˚C)	$\omega_{a,out}$ (kg_w/kg_a)	$T_{d,out}$ (˚C)	$m_{d,l}$ (kg/s)	η_{th} (%)	$X_{c,out}$ (W)	$X_{e,out}$ (W)	$X_{a,out}$ (W)	$X_{d,out}$ (W)	$X_{t,out}$ (W)	I_t (W)	η_{II} (%)
HPOCA-1	**24**	**35.02**	**0.0333**	**35.01**	**0.0031**	**57.21**	**13.58**	**181.92**	**195.50**	**4078.07**	**4273.57**	**1098.39**	**79.55**
HPOCA-2	**30**	**37.12**	**0.0385**	**37.11**	**0.0029**	**60.64**	**5.93**	**139.83**	**145.76**	**3950.24**	**4096.00**	**952.96**	**81.13**
HPOCA-3	**36**	**39.55**	**0.0452**	**39.54**	**0.0025**	**65.60**	**3.31**	**135.12**	**138.43**	**3787.48**	**3925.91**	**808.34**	**82.93**
HPOCA-4	**42**	**42.35**	**0.0540**	**42.34**	**0.0024**	**74.60**	**1.46**	**51.41**	**52.87**	**3725.03**	**3777.90**	**648.51**	**85.35**
HPOCA-5	**48**	**47.37**	**0.0653**	**47.37**	**0.0019**	**81.80**	**1.37**	**14.42**	**15.79**	**3677.692**	**3693.48**	**530.74**	**87.44**

5.5.4 Effect of variation in inlet Air Relative Humidity (HPOCH)

This study presents deviation in outlet parameters with varying the inlet relative humidity from 20% to 80% at constant inlet air DBT (36 ˚C), water temperature (56 ˚C), droplet diameter (250 μm) and RLG (0.5). Table 5.19 shows exit air DBT, specific humidity, droplet temperature and thermal efficiency of SCT increased with increased the air relative humidity. Table also shows 20% relative humidity air produce maximum cooling, i.e. up to 20.63 ˚C and 80% relative humidity air give maximum efficiency. Table 5.19 also shows as the relative humidity of air increases the change in total exergy of air, exergy of water, and SLE of SCT is decrease because evaporative heat and mass transfer between air and water droplet

decreased with increase the inlet air relative humidity. As relative humidity of air increases, the destruction in total exergy of the system relatively less because low relative humidity air absorbs more amount of water from droplets.

Table 5.19 Effect of variation in inlet air relative humidity (HPOCH)

1	2	3	4	5	6	7	8	9	10	11	12	13	14
Code	ϕ_{in} (˚C)	$T_{a,out}$ (˚C)	$\omega_{a,out}$ (kg_w/kg_a)	$T_{d,out}$ (˚C)	$m_{d,l}$ (kg/s)	η_{th} (%)	$X_{c,out}$ (W)	$X_{e,out}$ (W)	$X_{a,out}$ (W)	$X_{d,out}$ (W)	$X_{t,out}$ (W)	I_t (W)	η_{II} (%)
HPOCH-1	**20**	**35.38**	**0.0345**	**35.37**	**0.0036**	**56.94**	**0.10**	**274.51**	**274.60**	**13874.21**	**14148.81**	**1240.38**	**91.94**
HPOCH-2	**35**	**36.84**	**0.0380**	**36.83**	**0.0032**	**59.61**	**0.46**	**152.93**	**153.39**	**9103.54**	**9256.93**	**1061.64**	**89.71**
HPOCH-3	**50**	**38.24**	**0.0415**	**38.23**	**0.0029**	**62.39**	**1.85**	**97.40**	**99.25**	**6074.02**	**6173.27**	**923.16**	**86.99**
HPOCH-4	**65**	**39.55**	**0.0452**	**39.54**	**0.0025**	**65.60**	**3.31**	**135.12**	**138.43**	**3787.48**	**3925.91**	**808.34**	**82.93**
HPOCH-5	**80**	**40.81**	**0.0489**	**40.81**	**0.0024**	**69.23**	**5.23**	**34.43**	**39.67**	**2122.41**	**2162.08**	**715.45**	**75.14**

5.5.5 Effect of variation in inlet RLG (HPOCL)

In this study, RLG varied from 0.5 to 2.0, and constant inlet parameters of SCT are air DBT (36 ˚C), air relative humidity (65%), water droplet diameter 250 μm, and water temperature (56 ˚C). Table 5.20 shows as RLG increases exit air DBT, air specific humidity and droplet temperature increases because mass of water at inlet increases. Maximum and minimum water droplet temperature reduction is 16.46 ˚C and 09.46 ˚C which is obtained at 0.5 and 2 RLG respectively. The range (i.e. $T_{d,in} - T_{d,out}$) of SCT decreases by increases RLG hence the thermal efficiency of SCT also decreases by increases the RLG. Total exergy of air, exergy of water increase with increase the RLG because of exit air and water droplet temperature and mass of water increases with increases RLG. As the amount of water in water to air mass flow ratio increases destruction in exergy of the system along tower height increases because the amount of exergy release by water is more than the amount of exergy gain by air. SLE of SCT increases with increase the RLG.

Table 5.20 Effect of variation in inlet RLG (HPOCL)

1	2	3	4	5	6	7	8	9	10	11	12	13	14
Code	**RLG_{in}**	**$T_{a,out}$ (˚C)**	**$\omega_{a,out}$ (kg_w/kg_a)**	**$T_{d,out}$ (˚C)**	**$m_{d,l}$ (kg/s)**	**η_{th} (%)**	**$X_{c,out}$ (W)**	**$X_{e,out}$ (W)**	**$X_{a,out}$ (W)**	**$X_{d,out}$ (W)**	**$X_{t,out}$ (W)**	**I_t (W)**	**η_{II} (%)**
HPOCL-1	**0.5**	**39.55**	**0.0452**	**39.54**	**0.0025**	**65.60**	**3.31**	**135.12**	**138.43**	**3787.48**	**3925.91**	**808.34**	**82.93**
HPOCL-2	**1**	**42.74**	**0.0555**	**42.73**	**0.0037**	**52.89**	**10.42**	**253.32**	**263.74**	**7880.68**	**8144.42**	**1323.92**	**86.02**
HPOCL-3	**1.25**	**43.85**	**0.0595**	**43.84**	**0.0042**	**48.47**	**15.84**	**332.05**	**347.89**	**9964.21**	**10312.10**	**1523.27**	**87.13**
HPOCL-4	**1.5**	**44.75**	**0.0628**	**44.74**	**0.0046**	**44.88**	**20.73**	**401.66**	**422.39**	**12081.64**	**12504.03**	**1698.38**	**88.04**
HPOCL-5	**2**	**46.55**	**0.0663**	**46.54**	**0.0047**	**37.70**	**26.43**	**482.86**	**509.29**	**12877.88**	**13387.17**	**1762.05**	**88.37**

5.6 Three Dimensional Parallel Flow Multi Droplet SCT for Industrial Application

In this section 3-D multi droplet parallel flow CFD modelled to determine the effect of variation in inlet droplet diameters, water temperatures, air DBT, relative humidity of air and RLG on outlet parameters. The schematic diagram of 3-D parallel flow SCT is shown in Figure 3.1. Mesh of three dimensional parallel flow SCT is shown in Figure 5.7. Initial conditions used for computer simulation are same as 2-D multi droplets SCT used for industrial application.

5.6.1 Effect of variation in initial droplets diameter (HPUCR)

Table 5.21 shows the effect of changes in outlet parameters of SCT at constant inlet air DBT (36 ˚C), air relative humidity (65%), water temperature (56 ˚C), and RLG (0.5) by varying the multi droplet diameters from 31.81-318.18 µm to 254.55-2545.50 µm. As multi droplet diameter increases exit air DBT and water temperature increases and exit specific humidity, make up water required and thermal efficiency of SCT decreases because heat and mass transfer between air and water droplet decreases. It is also clear that 31.81-318.18 µm size water droplets produce maximum

cooling (16.11 °C) and maximum efficiency (64.21%). Total exergy of air and exergy destruction decrease as inlet droplet diameter increases. Exergy of water, exergy of system and SLE was increased from 83.39% to 97.75% with increasing the droplet diameter. It is due to heat and mass transfer between air and water decrease.

Table 5.21 Effect of variation in inlet droplet diameter (HPUCR)

1	2	3	4	5	6	7	8	9	10	11	12	13	14
Code	D_{in} (μm)	$T_{a,out}$ (˚C)	$\omega_{a,out}$ (kg_w/kg_a)	$T_{d,m,out}$ (˚C)	$m_{d,l}$ (kg/s)	η_{th} (%)	$X_{c,out}$ (W)	$X_{e,out}$ (W)	$X_{a,out}$ (W)	$X_{d,out}$ (W)	$X_{t,out}$ (W)	I_t (W)	η_{II} (%)
HPUCR-1	**31.81-318.18**	**39.9**	**0.0458**	**39.89**	**0.0026**	**64.21**	**2.19**	**116.29**	**118.48**	**3829.36**	**3947.84**	**786.42**	**83.39**
HPUCR-2	**63.63-636.36**	**45.18**	**0.0391**	**45.17**	**0.0021**	**43.16**	**1.61**	**92.4**	**94.01**	**4079.95**	**4173.96**	**560.30**	**88.17**
HPUCR-3	**127.27-1272.70**	**51.3**	**0.0323**	**51.29**	**0.0017**	**18.77**	**1.45**	**74.7**	**76.15**	**4381.24**	**4457.39**	**276.87**	**94.15**
HPUCR-4	**190.91-1909.10**	**53.64**	**0.0295**	**53.63**	**0.0014**	**9.45**	**1.29**	**61.62**	**62.91**	**4509.3**	**4572.21**	**162.05**	**96.58**
HPUCR-5	**254.55-2545.50**	**54.54**	**0.0286**	**54.53**	**0.0012**	**5.86**	**1.02**	**43.68**	**44.70**	**4583.27**	**4627.97**	**106.29**	**97.75**

5.6.2 Effect of variation in inlet Water Temperature (HPUCD)

The effect of variation of inlet water temperatures from 50 - 58 ˚C on various exit parameters are given in Table 5.22. The other important constant inlet parameters of SCT are air DBT (36 ˚C), air relative humidity (65%), water droplet diameter (250 μm), and RLG (0.5). Table 5.22 shows as inlet water temperature increases exit air DBT, air specific humidity, water temperature, makeup water required, and thermal efficiency of SCT increases. It was noted that thermal efficiency achieved by 3-D model was more then 2-D model for same inlet parameters. It also observed that when the temperature of inlet water is 58 ˚C, maximum cooling of droplet was achieved at 17.92 ˚C at constant air temperature. It is also noted when water droplet temperature increased, the specific humidity of air increased and more amount of water vapour mixed into air that results in increased in total exergy of air. The exergy destruction of system increases and SLE decreases by increases the inlet water droplet

temperature. Depicted destruction in total exergy of the system is more for higher temperature droplet because it transfers water content into air faster than lower temperature droplets.

Table 5.22 Effect of variation in inlet water temperature (HPUCD)

1	2	3	4	5	6	7	8	9	10	11	12	13	14
Code	$T_{d,in}$ (˚C)	$T_{a,out}$ (˚C)	$\omega_{a,out}$ (kg_w/kg_a)	$T_{d,m,out}$ (˚C)	$m_{d,l}$ (kg/s)	η_{th} (%)	$X_{c,out}$ (W)	$X_{e,out}$ (W)	$X_{a,out}$ (W)	$X_{d,out}$ (W)	$X_{t,out}$ (W)	I_t (W)	η_{II} (%)
HPUCD-1	**50**	**38.09**	**0.0417**	**38.08**	**0.002**	**62.44**	**0.58**	**79.03**	**79.61**	**3803.64**	**3883.25**	**523.13**	**88.13**
HPUCD-2	**52**	**38.71**	**0.043**	**38.70**	**0.0022**	**63.06**	**0.94**	**90.86**	**91.80**	**3812.12**	**3903.92**	**606.44**	**86.55**
HPUCD-3	**54**	**39.35**	**0.0444**	**39.34**	**0.0024**	**63.49**	**1.64**	**109.63**	**111.27**	**3814.19**	**3925.46**	**694.22**	**84.97**
HPUCD-4	**56**	**39.9**	**0.0458**	**39.89**	**0.0026**	**64.21**	**2.19**	**116.29**	**118.48**	**3829.36**	**3947.84**	**786.42**	**83.39**
HPUCD-5	**58**	**40.49**	**0.0474**	**40.48**	**0.0027**	**64.67**	**2.82**	**127.79**	**130.61**	**3840.48**	**3971.09**	**882.92**	**81.81**

5.6.3 Effect of variation in inlet air DBT (HPUCA)

In this section air DBT varied from 24 - 48 ˚C and constant inlet parameters of SCT are air relative humidity (65%), water droplet diameter (250 µm), water temperature (56 ˚C), and RLG (0.5). It is observed from Table 5.23 that exit air DBT, specific humidity and droplet temperatures increases relatively as inlet air DBT increases; it also shows at 24 ˚C DBT, air produce maximum cooling and it cool down water droplet up to 20.56 ˚C.

Table 5.23 Effect of variation in inlet air DBT (HPUCA)

1	2	3	4	5	6	7	8	9	10	11	12	13	14
Code	$T_{a,in}$ (˚C)	$T_{a,out}$ (˚C)	$\omega_{a,out}$ (kg_w/kg_a)	$T_{d,m,out}$ (˚C)	$m_{d,l}$ (kg/s)	η_{th} (%)	$X_{c,out}$ (W)	$X_{e,out}$ (W)	$X_{a,out}$ (W)	$X_{d,out}$ (W)	$X_{t,out}$ (W)	I_t (W)	η_{II} (%)
HPUCA-1	**24**	**35.45**	**0.0339**	**35.44**	**0.0026**	**56.03**	**16.34**	**181.56**	**197.90**	**4097.6**	**4295.50**	**1076.46**	**79.96**
HPUCA-2	**30**	**37.51**	**0.0391**	**37.5**	**0.0025**	**59.39**	**9.76**	**126.79**	**136.55**	**3981.38**	**4117.93**	**931.03**	**81.56**
HPUCA-3	**36**	**39.9**	**0.0458**	**39.89**	**0.0026**	**64.21**	**2.19**	**116.29**	**118.48**	**3829.36**	**3947.84**	**786.42**	**83.39**
HPUCA-4	**42**	**42.68**	**0.0547**	**42.67**	**0.0019**	**72.82**	**0.94**	**51.84**	**52.78**	**3747.05**	**3799.83**	**626.58**	**85.84**
CPUCA-5	**48**	**47.68**	**0.066**	**47.67**	**0.0011**	**78.94**	**0.01**	**11.56**	**11.57**	**3703.842**	**3715.41**	**508.81**	**87.95**

Table 5.23 also represents that increase in inlet air DBT temperature, the thermal efficiency of SCT increases. Maximum thermal efficiency (78.94%) was achieved at 48 ˚C inlet air DBT. With increase inlet air DBT, the convective exergy of air, evaporative exergy of air, total exergy of air, exergy of water, and total exergy of system increased. The SLE of the system was increased because of exergy destruction decreased with increasing the initial air DBT.

5.6.4 Effect of variation in inlet Air Relative Humidity (HPUCH)

In the present study, variation of inlet relative humidity from 20% to 80% and other important constant inlet parameters are air DBT (36 ˚C), water droplet diameter (250 μm), water temperature (56 ˚C), and RLG (0.5). Table 5.24 shows effects of variation of inlet relative humidity on outlet water and air parameters. It was observed that exit air DBT, specific humidity, droplet temperature and thermal efficiency of SCT increases with increase the air relative humidity.

Table 5.24 Effect of variation in inlet air relative humidity (HPUCH)

1	2	3	4	5	6	7	8	9	10	11	12	13	14
Code	ϕ_{in} (˚C)	$T_{a,out}$ (˚C)	$\omega_{a,out}$ (kg_w/kg_a)	$T_{d,m,out}$ (˚C)	$m_{d,l}$ (kg/s)	η_{th} (%)	$X_{c,out}$ (W)	$X_{e,out}$ (W)	$X_{a,out}$ (W)	$X_{d,out}$ (W)	$X_{t,out}$ (W)	I_t (W)	η_{II} (%)
HPUCH-1	**20**	**35.74**	**0.0351**	**35.73**	**0.0031**	**55.95**	**0.47**	**295.09**	**295.56**	**13875.18**	**14170.74**	**1218.46**	**92.08**
HPUCH-2	**35**	**37.20**	**0.0386**	**37.19**	**0.0027**	**58.49**	**0.15**	**175.32**	**175.47**	**9103.39**	**9278.86**	**1039.70**	**89.92**
HPUCH-3	**50**	**38.60**	**0.0421**	**38.59**	**0.0026**	**61.14**	**0.88**	**113.91**	**114.79**	**6080.41**	**6195.20**	**901.22**	**87.30**
HPUCH-4	**65**	**39.90**	**0.0458**	**39.89**	**0.0026**	**64.21**	**2.19**	**116.29**	**118.48**	**3829.36**	**3947.84**	**786.42**	**83.39**
HPUCH-5	**80**	**41.17**	**0.0495**	**41.16**	**0.0023**	**67.64**	**4.2**	**43.41**	**47.61**	**2136.4**	**2184.01**	**693.52**	**75.90**

Table 5.24 also shows at 20% relative humidity air produce maximum cooling (20.27 ˚C), and 80% relative humidity air gives maximum efficiency (67.64%). Table 5.24 further shows as the relative humidity of air increases the change in total exergy of air, exergy of water, and SLE of SCT is decreased. As relative humidity of air

increases, the destruction in total exergy of the system relatively decreases because low relative humidity air absorbs more amount of water from droplets.

5.6.5 Effect of variation in inlet RLG (HPUCL)

In this research RLG varied from 0.5 to 2.0, and constant inlet parameters of SCT are air DBT (36 ˚C), air relative humidity (65%), water droplet diameter 250 μm, and water temperature (56 ˚C). Table 5.25 shows as RLG increased exit air DBT, air specific humidity and droplet temperature increased because mass of water at inlet increased. Maximum and minimum water droplet temperature reduction is 16.11 ˚C and 09.18 ˚C which were obtained at 0.5 and 2 RLG respectively. The range of SCT decreased by increased the RLG hence the thermal efficiency of SCT also decreased by increased the RLG. Total exergy of air, exergy of water increased with increased the RLG because exit air and water droplet temperature and mass of water increased with increased the RLG. As the amount of water in RLG increased, destruction in exergy of the system along tower height increased because the amount of exergy supplied by water was more than amount of exergy accepted by air. SLE of SCT increases with increase the RLG.

Table 5.25 Effect of variation in inlet RLG (HPUCL)

1	2	3	4	5	6	7	8	9	10	11	12	13	14
Code	**RLG_{in}**	**$T_{a,out}$ (˚C)**	**$\omega_{a,out}$ (kg_w/kg_a)**	**$T_{d,m,out}$ (˚C)**	**$m_{d,l}$ (kg/s)**	**η_{th} (%)**	**$X_{c,out}$ (W)**	**$X_{e,out}$ (W)**	**$X_{a,out}$ (W)**	**$X_{d,out}$ (W)**	**$X_{t,out}$ (W)**	**I_t (W)**	**η_{II} (%)**
HPUCL-1	**0.5**	**39.9**	**0.0458**	**39.89**	**0.0026**	**64.21**	**2.19**	**116.29**	**118.48**	**3829.36**	**3947.84**	**786.42**	**83.39**
HPUCL-2	**1**	**43.06**	**0.0561**	**43.05**	**0.0038**	**51.61**	**9.45**	**238.63**	**248.08**	**7917.59**	**8165.67**	**1302.66**	**86.24**
HPUCL-3	**1.25**	**44.11**	**0.0601**	**44.1**	**0.0043**	**47.43**	**13.55**	**286.11**	**299.66**	**10031.58**	**10331.24**	**1504.13**	**87.29**
HPUCL-4	**1.5**	**45**	**0.0635**	**44.99**	**0.0047**	**43.88**	**18.67**	**314.36**	**333.03**	**12187.93**	**12520.96**	**1681.45**	**88.16**
HPUCL-5	**2**	**46.83**	**0.067**	**46.82**	**0.0048**	**36.59**	**26.73**	**323.58**	**350.31**	**13055.07**	**13405.38**	**1743.84**	**88.49**

5.7 Two Dimensional Counter flow Mono Droplet SCT for Industrial Application

In this research 2-D mono droplet counter flow MATLAB model used to determine the effect of variation in inlet droplet diameters, water temperatures, air DBT, relative humidity of air and RLG on outlet parameters. Initial conditions used for computer simulations are given in Table 5.2.

5.7.1 Effect of variation in initial droplets diameter (HCOMR)

In this section inlet water droplet diameter varied from 250 µm to 2000 µm and constant inlet parameters of SCT are air DBT (36 ˚C), air relative humidity (65%), water temperature (56 ˚C), and RLG (0.5). Table 5.26 shows as droplet diameter increased from 250 µm to 2000 µm, exit air DBT and water temperature increased and exit specific humidity, make up water required and thermal efficiency of SCT decreased because heat and mass transfer between air and water droplet decreased. It is also clear from Table 5.26 that 250 µm size water droplets give maximum cooling and maximum efficiency; it reduced droplet temperature up to 19.25 °C and maximum efficiency was 76.72%. Total exergy of air and exergy destruction decreased as inlet droplet diameter increased. Exergy destruction of system decreased with increased the droplet diameter. Exergy of water, exergy of system and SLE increased with increased the droplet diameter because heat and mass transfer between air and water decreased.

Table 5.26 Effect of variation in inlet droplet diameter (HCOMR)

1	2	3	4	5	6	7	8	9	10	11	12	13	14
Code	D_{in} (μm)	$T_{a,out}$ (˚C)	$\omega_{a,out}$ (kg_w/kg_a)	$T_{d,out}$ (˚C)	$m_{d,l}$ (kg/s)	η_{th} (%)	$X_{c,out}$ (W)	$X_{e,out}$ (W)	$X_{a,out}$ (W)	$X_{d,out}$ (W)	$X_{t,out}$ (W)	I_t (W)	η_{II} (%)
HCOMR-1	**250**	**36.76**	**0.0405**	**36.75**	**0.0017**	**76.72**	**1.05**	**78.23**	**79.28**	**3317.58**	**3396.86**	**1337.39**	**71.75**
HCOMR-2	**500**	**42.04**	**0.0338**	**42.03**	**0.0012**	**55.68**	**0.98**	**76.19**	**77.17**	**3545.81**	**3622.98**	**2.125**	**76.53**
HCOMR-3	**1000**	**48.16**	**0.0270**	**48.15**	**0.0008**	**31.29**	**0.67**	**23.54**	**24.21**	**3882.20**	**3906.41**	**1.223**	**82.51**
HCOMR-4	**1500**	**50.56**	**0.0246**	**50.55**	**0.0005**	**21.72**	**0.35**	**6.11**	**6.46**	**4014.77**	**4021.23**	**0.764**	**84.94**
HCOMR-5	**2000**	**51.47**	**0.0237**	**51.46**	**0.0003**	**18.09**	**0.12**	**2.32**	**2.44**	**4074.55**	**4076.99**	**0.524**	**86.12**

5.7.2 Effect of variation in inlet Water Temperature (HCOMD)

This research was based on the variation of inlet water temperature from 50 ˚C to 58 ˚C. The constant inlet parameters of SCT are air DBT (36 ˚C), air relative humidity (65%), water droplet diameter (250 μm), and RLG (0.5). Table 5.27 shows as inlet water temperature increased exit air DBT, air specific humidity, water temperature, makeup water required increased. The Thermal efficiency of SCT decreased with increased the Inlet water temperature. Obtain thermal efficiency by 50 ˚C water droplet was 78.88%. It also shows that when the temperature of inlet water is 58 ˚C, maximum cooling of the droplet was achieved (20.72 ˚C) as the high temperature difference between water and air (keeping air temperature constant). As inlet water droplet temperature increased, the specific humidity of air increased because due to increase in water temperature more water vapour is added in the air, the Table also shows that increased in inlet water temperature, additional water vapour mixed in air and increased total exergy of air. The exergy destruction of the system increased and SLE decreased by increased the inlet water droplet temperature. Depicted destruction in total exergy of the system was more for greater temperature

droplet because it transferred water content in to air faster than lesser temperature droplets.

Table 5.27 Effect of variation in inlet water temperature (HCOMD)

1	2	3	4	5	6	7	8	9	10	11	12	13	14
Code	$T_{d,in}$ (˚C)	$T_{a,out}$ (˚C)	$\omega_{a,out}$ (kg_w/kg_a)	$T_{d,out}$ (˚C)	$m_{d,l}$ (kg/s)	η_{th} (%)	$X_{c,out}$ (W)	$X_{e,out}$ (W)	$X_{a,out}$ (W)	$X_{d,out}$ (W)	$X_{t,out}$ (W)	I_t (W)	η_{II} (%)
HCOMD-1	**50**	**34.95**	**0.0363**	**34.94**	**0.0011**	**78.88**	**0.11**	**49.66**	**49.77**	**3282.30**	**3332.07**	**1074.31**	**75.62**
HCOMD-2	**52**	**35.57**	**0.0377**	**35.56**	**0.0013**	**77.95**	**0.15**	**60.45**	**60.60**	**3292.22**	**3352.82**	**1157.54**	**74.34**
HCOMD-3	**54**	**36.21**	**0.0391**	**36.20**	**0.0015**	**77.08**	**0.18**	**65.03**	**65.21**	**3309.22**	**3374.43**	**1245.25**	**73.04**
HCOMD-4	**56**	**36.76**	**0.0405**	**36.75**	**0.0017**	**76.72**	**1.05**	**78.23**	**79.28**	**3317.58**	**3396.86**	**1337.40**	**71.75**
HCOMD-5	**58**	**37.29**	**0.0417**	**37.28**	**0.0018**	**76.48**	**1.65**	**81.95**	**83.60**	**3336.51**	**3420.11**	**1433.90**	**70.46**

5.7.3 Effect of variation in inlet air DBT (HCOMA)

In this section inlet air DBT was varied from 24 - 48 ˚C and constant inlet parameters of SCT are air relative humidity (65%), water droplet diameter (250 µm), water temperature (56 ˚C), and RLG (0.5). Table 5.28 shows exit air DBT, specific humidity and droplet temperatures increases relatively as inlet air DBT increases, it also shows 24 ˚C DBT air produce maximum cooling, and it cools down water droplet up to 24.66 ˚C. Table 5.28 also represents that increased in inlet air DBT temperature, the thermal efficiency of SCT increased. The convective exergy of air, evaporative exergy of air, total exergy of air, exergy of water, total exergy of system and exergy destruction decreased with increased the inlet air DBT temperature. The SLE of system increased with increased the initial air DBT.

Table 5.28 Effect of variation in inlet air DBT (HCOMA)

1	2	3	4	5	6	7	8	9	10	11	12	13	14
Code	$T_{d,in}$ (˚C)	$T_{a,out}$ (˚C)	$\omega_{a,out}$ (kg_w/kg_a)	$T_{d,out}$ (˚C)	$m_{d,l}$ (kg/s)	η_{th} (%)	$X_{c,out}$ (W)	$X_{e,out}$ (W)	$X_{a,out}$ (W)	$X_{d,out}$ (W)	$X_{t,out}$ (W)	I_t (W)	η_{II} (%)
HCOMA-1	**24**	**31.35**	**0.0287**	**31.34**	**0.0042**	**67.21**	**21.64**	**224.82**	**246.46**	**3495.40**	**3741.86**	**1630.10**	**69.66**
HCOMA-2	**30**	**33.49**	**0.0338**	**33.48**	**0.0035**	**72.30**	**12.93**	**184.94**	**197.87**	**3367.52**	**3565.39**	**1483.57**	**70.62**
HCOMA-3	**36**	**36.76**	**0.0405**	**36.75**	**0.0017**	**76.72**	**1.05**	**78.23**	**79.28**	**3317.58**	**3396.86**	**1337.39**	**71.75**
HCOMA-4	**42**	**39.46**	**0.0493**	**39.45**	**0.0024**	**90.39**	**1.01**	**65.76**	**66.77**	**3184.13**	**3250.90**	**1175.51**	**73.44**
HCOMA-5	**48**	**45.48**	**0.0606**	**45.47**	**0.0019**	**99.81**	**0.74**	**48.36**	**49.10**	**3118.83**	**3167.93**	**1056.29**	**74.99**

5.7.4 Effect of variation in inlet Air Relative Humidity (HCOMH)

Table 5.29 shows the effect of the deviation in exit parameters of SCT at constant inlet air DBT (36 ˚C), water temperature (56 ˚C), water droplet diameter (250), and RLG (0.5) by varying the inlet air relative humidity from 20% to 80%. Table 5.29 shows deviation in exit parameters with increased the inlet air relative humidity. Table 5.29 shows exit air DBT, specific humidity, droplet temperature and thermal efficiency of SCT increased with increased the inlet air relative humidity.

Table 5.29 Effect of variation in inlet air relative humidity (HCOMH)

1	2	3	4	5	6	7	8	9	10	11	12	13	14
Code	ϕ_{in} (˚C)	$T_{a,out}$ (˚C)	$\omega_{a,out}$ (kg_w/kg_a)	$T_{d,out}$ (˚C)	$m_{d,l}$ (kg/s)	η_{th} (%)	$X_{c,out}$ (W)	$X_{e,out}$ (W)	$X_{a,out}$ (W)	$X_{d,out}$ (W)	$X_{t,out}$ (W)	I_t (W)	η_{II} (%)
HCOMH-1	**20**	**32.57**	**0.0299**	**32.56**	**0.0039**	**64.70**	**0.98**	**504.92**	**505.90**	**13113.76**	**13619.66**	**1769.53**	**88.50**
HCOMH-2	**35**	**34.03**	**0.0334**	**34.02**	**0.0035**	**68.35**	**0.75**	**342.76**	**343.51**	**8384.28**	**8727.79**	**1590.78**	**84.58**
HCOMH-3	**50**	**35.43**	**0.0368**	**35.42**	**0.0031**	**72.26**	**0.49**	**216.34**	**216.83**	**5427.27**	**5644.10**	**1452.33**	**79.53**
HCOMH-4	**65**	**36.76**	**0.0405**	**36.75**	**0.0017**	**76.72**	**1.05**	**78.23**	**79.28**	**3317.58**	**3396.86**	**1337.39**	**71.75**
HCOMH-5	**80**	**38.02**	**0.0439**	**38.02**	**0.0023**	**81.95**	**1.17**	**69.76**	**70.93**	**1561.99**	**1632.92**	**1244.61**	**56.75**

Table 5.29 also shows 20% relative humidity air produced highest cooling, i.e. up to 23.44 ˚C and 80% relative humidity air give highest thermal efficiency (81.95%). Table 5.29 also shows as the relative humidity of air increases the change in total exergy of air, exergy of water, and SLE of SCT is decreased. As relative

humidity of air was increased, the destruction in total exergy of system was relatively fewer because low relative humidity air absorbed more amount of water from droplets.

5.7.5 Effect of variation in inlet RLG (HCOML)

In this study inlet RLG was varied from 0.5 to 2, and constant inlet parameters of SCT are air DBT (36 ˚C), air relative humidity (65%), water droplet diameter 250 μm, and water temperature (56 ˚C). Table 5.30 shows as RLG increased exit air DBT, air specific humidity and droplet temperature increased because mass of water at inlet increased. Maximum and minimum water droplet temperature reduction is 19.25 ˚C and 11.89 ˚C which obtained at 0.5 and 2 RLG respectively. The range (i.e. $T_{d,in} - T_{d,out}$) of SCT decreased by increased RLG hence the thermal efficiency of SCT also decreased by increased the RLG. Total exergy of air, exergy of water increased with increasing the RLG because exit air and water droplet temperature and mass of water increased with increased the RLG. As the amount of water in RLG increased destruction in exergy of the system along tower height increased because the amount of exergy release by water is more than the amount of exergy gain by air. SLE of SCT increased with increased the RLG.

Table 5.30 Effect of variation in inlet RLG (HCOML)

1	2	3	4	5	6	7	8	9	10	11	12	13	14
Code	**RLG_{in}**	**$T_{a,out}$ (˚C)**	**$\omega_{a,out}$ (kg_w/kg_a)**	**$T_{d,out}$ (˚C)**	**$m_{d,l}$ (kg/s)**	**η_{th} (%)**	**$X_{c,out}$ (W)**	**$X_{e,out}$ (W)**	**$X_{a,out}$ (W)**	**$X_{d,out}$ (W)**	**$X_{t,out}$ (W)**	**I_t (W)**	**η_{II} (%)**
HCOML-1	**0.50**	**36.76**	**0.0405**	**36.75**	**0.0017**	**76.72**	**1.05**	**78.23**	**79.28**	**3317.58**	**3396.86**	**1337.39**	**71.75**
HCOML-2	**1.00**	**40.36**	**0.0508**	**40.35**	**0.0029**	**62.38**	**6.12**	**176.86**	**182.98**	**7431.77**	**7614.75**	**1853.59**	**80.42**
HCOML-3	**1.25**	**41.66**	**0.0548**	**41.65**	**0.0034**	**57.19**	**8.30**	**246.11**	**254.41**	**9535.75**	**9790.16**	**2045.21**	**82.72**
HCOML-4	**1.50**	**42.73**	**0.0577**	**42.72**	**0.0038**	**52.93**	**10.23**	**363.89**	**374.12**	**11612.82**	**11986.94**	**2215.47**	**84.40**
HCOML-5	**2.00**	**44.12**	**0.0614**	**44.11**	**0.0039**	**47.39**	**17.65**	**343.23**	**360.88**	**12502.90**	**12863.78**	**2285.44**	**84.91**

5.8 Two Dimensional Counter flow Multi Droplet SCT for Industrial Application

This research is based on 2-D multi droplet counter flow MATLAB model to determine the effect of variation in inlet droplet diameters, water temperatures, air DBT, relative humidity of air and RLG on outlet parameters. Initial conditions used for computer simulation are given in Table 5.3.

5.8.1 Effect of variation in initial droplets diameter (HCUMR)

The effect of variation of inlet multi droplet diameters on outlet air DBT, air specific humidity, water temperature, makeup water required, thermal efficiency, convective exergy of air, evaporative exergy of air, total exergy of air, water exergy, total exergy of system, exergy destruction and SLE at constant inlet air DBT (36 ˚C), air relative humidity (65%), water temperature (56 ˚C), and RLG (0.5) are given in Table 5.31.

Table 5.31 Effect of variation in inlet droplet diameter (HCUMR)

1	2	3	4	5	6	7	8	9	10	11	12	13	14
Code	D_{in} (µm)	$T_{a,out}$ (˚C)	$\omega_{a,out}$ (kg_w/kg_a)	$T_{d,m,out}$ (˚C)	$m_{d,l}$ (kg/s)	η_{th} (%)	$X_{c,out}$ (W)	$X_{e,out}$ (W)	$X_{a,out}$ (W)	$X_{d,out}$ (W)	$X_{t,out}$ (W)	I_t (W)	η_{II} (%)
HCUMR-1	**31.81-318.18**	**37.12**	**0.0411**	**37.11**	**0.0018**	**75.29**	**0.04**	**59.22**	**59.26**	**3367.45**	**3426.71**	**1307.54**	**72.38**
HCUMR-2	**63.63-636.36**	**42.4**	**0.0344**	**42.39**	**0.0013**	**54.24**	**0.01**	**76.58**	**76.59**	**3576.24**	**3652.83**	**1081.42**	**77.16**
HCUMR-3	**127.27-1272.70**	**48.52**	**0.0276**	**48.51**	**0.0009**	**29.85**	**0**	**13.05**	**13.05**	**3923.21**	**3936.26**	**797.99**	**83.14**
HCUMR-4	**190.91-1909.10**	**50.91**	**0.0251**	**50.9**	**0.0006**	**20.33**	**0**	**5.14**	**5.14**	**4045.94**	**4051.08**	**683.17**	**85.57**
HCUMR-5	**254.55-2545.50**	**51.82**	**0.0242**	**51.81**	**0.0004**	**16.70**	**0**	**3.93**	**3.93**	**4102.91**	**4106.84**	**627.41**	**86.75**

As multi droplet diameter increased exit air DBT and water temperature increased and exit specific humidity, make up water required and thermal efficiency of SCT decreased because heat and mass transfer between air and water droplet

decreased. For smaller size droplet the decreased in droplet temperature and increased in specific humidity of air is relatively faster because smaller size droplets cover larger area in SCT. It is also clear that 250 µm size water droplets produce maximum cooling; it reduces droplet temperature up to 18.89 °C. Total exergy of air is the sum of exergy due to conductive and evaporative heat transfer. Total exergy of air and exergy destruction decreased as inlet droplet diameter increased. Exergy of water, exergy of system and SLE increased with increased the droplet diameter because heat and mass transfer between air and water decreased.

5.8.2 Effect of variation in inlet Water Temperature (HCUMD)

The Inlet water temperature was varied from 50 ˚C to 58 ˚C in this research and its effects on various exit parameters are given in Table 5.32. The constant important inlet parameters used for this study are air DBT (36 ˚C), air relative humidity (65%), multi droplet diameter (31.81-318.18 µm), and RLG (0.5).

Table 5.32 Effect of variation in inlet water temperature (HCUMD)

1	2	3	4	5	6	7	8	9	10	11	12	13	14
Code	$T_{d,in}$ (˚C)	$T_{a,out}$ (˚C)	$\omega_{a,out}$ (kg_w/kg_a)	$T_{d,m,out}$ (˚C)	$m_{d,l}$ (kg/s)	η_{th} (%)	$X_{c,out}$ (W)	$X_{e,out}$ (W)	$X_{a,out}$ (W)	$X_{d,out}$ (W)	$X_{t,out}$ (W)	I_t (W)	η_{II} (%)
HCUMD-1	**50**	**35.31**	**0.0369**	**35.30**	**0.0012**	**77.00**	**0.00**	**37.19**	**37.19**	**3324.73**	**3361.92**	**1044.46**	**76.30**
HCUMD-2	**52**	**35.93**	**0.0383**	**35.92**	**0.0014**	**76.24**	**0.00**	**43.64**	**43.64**	**3339.03**	**3382.67**	**1127.69**	**75.00**
HCUMD-3	**54**	**36.57**	**0.0397**	**36.56**	**0.0016**	**75.53**	**0.01**	**51.61**	**51.62**	**3352.66**	**3404.28**	**1215.40**	**73.69**
HCUMD-4	**56**	**37.12**	**0.0411**	**37.11**	**0.0018**	**75.29**	**0.04**	**59.22**	**59.26**	**3367.45**	**3426.71**	**1307.55**	**72.38**
HCUMD-5	**58**	**37.66**	**0.0424**	**37.65**	**0.0019**	**75.12**	**0.96**	**72.91**	**73.87**	**3375.98**	**3449.85**	**1404.16**	**71.07**

Table 5.32 shows as inlet water temperature increased exit air DBT, air specific humidity, water temperature, and makeup water required increased. The Thermal efficiency of SCT decreased with increased the inlet water temperature. It also observed that when the temperature of inlet water is 58 ˚C, maximum cooling of the droplet was achieved at 18.19 ˚C. Specific humidity of air increased with increase

in inlet water temperature because more water vapour mixed in air. Similarly the exergy destruction of system increased, and SLE decreased with increased the inlet water droplet temperature.

5.8.3 Effect of variation in inlet air DBT (HCUMA)

This research based on the variation of inlet air DBT from 24 ˚C to 48 ˚C. Table 5.33 shows deviations in outlet parameters at constant inlet air relative humidity (65 %), water temperature (56 ˚C), and droplet diameter (31.81-318.18 µm) and RLG (0.5). It was observed from Table 5.33 that exit air DBT, specific humidity, water droplet temperatures, and thermal efficiency of SCT increased relatively as inlet air DBT increased; it also shows 24 ˚C DBT air produce maximum cooling and it cool down water droplet up to 24.23 ˚C. The total exergy of air, exergy of water, and total exergy of system decreased with increased the inlet air DBT temperature. The SLE of the system increased because exergy destruction decreased with increasing the initial air DBT.

Table 5.33 Effect of variation in inlet air DBT (HCUMA)

1	2	3	4	5	6	7	8	9	10	11	12	13	14
Code	$T_{a,in}$ (˚C)	$T_{a,out}$ (˚C)	$\omega_{a,out}$ (kg_w/kg_a)	$T_{d,m,out}$ (˚C)	$m_{d,l}$ (kg/s)	η_{th} (%)	$X_{c,out}$ (W)	$X_{e,out}$ (W)	$X_{a,out}$ (W)	$X_{d,out}$ (W)	$X_{t,out}$ (W)	I_t (W)	η_{II} (%)
HCUMA-1	**24**	**31.78**	**0.0292**	**31.77**	**0.0026**	**66.04**	**21.53**	**222.29**	**243.82**	**3529.24**	**3773.06**	**1598.90**	**70.24**
HCUMA-2	**30**	**33.88**	**0.0344**	**33.87**	**0.0025**	**71.04**	**5.69**	**144.91**	**150.6**	**3445.23**	**3595.83**	**1453.13**	**71.22**
HCUMA-3	**36**	**37.12**	**0.0411**	**37.11**	**0.0018**	**75.29**	**0.04**	**59.22**	**59.26**	**3367.45**	**3426.71**	**1307.54**	**72.38**
HCUMA-4	**42**	**39.78**	**0.0499**	**39.77**	**0.0017**	**88.64**	**0.02**	**24.86**	**24.88**	**3255.66**	**3280.54**	**1145.87**	**74.11**
HCUMA-5	**48**	**45.5**	**0.0612**	**45.49**	**0.0014**	**99.62**	**0.01**	**18.86**	**18.87**	**3178.2**	**3197.07**	**1027.15**	**75.68**

5.8.4 Effect of variation in inlet Air Relative Humidity (HCUMH)

The effects of deviation of inlet relative humidity from 20% to 80% on the exit parameters at constant inlet air DBT (36 ˚C), water temperature (56 ˚C), droplet diameter (31.81-318.18 µm), and RLG (0.5) are given in Table 5.34.

Table 5.34 Effect of variation in inlet air relative humidity (HCUMH)

1	2	3	4	5	6	7	8	9	10	11	12	13	14
Code	ϕ_{in} (%)	$T_{a,out}$ (˚C)	$\omega_{a,out}$ (kg_w/kg_a)	$T_{d,m,out}$ (˚C)	$m_{d,l}$ (kg/s)	η_{th} (%)	$X_{c,out}$ (W)	$X_{e,out}$ (W)	$X_{a,out}$ (W)	$X_{d,out}$ (W)	$X_{t,out}$ (W)	I_t (W)	η_{II} (%)
HCUMH-1	**20**	**32.93**	**0.0305**	**32.92**	**0.0036**	**63.70**	**2.03**	**536.18**	**538.21**	**13111.32**	**13649.53**	**1739.66**	**88.70**
HCUMH-2	**35**	**34.39**	**0.0340**	**34.38**	**0.0031**	**67.23**	**1.57**	**238.67**	**240.24**	**8517.41**	**8757.65**	**1560.92**	**84.87**
HCUMH-3	**50**	**35.79**	**0.0374**	**35.78**	**0.0027**	**71.00**	**1.04**	**150.48**	**151.52**	**5522.44**	**5673.96**	**1422.47**	**79.96**
HCUMH-4	**65**	**37.12**	**0.0411**	**37.11**	**0.0018**	**75.29**	**0.04**	**59.22**	**59.26**	**3367.45**	**3426.71**	**1307.54**	**72.38**
HCUMH-5	**80**	**38.39**	**0.0446**	**38.38**	**0.0023**	**80.31**	**0.00**	**34.76**	**34.76**	**1628.01**	**1662.77**	**1214.76**	**57.78**

It was observed that exit air DBT, specific humidity, droplet temperature and thermal efficiency of SCT increased with increased the air relative humidity. Table 5.34 also shows 20% relative humidity air produced maximum cooling, i.e. up to 23.08 ˚C and 80% relative humidity air give maximum thermal efficiency (80.31%) of SCT. Table 5.34 also shows as the relative humidity of air increased the change in total exergy of air, exergy of water, and SLE of SCT was decreased. As relative humidity of air increased, the destruction in total exergy of system relatively decreased because low relative humidity air absorbs more amount of water from droplets.

5.8.5 Effect of variation in inlet RLG (HCUML)

This study was based on the variation of RLG from 0.5 to 2.0. The constant inlet parameters of this study was air DBT (36 ˚C), air relative humidity (65%), water temperature (56 ˚C), and droplet diameter (31.81-318.18 µm). Table 5.35 shows that

as RLG increased, exit air DBT, air specific humidity and droplet temperature increased because the mass of water at inlet increased. Maximum and minimum water droplet temperature reduction is 18.89 ˚C and 11.59 ˚C which obtained at 0.5 and 2 RLG respectively. The range of SCT decreased by increasing the RLG hence the thermal efficiency of SCT also decreased by increasing the RLG. Total exergy of air, exergy of water increased with increasing the RLG because exit air and water droplet temperature and mass of water increased with increasing the RLG. As the amount of water in water to air mass flow ratio increases destruction in exergy of system along tower height increases because the amount of exergy release by water is more than the amount of exergy gained by air. SLE of SCT increases with increase in the RLG.

Table 5.35 Effect of variation in inlet RLG (HCUML)

1	2	3	4	5	6	7	8	9	10	11	12	13	14
Code	**RLG**$_{in}$	$T_{a,out}$ (˚C)	$\omega_{a,out}$ (kg_w/kg_a)	$T_{d,m,out}$ (˚C)	$m_{d,l}$ (kg/s)	η_{th} (%)	$X_{c,out}$ (W)	$X_{e,out}$ (W)	$X_{a,out}$ (W)	$X_{d,out}$ (W)	$X_{t,out}$ (W)	I_t (W)	η_{II} (%)
HCUML-1	**0.5**	**37.12**	**0.0411**	**37.11**	**0.0018**	**75.29**	**0.04**	**59.22**	**59.26**	**3367.45**	**3426.71**	**1307.54**	**72.38**
HCUML-2	**1**	**40.69**	**0.0514**	**40.68**	**0.0030**	**61.06**	**4.43**	**212.36**	**216.79**	**7426.95**	**7643.74**	**1824.60**	**80.73**
HCUML-3	**1.25**	**41.92**	**0.0554**	**41.91**	**0.0035**	**56.16**	**7.32**	**265.33**	**272.65**	**9545.18**	**9817.83**	**2017.54**	**82.95**
HCUML-4	**1.5**	**42.94**	**0.0584**	**42.93**	**0.0039**	**52.09**	**11.23**	**311.68**	**322.91**	**11687.65**	**12010.56**	**2191.85**	**84.57**
HCUML-5	**2**	**44.41**	**0.0621**	**44.41**	**0.0040**	**46.19**	**15.79**	**311.06**	**326.85**	**12562.87**	**12889.72**	**2259.50**	**85.09**

5.9 Three Dimensional Counter flow Mono Droplet SCT for Industrial Application

This research is based on 3-D mono droplet counter flow CFD model to determine the effect of variation in inlet droplet diameters, water temperatures, air DBT, relative humidity of air and RLG on outlet parameters. Schematic diagram of 3-D counter flow SCT is shown in Figure 3.2. The mesh of 3-D counter flow SCT is

shown in Figure 5.8. Initial conditions used for computer simulation are given in Table 5.2.

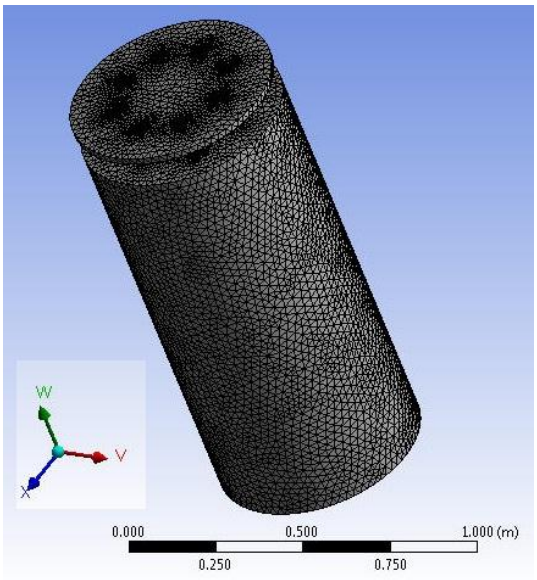

Figure 5.8 Mesh of three dimensional counter flow SCT

5.9.1 Effect of variation in initial droplets diameter (HCOCR)

Table 5.36 shows the variation in SCT exit parameters by varying inlet droplet diameter. The other significant constant inlet parameters of SCT are air DBT (36 ˚C), air relative humidity (65%), water temperature (56 ˚C), and RLG (0.5). As droplet diameter increases from 250 µm to 2000 µm, exit air DBT and water temperature increases and exit specific humidity, make up water required and thermal efficiency of SCT decreases because heat and mass transfer between air and water droplet decreases. Maximum and minimum water droplet temperature reduction is 18.55 ˚C and 03.89 ˚C which obtained at 250 µm and 2000 µm respectively. Maximum SCT efficiency was achieved with 250 µm droplet diameter and it was 73.93%. Total exergy of water and exergy of the system increased with increase in the droplet diameter. The SLE of SCT increased and exergy destruction of system decreased with

increased the droplet diameters because heat and mass transfer between air and water decreases.

Table 5.36 Effect of variation in inlet droplet diameter (HCOCR)

1	2	3	4	5	6	7	8	9	10	11	12	13	14
Code	D_{in} (μm)	$T_{a,out}$ (˚C)	$\omega_{a,out}$ (kg_w/kg_a)	$T_{d,out}$ (˚C)	$m_{d,l}$ (kg/s)	η_{th} (%)	$X_{c,out}$ (W)	$X_{e,out}$ (W)	$X_{a,out}$ (W)	$X_{d,out}$ (W)	$X_{t,out}$ (W)	I_t (W)	η_{II} (%)
HCOCR-1	**250**	**37.46**	**0.0417**	**37.45**	**0.0019**	**73.93**	**1.36**	**84.41**	**85.77**	**3371.06**	**3456.83**	**1277.42**	**73.02**
HCOCR-2	**500**	**42.74**	**0.0350**	**42.73**	**0.0014**	**52.87**	**1.27**	**76.19**	**77.46**	**3605.49**	**3682.95**	**1051.31**	**77.79**
HCOCR-3	**1000**	**48.86**	**0.0282**	**48.85**	**0.0010**	**28.49**	**1.14**	**23.54**	**24.68**	**3941.7**	**3966.38**	**767.88**	**83.78**
HCOCR-4	**1500**	**51.24**	**0.0256**	**51.23**	**0.0007**	**19.00**	**0.67**	**6.11**	**6.78**	**4074.42**	**4081.20**	**653.06**	**86.21**
HCOCR-5	**2000**	**52.15**	**0.0247**	**52.14**	**0.0005**	**15.38**	**0.45**	**7.87**	**8.32**	**4128.64**	**4136.96**	**597.30**	**87.38**

5.9.2 Effect of variation in inlet Water Temperature (HCOCD)

This study was based on the variation of inlet water temperature from 50 ˚C to 58 ˚C. The constant initial key parameters of SCT are air DBT (36 ˚C), air relative humidity (65%), water droplet diameter (250 μm), and RLG (0.5). Table 5.37 is shown as inlet water temperature increased exit air DBT, air specific humidity, water temperature, and makeup water required increased. It also shows that when the temperature of inlet water is 58 ˚C, maximum cooling of the droplet is achieved (20 ˚C) as the high temperature difference between water and air (keeping air temperature constant). Maximum SCT efficiency (75.18%) achieved by 50 ˚C inlet droplet temperature. As inlet water droplet temperature increased, the specific humidity of air increased because due to rise in water temperature more water vapour is added in air. Table 5.37 shows the thermal efficiency of SCT deceased by increased the water droplet temperature. Table 5.37 also shows that increased in inlet water temperature, more quantity of water vapour mixed in the air and increased total exergy of air. The exergy destruction of the system increased and SLE decreased by increased the inlet water droplet temperature. Depicted destruction in total exergy of the system is more

for higher temperature droplet because it transfers water content in to air faster than lower temperature droplets.

Table 5.37 Effect of variation in inlet water temperature (HCOCD)

1	2	3	4	5	6	7	8	9	10	11	12	13	14
Code	$T_{d,in}$ (˚C)	$T_{a,out}$ (˚C)	$\omega_{a,out}$ (kg_w/kg_a)	$T_{d,out}$ (˚C)	$m_{d,l}$ (kg/s)	η_{th} (%)	$X_{c,out}$ (W)	$X_{e,out}$ (W)	$X_{a,out}$ (W)	$X_{d,out}$ (W)	$X_{t,out}$ (W)	I_t (W)	η_{II} (%)
HCOCD-1	**50**	**35.65**	**0.0375**	**35.64**	**0.0013**	**75.18**	**2.16**	**37.52**	**39.68**	**3352.38**	**3392.06**	**1014.32**	**76.98**
HCOCD-2	**52**	**36.27**	**0.0389**	**36.26**	**0.0015**	**74.60**	**1.84**	**60.45**	**62.29**	**3350.51**	**3412.80**	**1097.56**	**75.67**
HCOCD-3	**54**	**36.91**	**0.0403**	**36.90**	**0.0017**	**74.03**	**1.45**	**65.03**	**66.48**	**3367.92**	**3434.40**	**1185.28**	**74.34**
HCOCD-4	**56**	**37.46**	**0.0417**	**37.45**	**0.0019**	**73.93**	**1.36**	**84.41**	**85.77**	**3371.06**	**3456.83**	**1277.42**	**73.02**
HCOCD-5	**58**	**38.01**	**0.0431**	**38.00**	**0.0020**	**73.80**	**1.01**	**98.29**	**99.30**	**3380.66**	**3479.96**	**1374.05**	**71.69**

5.9.3 Effect of variation in inlet air DBT (HCOCA)

In this research, constant inlet parameters of SCT are air relative humidity (65%), water droplet diameter (250 μm), water temperature (56 ˚C), RLG (0.5), and inlet DBT of air was varied from 24 - 48 ˚C. Table 5.38 shows exit air DBT, air specific humidity and droplet temperatures increased as inlet air DBT increased, it also shows 24 ˚C DBT air produce maximum cooling, and it cools down water droplet up to 23.80 ˚C.

Table 5.38 Effect of variation in inlet air DBT (HCOCA)

1	2	3	4	5	6	7	8	9	10	11	12	13	14
Code	$T_{a,in}$ (˚C)	$T_{a,out}$ (˚C)	$\omega_{a,out}$ (kg_w/kg_a)	$T_{d,out}$ (˚C)	$m_{d,l}$ (kg/s)	η_{th} (%)	$X_{c,out}$ (W)	$X_{e,out}$ (W)	$X_{a,out}$ (W)	$X_{d,out}$ (W)	$X_{t,out}$ (W)	I_t (W)	η_{II} (%)
HCOCA-1	**24**	**32.21**	**0.0298**	**32.2**	**0.0037**	**64.87**	**20.32**	**218.81**	**239.13**	**3565.13**	**3804.26**	**1567.70**	**70.82**
HCOCA-2	**30**	**34.26**	**0.0351**	**34.25**	**0.0032**	**69.82**	**10.87**	**184.94**	**195.81**	**3430.96**	**3626.77**	**1422.19**	**71.83**
HCOCA-3	**36**	**37.46**	**0.0417**	**37.45**	**0.0019**	**73.93**	**1.36**	**84.41**	**85.77**	**3371.06**	**3456.83**	**1277.42**	**73.02**
HCOCA-4	**42**	**40.09**	**0.0505**	**40.08**	**0.0023**	**86.95**	**1.03**	**39.76**	**40.79**	**3269.39**	**3310.18**	**1116.23**	**74.78**
HCOCA-5	**48**	**45.78**	**0.0618**	**45.77**	**0.0018**	**96.97**	**0.91**	**10.72**	**11.63**	**3214.58**	**3226.21**	**998.02**	**76.37**

Table 5.38 also represents that increased in inlet air DBT, the thermal efficiency of SCT increased, and maximum thermal efficiency (96.97%) achieved at 48 ˚C. The convective exergy of air, evaporative exergy of air, total exergy of air, exergy of water, and total exergy of system decreased with increased the inlet air DBT temperature. The SLE of the system increased because exergy destruction decreased with increased the initial air DBT.

5.9.4 Effect of variation in inlet Air Relative Humidity (HCOCH)

In present research the Table 5.39 shows the effect of deviation in exit parameters of SCT at constant inlet air DBT (36 ˚C), water temperature (56 ˚C), water droplet diameter (250 µm), and RLG (0.5) by varying the inlet air relative humidity from 20% to 80%. Table 5.39 shows exit air DBT, specific humidity, droplet temperature and thermal efficiency of SCT increased with increased the air relative humidity. Table 5.39 also shows 20% relative humidity air produce maximum cooling, i.e. up to 22.73 ˚C and 80% relative humidity air give maximum efficiency (78.76%). Table 5.39 also shows as the relative humidity of air increased the change in total exergy of air, exergy of water, and SLE of SCT is decreased. As relative humidity of air was increased, the destruction in total exergy of the system relatively less because low relative humidity air absorb more amount of water from water droplets.

Table 5.39 Effect of variation in inlet air relative humidity (HCOCH)

1	2	3	4	5	6	7	8	9	10	11	12	13	14
Code	ϕ_{in} (%)	$T_{a,out}$ (˚C)	$\omega_{a,out}$ (kg_w/kg_a)	$T_{d,out}$ (˚C)	$m_{d,l}$ (kg/s)	η_{th} (%)	$X_{c,out}$ (W)	$X_{e,out}$ (W)	$X_{a,out}$ (W)	$X_{d,out}$ (W)	$X_{t,out}$ (W)	I_t (W)	η_{II} (%)
HCOCH-1	**20**	**33.28**	**0.0311**	**33.27**	**0.0035**	**62.74**	**4.73**	**394.44**	**399.17**	**13280.5**	**13679.67**	**1709.53**	**88.89**
HCOCH-2	**35**	**34.74**	**0.0346**	**34.73**	**0.0034**	**66.14**	**3.71**	**342.76**	**346.47**	**8441.32**	**8787.79**	**1530.77**	**85.16**

HCOCH-3	**50**	**36.14**	**0.038**	**36.13**	**0.0031**	**69.77**	**2.43**	**216.34**	**218.77**	**5485.32**	**5704.09**	**1392.33**	**80.38**
HCOCH-4	**65**	**37.46**	**0.0417**	**37.45**	**0.0019**	**73.93**	**1.36**	**84.41**	**85.77**	**3371.06**	**3456.83**	**1277.42**	**73.02**
HCOCH-5	**80**	**38.73**	**0.0453**	**38.72**	**0.0021**	**78.76**	**0.11**	**66.12**	**66.23**	**1626.66**	**1692.89**	**1184.64**	**58.83**

5.9.5 Effect of variation in inlet RLG (HCOCL)

In This section variation of RLG was 0.5 to 2.0, and the constant inlet parameters of SCT was air DBT (36 ˚C), air relative humidity (65%), water temperature (56 ˚C), water droplet diameter (250 μm), and RLG (0.5). Table 5.40 shows as RLG increased in exit air DBT, air specific humidity and droplet temperature increased because the mass of water at inlet increased. Maximum and minimum water droplet temperature reduction was 18.55 ˚C and 11.31 ˚C which were obtained at 0.5 and 2 RLG respectively. The range of SCT decreased by increased RLG hence the thermal efficiency of SCT also decreased by increasing the RLG. Total exergy of air, exergy of water increased with increasing the RLG because exit air and water droplet temperature and mass of water increased with increased the RLG. As the amount of water in RLG increased destruction in exergy of system along tower height increased because the amount of exergy released by water was more than the amount of exergy gain by air. SLE of SCT increased with increased the RLG.

Table 5.40 Effect of variation in inlet RLG (HCOCL)

1	2	3	4	5	6	7	8	9	10	11	12	13	14
Code	**RLG**$_{in}$	$T_{a,out}$ (˚C)	$\omega_{a,out}$ (kg_w/kg_a)	$T_{d,out}$ (˚C)	$m_{d,l}$ (kg/s)	η_{th} (%)	$X_{c,out}$ (W)	$X_{e,out}$ (W)	$X_{a,out}$ (W)	$X_{d,out}$ (W)	$X_{t,out}$ (W)	I_t (W)	η_{II} (%)
HCOCL-1	**0.50**	**37.46**	**0.0417**	**37.45**	**0.0019**	**73.93**	**1.36**	**84.41**	**85.77**	**3371.06**	**3456.83**	**1277.42**	**73.02**
HCOCL-2	**1.00**	**41.00**	**0.0520**	**40.99**	**0.0031**	**59.82**	**7.22**	**176.86**	**184.08**	**7489.00**	**7673.08**	**1795.26**	**81.04**
HCOCL-3	**1.25**	**42.17**	**0.0560**	**42.16**	**0.0036**	**55.16**	**9.49**	**246.11**	**255.60**	**9590.21**	**9845.81**	**1989.56**	**83.19**
HCOCL-4	**1.50**	**43.17**	**0.0591**	**43.16**	**0.0040**	**51.18**	**12.78**	**363.89**	**376.67**	**11657.88**	**12034.55**	**2167.86**	**84.74**
HCOCL-5	**2.00**	**44.69**	**0.0628**	**44.69**	**0.0041**	**45.08**	**20.15**	**336.26**	**356.41**	**12559.78**	**12916.19**	**2233.03**	**85.26**

5.10 Three Dimensional Counter flow Multi Droplet SCT for Industrial Application

In this research, 3-D multi droplet counter flow CFD model used to determine the effect of variation in inlet droplet diameters, water temperatures, air DBT, relative humidity of air and RLG on outlet parameters. Schematic diagram of 3-D counter flow SCT is shown in Figure 3.2. The mesh of 3-D counter flow SCT is shown in Figure 5.8. Initial conditions used for computer simulation are given in Table 5.3.

5.10.1 Effect of variation in initial droplets diameter (HCUCR)

This study represents the variation of outlet water and air parameters with varying the inlet droplet diameter. The other inlet parameters for this study are air DBT (36 ˚C), air relative humidity (65%), water temperature (56 ˚C), and RLG (0.5). Table 5.41 shows as multi droplet diameter increased exit air DBT and water temperature increased and exit specific humidity, make up water required and thermal efficiency of SCT decreased because heat and mass transfer between air and water droplet decreased.

Table 5.41 Effect of variation in inlet droplet diameter (HCUCR)

1	2	3	4	5	6	7	8	9	10	11	12	13	14
Code	D_{in} (µm)	$T_{a,out}$ (˚C)	$\omega_{a,out}$ (kg_w/kg_a)	$T_{d,m,out}$ (˚C)	$m_{d,l}$ (kg/s)	η_{th} (%)	$X_{c,out}$ (W)	$X_{e,out}$ (W)	$X_{a,out}$ (W)	$X_{d,out}$ (W)	$X_{t,out}$ (W)	I_t (W)	η_{II} (%)
HCUCR-1	**31.81-318.18**	**37.84**	**0.0423**	**37.83**	**0.002**	**72.42**	**0.95**	**73.62**	**74.57**	**3412.90**	**3487.47**	**1246.78**	**73.66**
HCUCR-2	**63.63-636.36**	**43.12**	**0.0356**	**43.11**	**0.0015**	**51.38**	**0.82**	**76.58**	**77.4**	**3636.19**	**3713.59**	**1020.66**	**78.44**
HCUCR-3	**127.27-1272.70**	**49.24**	**0.0288**	**49.23**	**0.0011**	**26.98**	**0.64**	**13.05**	**13.69**	**3983.33**	**3997.02**	**737.23**	**84.43**
HCUCR-4	**190.91-1909.10**	**51.61**	**0.0261**	**51.6**	**0.0008**	**17.54**	**0.58**	**5.14**	**5.72**	**4106.12**	**4111.84**	**622.41**	**86.85**
HCUCR-5	**254.55-2545.50**	**52.52**	**0.0252**	**52.51**	**0.0006**	**13.91**	**0.39**	**2.14**	**2.53**	**4165.07**	**4167.6**	**566.65**	**88.03**

It is also clear that 31.81-318.18 µm size water droplets produce maximum cooling (18.17 °C) and maximum efficiency (72.42%). Total exergy of air and exergy destruction decreased as inlet droplet diameter increased. Exergy of water, exergy of system and SLE increased with increased the droplet diameter because heat and mass transfer between air and water decreased.

5.10.2 Effect of variation in inlet Water Temperature (HCUCD)

The change of inlet water temperatures from 50 - 58 ˚C on different outlet parameters are given in Table 5.42. The other fixed inlet parameters are air DBT (36 ˚C), air relative humidity (65%), multi droplet diameter (31.81-318.18 µm), and RLG (0.5). Table 5.42 shows as inlet water temperature increased exit air DBT, air specific humidity, water temperature, and makeup water required increased. It also observed that when the temperature of inlet water is 58 ˚C, maximum cooling of droplet was 19.61 ˚C at the high temperature difference between water and air (keeping air temperature constant).

Table 5.42 Effect of variation in inlet water temperature (HCUCD)

1	2	3	4	5	6	7	8	9	10	11	12	13	14
Code	$T_{d,in}$ (˚C)	$T_{a,out}$ (˚C)	$\omega_{a,out}$ (kg_w/kg_a)	$T_{d,m,out}$ (˚C)	$m_{d,l}$ (kg/s)	η_{th} (%)	$X_{c,out}$ (W)	$X_{e,out}$ (W)	$X_{a,out}$ (W)	$X_{d,out}$ (W)	$X_{t,out}$ (W)	I_t (W)	η_{II} (%)
HCUCD-1	**50**	**36.03**	**0.0381**	**36.02**	**0.0014**	**73.23**	**0.43**	**26.16**	**26.59**	**3396.29**	**3422.88**	**983.49**	**77.68**
HCUCD-2	**52**	**36.65**	**0.0395**	**36.64**	**0.0016**	**72.83**	**0.61**	**37.64**	**38.25**	**3405.31**	**3443.56**	**1066.80**	**76.35**
HCUCD-3	**54**	**37.29**	**0.0409**	**37.28**	**0.0018**	**72.41**	**0.87**	**54.61**	**55.48**	**3409.61**	**3465.09**	**1154.59**	**75.01**
HCUCD-4	**56**	**37.84**	**0.0423**	**37.83**	**0.0020**	**72.42**	**0.95**	**73.62**	**74.57**	**3412.90**	**3487.47**	**1246.78**	**73.66**
HCUCD-5	**58**	**38.4**	**0.0438**	**38.39**	**0.0021**	**72.39**	**1.36**	**109.16**	**110.52**	**3400.04**	**3510.56**	**1343.45**	**72.32**

The thermal efficiency of SCT decreased with increased the inlet water temperature. As inlet water droplet temperature increased, the specific humidity of air increased because due to increase in water temperature more water vapour is added in

the air, Table 5.42 also shows that increased in inlet water temperature, more quantity of water vapour mixed in the air and increased total exergy of air. The exergy destruction of the system increased, and SLE decreased by increased the inlet water droplet temperature. Depicted destruction in total exergy of the system was more for higher temperature droplet because it transfers water content in to air faster than lower temperature droplets.

5.10.3 Effect of variation in inlet air DBT (HCUCA)

In present section DBT of air was varied from 24 - 48 ˚C and other important inlet parameters are air relative humidity (65%), water temperature (56 ˚C), multi droplet diameter (31.81-318.18 µm), and RLG (0.5). From Table 5.43 it was observed that exit air DBT, specific humidity and droplet temperatures increased relatively as inlet air DBT increased; it also shows 24 ˚C DBT air produce highest cooling and it cool down water droplet up to 23.34 ˚C. Table 5.43 also represents that increased in inlet air DBT temperature, the thermal efficiency of SCT increased. Maximum thermal efficiency attained was 93.93% by 48 ˚C inlet air DBT. The convective exergy of air, evaporative exergy of air, total exergy of air, exergy of water, and total exergy of system decreased with increased the inlet air DBT temperature. The SLE of system increased because exergy destruction decreased with increased the initial air DBT.

Table 5.43 Effect of variation in inlet air DBT (HCUCA)

1	2	3	4	5	6	7	8	9	10	11	12	13	14
Code	$T_{a,in}$ (˚C)	$T_{a,out}$ (˚C)	$\omega_{a,out}$ (kg_w/kg_a)	$T_{d,m,out}$ (˚C)	$m_{d,l}$ (kg/s)	η_{th} (%)	$X_{c,out}$ (W)	$X_{e,out}$ (W)	$X_{a,out}$ (W)	$X_{d,out}$ (W)	$X_{t,out}$ (W)	I_t (W)	η_{II} (%)
HCUCA-1	**24**	**32.67**	**0.0304**	**32.66**	**0.0026**	**63.61**	**2.52**	**208.63**	**211.15**	**3624.31**	**3835.46**	**1536.50**	**71.40**
HCUCA-2	**30**	**34.68**	**0.0356**	**34.67**	**0.0025**	**68.48**	**1.93**	**144.91**	**146.84**	**3510.87**	**3657.71**	**1391.25**	**72.44**
HCUCA-3	**36**	**37.84**	**0.0423**	**37.83**	**0.0020**	**72.42**	**0.95**	**73.62**	**74.57**	**3412.90**	**3487.47**	**1246.78**	**73.66**
HCUCA-4	**42**	**40.44**	**0.0511**	**40.43**	**0.0017**	**85.04**	**0.54**	**59.76**	**60.3**	**3279.52**	**3339.82**	**1086.59**	**75.45**
HCUCA-5	**48**	**46.1**	**0.0624**	**46.09**	**0.0013**	**93.93**	**0.16**	**26.68**	**26.84**	**3228.51**	**3255.35**	**968.87**	**77.06**

5.10.4 Effect of variation in inlet Air Relative Humidity (HCUCH)

In This research inlet relative humidity varied from 20% to 80% and inlet constant parameters of SCT are air DBT (36 ˚C), multi droplet diameter (31.81-318.18 μm, water temperature (56 ˚C), and RLG (0.5). Table 5.44 shows effects of variation of inlet relative humidity on outlet water and air parameters.

Table 5.44 Effect of variation in inlet air relative humidity (HCUCH)

1	2	3	4	5	6	7	8	9	10	11	12	13	14
Code	ϕ_{in} (%)	$T_{a,out}$ (˚C)	$\omega_{a,out}$ (kg_w/kg_a)	$T_{d,m,out}$ (˚C)	$m_{d,l}$ (kg/s)	η_{th} (%)	$X_{c,out}$ (W)	$X_{e,out}$ (W)	$X_{a,out}$ (W)	$X_{d,out}$ (W)	$X_{t,out}$ (W)	I_t (W)	η_{II} (%)
HCUCH-1	**20**	**33.66**	**0.0317**	**33.65**	**0.0035**	**61.69**	**1.91**	**455.37**	**457.28**	**13253.05**	**13710.33**	**1678.86**	**89.09**
HCUCH-2	**35**	**35.12**	**0.0352**	**35.11**	**0.0029**	**64.96**	**1.52**	**238.67**	**240.19**	**8578.26**	**8818.45**	**1500.12**	**85.46**
HCUCH-3	**50**	**36.52**	**0.0386**	**36.51**	**0.0027**	**68.43**	**1.02**	**150.48**	**151.5**	**5583.24**	**5734.74**	**1361.69**	**80.81**
HCUCH-4	**65**	**37.84**	**0.0423**	**37.83**	**0.0020**	**72.42**	**0.95**	**73.62**	**74.57**	**3412.90**	**3487.47**	**1246.78**	**73.66**
HCUCH-5	**80**	**39.11**	**0.046**	**39.1**	**0.0022**	**77.03**	**0.27**	**93.55**	**93.82**	**1629.71**	**1723.53**	**1154.00**	**59.90**

It was observed that exit air DBT, specific humidity, droplet temperature and thermal efficiency of SCT increased with increased the air relative humidity. Table 5.44 also shows 20% relative humidity air produce maximum cooling (22.35 ˚C), and 80% relative humidity air give maximum efficiency (77.03%). Table 5.44 also shows as relative humidity of air increased the change in total exergy of air, exergy of water, and SLE of SCT was decreased. As relative humidity of air increased, the destruction

in total exergy of the system relatively decreased because low relative humidity air absorbs more amount of water from droplets.

5.10.5 Effect of variation in inlet RLG (HCUCL)

In this section variation of RLG was from 0.5 to 2.0 and inlet constant parameters of SCT are air DBT (36 ˚C), air relative humidity (65%), multi droplet diameter (31.81-318.18 µm), and water temperature (56 ˚C). Table 5.45 shows as RLG increased exit air DBT, air specific humidity, droplet temperature, and makeup water required increased because the mass of water at inlet increased.

Table 5.45 Effect of variation in inlet RLG (HCUCL)

1	2	3	4	5	6	7	8	9	10	11	12	13	14
Code	**RLG**$_{in}$	$T_{a,out}$ (˚C)	$\omega_{a,out}$ (kg_w/kg_a)	$T_{d,m,out}$ (˚C)	$m_{d,l}$ (kg/s)	η_{th} (%)	$X_{c,out}$ (W)	$X_{e,out}$ (W)	$X_{a,out}$ (W)	$X_{d,out}$ (W)	$X_{t,out}$ (W)	I_t (W)	η_{II} (%)
HCUCL-1	**0.5**	**37.84**	**0.0423**	**37.83**	**0.0020**	**72.42**	**0.95**	**73.62**	**74.57**	**3412.90**	**3487.47**	**1246.78**	**73.66**
HCUCL-2	**1**	**41.34**	**0.0526**	**41.33**	**0.0032**	**58.47**	**5.68**	**212.36**	**218.04**	**7484.46**	**7702.5**	**1765.84**	**81.35**
HCUCL-3	**1.25**	**42.45**	**0.0566**	**42.44**	**0.0037**	**54.05**	**8.51**	**265.33**	**273.84**	**9600.11**	**9873.95**	**1961.42**	**83.43**
HCUCL-4	**1.5**	**43.40**	**0.0599**	**43.39**	**0.0041**	**50.26**	**12.91**	**311.68**	**324.59**	**11733.83**	**12058.42**	**2143.99**	**84.90**
HCUCL-5	**2**	**44.99**	**0.0636**	**44.98**	**0.0042**	**43.92**	**17.63**	**310.81**	**328.44**	**12614.27**	**12942.71**	**2206.51**	**85.43**

Maximum and minimum water droplet temperature reduction is 18.17 ˚C and 11.02 ˚C which were obtained at 0.5 and 2 RLG respectively. The range of SCT decreased by increased the RLG hence the thermal efficiency of SCT also decreased by increasing the RLG. The total exergy of air, exergy of water increased with increasing the RLG because exit air and water droplet temperature and mass of water increased with increased the RLG. As RLG increased destruction in exergy of system along tower height increased because the amount of exergy release by water is more than amount of exergy gain by air. SLE of SCT increased with increased the RLG.

5.11 Comparative Study of SCT with Change in Initial Droplet Diameter for Industrial Application

In this section the effects on exit parameters (i.e. water droplet temperature, thermal efficiency, SLE) due to variation in inlet droplet diameter of SCT, the exit parameter results were studies for parallel flow and counter flow configuration using 2-D MATLAB model and 3-D CFD model. These results are compared for mono-droplet and multi-droplet diameter.

5.11.1 Variation in outlet water temperature with change of initial droplets diameter

The variation of outlet water temperature with varying inlet droplet diameter for parallel and counter-flow configuration is shown in Figure 5.9. It was observed that the outlet water temperature increased with the increasing the inlet droplet diameter in all the cases of parallel flow and counter flow SCT.

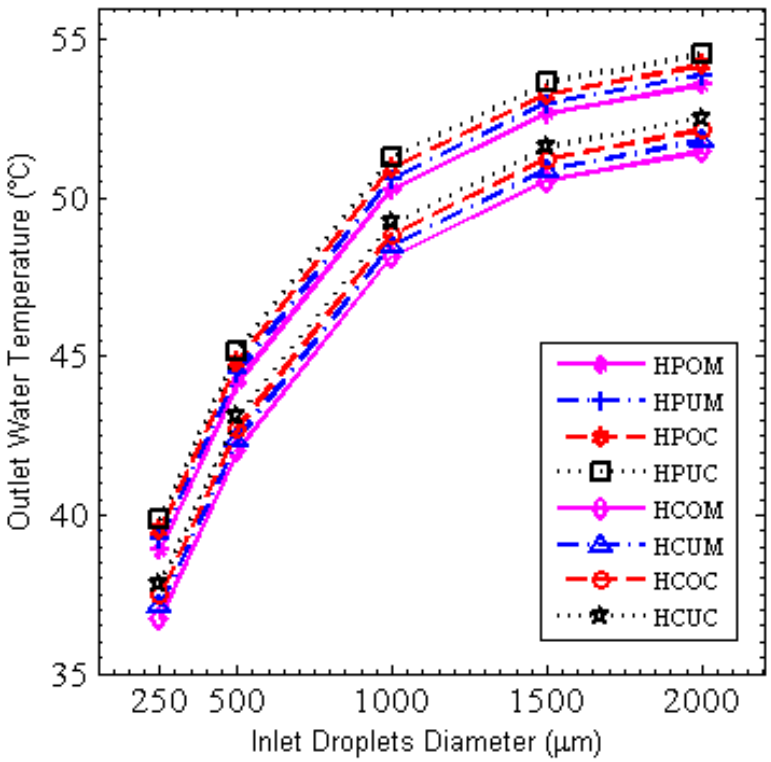

Figure 5.9 Outlet water temperature with variation in inlet droplet diameter

Figure 5.9 shows parallel flow SCT predicted higher exit water temperature in comparison to counter flow SCT because heat and mass transfer in counter flow SCT was more than parallel flow SCT. Figure 5.9 also shows that parallel and counter multi droplet SCT predicted exit water temperature higher than the mono droplet in both the cases of 2-D and 3-D. The multi droplet models were closer to the validation test as they described more realistic phenomena because mono droplet models considered more assumption compared to multi droplet models. The multi droplet 3-D CFD model predicted higher outlet water temperature compared to multi droplet 2-D model of MATLAB, However 3-D CFD model with least error in the validation test as shown in the Figures 5.1 - 5.4. The minimum and maximum temperature obtained by parallel flow configurations are 38.89 ˚C and 54.53 ˚C, and counter flow configurations are 36.75 ˚C and 52.51 ˚C respectively.

5.11.2 Variation in thermal efficiency of SCT with change of initial droplets diameter

The variation of thermal efficiency of SCT with varying inlet droplet diameter for parallel and counter-flow configuration is shown in Figure 5.10. It is observed that thermal efficiency of SCT decreased with the increasing in the inlet droplet diameter in all the cases of parallel flow and counter flow models because heat and mass transfer between air and water droplet decreases with increase the droplet diameter. Thermal efficiency for parallel flow cases was lower than counter flow cases for same inlet droplet diameter. Figure 5.10 shows that parallel and counter multi droplet SCT predicted thermal efficiency lower than the mono droplet in both the cases of 2-D and 3-D. The multi droplet models were closer to the validation test as they described more accurate results because mono droplet models considered more assumption compared to multi droplet models. The multi droplet 3-D CFD model predicted least thermal efficiency compared to multi droplet 2-D model of MATLAB, However 3-D CFD model with least error in the validation test as shown in Figures 5.1 - 5.4. The minimum and maximum thermal efficiency attained by parallel flow configurations are 5.86% and 68.19%, and counter flow configurations are 13.91% and 76.72% respectively. The maximum thermal efficiency achieved by parallel and counter flow 3-D CFD multi droplet model was 64.21% and 72.42% respectively.

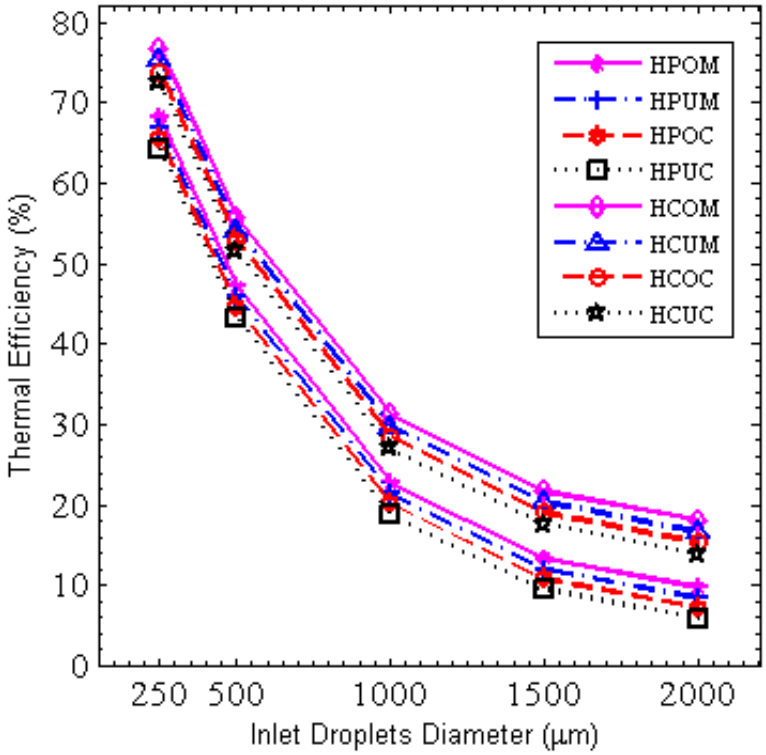

Figure 5.10 Thermal efficiency of SCT with variation in inlet droplet diameter

5.11.3 Variation in SLE of SCT with change of initial droplets diameter

The variation of SLE of SCT with varying inlet droplet diameter for parallel and counter-flow configuration is shown in Figure 5.11. It is observed that SLE of SCT was increased with the increasing the inlet droplet diameter for all the cases of parallel flow and counter flow models because total exergy of system increases with increases the droplet diameter. Figure 5.11 shows parallel flow SCT predicted higher SLE in comparison to counter flow SCT because heat and mass transfer in counter flow SCT was more than parallel flow SCT. Figure 5.11 also shows that parallel and counter multi droplet SCT predicted SLE higher than the mono droplet in both the cases of 2-D and 3-D. The minimum and maximum SLE attained by parallel flow

configurations are 81.61% and 97.75%, and counter flow configurations are 71.75% and 88.03% respectively.

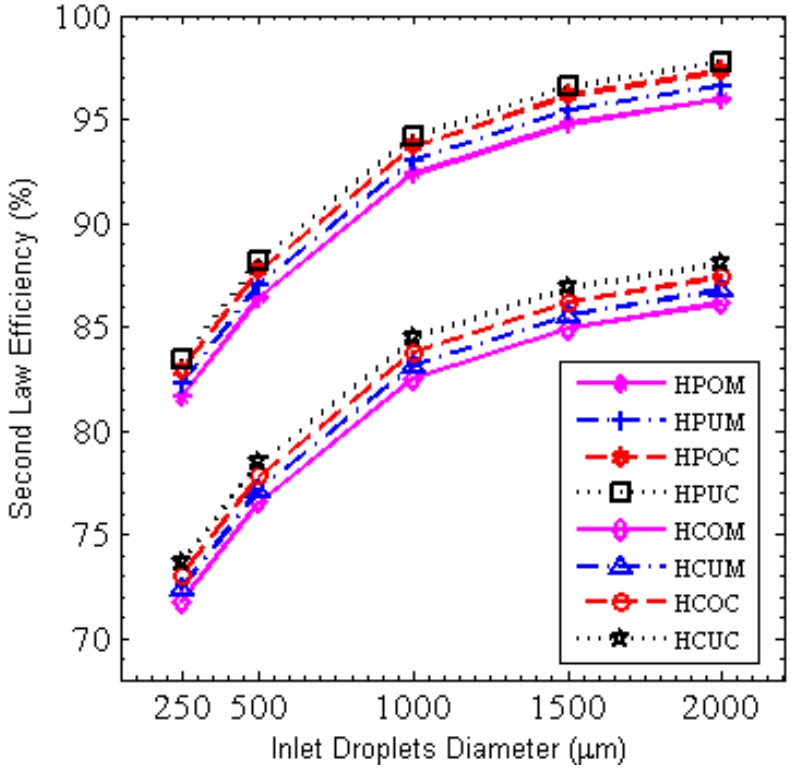

Figure 5.11 SLE of SCT with variation in inlet droplet diameter

5.12 Comparative Study of SCT with Change in Initial Water Temperature for Industrial Application

In order to study the effects of inlet water temperatures from 50 ˚C to 58 ˚C on exit parameters (i.e. water droplet temperature, thermal efficiency and SLE). The exit parameter results were obtained for parallel flow and counter flow configuration using 2-D MATLAB model and 3-D CFD model. Due to some error, outlet results of 2-D MATLAB models and 3-D CFD models for all configurations (mono droplet, multi droplet, parallel flow and counter flow) were different.

5.12.1 Variation in outlet water temperature with changes in inlet water temperature

The variation of outlet water temperature with varying inlet water temperature from 50 ˚C to 58 ˚C for parallel and counter-flow configuration is shown in Figure 5.12.

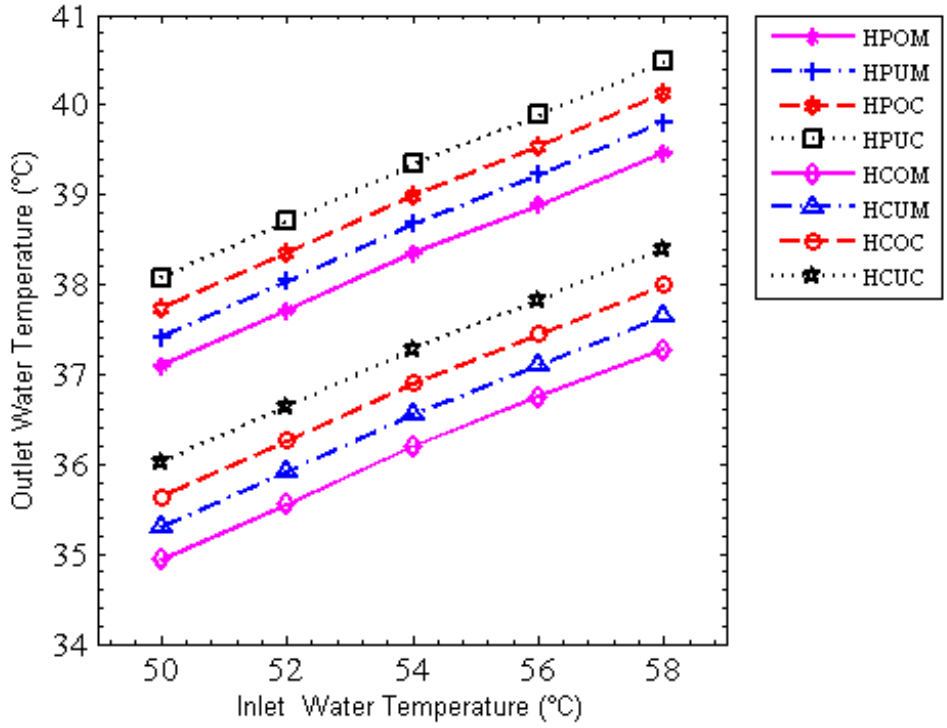

Figure 5.12 Outlet water temperature with variation of inlet water temperature

It is observed that the outlet water temperature increased with the increase in the inlet water temperature in all the cases (parallel flow and counter flow SCT). Figure 5.12 also shows parallel flow SCT predicted higher exit water temperature in comparison to counter flow SCT because heat and mass transfer in counter flow SCT was more than parallel flow SCT. Figure 5.12 also shows that parallel and counter multi droplet SCT predicted exit water temperature higher than the mono droplet in both the cases of 2-D and 3-D. The multi droplet models were closer to the validation

test as they described more realistic phenomena because mono droplet models considered more assumption compared to multi droplet models. The multi droplet 3-D CFD model predicted higher outlet water temperature compared to multi droplet 2-D model of MATLAB, However 3-D CFD model with least error in the validation test as shown in the Figures 5.1 - 5.4. The minimum outlet water temperature was obtained at 50 ˚C inlet water temperature droplets for parallel flow and counter flow models are 37.09 ˚C and 34.94 ˚C respectively. Maximum exit water temperature obtains by 58 ˚C inlet water temperature droplets for parallel flow and counter flow model are 40.48 ˚C and 38.39 ˚C respectively.

5.12.2 Variation in thermal efficiency of SCT with change of initial water temperature

The variations of thermal efficiency of SCT with varying inlet water temperature for parallel and counter flow configuration are shown in Figure 5.13. Figure 5.13 shows the thermal efficiency of all 2-D and 3-D cases of counter flow SCT was higher than parallel flow SCT. Figure 5.13 also shows parallel and counter multi droplet SCT predicted thermal efficiency lower than the mono droplet in both the cases of 2-D and 3-D. The multi droplet models were closer to the validation test as they described more accurate phenomena because mono droplet models considered more assumption compared to multi droplet models. The multi droplet 3-D CFD model predicted least thermal efficiency compared to multi droplet 2-D model of MATLAB, However 3-D CFD model with least error in the validation test as shown in Figures 5.1 - 5.4. The overall maximum thermal efficiency obtained by 58 ˚C inlet water temperature parallel flow mono droplet MATLAB model was 68.40%. The overall maximum thermal efficiency obtained by 50 ˚C inlet water temperature

counter flow mono droplet MATLAB model was 78.44%. The maximum thermal efficiency attains by parallel and counter flow 3-D CFD models are 64.67% and 73.23% respectively.

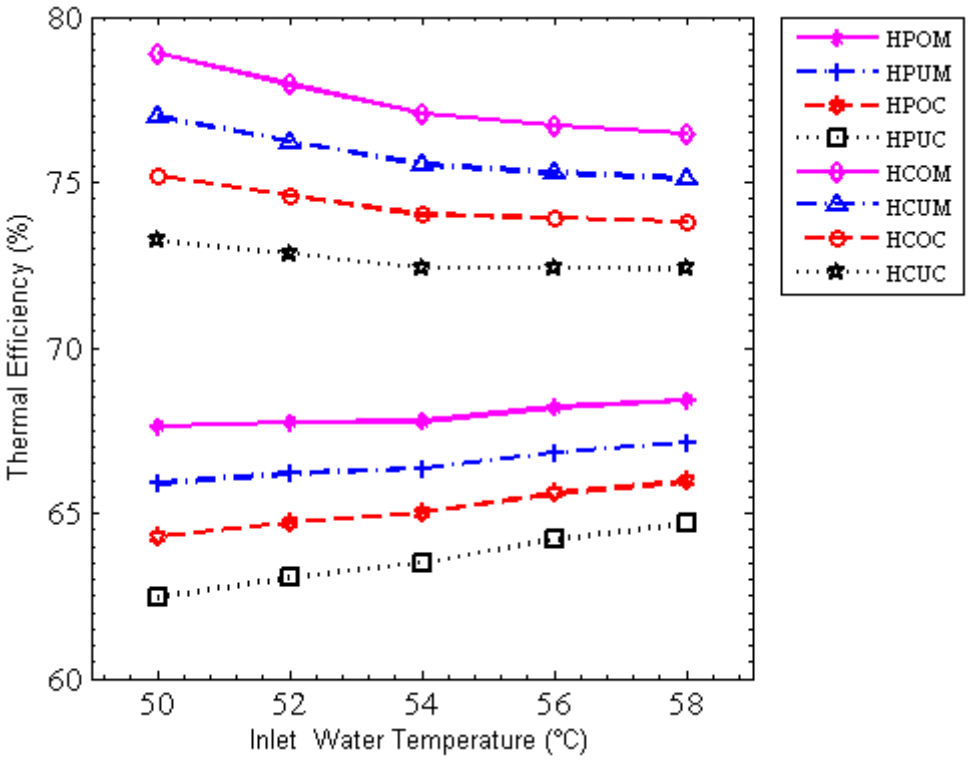

Figure 5.13 Thermal efficiency of SCT with variation in inlet water temperature

5.12.3 Variation in SLE of SCT with change of initial water temperature

The variation of SLE of SCT with varying inlet water temperature for parallel and counter-flow configuration are shown in Figure 5.14. It was observed that SLE of SCT decreased with the increasing the inlet water temperature for all the cases of parallel flow and counter flow models because total system exergy destruction increased with increasing the inlet water temperature. Figure 5.14 shows parallel flow SCT predicted higher SLE in comparison to counter flow SCT because heat and mass transfer in counter flow SCT was more than parallel flow SCT.

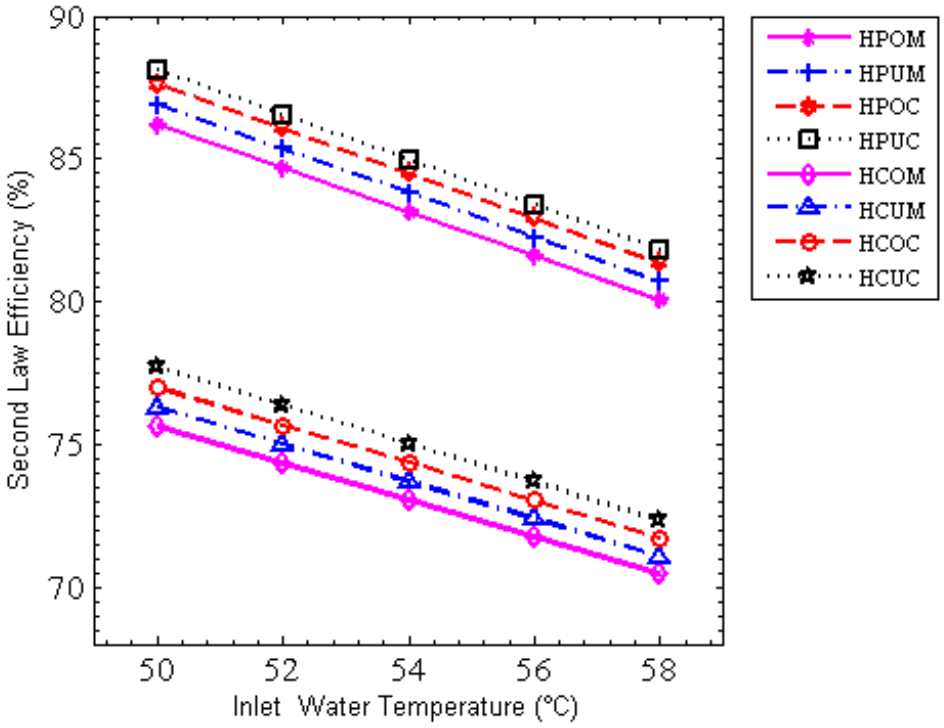

Figure 5.14 SLE of SCT with variation in inlet water temperature

Figure 5.14 also shows that parallel and counter multi droplet SCT predicted SLE higher than the mono droplet in both the cases of 2-D and 3-D. The maximum and minimum SLE efficiency were obtained at 50 ˚C and 58 ˚C inlet water temperature respectively for parallel flow and counter flow models. Maximum and minimum SLE attained by parallel flow configurations are 88.13% and 80.06%, and counter flow configurations are 77.68% and 70.46% respectively.

5.13 Comparative Study of SCT with Change in Inlet air DBT for Industrial Application

In order to study the effects of inlet air DBT from 24 ˚C to 42 ˚C on exit parameters (i.e. water droplet temperature, thermal efficiency and SLE), the exit parameter results were obtained for parallel flow and counter flow configuration using

2-D MATLAB model and 3-D CFD model. These exit parameter results were compared for the cases of mono-droplet and multi-droplet diameter. Outlet results of 2-D MATLAB models and 3-D CFD models for mono and multi droplet for parallel flow and counter flow configurations are different due to some error.

5.13.1 Variation in outlet water temperature with changes in inlet air temperature

The variation of outlet water temperature with varying inlet air DBT from 24 ˚C to 48 ˚C for parallel and counter-flow configuration is shown in Figure 5.15. It was observed that the outlet water temperature increased with the increasing the inlet air DBT for all the cases of parallel flow and counter flow SCT. Figure 5.15 shows parallel flow SCT predicted higher exit water temperature in comparison to counter flow SCT because heat and mass transfer in counter flow SCT was more than parallel flow SCT. Figure 5.15 also shows counter flow model water droplet cools down faster because relative velocity of water droplet in counter flow model was more than parallel flow model. The parallel and counter flow multi droplet SCT predicted exit water temperature higher than the mono droplet in both the cases of 2-D and 3-D. The multi droplet models were closer to the validation test as they described more exact results because mono droplet models considered extra assumption compared to multi droplet models. The multi droplet 3-D CFD model predicted higher outlet water temperature compared to multi droplet 2-D model of MATLAB, However 3-D CFD model has least error in the validation test as shown in the Figures 5.1 - 5.4. The minimum and maximum exit water temperature was obtained at 24 ˚C and 48 ˚C inlet air DBT respectively for parallel flow and counter flow models. Minimum and

maximum exit water temperature attained by parallel flow configurations are 34.21 ˚C and 47.67 ˚C, and counter flow configurations are 31.34 ˚C and 46.09 ˚C respectively.

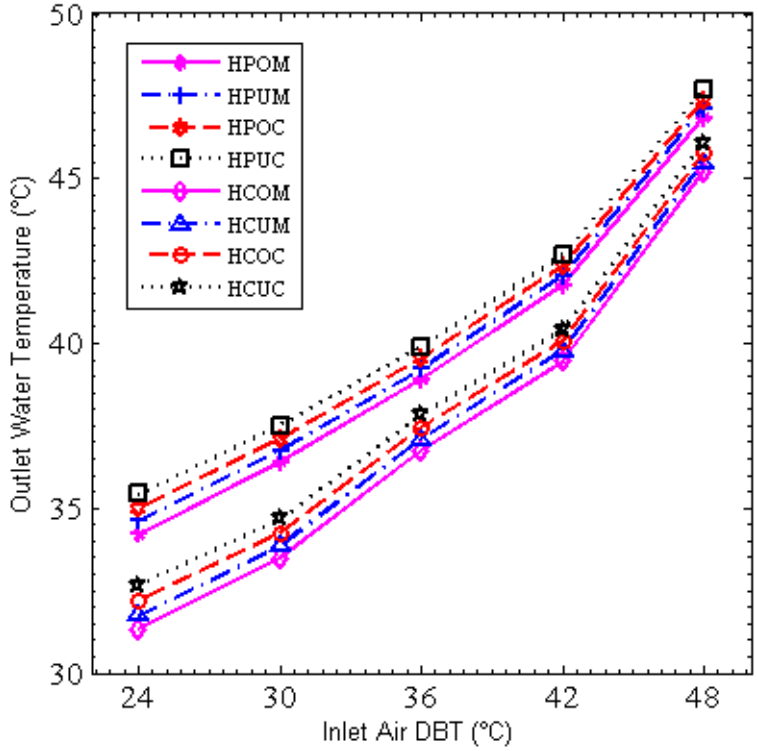

Figure 5.15 Outlet water temperature with variation in inlet air temperature

5.13.2 Variation in thermal efficiency of SCT with change of initial air temperature.

The variation of thermal efficiency of SCT with varying inlet air DBT for parallel and counter flow configuration are shown in Figure 5.16. It was observed that thermal efficiency of SCT increased with the increasing inlet the air DBT for all the cases of parallel flow and counter flow models. The thermal efficiency obtained from counter flow model was more than parallel flow models for same inlet air DBT because range (i.e. $T_{d,in} - T_{d,out}$) of SCT is more for counter flow models.

Figure 5.16 shows parallel and counter multi droplet SCT predicted thermal efficiency lower than the mono droplet in both the cases of 2-D and 3-D. The multi droplet

models were closer to the validation test as they described more accurate phenomena because mono droplet models considered more assumption compared to multi droplet models.

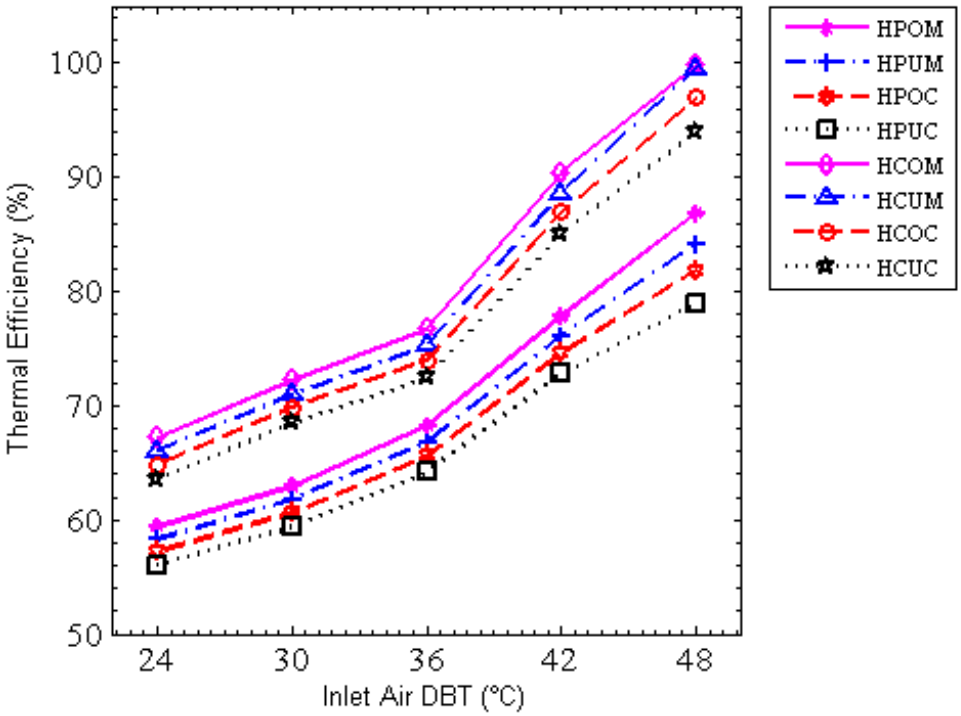

Figure 5.16 Thermal efficiency of SCT with variation in inlet air temperature

The multi droplet 3-D CFD model predicted least thermal efficiency compared to multi droplet 2-D model of MATLAB, However 3-D CFD model with least error in the validation test as shown in Figures 5.1 - 5.4. The minimum and maximum thermal efficiency obtained at 24 ˚C and 48 ˚C inlet air DBT respectively for all parallel flow and counter flow models. The minimum and maximum thermal efficiency attained by 3-D CFD parallel flow model was 56.03% and 78.94%, similarly minimum and maximum thermal efficiency attained by 3-D CFD counter flow model was 63.61% and 93.93%.

5.13.3 Variation in SLE of SCT with change of initial air temperature

The variation of SLE of SCT with varying inlet air DBT for parallel and counter-flow configuration are shown in Figure 5.17.

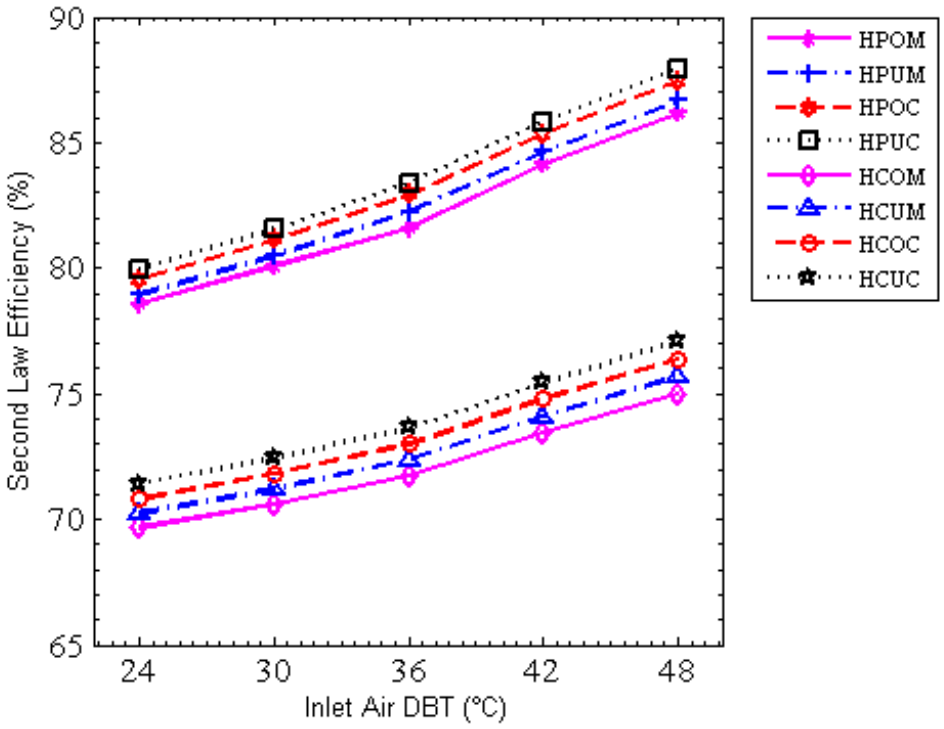

Figure 5.17 SLE of SCT with variation in inlet air temperature

It was observed that SLE of SCT increased with the increasing the inlet air DBT for all the cases of parallel flow and counter flow models because total system exergy decreased with increasing the inlet air DBT. The SLE for parallel flow cases was higher than counter flow cases for same inlet air DBT. Figure 5.17 shows parallel flow SCT predicted higher SLE in comparison to counter flow SCT because heat and mass transfer in counter flow SCT was more than parallel flow SCT. Figure 5.17 also shows that parallel and counter multi droplet SCT predicted SLE higher than the mono droplet in both the cases of 2-D and 3-D. Maximum and minimum SLE

efficiency obtained by 24 ˚C and 48 ˚C inlet air DBT respectively for parallel flow and counter flow models. Minimum and maximum SLE attained by parallel flow configurations are 78.57% and 87.95%, and counter flow configurations are 69.66% and 77.06% respectively.

5.14 Comparative Study of SCT with Change in Inlet Air Relative Humidity for Industrial Application

In order to present the effects of inlet air relative humidity from 20% to 80% on exit parameters (i.e. water droplet temperature, thermal efficiency and SLE), the exit parameter results were obtained for parallel flow and counter flow configuration using 2-D MATLAB model and 3-D CFD model. These exit parameter results were compared for the cases of mono-droplet and multi-droplet diameter.

5.14.1 Variation in outlet water temperature with changes in inlet air relative humidity

The variation of outlet water temperature with varying inlet air relative humidity from 20% to 80% for parallel flow and counter flow configuration is shown in Figure 5.18. In this study, it is observed that the outlet water temperature increased with the increasing the inlet air relative humidity in all the cases of parallel flow and counter flow SCT. Figure 5.18 shows parallel flow SCT predicted higher exit water temperature in comparison to counter flow SCT because heat and mass transfer in counter flow SCT was more than parallel flow SCT. Figure 5.18 also shows that parallel and counter multi droplet SCT predicted outlet water temperature higher than the mono droplet in both the cases of 2-D and 3-D.

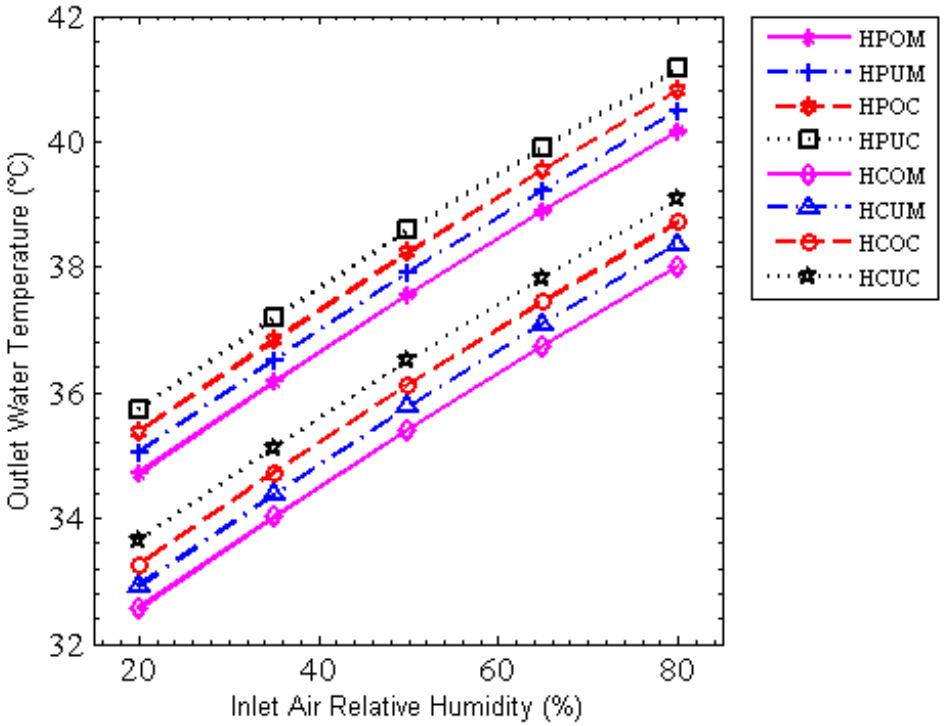

Figure 5.18 Outlet water temperature with variation in inlet air relative humidity

The multi droplet models were closer to the validation test as they described more realistic phenomena because mono droplet models considered more assumption compared to multi droplet models. The multi droplet 3-D CFD model predicted higher outlet water temperature compared to multi droplet 2-D model of MATLAB, However 3-D CFD model with least error in the validation test as shown in the Figures 5.1 - 5.4. The minimum and maximum exit water temperature obtained by 20% and 80% inlet air relative humidity respectively for parallel flow and counter flow models. Minimum and maximum exit water temperature attain by parallel flow configurations are 34.71 ˚C and 41.16 ˚C, and counter flow configurations are 32.56 ˚C and 39.1 ˚C respectively.

5.14.2 Variation in thermal efficiency of SCT with change of initial air relative humidity.

The variation of thermal efficiency of SCT with varying inlet air DBT for parallel and counter flow configuration are studied and shown in Figure 5.19.

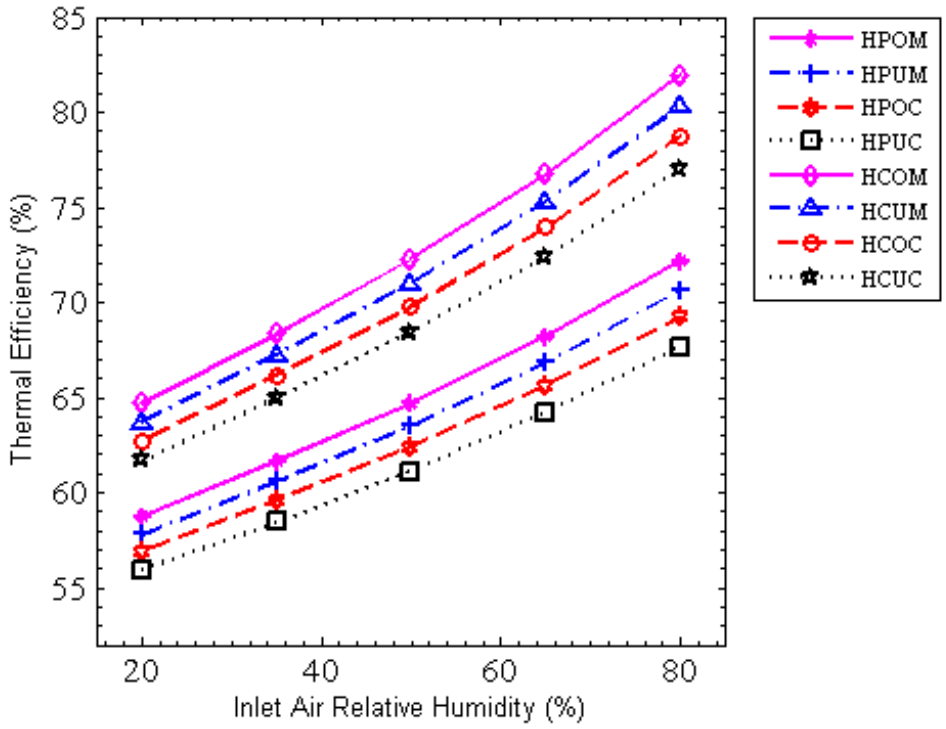

Figure 5.19 Thermal efficiency of SCT with variation in inlet air relative humidity

It is observed that thermal efficiency of SCT increased with the increase in the inlet air relative humidity in all the cases of parallel flow and counter flow models. Thermal efficiency obtains from counter flow models are more than parallel flow models for same inlet air relative humidity because evaporative heat transfer increased with increasing the inlet air relative humidity. Figure 5.19 shows that parallel and counter multi droplet SCT predicted thermal efficiency lower than the mono droplet in both the cases of 2-D and 3-D. The multi droplet models were closer to the validation test as they described more accurate phenomena because mono

droplet models considered more assumption compared to multi droplet models. The multi droplet 3-D CFD model predicted least thermal efficiency compared to multi droplet 2-D model of MATLAB, However 3-D CFD model with least error in the validation test as shown in Figures 5.1 - 5.4. Minimum and maximum thermal efficiency was obtained at 20% and 80% inlet air relative humidity respectively for all parallel flow and counter flow models. Minimum and maximum thermal efficiency attained by parallel flow configurations are 55.95% and 72.20%, and counter flow configurations are 61.69% and 81.95% respectively.

5.14.3 Variation in SLE of SCT with change of initial air relative humidity.

The variation of SLE of SCT with varying inlet air relative humidity for parallel and counter-flow configuration is shown in Figure 5.20. It is observed that SLE of SCT decreased with the increasing the inlet air relative humidity for all the cases of parallel flow and counter flow models as total system exergy decreased with increasing the inlet air relative humidity. Figure 5.20 shows parallel flow SCT predicted higher SLE in comparison to counter flow SCT because heat and mass transfer in counter flow SCT was more than parallel flow SCT. The Figure also shows that parallel and counter multi droplet SCT predicted SLE higher than the mono droplet in both the cases of 2-D and 3-D. In this case maximum and minimum SLE were obtained at 20% and 80% initial air relative humidity respectively for parallel flow and counter flow models. Maximum and minimum SLE attained by parallel flow configurations are 92.08% and 72.95%, and counter flow configurations are 89.09% and 56.75% respectively.

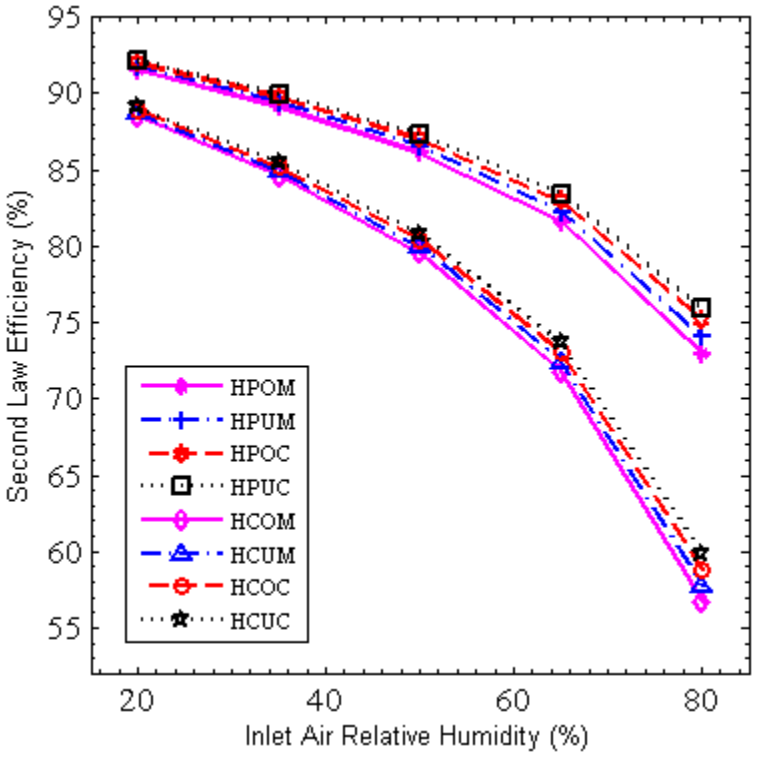

Figure 5.20 SLE of SCT with variation in inlet air relative humidity

5.15 Comparative Study of SCT with Change in Inlet RLG for Industrial Application

In order to studied the effects of inlet RLG from 0.5 to 2 on exit parameters (i.e. water droplet temperature, thermal efficiency and SLE). The exit parameter results were obtained for parallel flow and counter flow configuration using 2-D MATLAB model and 3-D CFD model. These exit parameter results was compared for the cases of mono-droplet and multi-droplet diameter. The outlet results of 2-D MATLAB models and 3-D CFD models for the mono and multi droplet for parallel flow and counter flow configurations are noted differently due to some error.

5.15.1 Variation in outlet water temperature with changes in inlet RLG.

In the present study, the variation of outlet water temperature with varying inlet RLG from 0.5 to 2 for parallel and counter-flow configuration is shown in Figure 5.21.

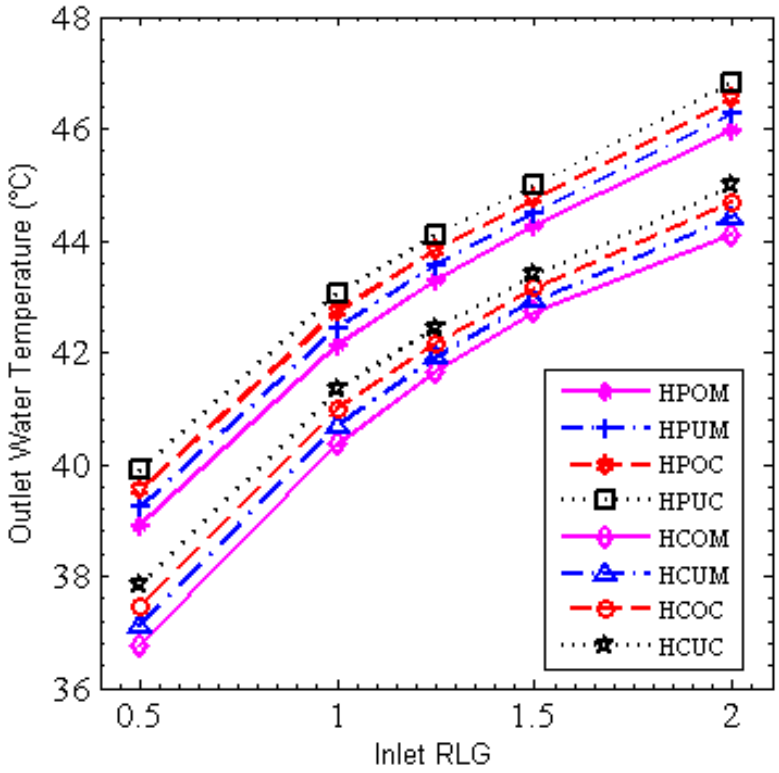

Figure 5.21 Outlet water temperature with variation in inlet RLG

It is observed that the outlet water temperature increased with the increasing the inlet RLG in all the cases of parallel flow and counter flow SCT. It is also observed, exit water temperature for parallel flow cases were greater than counter flow cases for same inlet RLG. In counter flow model water droplet cooled down faster because heat and mass transfer in counter flow SCT was more than parallel flow SCT. Figure 5.9 also shows that parallel and counter multi droplet SCT predicted exit water temperature higher than the mono droplet in both the cases of 2-D and 3-D.

The multi droplet models were closer to the validation test as they described more realistic phenomena because mono droplet models considered more assumption compared to multi droplet models. The multi droplet 3-D CFD model predicted higher outlet water temperature compared to multi droplet 2-D model of MATLAB. The minimum and maximum exit water temperature attained by parallel flow configurations are 38.89 ˚C and 46.82 ˚C, and counter flow configurations are 36.75 ˚C and 44.98 ˚C respectively.

5.15.2 Variation in thermal efficiency of SCT with change of initial RLG.

The variation of thermal efficiency of SCT with varying inlet air DBT for parallel and counter flow configuration are shown in Figure 5.22. It is observed from Figure 5.22 that thermal efficiency of SCT decreased with the increasing the inlet RLG for all the cases of parallel flow and counter flow SCT models. The thermal efficiency obtained from counter flow models was more than parallel flow models for same inlet RLG. Figure 5.22 also shows the thermal efficiency of all 2-D and 3-D cases of counter flow SCT was higher than parallel flow SCT. Figure 5.22 also shows parallel and counter multi droplet SCT predicted thermal efficiency lower than the mono droplet in both the cases of 2-D and 3-D. The multi droplet models were closer to the validation test as they described more accurate phenomena because mono droplet models considered more assumption compared to multi droplet models. The multi droplet 3-D CFD model predicted least thermal efficiency compared to multi droplet 2-D model of MATLAB, however 3-D CFD model with least error in the validation test as shown in Figures 5.1 - 5.4. The maximum and minimum thermal efficiency obtained at 0.5 and 2 inlet RLG respectively for all parallel flow and

counter flow models. The overall maximum and minimum thermal efficiency attains by parallel flow configurations are 68.19% and 36.59%, and counter flow configurations are 76.72% and 43.92% respectively. The maximum thermal efficiency attained by 3-D CFD parallel flow and counter flow model were 64.21% and 72.41% respectively.

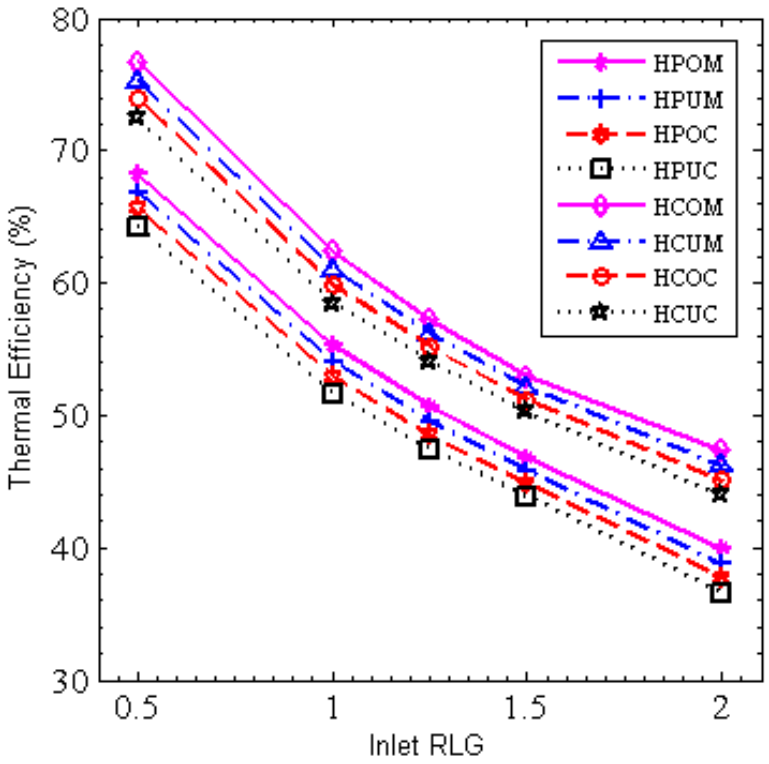

Figure 5.22 Thermal efficiency of SCT with variation in inlet RLG

5.15.3 Variation in SLE of SCT with change of initial RLG.

The variation of SLE of SCT with varying inlet RLG for parallel and counter-flow configuration are shown in Figure 5.23. It is observed that SLE of SCT increased with the increasing the inlet RLG for all the cases of parallel flow and counter flow models. It was also noticed that SLE for parallel flow cases was higher than counter flow cases for same inlet RLG. Figure 5.23 shows parallel flow SCT predicted higher SLE in comparison to counter flow SCT because heat and mass transfer in counter

flow SCT was more than parallel flow SCT. Figure 5.23 also shows that parallel and counter multi droplet SCT predicted SLE higher than the mono droplet in both the cases of 2-D and 3-D. The minimum and maximum SLE attained by parallel flow configurations were 81.60% and 88.49%, and counter flow configurations were 71.75% and 85.43% respectively.

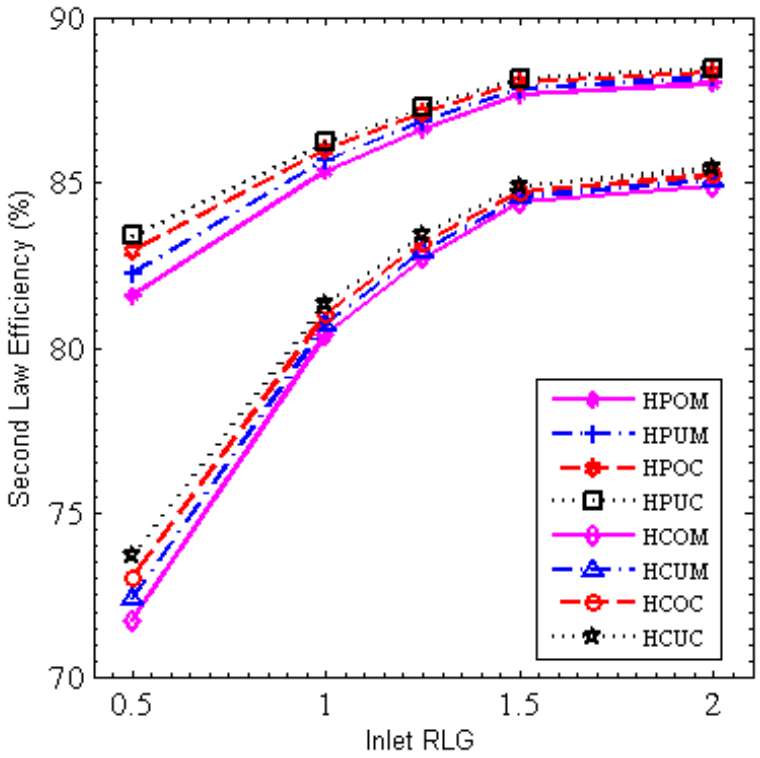

Figure 5.23 SLE of SCT with variation in inlet RLG

5.16 Two Dimensional Parallel Flow Mono Droplet SCT for Air Cooling Application

This study based on 2-D mono droplet parallel flow MATLAB model to determine the effect of variation in inlet droplet diameters, water temperatures, air DBT, relative humidity of air and RLG on outlet parameters. Initial conditions used for computer simulation are given in Table 5.4.

5.16.1 Effect of variation in initial droplets diameter (NPOMR)

This research based on variation of inlet water droplet diameter from 200 µm to 1000 µm. The inlet constant parameters used in this research are air DBT (40 ˚C), air relative humidity (20%), water temperature (34 ˚C), and RLG (0.5). Table 5.46 shows the variation of air DBT, air specific humidity, water temperature, makeup water required, thermal efficiency, convective exergy of air, evaporative exergy of air, total exergy of air, water exergy, total exergy of system, exergy destruction, and SLE with varying inlet droplet diameter. As droplet diameter increased from 200 µm to 1000 µm, exit air DBT and water temperature increased and exit specific humidity, make up water required and thermal efficiency of SCT decreased because heat and mass transfer between air and water droplet decreased. Water droplet of 200 µm produced maximum drop in inlet air DBT (12.53 ˚C) and maximum thermal efficiency (56.57%). Total exergy of air and exergy destruction decreased as inlet droplet diameter increased. Exergy of water, exergy of system and SLE increased with increasing the droplet diameter as heat and mass transfer between air and water decreased.

Table 5.46 Effect of variation in inlet droplet diameter (NPOMR)

1	2	3	4	5	6	7	8	9	10	11	12	13	14
Code	D_{in} (µm)	$T_{a,out}$ (˚C)	$\omega_{a,out}$ (kg_w/kg_a)	$T_{d,out}$ (˚C)	$m_{d,l}$ (kg/s)	η_{th} (%)	$X_{c,out}$ (W)	$X_{e,out}$ (W)	$X_{a,out}$ (W)	$X_{d,out}$ (W)	$X_{t,out}$ (W)	I_t (W)	η_{II} (%)
NPOMR-1	**200**	**27.47**	**0.0235**	**27.46**	**0.0017**	**56.57**	**31.54**	**125.38**	**156.92**	**13708.07**	**13864.99**	**424.38**	**97.03**
NPOMR-2	**400**	**31.27**	**0.0219**	**28.17**	**0.0015**	**50.43**	**16.02**	**95.66**	**111.68**	**13829.61**	**13941.29**	**348.08**	**97.56**
NPOMR-3	**600**	**35.65**	**0.0183**	**28.75**	**0.0010**	**45.42**	**3.93**	**50.87**	**54.80**	**13944.67**	**13999.47**	**289.90**	**97.97**
NPOMR-4	**800**	**37.50**	**0.0159**	**29.97**	**0.0007**	**34.86**	**1.28**	**27.16**	**28.44**	**14034.31**	**14062.75**	**226.62**	**98.41**
NPOMR-5	**1000**	**38.34**	**0.0143**	**30.88**	**0.0006**	**26.99**	**0.56**	**15.75**	**16.31**	**14094.07**	**14110.38**	**178.99**	**98.75**

5.16.2 Effect of variation in inlet Water Temperature (NPOMD)

In this study the inlet fixed parameters are air DBT (40 ˚C), air relative humidity (20%), water droplet diameter (200 µm), RLG (0.5) and inlet water temperature varied from 28 ˚C to 36 ˚C. Table 5.47 shows variation of exit parameters of SCT by varying the inlet water droplet temperature. Table 5.47 also shows that inlet water temperature increases exit air DBT, air specific humidity, water temperature, makeup water required the thermal efficiency of SCT increases. Maximum cooling in exit air DBT achieved (14.46 ˚C) at 28 ˚C inlet water temperature as the high temperature difference between inlet water and air (keeping air DBT constant) and also maximum thermal efficiency achieved (54.94%) at 36 ˚C inlet water temperature. As inlet water droplet temperature increased specific humidity, evaporative exergy and total exergy of air increased due to increase in water temperature, more water vapour was added in air. The exergy destruction of system was increased and SLE decreased by increasing the inlet water droplet temperature. Destruction in total exergy of system increased as inlet water temperature increased because it transfers water content in to air faster than lower temperature droplets.

Table 5.47 Effect of variation in inlet water temperature (NPOMD)

1	2	3	4	5	6	7	8	9	10	11	12	13	14
Code	$T_{d,in}$ (˚C)	$T_{a,out}$ (˚C)	$\omega_{a,out}$ (kg_w/kg_a)	$T_{d,out}$ (˚C)	$m_{d,l}$ (kg/s)	η_{th} (%)	$X_{c,out}$ (W)	$X_{e,out}$ (W)	$X_{a,out}$ (W)	$X_{d,out}$ (W)	$X_{t,out}$ (W)	I_t (W)	η_{II} (%)
NPOMD-1	**28**	**25.54**	**0.0208**	**25.53**	**0.0014**	**44.42**	**44.43**	**80.98**	**125.41**	**13832.50**	**13957.91**	**214.26**	**98.49**
NPOMD-2	**30**	**26.31**	**0.0218**	**26.31**	**0.0015**	**48.81**	**39.81**	**94.61**	**134.42**	**13812.58**	**13947.00**	**257.77**	**98.19**
NPOMD-3	**32**	**27.07**	**0.0229**	**27.07**	**0.0016**	**51.57**	**35.52**	**109.40**	**144.92**	**13792.70**	**13937.62**	**306.26**	**97.85**
NPOMD-4	**34**	**27.47**	**0.0235**	**27.46**	**0.0017**	**56.57**	**31.54**	**125.38**	**156.92**	**13708.07**	**13864.99**	**424.38**	**97.03**
NPOMD-5	**36**	**28.55**	**0.0250**	**28.55**	**0.0019**	**54.94**	**27.87**	**142.57**	**170.44**	**13752.91**	**13923.35**	**417.77**	**97.09**

5.16.3Effect of variation in inlet air DBT (NPOMA)

This section represents variation of inlet air DBT from 36 - 40 ˚C and constant inlet parameters are air relative humidity (20%), water droplet diameter (200 µm), water temperature (34 ˚C), and RLG (0.5). Table 5.48 shows exit air DBT, specific humidity and droplet temperatures increased relatively as inlet air DBT increases, it also shows 36 ˚C DBT air produce maximum cooling and it cool down water droplet up to 09.92 ˚C. Table shows that increased in inlet air DBT thermal efficiency of SCT increased and maximum thermal efficiency achieved (55.73%) by 36 ˚C inlet air DBT. The convective exergy of air, evaporative exergy of air, total exergy of air, exergy of water, total exergy of system and exergy destruction decreased with increasing the inlet air DBT temperature. The SLE of system increased with increasing the initial air DBT.

Table 5.48 Effect of variation in inlet air DBT (NPOMA)

1	2	3	4	5	6	7	8	9	10	11	12	13	14
Code	$T_{a,in}$ (˚C)	$T_{a,out}$ (˚C)	$\omega_{a,out}$ (kg_w/kg_a)	$T_{d,out}$ (˚C)	$m_{d,l}$ (kg/s)	η_{th} (%)	$X_{c,out}$ (W)	$X_{e,out}$ (W)	$X_{a,out}$ (W)	$X_{d,out}$ (W)	$X_{t,out}$ (W)	I_t (W)	η_{II} (%)
NPOMA-1	**36**	**26.08**	**0.0221**	**26.07**	**0.0018**	**55.73**	**19.85**	**151.14**	**170.99**	**13497.53**	**13668.52**	**467.01**	**96.70**
NPOMA-2	**38**	**26.76**	**0.0229**	**26.75**	**0.0018**	**55.94**	**25.44**	**138.13**	**163.57**	**13457.69**	**13621.26**	**449.72**	**96.80**
NPOMA-3	**40**	**27.47**	**0.0235**	**27.46**	**0.0017**	**56.57**	**31.54**	**125.38**	**156.92**	**13417.55**	**13574.47**	**428.28**	**96.94**
NPOMA-4	**42**	**28.20**	**0.0251**	**28.19**	**0.0016**	**57.07**	**38.07**	**112.95**	**151.02**	**13377.21**	**13528.23**	**404.20**	**97.10**
NPOMA-5	**44**	**28.97**	**0.0262**	**28.96**	**0.0015**	**57.53**	**44.97**	**100.88**	**145.85**	**13336.67**	**13482.52**	**380.37**	**97.26**

5.16.4 Effect of variation in inlet Air Relative Humidity (NPOMH)

In this research inlet relative humidity varies from 20% to 40% and constant inlet values are air DBT (40 ˚C), water droplet diameter (200 µm), water temperature (34 ˚C), and RLG (0.5). Table 5.49 shows exit air DBT, specific humidity, droplet temperature and thermal efficiency of SCT increased with increasing the air relative

humidity. Table 5.49 also shows 20% relative humidity air produce maximum air cooling, i.e. up to 12.53 ˚C and 80% relative humidity air give maximum thermal efficiency (59.51). Table also shows as relative humidity of air increased the change in total exergy of air, exergy of water, and SLE of SCT decreased. As relative humidity of air increased, the destruction in total exergy of system relatively decreased.

Table 5.49 Effect of variation in inlet air relative humidity (NPOMH)

1	2	3	4	5	6	7	8	9	10	11	12	13	14
Code	ϕ_{in} (%)	$T_{a,out}$ (˚C)	$\omega_{a,out}$ (kg_w/kg_a)	$T_{d,out}$ (˚C)	$m_{d,l}$ (kg/s)	η_{th} (%)	$X_{c,out}$ (W)	$X_{e,out}$ (W)	$X_{a,out}$ (W)	$X_{d,out}$ (W)	$X_{t,out}$ (W)	I_t (W)	η_{II} (%)
NPOMH-1	**20**	**27.47**	**0.0235**	**27.46**	**0.0017**	**56.57**	**31.54**	**125.38**	**156.92**	**13417.55**	**13574.47**	**428.28**	**96.94**
NPOMH-2	**25**	**28.60**	**0.0251**	**28.59**	**0.0016**	**57.09**	**27.56**	**88.34**	**115.90**	**11850.07**	**11650.57**	**396.63**	**96.71**
NPOMH-3	**30**	**29.35**	**0.0263**	**29.35**	**0.0014**	**58.08**	**23.94**	**62.52**	**86.46**	**10279.99**	**10083.71**	**374.72**	**96.42**
NPOMH-4	**35**	**30.09**	**0.0275**	**30.09**	**0.0013**	**59.59**	**20.67**	**44.01**	**64.68**	**8953.17**	**8762.70**	**425.14**	**95.37**
NPOMH-5	**40**	**30.81**	**0.0287**	**30.81**	**0.0011**	**62.13**	**17.71**	**30.54**	**48.25**	**7804.37**	**7621.26**	**421.27**	**94.76**

5.16.5 Effect of variation in inlet RLG (NPOML)

In this section inlet RLG varied from 0.5 to 1.5. The fixed inlet parameters used fro study was air DBT (40 ˚C), air relative humidity (20%), water droplet diameter (200 µm), and water temperature (34 ˚C). Table 5.50 shows as RLG increased exit air DBT, air specific humidity and droplet temperature increases as mass of water at inlet increased. Maximum and minimum water droplet temperature reduction is 12.53 ˚C and 09.97 ˚C which obtained at 0.5 and 1.5 RLG respectively. Range and thermal efficiency of SCT decreased with increasing the RLG. Total exergy of air, exergy of water increased with increasing the RLG as exit air DBT, water droplet temperature and mass of water increased with increase the RLG. As the amount of water in RLG increased destruction in exergy of the system along tower

height increases as the amount of exergy release by water is more than the amount of exergy gain by air. SLE of SCT increased with increase the RLG.

Table 5.50 Effect of variation in inlet RLG (NPOML)

1	2	3	4	5	6	7	8	9	10	11	12	13	14
Code	**RLG_{in}**	**$T_{a,out}$ (˚C)**	**$\omega_{a,out}$ (kg_w/kg_a)**	**$T_{d,out}$ (˚C)**	**$m_{d,l}$ (kg/s)**	**η_{th} (%)**	**$X_{c,out}$ (W)**	**$X_{e,out}$ (W)**	**$X_{a,out}$ (W)**	**$X_{d,out}$ (W)**	**$X_{t,out}$ (W)**	**I_t (W)**	**η_{II} (%)**
NPOML-1	**0.5**	**27.47**	**0.0235**	**27.46**	**0.0017**	**56.57**	**31.54**	**125.38**	**156.92**	**13708.07**	**13864.99**	**424.38**	**97.03**
NPOML-2	**0.75**	**28.40**	**0.0249**	**28.39**	**0.0018**	**48.53**	**26.87**	**148.02**	**174.89**	**20742.24**	**20917.13**	**516.94**	**97.59**
NPOML-3	**1**	**29.10**	**0.0260**	**29.09**	**0.0019**	**42.47**	**23.69**	**165.99**	**189.68**	**27794.58**	**27984.26**	**594.49**	**97.92**
NPOML-4	**1.25**	**29.62**	**0.0268**	**29.61**	**0.0020**	**37.98**	**21.41**	**180.64**	**202.05**	**34859.36**	**35061.41**	**662.02**	**98.15**
NPOML-5	**1.5**	**30.03**	**0.0275**	**30.02**	**0.0021**	**34.43**	**19.69**	**192.82**	**212.51**	**41933.05**	**42145.56**	**722.56**	**98.31**

5.17 Two Dimensional Parallel Flow Multi Droplet SCT for Air Cooling Application

This study based on 2-D multi droplet parallel flow MATLAB model to determine the effect of variation in inlet droplet diameters, water temperatures, air DBT, relative humidity of air and RLG on outlet parameters. Initial conditions used for computer simulation are given in Table 5.5.

5.17.1 Effect of variation in initial droplets diameter (NPUMR)

This research represents the variation of outlet parameters of SCT with varying the inlet multi droplet diameters. The constant inlet parameters used for this study was air DBT (40 ˚C), air relative humidity (20%), and water temperature (34 ˚C). Table 5.51 shows as multi droplet diameter increase exit air DBT and water temperature increased and exit specific humidity, make up water required and thermal efficiency of SCT decreased as heat and mass transfer between air and water droplet decreased. Maximum drop in inlet air DBT (12.22 ˚C) and maximum thermal

efficiency (53.89%) achieved by 25.45 - 254.54 µm multi droplet diameters. Convective, evaporative, total exergy of air and exergy destruction decreased as inlet droplet diameter increases. Exergy of water, exergy of system and SLE increased with increasing the multi droplet diameters because heat and mass transfer between air and water decreased.

Table 5.51 Effect of variation in inlet droplet diameter (NPUMR)

1	2	3	4	5	6	7	8	9	10	11	12	13	14
Code	D_{in} (µm)	$T_{a,out}$ (˚C)	$\omega_{a,out}$ (kg_w/kg_a)	$T_{d,m,out}$ (˚C)	$m_{d,l}$ (kg/s)	η_{th} (%)	$X_{c,out}$ (W)	$X_{e,out}$ (W)	$X_{a,out}$ (W)	$X_{d,out}$ (W)	$X_{t,out}$ (W)	I_t (W)	η_{II} (%)
NPUMR-1	25.45-254.54	27.78	0.0238	27.77	0.0018	53.89	31.96	123.63	155.59	13491.5	13647.09	290.17	97.46
NPUMR-2	50.90-509.09	30.96	0.0201	29.39	0.0013	39.85	17.14	72.02	89.16	13619.55	13708.70	294.26	97.90
NPUMR-3	76.36-763.64	36.15	0.0153	31.04	0.0007	25.62	3.05	22.46	25.51	13785.41	13810.93	192.09	98.63
NPUMR-4	101.81-1018.18	38.40	0.0129	31.99	0.0004	17.42	0.52	7.60	8.12	13871.18	13879.29	123.57	99.12
NPUMR-5	127.27-1272.73	39.19	0.0118	32.53	0.0002	12.72	0.13	3.33	3.46	13912.74	13916.20	86.58	99.38

5.17.2 Effect of variation in inlet Water Temperature (NPUMD)

In this section the effect of variation of inlet water temperatures from 28 ˚C to 36 ˚C on various exit parameters are given in Table 5.52. The other important constant inlet parameters are air DBT (40 ˚C), air relative humidity (20%), water droplet diameters (25.45 – 254.54 µm), and RLG (0.5).

Table 5.52 Effect of variation in inlet water temperature (NPUMD)

1	2	3	4	5	6	7	8	9	10	11	12	13	14
Code	$T_{d,in}$ (˚C)	$T_{a,out}$ (˚C)	$\omega_{a,out}$ (kg_w/kg_a)	$T_{d,m,out}$ (˚C)	$m_{d,l}$ (kg/s)	η_{th} (%)	$X_{c,out}$ (W)	$X_{e,out}$ (W)	$X_{a,out}$ (W)	$X_{d,out}$ (W)	$X_{t,out}$ (W)	I_t (W)	η_{II} (%)
NPUMD-1	28	25.49	0.0208	25.50	0.0014	44.93	44.76	80.19	124.95	13550.29	13675.24	22.37	98.47
NPUMD-2	30	26.25	0.0218	26.27	0.0015	49.29	40.18	93.52	133.70	13530.66	13664.36	29.71	98.16
NPUMD-3	32	27.00	0.0228	27.03	0.0016	51.98	35.92	108.00	143.92	13511.08	13655.00	38.54	97.83
NPUMD-4	34	27.74	0.0238	27.77	0.0017	53.85	31.96	123.63	155.59	13491.50	13647.09	48.96	97.46
NPUMD-5	36	28.46	0.0249	28.50	0.0019	55.28	28.30	140.44	168.74	13471.87	13640.61	61.10	97.06

Table 5.52 shows as inlet water temperature increases exit air DBT, air specific humidity, water temperature, makeup water required, and thermal efficiency of SCT increased. It also observed that when the temperature of inlet water is 28 ˚C, maximum cooling of air was achieved (14.51 ˚C) as high temperature difference between water and air (keeping air temperature constant), increases sensible cooling as well as evaporative cooling. As inlet water droplet temperature increases, the specific humidity of air increased because due to increase in water temperature more water vapour is added in the air, Table 5.52 also shows that increased in inlet water temperature, more quantity of water vapour mixed in the air and increased evaporative and total exergy of air. The exergy destruction of the system was increased and SLE decreased by increasing the inlet water droplet temperature. Depicted destruction in total exergy of the system was more for higher temperature droplet because it transfers water content into air faster than lower temperature droplets.

5.17.3Effect of variation in inlet air DBT (NPUMA)

This study was based on variation of air DBT 36 - 44 ˚C. The constant inlet parameters taken for this study was air relative humidity (20%), water temperature (34 ˚C), multi droplet diameter (25.45 – 254.54 µm), and RLG (0.5). It was observed from Table 5.53 that exit air DBT, specific humidity and droplet temperatures increased relatively as inlet air DBT increases; it also shows 44 ˚C DBT air produced maximum cooling and it cool down air DBT up to 14.73 ˚C. Table 5.53 also represents that increase in inlet air DBT temperature, the thermal efficiency of SCT increased. Convective exergy of air increased with increasing the inlet air DBT. Evaporative exergy of air, total exergy of air, water exergy, total exergy of system and

exergy destruction decreased with increasing the inlet air DBT. The SLE of the system increased as exergy destruction decreased with increasing the initial air DBT.

Table 5.53 Effect of variation in inlet air DBT (NPUMA)

1	2	3	4	5	6	7	8	9	10	11	12	13	14
Code	$T_{a,in}$ (˚C)	$T_{a,out}$ (˚C)	$\omega_{a,out}$ (kg_w/kg_a)	$T_{d,m,out}$ (˚C)	$m_{d,l}$ (kg/s)	η_{th} (%)	$X_{c,out}$ (W)	$X_{e,out}$ (W)	$X_{a,out}$ (W)	$X_{d,out}$ (W)	$X_{t,out}$ (W)	I_t (W)	η_{II} (%)
NPUMA-1	**36**	**26.45**	**0.0219**	**26.44**	**0.0020**	**53.13**	**20.25**	**148.94**	**169.19**	**13571.96**	**13741.15**	**391.31**	**97.21**
NPUMA-2	**38**	**27.08**	**0.0228**	**27.07**	**0.0019**	**53.47**	**25.86**	**136.17**	**162.03**	**13531.85**	**13693.88**	**373.78**	**97.32**
NPUMA-3	**40**	**27.78**	**0.0238**	**27.77**	**0.0018**	**53.89**	**31.96**	**123.63**	**155.59**	**13491.5**	**13647.09**	**290.17**	**97.46**
NPUMA-4	**42**	**28.51**	**0.0249**	**28.5**	**0.0017**	**54.03**	**38.5**	**111.4**	**149.9**	**13450.94**	**13600.84**	**336.81**	**97.62**
NPUMA-5	**44**	**29.27**	**0.0261**	**29.26**	**0.0016**	**54.11**	**45.39**	**99.51**	**144.9**	**13410.23**	**13555.13**	**317.1**	**97.78**

5.17.4 Effect of variation in inlet Air Relative Humidity (NPUMH)

The effects of deviation of inlet relative humidity from 20% to 40% on the exit parameters at constant inlet air DBT (40 ˚C), water temperature (34 ˚C), droplet diameter (25.45 – 254.54 μm), and RLG (0.5) are given in Table 5.54. Table 5.54 shows effects of variation of inlet relative humidity on outlet water and air parameters. It was observed that exit air DBT, specific humidity, droplet temperature and thermal efficiency of SCT increased with increasing the air relative humidity. Table 5.54 also shows 20% relative humidity air produced maximum cooling of air, i.e. up to 12.22 ˚C and 40% relative humidity air gave the maximum thermal efficiency of SCT (56.87%). Table 5.54 also shows as the relative humidity of air increases the change in total exergy of air, exergy of water, and SLE of SCT decreased. As relative humidity of air increased, the destruction in total exergy of the system relatively decreased.

Table 5.54 Effect of variation in inlet air relative humidity (NPUMH)

1	2	3	4	5	6	7	8	9	10	11	12	13	14
Code	ϕ_{in} (%)	$T_{a,out}$ (˚C)	$\omega_{a,out}$ (kg_w/kg_a)	$T_{d,m,out}$ (˚C)	$m_{d,l}$ (kg/s)	η_{th} (%)	$X_{c,out}$ (W)	$X_{e,out}$ (W)	$X_{a,out}$ (W)	$X_{d,out}$ (W)	$X_{t,out}$ (W)	I_t (W)	η_{II} (%)
NPUMH-1	**20.00**	**27.78**	**0.0238**	**27.77**	**0.0018**	**53.89**	**31.96**	**123.63**	**155.59**	**13491.5**	**13647.09**	**290.17**	**97.46**
NPUMH-2	**25.00**	**28.55**	**0.0249**	**28.54**	**0.0016**	**54.02**	**27.72**	**86.92**	**114.65**	**11608.48**	**11723.12**	**239.66**	**97.31**
NPUMH-3	**30.00**	**29.31**	**0.0261**	**29.30**	**0.0014**	**54.49**	**24.06**	**61.36**	**85.43**	**10070.76**	**10156.18**	**196.34**	**97.11**
NPUMH-4	**35.00**	**30.04**	**0.0273**	**30.03**	**0.0012**	**55.40**	**20.75**	**43.06**	**63.81**	**8771.21**	**8835.03**	**158.74**	**96.16**
NPUMH-5	**40.00**	**30.76**	**0.0285**	**30.75**	**0.0010**	**56.87**	**17.76**	**29.77**	**47.52**	**7645.95**	**7693.48**	**125.82**	**95.66**

5.17.5 Effect of variation in inlet RLG (NPUML)

The Inlet RLG was varied from 0.5 to 1.5 in this research and its effects on various exit parameters are given in Table 5.55. The constant important inlet parameters used for this study are air DBT (40 ˚C), air relative humidity (20%), water droplet temperature (34 ˚C), and multi droplet diameter (25.45 – 254.54 µm). Table 5.55 shows exit air DBT, specific humidity of air and water droplet temperature increased with increasing the RLG. Maximum and minimum air DBT reduction was 12.22 ˚C and 09.66 ˚C which is obtained at 0.5 and 1.5 RLG respectively. The range of SCT decreased by increasing the RLG hence thermal efficiency of SCT also decreased by increase the RLG. Maximum thermal efficiency (53.89%) achieved by 0.5 RLG. Total exergy of air, exergy of water increased with increasing the RLG as exit air and water droplet temperature and mass of water increased with increases the RLG. As the amount of water in water to air mass flow ratio increased destruction in exergy of the system along tower height increase because the amount of exergy release by water is more than the amount of exergy gain by air. SLE of SCT increases with increase the RLG.

Table 5.55 Effect of variation in inlet RLG (NPUML)

1	2	3	4	5	6	7	8	9	10	11	12	13	14
Code	**RLG**$_{in}$	$T_{a,out}$ (˚C)	$\omega_{a,out}$ (kg_w/kg_a)	$T_{d,m,out}$ (˚C)	$m_{d,l}$ (kg/s)	η_{th} (%)	$X_{c,out}$ (W)	$X_{e,out}$ (W)	$X_{a,out}$ (W)	$X_{d,out}$ (W)	$X_{t,out}$ (W)	I_t (W)	η_{II} (%)
NPUML-1	**0.5**	**27.78**	**0.0238**	**27.77**	**0.0018**	**53.89**	**31.96**	**123.63**	**155.59**	**13491.5**	**13647.09**	**290.17**	**97.46**
NPUML-2	**0.75**	**28.72**	**0.0252**	**28.71**	**0.0019**	**45.76**	**27.2**	**146**	**173.2**	**20414.67**	**20587.87**	**416.25**	**98.02**
NPUML-3	**1**	**29.41**	**0.0263**	**29.4**	**0.0020**	**39.79**	**23.99**	**163.89**	**187.88**	**27355.49**	**27543.37**	**462.13**	**98.35**
NPUML-4	**1.25**	**29.93**	**0.0271**	**29.92**	**0.0021**	**35.29**	**21.67**	**178.53**	**200.2**	**34308.46**	**34508.66**	**498.23**	**98.58**
NPUML-5	**1.5**	**30.34**	**0.0278**	**30.33**	**0.0022**	**31.75**	**19.93**	**190.72**	**210.65**	**41270.17**	**41480.82**	**527.44**	**98.74**

5.18 Three Dimensional Parallel Flow Mono Droplet SCT for Air Cooling Application

This study based on 3-D mono droplet parallel flow CFD model to determine the effect of variation in inlet droplet diameters, water temperatures, air DBT, relative humidity of air and RLG on outlet parameters. The schematic diagram of 3-D parallel flow SCT is shown in Figure 3.1. Mesh of three dimensional parallel flow SCT shown in Figure 5.7. Initial conditions used for computer simulation are same as 2-D parallel flow mono droplets SCT used for air cooling application.

5.18.1 Effect of variation in initial droplets diameter (NPOCR)

Table 5.56 shows the variation in air and water droplet outlet parameters by changing inlet droplet diameter from 200 - 1000 µm, and the fixed inlet parameters of SCT are air DBT (40 ˚C), air relative humidity (20%), water temperature (34 ˚C), and RLG (0.5). Table 5.56 shows as droplet diameter increasing from 200 µm to 1000 µm, exit air DBT and water temperature increased and exit specific humidity, make up water required and thermal efficiency of SCT decreased because heat and mass transfer between air and water droplet decreased. Maximum and minimum air DBT

reduction is 11.88 ˚C and 0.48 ˚C which is obtain at 200 µm and 1000 µm respectively. Maximum SCT efficiency achieved with 200 µm droplet diameter and it was 50.95%**.** Total exergy of air is the sum of convective and evaporative exergy of air. Exergy of water and exergy of system increased with increases the droplet diameter. SLE of SCT increased with increase the droplet diameter. Convective, evaporative, total exergy of air and exergy destruction of system decreased with increasing the droplet diameters because heat and mass transfer between air and water decreased.

Table 5.56 Effect of variation in inlet droplet diameter (NPOCR)

1	2	3	4	5	6	7	8	9	10	11	12	13	14
Code	D_{in} (µm)	$T_{a,out}$ (˚C)	$\omega_{a,out}$ (kg_w/kg_a)	$T_{d,out}$ (˚C)	$m_{d,l}$ (kg/s)	η_{th} (%)	$X_{c,out}$ (W)	$X_{e,out}$ (W)	$X_{a,out}$ (W)	$X_{d,out}$ (W)	$X_{t,out}$ (W)	I_t (W)	η_{II} (%)
NPOCR-1	**200**	**28.12**	**0.0241**	**28.11**	**0.0019**	**50.95**	**29.81**	**133.77**	**163.58**	**13552.30**	**13715.88**	**286.87**	**97.95**
NPOCR-2	**400**	**31.30**	**0.0215**	**29.73**	**0.0015**	**36.91**	**14.61**	**95.66**	**110.27**	**13654.83**	**13765.10**	**237.65**	**98.30**
NPOCR-3	**600**	**36.49**	**0.0179**	**31.38**	**0.0012**	**22.68**	**3.44**	**50.87**	**54.31**	**13761.46**	**13815.77**	**186.98**	**98.66**
NPOCR-4	**800**	**38.73**	**0.0152**	**32.32**	**0.0010**	**14.56**	**0.96**	**27.16**	**28.12**	**13840.15**	**13868.27**	**134.48**	**99.04**
NPOCR-5	**1000**	**39.52**	**0.0143**	**32.86**	**0.0009**	**9.86**	**0.57**	**16.02**	**16.59**	**13905.16**	**13921.75**	**81.00**	**99.42**

5.18.2 Effect of variation in inlet Water Temperature (NPOCD)

The effects of variation of inlet water droplet temperature from 28 to 36 ˚C on exit air and water droplet parameters are given in Table 5.57. The unchanged inlet parameters used for this study are air DBT (40 ˚C), air relative humidity (20%), water droplet diameter (200 µm), and RLG (0.5). Table 5.57 shows as inlet water temperature increase exit air DBT, air specific humidity, water temperature, makeup water required, thermal efficiency of SCT increased. It also shows in Table when temperature of inlet water is 28 ˚C maximum cooling of air achieved (14.14 ˚C) due to high temperature difference between water and air (keeping air temperature

constant). The maximum SCT efficiency (52.88%) achieved by 36 ˚C inlet droplet temperature due to increase in sensible cooling as well as evaporative cooling. As inlet water droplet temperature increase, the specific humidity of air increased because due to increase in water temperature more water vapour is added in air. Table 5.57 also shows that increase in inlet water temperature, more quantity of water vapour mixed in air hence increased total exergy of air. The exergy destruction of system was increased and SLE decreased by increasing the inlet water droplet temperature. Depicted destruction in total exergy of system is more for higher temperature droplet because it transfers water content in to air faster than lower temperature droplets.

Table 5.57 Effect of variation in inlet water temperature (NPOCD)

1	2	3	4	5	6	7	8	9	10	11	12	13	14
Code	$T_{d,in}$ (˚C)	$T_{a,out}$ (˚C)	$\omega_{a,out}$ (kg_w/kg_a)	$T_{d,out}$ (˚C)	$m_{d,l}$ (kg/s)	η_{th} (%)	$X_{c,out}$ (W)	$X_{e,out}$ (W)	$X_{a,out}$ (W)	$X_{d,out}$ (W)	$X_{t,out}$ (W)	I_t (W)	η_{II} (%)
NPOCD-1	**28**	**25.86**	**0.0214**	**25.85**	**0.0016**	**38.67**	**41.85**	**88.59**	**130.44**	**13614.74**	**13745.18**	**142.71**	**98.97**
NPOCD-2	**30**	**26.63**	**0.0225**	**26.62**	**0.0017**	**44.71**	**36.87**	**104.72**	**141.59**	**13592.34**	**13733.93**	**185.89**	**98.66**
NPOCD-3	**32**	**27.38**	**0.0236**	**27.37**	**0.0018**	**48.43**	**32.38**	**121.97**	**154.35**	**13569.82**	**13724.17**	**233.93**	**98.32**
NPOCD-4	**34**	**28.12**	**0.0241**	**28.11**	**0.0019**	**50.95**	**29.81**	**133.77**	**163.58**	**13552.30**	**13715.88**	**286.87**	**97.95**
NPOCD-5	**36**	**28.85**	**0.0255**	**28.83**	**0.0020**	**52.88**	**26.06**	**151.04**	**177.10**	**13531.88**	**13708.98**	**344.48**	**97.55**

5.18.3 Effect of variation in inlet air DBT (NPOCA)

The effects of deviation of inlet air DBT from 36 - 44 ˚C on the exit parameters at constant inlet air relative humidity (20%), water temperature (34 ˚C), droplet diameter (200 µm), and RLG (0.5) are given in Table 5.58. Table 5.58 shows exit air DBT, air specific humidity and droplet temperatures increased relatively as inlet air DBT increases, it also shows 44 ˚C DBT air produced maximum cooling and it cool down water droplet up to 14.40 ˚C. Table 5.58 also represents that increase in

inlet air DBT, thermal efficiency of SCT decreased, and maximum thermal efficiency (51.58%) achieved at 36 ˚C. The total exergy of air, exergy of water, total exergy of system, and exergy destruction decreased with increasing the inlet air DBT. The SLE of system increased with increase the initial air DBT.

Table 5.58 Effect of variation in inlet air DBT (NPOCA)

1	2	3	4	5	6	7	8	9	10	11	12	13	14
Code	$T_{a,in}$ (˚C)	$T_{a,out}$ (˚C)	$\omega_{a,out}$ (kg_w/kg_a)	$T_{d,out}$ (˚C)	$m_{d,l}$ (kg/s)	η_{th} (%)	$X_{c,out}$ (W)	$X_{e,out}$ (W)	$X_{a,out}$ (W)	$X_{d,out}$ (W)	$X_{t,out}$ (W)	I_t (W)	η_{II} (%)
NPOCA-1	**36**	**26.67**	**0.0224**	**26.66**	**0.0021**	**51.58**	**22.23**	**145.59**	**167.82**	**13642.15**	**13809.97**	**325.57**	**97.70**
NPOCA-2	**38**	**27.37**	**0.0234**	**27.36**	**0.0020**	**51.23**	**28.41**	**139.93**	**168.34**	**13594.35**	**13762.69**	**308.29**	**97.81**
NPOCA-3	**40**	**28.12**	**0.0241**	**28.11**	**0.0019**	**50.95**	**29.81**	**133.77**	**163.58**	**13552.30**	**13715.88**	**286.87**	**97.95**
NPOCA-4	**42**	**28.85**	**0.0256**	**28.84**	**0.0018**	**50.69**	**41.33**	**117.22**	**158.55**	**13511.07**	**13669.62**	**262.81**	**98.11**
NPOCA-5	**44**	**29.60**	**0.0268**	**29.59**	**0.0017**	**50.34**	**48.78**	**94.21**	**142.99**	**13480.92**	**13623.91**	**238.98**	**98.28**

5.18.4 Effect of variation in inlet Air Relative Humidity (NPOCH)

This study was based on variation of inlet relative humidity from 20% to 40%. The fixed inlet parameters of this study was air DBT (36 ˚C), water droplet temperature (34 ˚C), droplet diameter (200 µm) and RLG (0.5). Table 5.59 shows exit air DBT, specific humidity, droplet temperature and thermal efficiency of SCT increased with increasing the air relative humidity.

Table 5.59 Effect of variation in inlet air relative humidity (NPOCH)

1	2	3	4	5	6	7	8	9	10	11	12	13	14
Code	ϕ_{in} (%)	$T_{a,out}$ (˚C)	$\omega_{a,out}$ (kg_w/kg_a)	$T_{d,out}$ (˚C)	$m_{d,l}$ (kg/s)	η_{th} (%)	$X_{c,out}$ (W)	$X_{e,out}$ (W)	$X_{a,out}$ (W)	$X_{d,out}$ (W)	$X_{t,out}$ (W)	I_t (W)	η_{II} (%)
NPOCH-1	**20**	**28.12**	**0.0241**	**28.11**	**0.0019**	**50.95**	**29.81**	**133.77**	**163.58**	**13824.30**	**13987.88**	**301.49**	**97.89**
NPOCH-2	**25**	**28.77**	**0.0254**	**28.76**	**0.0016**	**52.82**	**26.70**	**88.34**	**115.04**	**11752.86**	**11867.90**	**398.43**	**96.75**
NPOCH-3	**30**	**29.49**	**0.0265**	**29.48**	**0.0014**	**54.20**	**23.32**	**62.52**	**85.84**	**10046.90**	**10132.74**	**482.25**	**95.46**
NPOCH-4	**35**	**30.5**	**0.0282**	**30.19**	**0.0012**	**55.87**	**18.98**	**44.01**	**62.99**	**8653.61**	**8716.60**	**503.93**	**94.53**
NPOCH-5	**40**	**30.98**	**0.0289**	**30.97**	**0.0011**	**56.53**	**17.01**	**27.36**	**44.37**	**7428.08**	**7472.45**	**541.88**	**93.24**

Table 5.59 also shows 20% relative humidity air produced maximum cooling, i.e. up to 11.88 ˚C and 40% relative humidity air gave maximum thermal efficiency (56.53%). Table 5.59 also shows as relative humidity of air increased the change in total exergy of air, exergy of water, and SLE of SCT is decrease. As relative humidity of air increase the destruction in total exergy of system increased.

5.18.5 Effect of variation in inlet RLG (NPOCL)

In this section inlet RLG was varied from 0.5 to 1.5, and persistent inlet parameters of SCT are air DBT (40 ˚C), air relative humidity (20%), Water temperature (34 ˚C), and water droplet diameter (200 μm). Table 5.60 shows as RLG increased exit air DBT, air specific humidity and droplet temperature increases because mass of water at inlet increased.

Table 5.60 Effect of variation in inlet RLG (NPOCL)

1	2	3	4	5	6	7	8	9	10	11	12	13	14
Code	**RLG_{in}**	**$T_{a,out}$ (˚C)**	**$\omega_{a,out}$ (kg_w/kg_a)**	**$T_{d,out}$ (˚C)**	**$m_{d,l}$ (kg/s)**	**η_{th} (%)**	**$X_{c,out}$ (W)**	**$X_{e,out}$ (W)**	**$X_{a,out}$ (W)**	**$X_{d,out}$ (W)**	**$X_{t,out}$ (W)**	**I_t (W)**	**η_{II} (%)**
NPOCL-1	**0.5**	**28.12**	**0.0241**	**28.11**	**0.0019**	**50.95**	**29.81**	**133.77**	**163.58**	**13824.30**	**13987.88**	**301.50**	**97.89**
NPOCL-2	**0.75**	**29.06**	**0.0255**	**29.05**	**0.0020**	**42.82**	**25.22**	**157.38**	**182.60**	**20918.86**	**21101.46**	**332.60**	**98.45**
NPOCL-3	**1**	**29.75**	**0.0266**	**29.74**	**0.0021**	**36.85**	**22.38**	**174.48**	**196.86**	**28033.18**	**28230.04**	**348.71**	**98.78**
NPOCL-4	**1.25**	**30.26**	**0.0274**	**30.25**	**0.0022**	**32.44**	**20.29**	**180.66**	**200.95**	**35167.68**	**35368.63**	**354.80**	**99.01**
NPOCL-5	**1.5**	**30.61**	**0.0281**	**30.66**	**0.0023**	**28.89**	**18.51**	**201.29**	**219.80**	**42294.43**	**42514.23**	**353.89**	**99.17**

The maximum and minimum air DBT reduction was 11.88 ˚C and 09.36 ˚C which obtained at 0.5 and 1.5 RLG respectively. The range of SCT was decreased by increasing the RLG hence thermal efficiency of SCT also decreased by increasing the RLG. Total exergy of air, exergy of water, and exergy of system increased with increasing the RLG because mass of water increased with increasing the RLG. As amount of water in water to air mass flow ratio increase destruction in exergy of

system along tower height increased because amount of exergy release by water was more than amount of exergy gain by air. SLE of SCT increased with increasing the RLG.

5.19 Three Dimensional Parallel Flow Multi Droplet SCT for Air Cooling Application

This study based on 3-D multi droplet parallel flow CFD model to determine the effect of variation in inlet droplet diameters, water temperatures, air DBT, relative humidity of air and RLG on outlet parameters. The schematic diagram of 3-D parallel flow SCT is shown in Figure 3.1. Mesh of three dimensional parallel flow SCT shown in Figure 5.7. Initial conditions used for computer simulation are same as 2-D parallel flow multi droplets SCT used for air cooling application.

5.19.1 Effect of variation in initial droplets diameter (NPUCR)

The effect of variation of inlet multi droplet diameters on outlet air DBT, air specific humidity, water temperature, makeup water required, thermal efficiency, convective exergy of air, evaporative exergy of air, total exergy of air, water exergy, total exergy of system, exergy destruction and SLE at constant inlet air DBT (40 ˚C), air relative humidity (20%), water temperature (34 ˚C), and RLG (0.5) are given in Table 5.61. Table 5.61 shows as multi droplet diameter increases exit air DBT and water temperature increased and exit specific humidity, make up water required and thermal efficiency of SCT decreased because heat and mass transfer between air and water droplet decreased. It is also clear that 25.45-254.54 μm size water droplets produce maximum cooling (11.53 ˚C) and maximum efficiency (47.92%). Total

exergy of air and exergy destruction decreased as inlet droplet diameter increases. Exergy of water, exergy of system and SLE increased with increasing the droplet diameter because heat and mass transfer between air and water decreases.

Table 5.61 Effect of variation in inlet droplet diameter (NPUCR)

1	2	3	4	5	6	7	8	9	10	11	12	13	14
Code	D_{in} (µm)	$T_{a,out}$ (˚C)	$\omega_{a,out}$ (kg_w/kg_a)	$T_{d,m,out}$ (˚C)	$m_{d,l}$ (kg/s)	η_{th} (%)	$X_{c,out}$ (W)	$X_{e,out}$ (W)	$X_{a,out}$ (W)	$X_{d,out}$ (W)	$X_{t,out}$ (W)	I_t (W)	η_{II} (%)
NPUCR-1	25.45-254.54	28.47	0.0244	28.46	0.002	47.92	30.18	131.98	162.16	13620.81	13782.97	219.78	98.43
NPUCR-2	50.90-509.09	31.65	0.0198	30.08	0.0016	33.88	16.02	72.02	88.04	13744.15	13832.19	170.56	98.78
NPUCR-3	76.36-763.64	36.84	0.0148	31.72	0.0013	19.74	2.61	22.46	25.07	13857.79	13882.86	119.89	99.14
NPUCR-4	101.81-1018.18	39.08	0.0125	32.66	0.0011	11.62	0.36	7.59	7.95	13927.41	13935.36	67.39	99.52
NPUCR-5	127.27-1272.73	39.87	0.0115	33.20	0.0010	6.92	0.02	2.05	2.07	13986.77	13988.84	13.91	99.90

5.19.2 Effect of variation in inlet Water Temperature (NPUCD)

This research based on the variation of inlet water temperature from 28 ˚C to 36 ˚C. Table 5.62 shows deviations in outlet parameters at constant inlet air DBT (40 ˚C), air relative humidity (20 %), multi droplet diameter (25.45-254.54 µm) and RLG (0.5). Table 5.62 also shows as inlet water temperature increases exit air DBT, air specific humidity, water temperature, makeup water required, and thermal efficiency of SCT increased. It also observed that maximum cooling of air (13.78 ˚C) was achieved by 28 ˚C inlet water temperature, as high temperature difference between water and air (keeping air temperature constant) increased sensible cooling as well as evaporative cooling. As inlet water droplet temperature increase the specific humidity of air increased because due to increase in water temperature more water vapour is added in air. Table 5.62 also shows that increase in inlet water temperature, more quantity of water vapour mixed in air and increased total exergy of air. The exergy

destruction of system was increased and SLE decreased by increasing the inlet water droplet temperature. The depicted destruction in total exergy of system was more for higher temperature droplet because it transfers water content in to air faster than lower temperature droplets.

Table 5.62 Effect of variation in inlet water temperature (NPUCD)

1	2	3	4	5	6	7	8	9	10	11	12	13	14
Code	$T_{d,in}$ (˚C)	$T_{a,out}$ (˚C)	$\omega_{a,out}$ (kg_w/kg_a)	$T_{d,m,out}$ (˚C)	$m_{d,l}$ (kg/s)	η_{th} (%)	$X_{c,out}$ (W)	$X_{e,out}$ (W)	$X_{a,out}$ (W)	$X_{d,out}$ (W)	$X_{t,out}$ (W)	I_t (W)	η_{II} (%)
NPUCD-1	**28**	**26.22**	**0.0211**	**26.21**	**0.0017**	**32.19**	**43.37**	**84.23**	**127.6**	**13685.43**	**13813.03**	**74.85**	**99.46**
NPUCD-2	**30**	**26.99**	**0.0222**	**26.98**	**0.0018**	**39.95**	**38.51**	**93.52**	**132.03**	**13669.43**	**13801.46439**	**118.36**	**99.15**
NPUCD-3	**32**	**27.73**	**0.0225**	**27.72**	**0.0019**	**44.77**	**34.26**	**108.07**	**142.33**	**13649.15**	**13791.47905**	**166.62**	**98.81**
NPUCD-4	**34**	**28.47**	**0.0244**	**28.46**	**0.002**	**47.92**	**30.18**	**131.98**	**162.16**	**13620.81**	**13782.97**	**219.78**	**98.43**
NPUCD-5	**36**	**29.2**	**0.0232**	**29.18**	**0.0021**	**50.29**	**26.72**	**147.67**	**174.39**	**13601.49**	**13775.87571**	**277.58**	**98.02**

5.19.3 Effect of variation in inlet air DBT (NPUCA)

Table 5.63 shows the effect of deviation in exit parameters of SCT at constant inlet air relative humidity (20%), water temperature (34 ˚C), water droplet diameter (25.45-254.54 µm) and RLG (0.5) by varying the air DBT from 36 - 44 ˚C. It was observed from Table 5.63 that exit air DBT, specific humidity and droplet temperatures increased relatively as inlet air DBT increases; it also shows 44 ˚C DBT air produced maximum cooling and it cool down exit air up to 14.06 ˚C. Table 5.63 also represents that increase in inlet air DBT temperature the thermal efficiency of SCT decreased. The maximum thermal efficiency (48.49%) achieved by 28 ˚C inlet air DBT. The total exergy of air, exergy of water, and total exergy of system was decreased with increasing the inlet air DBT temperature. The SLE of system increased as exergy destruction decreased with increase the inlet air DBT.

Table 5.63 Effect of variation in inlet air DBT (NPUCA)

1	2	3	4	5	6	7	8	9	10	11	12	13	14
Code	$T_{a,in}$ (˚C)	$T_{a,out}$ (˚C)	$\omega_{a,out}$ (kg_w/kg_a)	$T_{d,m,out}$ (˚C)	$m_{d,l}$ (kg/s)	η_{th} (%)	$X_{c,out}$ (W)	$X_{e,out}$ (W)	$X_{a,out}$ (W)	$X_{d,out}$ (W)	$X_{t,out}$ (W)	I_t (W)	η_{II} (%)
NPUCA-1	**36**	**27.11**	**0.0216**	**27.1**	**0.0022**	**48.49**	**22.52**	**143.75**	**166.27**	**13712.51157**	**13878.78**	**256.75**	**98.18**
NPUCA-2	**38**	**27.78**	**0.0221**	**27.77**	**0.0021**	**48.07**	**29.12**	**136.17**	**165.29**	**13665.39863**	**13830.68863**	**240.29**	**98.29**
NPUCA-3	**40**	**28.47**	**0.0244**	**28.46**	**0.002**	**47.92**	**30.18**	**131.98**	**162.16**	**13620.81**	**13782.97**	**219.78**	**98.43**
NPUCA-4	**42**	**29.19**	**0.0255**	**29.18**	**0.0019**	**47.35**	**42.03**	**111.41**	**153.44**	**13583.05327**	**13736.49327**	**195.94**	**98.59**
NPUCA-5	**44**	**29.94**	**0.0265**	**29.93**	**0.0018**	**46.46**	**48.11**	**94.81**	**142.92**	**13547.23**	**13690.15**	**172.74**	**98.75**

5.19.4 Effect of variation in inlet Air Relative Humidity (NPUCH)

In this section air relative humidity varied from 20% to 40%, and constant inlet parameters of SCT are air DBT (40 ˚C), water temperature (34 ˚C), water droplet diameter (200 µm) and RLG (0.5). Table 5.64 shows exit air DBT, specific humidity, droplet temperature and thermal efficiency of SCT increased with increasing the air relative humidity.

Table 5.64 Effect of variation in inlet air relative humidity (NPUCH)

1	2	3	4	5	6	7	8	9	10	11	12	13	14
Code	ϕ_{in} (%)	$T_{a,out}$ (˚C)	$\omega_{a,out}$ (kg_w/kg_a)	$T_{d,m,out}$ (˚C)	$m_{d,l}$ (kg/s)	η_{th} (%)	$X_{c,out}$ (W)	$X_{e,out}$ (W)	$X_{a,out}$ (W)	$X_{d,out}$ (W)	$X_{t,out}$ (W)	I_t (W)	η_{II} (%)
NPUCH-1	**20**	**28.47**	**0.0244**	**28.46**	**0.002**	**47.92**	**30.18**	**131.98**	**162.16**	**13620.81**	**13782.97**	**219.78**	**98.43**
NPUCH-2	**25**	**29.24**	**0.0254**	**29.23**	**0.0018**	**47.19**	**26.48**	**86.92**	**113.4**	**11674.41**	**11858.66**	**188.54**	**98.44**
NPUCH-3	**30**	**29.98**	**0.0265**	**29.97**	**0.0016**	**46.73**	**23.01**	**61.36**	**84.37**	**10149.02**	**10291.37**	**167.06**	**98.40**
NPUCH-4	**35**	**30.71**	**0.0278**	**30.70**	**0.0014**	**46.04**	**19.61**	**43.06**	**62.67**	**8904.61**	**8970.01**	**217.83**	**97.63**
NPUCH-5	**40**	**31.42**	**0.0291**	**31.41**	**0.0012**	**45.32**	**16.36**	**23.55**	**39.91**	**7804.08**	**7828.11**	**214.41**	**97.33**

Table 5.64 also shows 20% relative humidity air produce maximum cooling (11.53 ˚C), and maximum efficiency (47.92%). Table 5.64 also shows as relative humidity of air increases the change in total exergy of air, exergy of water, and SLE of SCT decreased. As relative humidity of air increases, the destruction in total exergy

of system relatively decreased because low relative humidity air absorbs more amount of water from droplets.

5.19.5 Effect of variation in inlet RLG (NPUCL)

In this section inlet RLG was varied from 0.5 to 1.5, and constant inlet parameters of SCT are air DBT (40 ˚C), air relative humidity (20%), water droplet diameter (200 μm), and water temperature (34 ˚C). Table 5.65 shows as RLG increases exit air DBT, air specific humidity and droplet temperature increased because the mass of water at inlet increased.

Table 5.65 Effect of variation in inlet RLG (NPUCL)

1	2	3	4	5	6	7	8	9	10	11	12	13	14
Code	**RLG**$_{in}$	$T_{a,out}$ (˚C)	$\omega_{a,out}$ (kg_w/kg_a)	$T_{d,m,out}$ (˚C)	$m_{d,l}$ (kg/s)	η_{th} (%)	$X_{c,out}$ (W)	$X_{e,out}$ (W)	$X_{a,out}$ (W)	$X_{d,out}$ (W)	$X_{t,out}$ (W)	I_t (W)	η_{II} (%)
NPUCL-1	**0.5**	**28.47**	**0.0244**	**28.46**	**0.002**	**47.92**	**30.18**	**131.98**	**162.16**	**13620.81**	**13782.97**	**219.78**	**98.43**
NPUCL-2	**0.75**	**29.4**	**0.0258**	**29.39**	**0.0021**	**39.88**	**26.55**	**146**	**172.55**	**20618.29**	**20790.84**	**213.28**	**98.98**
NPUCL-3	**1**	**30.08**	**0.0269**	**30.07**	**0.0022**	**34.00**	**22.94**	**163.89**	**186.83**	**27627.84**	**27814.67**	**190.84**	**99.32**
NPUCL-4	**1.25**	**30.58**	**0.0277**	**30.57**	**0.0023**	**29.67**	**20.39**	**178.53**	**198.92**	**34646.67**	**34845.59**	**161.28**	**99.54**
NPUCL-5	**1.5**	**30.99**	**0.0284**	**30.98**	**0.0024**	**26.12**	**18.85**	**198.27**	**217.12**	**41667.63**	**41884.75**	**123.50**	**99.71**

The maximum and minimum air DBT reduction was 11.53 ˚C and 09.01 ˚C which obtained at 0.5 and 1.5 RLG respectively. The range of SCT was decreased by increasing the RLG hence the thermal efficiency of SCT also decreased by increasing the RLG. The total exergy of air, exergy of water increased with increasing the RLG as exit air and water droplet temperature and mass of water increased with increasing the RLG. As the amount of water in water to air mass flow ratio increases destruction in exergy of the system along tower height decreased. SLE of SCT was increased with increasing the RLG.

5.20 Two Dimensional Counter flow Mono Droplet SCT for Air Cooling Application

This study based on 2-D mono droplet counter flow MATLAB model to determine the effect of variation in inlet droplet diameters, water temperatures, air DBT, relative humidity of air and RLG on outlet parameters. Initial conditions used for computer simulation are same as 2-D parallel flow mono droplets SCT used for air cooling application.

5.20.1 Effect of variation in initial droplets diameter (NCOMR)

Table 5.66 shows the variation of water and air exit parameters by varying inlet droplet diameters. The fixed inlet parameters used for this study are air DBT (40 ˚C), air relative humidity (20%), water temperature (34 ˚C), and RLG (0.5).

Table 5.66 Effect of variation in inlet droplet diameter (NCOMR)

1	2	3	4	5	6	7	8	9	10	11	12	13	14
Code	D_{in} (µm)	$T_{a,out}$ (˚C)	$\omega_{a,out}$ (kg_w/kg_a)	$T_{d,out}$ (˚C)	$m_{d,l}$ (kg/s)	η_{th} (%)	$X_{c,out}$ (W)	$X_{e,out}$ (W)	$X_{a,out}$ (W)	$X_{d,out}$ (W)	$X_{t,out}$ (W)	I_t (W)	η_{II} (%)
NCOMR-1	**200**	**25.41**	**0.0219**	**25.4**	**0.0011**	**74.39**	**38.99**	**89.25**	**128.24**	**11369.70**	**11497.94**	**2504.81**	**82.11**
NCOMR-2	**400**	**28.59**	**0.0227**	**27.02**	**0.0007**	**60.35**	**28.34**	**88.34**	**116.68**	**11430.47691**	**11547.16**	**2455.59**	**82.46**
NCOMR-3	**600**	**33.78**	**0.0195**	**28.69**	**0.0004**	**45.95**	**25.65**	**62.52**	**88.17**	**11509.66143**	**11597.83**	**2404.92**	**82.83**
NCOMR-4	**800**	**36.03**	**0.0181**	**29.66**	**0.0002**	**37.57**	**24.657**	**44.01**	**68.67**	**11581.66013**	**11650.33**	**2352.42**	**83.20**
NCOMR-5	**1000**	**36.82**	**0.0163**	**30.20**	**0.0001**	**32.87**	**21.48**	**37.69**	**59.17**	**11644.64154**	**11703.81**	**2298.94**	**83.58**

As droplet diameter increases from 200 µm to 1000 µm, exit air DBT and water temperature increased and exit specific humidity, makeup water required and thermal efficiency of SCT decreased as heat and mass transfer between air and water droplet decreased. It is also clear from Table that 200 µm size water droplets gave maximum cooling and maximum efficiency; it reduced droplet temperature up to

14.59 °C and maximum efficiency was 74.39%. Total exergy of air decreased as inlet droplet diameter increases. The exergy destruction of system decreased with increase the droplet diameter. The exergy of water, exergy of system and SLE was increased with increasing the droplet diameter because heat and mass transfer between air and water decreased.

5.20.2 Effect of variation in inlet Water Temperature (NCOMD)

This research based on variation of inlet water temperature from 28 - 36 ˚C. The inlet persistent parameters used in this research are air DBT (40 ˚C), air relative humidity (20%), water droplet diameter (200 µm), and RLG (0.5). Table 5.67 shows as inlet water temperature increases exit air DBT, air specific humidity, water temperature, makeup water required increased. The thermal efficiency of SCT was decreased with increasing the inlet water temperature. The maximum thermal efficiency obtain by 28 ˚C water droplet was 87.95%. It also shows that when temperature of inlet water is 28 ˚C maximum cooling of droplet achieved (16.91 ˚C) as high temperature difference between water and air (keeping air temperature constant). As inlet water droplet temperature increases, the specific humidity of air increased because due to increase in water temperature more water vapour added in the air, Table 5.67 also shows that increased in inlet water temperature, more quantity of water vapour mixed in air and increased total exergy of air. The exergy destruction of system was increased and SLE decreased by increasing the inlet water droplet temperature. The depicted destruction in total exergy of system was more for higher temperature droplet because it transfers water content in to air faster than lower temperature droplets.

Table 5.67 Effect of variation in inlet water temperature (NCOMD)

1	2	3	4	5	6	7	8	9	10	11	12	13	14
Code	$T_{d,in}$ (˚C)	$T_{a,out}$ (˚C)	$\omega_{a,out}$ (kg_w/kg_a)	$T_{d,out}$ (˚C)	$m_{d,l}$ (kg/s)	η_{th} (%)	$X_{c,out}$ (W)	$X_{e,out}$ (W)	$X_{a,out}$ (W)	$X_{d,out}$ (W)	$X_{t,out}$ (W)	I_t (W)	η_{II} (%)
NCOMD-1	**28**	**23.09**	**0.0201**	**23.11**	**0.0008**	**87.95**	**47.79**	**51.06**	**98.85**	**11424.43**	**11523.28**	**2364.60**	**82.97**
NCOMD-2	**30**	**23.86**	**0.0207**	**23.87**	**0.0009**	**81.08**	**44.10**	**64.61**	**108.71**	**11404.40**	**11513.11**	**2406.72**	**82.71**
NCOMD-3	**32**	**24.65**	**0.0217**	**24.66**	**0.0010**	**76.78**	**40.24**	**76.45**	**116.69**	**11387.82**	**11504.51**	**2453.59**	**82.42**
NCOMD-4	**34**	**25.41**	**0.0219**	**25.4**	**0.0011**	**74.39**	**38.99**	**89.25**	**128.24**	**11369.70**	**11497.94**	**2504.82**	**82.11**
NCOMD-5	**36**	**26.15**	**0.0233**	**26.16**	**0.0012**	**72.57**	**33.70**	**115.27**	**148.97**	**11343.83**	**11492.80**	**2560.66**	**81.78**

5.20.3 Effect of variation in inlet air DBT (NCOMA)

In this section inlet DBT of air has been varied from 36 - 44 ˚C and other constant inlet parameters of SCT are air relative humidity (20%), water temperature (34 ˚C), water droplet diameter (200 µm), and RLG (0.5). Table 5.68 shows exit air DBT, specific humidity and droplet temperatures increased relatively as inlet air DBT increases; it also shows 24 ˚C DBT air produced maximum cooling and it cool down water droplet up to 16.02 ˚C.

Table 5.68 Effect of variation in inlet air DBT (NCOMA)

1	2	3	4	5	6	7	8	9	10	11	12	13	14
Code	$T_{a,in}$ (˚C)	$T_{a,out}$ (˚C)	$\omega_{a,out}$ (kg_w/kg_a)	$T_{d,out}$ (˚C)	$m_{d,l}$ (kg/s)	η_{th} (%)	$X_{c,out}$ (W)	$X_{e,out}$ (W)	$X_{a,out}$ (W)	$X_{d,out}$ (W)	$X_{t,out}$ (W)	I_t (W)	η_{II} (%)
NCOMA-1	**36**	**23.98**	**0.0210**	**23.97**	**0.0013**	**70.48**	**11.87**	**169.69**	**181.56**	**11408.75**	**11590.31**	**2545.22**	**81.99**
NCOMA-2	**38**	**24.67**	**0.0214**	**24.66**	**0.0012**	**72.07**	**16.17**	**138.14**	**154.31**	**11389.64**	**11543.95**	**2527.03**	**82.04**
NCOMA-3	**40**	**25.41**	**0.0219**	**25.4**	**0.0011**	**74.39**	**38.99**	**89.25**	**128.24**	**11369.70**	**11497.94**	**2504.81**	**82.11**
NCOMA-4	**42**	**26.15**	**0.0239**	**26.14**	**0.0010**	**77.21**	**35.44**	**112.95**	**148.39**	**11304.14**	**11452.53**	**2479.90**	**82.20**
NCOMA-5	**44**	**26.95**	**0.0251**	**26.94**	**0.0009**	**80.59**	**44.97**	**112.79**	**157.76**	**11249.39**	**11407.15**	**2455.74**	**82.29**

Table 5.68 also represents that increased in inlet air DBT temperature, the thermal efficiency of SCT increases. The maximum thermal efficiency (80.59%) achieved by 44 ˚C inlet air DBT. Total exergy of the air, exergy of water, exergy of

the system, and exergy destruction was decreased with increasing the inlet air DBT. The SLE of the system was increased with increasing the initial air DBT.

5.20.4 Effect of variation in inlet Air Relative Humidity (NCOMH)

This study is based on variation of inlet relative humidity from 20% to 40%, and other constant inlet parameters are air DBT (40 ˚C), water temperature (34 ˚C), droplet diameter (200 µm) and RLG (0.5). Table 5.69 shows exit air DBT, specific humidity, droplet temperature and thermal efficiency of SCT was increased with increasing the inlet air relative humidity.

Table 5.69 Effect of variation in inlet air relative humidity (NCOMH)

1	2	3	4	5	6	7	8	9	10	11	12	13	14
Code	ϕ_{in} (%)	$T_{a,out}$ (˚C)	$\omega_{a,out}$ (kg_w/kg_a)	$T_{d,out}$ (˚C)	$m_{d,l}$ (kg/s)	η_{th} (%)	$X_{c,out}$ (W)	$X_{e,out}$ (W)	$X_{a,out}$ (W)	$X_{d,out}$ (W)	$X_{t,out}$ (W)	I_t (W)	η_{II} (%)
NCOMH-1	**20**	**25.41**	**0.0219**	**25.4**	**0.0011**	**74.39**	**38.99**	**89.25**	**128.24**	**11369.70**	**11497.94**	**2504.81**	**82.11**
NCOMH-2	**25**	**26.18**	**0.0238**	**26.17**	**0.0009**	**77.49**	**31.56**	**78.34**	**109.90**	**11064.76**	**9575.31**	**2471.88**	**79.48**
NCOMH-3	**30**	**26.96**	**0.0251**	**26.95**	**0.0007**	**81.72**	**27.21**	**62.52**	**89.73**	**9612.67**	**8009.71**	**2448.72**	**76.59**
NCOMH-4	**35**	**27.72**	**0.0265**	**27.71**	**0.0005**	**87.80**	**23.17**	**44.01**	**67.18**	**8382.62**	**6689.62**	**2418.22**	**72.81**
NCOMH-5	**40**	**28.44**	**0.0280**	**28.43**	**0.0003**	**97.50**	**19.43**	**38.39**	**57.82**	**7320.88**	**5549.20**	**2393.32**	**69.00**

Table 5.69 also shows 20% relative humidity air produced maximum cooling, i.e. up to 14.59 ˚C and 40% relative humidity air gave maximum thermal efficiency (97.50%). Table 5.69 also shows as relative humidity of air increases the change in total exergy of air, exergy of water, and SLE of SCT is decreased. The destruction in total exergy of the system relatively decreased with increases the relative humidity of air, because low relative humidity air absorbs more amount of water from droplets.

5.20.5 Effect of variation in inlet RLG (NCOML)

In this study inlet RLG was varied from 0.5 to 1.5, and others important constant inlet parameters of SCT are air DBT (40 ˚C), air relative humidity (20%), water droplet diameter (200 μm), and water temperature (34 ˚C). Table 5.70 shows as RLG increases exit air DBT, air specific humidity and droplet temperature, makeup water required increased because the mass of water at inlet increased.

Table 5.70 Effect of variation in inlet RLG (NCOML)

1	2	3	4	5	6	7	8	9	10	11	12	13	14
Code	**RLG_{in}**	**$T_{a,out}$ (˚C)**	**$\omega_{a,out}$ (kg_w/kg_a)**	**$T_{d,out}$ (˚C)**	**$m_{d,l}$ (kg/s)**	**η_{th} (%)**	**$X_{c,out}$ (W)**	**$X_{e,out}$ (W)**	**$X_{a,out}$ (W)**	**$X_{d,out}$ (W)**	**$X_{t,out}$ (W)**	**I_t (W)**	**η_{II} (%)**
NCOML-1	**0.5**	**25.41**	**0.0219**	**25.4**	**0.0011**	**74.39**	**38.99**	**89.25**	**128.24**	**11369.70**	**11497.94**	**2504.81**	**82.11**
NCOML-2	**0.75**	**26.34**	**0.0233**	**26.33**	**0.0012**	**66.35**	**33.78**	**148.02**	**181.80**	**17179.46**	**17361.26**	**3642.86**	**82.66**
NCOML-3	**1**	**27.04**	**0.0244**	**27.03**	**0.0013**	**60.29**	**30.26**	**165.99**	**196.25**	**23047.67**	**23243.92**	**4761.59**	**83.00**
NCOML-4	**1.25**	**27.6**	**0.0252**	**27.59**	**0.0014**	**55.45**	**27.76**	**180.64**	**208.40**	**28917.55**	**29125.95**	**5880.92**	**83.20**
NCOML-5	**1.5**	**28.01**	**0.0259**	**28**	**0.0015**	**51.90**	**25.98**	**148.25**	**174.23**	**34853.89**	**35028.12**	**6980.13**	**83.38**

The maximum and minimum water droplet temperature reduction was 14.59 ˚C and 11.99 ˚C which was obtained at 0.5 and 1.5 RLG respectively. The range of SCT was decreased by increasing the RLG hence the thermal efficiency of SCT also decreased by increasing the RLG. The maximum thermal efficiency (74.39%) achieved by 0.5 RLG. Total exergy of air, exergy of water increased with increasing the RLG because exit air and water droplet temperature and mass of water increased with increases RLG. As the amount of water in water to air mass flow ratio increased destruction in exergy of the system along tower height increases because amount of exergy release by water is more than the amount of exergy gain by air. The SLE of SCT also increased with increasing the RLG.

5.21 Two Dimensional Counter flow Multi Droplet SCT for Air Cooling Application

This study based on 2-D multi droplet counter flow MATLAB model to determine the effect of variation in inlet droplet diameters, water temperatures, air DBT, relative humidity of air and RLG on outlet parameters. The schematic diagram of 2-D counter flow SCT is shown in Figure 1.2. Initial conditions used for computer simulation are same as 2-D parallel flow multi droplets SCT used for air cooling application.

5.21.1 Effect of variation in initial droplets diameter (NCUMR)

This section of research was based on the variation of inlet multi droplet diameters from 25.45 - 254.54 µm to 127.27 - 1272.73 µm. The other important constant inlet parameters air DBT (40 ˚C), air relative humidity (20%), water temperature (34 ˚C), and RLG (0.5). Table 5.71 shows as multi droplet diameter increase exit air DBT and water temperature increased and exit specific humidity, makeup water required and thermal efficiency of SCT decreased because heat and mass transfer between air and water droplet decreased. For smaller size droplets the decreased in droplet temperature and increased in specific humidity of air relatively faster because smaller size droplets cover the larger area in SCT. It is also clear that droplets between 25.45 - 254.54 µm produce maximum cooling and maximum efficiency; it reduced droplet temperature up to 14.24 °C. The total exergy of air and exergy destruction decreased as inlet droplet diameter increases. The exergy of water, exergy of system and SLE increased with increases the droplet diameter because heat and mass transfer between air and water decreased.

Table 5.71 Effect of variation in inlet droplet diameter (NCUMR)

1	2	3	4	5	6	7	8	9	10	11	12	13	14
Code	D_{in} (µm)	$T_{a,out}$ (˚C)	$\omega_{a,out}$ (kg_w/kg_a)	$T_{d,m,out}$ (˚C)	$m_{d,l}$ (kg/s)	η_{th} (%)	$X_{c,out}$ (W)	$X_{e,out}$ (W)	$X_{a,out}$ (W)	$X_{d,out}$ (W)	$X_{t,out}$ (W)	I_t (W)	η_{II} (%)
NCUMR-1	**25.45-254.54**	**25.76**	**0.0222**	**25.75**	**0.0012**	**71.37**	**36.98**	**100.03**	**137.01**	**11428.78**	**11565.79**	**2436.97**	**82.60**
NCUMR-2	**50.90-509.09**	**28.94**	**0.0185**	**27.37**	**0.0008**	**57.32**	**24.44**	**72.02**	**96.46**	**11518.54271**	**11615.00**	**2387.75**	**82.95**
NCUMR-3	**76.36-763.64**	**34.13**	**0.0137**	**29.04**	**0.0005**	**42.92**	**10.13**	**22.46**	**32.59**	**11633.08723**	**11665.68**	**2337.07**	**83.31**
NCUMR-4	**101.81-1018.18**	**36.38**	**0.0113**	**30.00**	**0.0003**	**34.63**	**4.27**	**7.59**	**11.86**	**11706.31293**	**11718.17**	**2284.58**	**83.68**
NCUMR-5	**127.27-1272.73**	**37.17**	**0.0102**	**30.54**	**0.0002**	**29.93**	**3.98**	**4.81**	**8.79**	**11762.86734**	**11771.66**	**2231.09**	**84.07**

5.21.2 Effect of variation in inlet Water Temperature (NCUMD)

The effect of variation of inlet water temperatures from 28 ˚C to 36 ˚C on various exit parameters are given in the Table 5.72. The other fixed parameters of SCT are air DBT (40 ˚C), air relative humidity (20%), multi droplet diameters (25.45 - 254.54 µm), and RLG (0.5). Table 5.72 shows as inlet water temperature increases exit air DBT, air specific humidity, water temperature, and makeup water required increased. The thermal efficiency of SCT decreased with increase the inlet water temperature. It also observed that when the temperature of inlet water is 28 ˚C, maximum cooling of droplet achieved (16.55 ˚C) as high temperature difference between water and air (keeping air temperature constant). As inlet water droplet temperature increases, the specific humidity of air increased because due to increasing in water temperature more water vapour was added in air, Table 5.72 also shows that increase in inlet water temperature, more quantity of water vapour mixed in air and increased total exergy of air. The exergy destruction of the system also increased, and SLE decreased by increases the inlet water droplet temperature. The depicted destruction in total exergy of the system is more for higher temperature droplet because it transfers water content into air faster than lower temperature droplets.

Table 5.72 Effect of variation in inlet water temperature (NCUMD)

1	2	3	4	5	6	7	8	9	10	11	12	13	14
Code	$T_{d,in}$ (˚C)	$T_{a,out}$ (˚C)	$\omega_{a,out}$ (kg_w/kg_a)	$T_{d,m,out}$ (˚C)	$m_{d,l}$ (kg/s)	η_{th} (%)	$X_{c,out}$ (W)	$X_{e,out}$ (W)	$X_{a,out}$ (W)	$X_{d,out}$ (W)	$X_{t,out}$ (W)	I_t (W)	η_{II} (%)
NCUMD-1	**28**	**23.45**	**0.0199**	**23.45**	**0.0009**	**81.83**	**48.55**	**69.14**	**117.69**	**11473.95**	**11591.64**	**2296.24**	**83.47**
NCUMD-2	**30**	**24.22**	**0.0207**	**24.22**	**0.0010**	**76.46**	**44.64**	**93.52**	**138.16**	**11443.31**	**11581.47**	**2338.36**	**83.20**
NCUMD-3	**32**	**25.01**	**0.0215**	**25.01**	**0.0011**	**73.12**	**40.46**	**108.07**	**148.53**	**11424.34**	**11572.87**	**2385.23**	**82.91**
NCUMD-4	**34**	**25.76**	**0.0222**	**25.75**	**0.0012**	**71.37**	**36.98**	**100.03**	**137.01**	**11428.78**	**11565.79**	**2436.97**	**82.60**
NCUMD-5	**36**	**26.5**	**0.0231**	**26.51**	**0.0013**	**69.99**	**34.58**	**111.95**	**146.53**	**11413.46**	**11559.99**	**2493.47**	**82.26**

5.21.3Effect of variation in inlet air DBT (NCUMA)

This section of research represents the variation of inlet air DBT from 36 - 44 ˚C, and other constant important parameters of SCT are air relative humidity (20%), water droplet temperature (34 ˚C), multi droplet diameters (25.45 - 254.54 µm), and RLG (0.5). It was observed from Table 5.73 that exit air DBT, specific humidity, water droplet temperatures, and thermal efficiency of SCT increased relatively as inlet air DBT increases.

Table 5.73 Effect of variation in inlet air DBT (NCUMA)

1	2	3	4	5	6	7	8	9	10	11	12	13	14
Code	$T_{a,in}$ (˚C)	$T_{a,out}$ (˚C)	$\omega_{a,out}$ (kg_w/kg_a)	$T_{d,m,out}$ (˚C)	$m_{d,l}$ (kg/s)	η_{th} (%)	$X_{c,out}$ (W)	$X_{e,out}$ (W)	$X_{a,out}$ (W)	$X_{d,out}$ (W)	$X_{t,out}$ (W)	I_t (W)	η_{II} (%)
NCUMA-1	**36**	**24.34**	**0.0204**	**24.33**	**0.0014**	**67.96**	**11.63**	**168.55**	**180.18**	**11478.28**	**11658.46**	**2477.07**	**82.48**
NCUMA-2	**38**	**25.03**	**0.0213**	**25.02**	**0.0013**	**69.29**	**16.75**	**136.17**	**152.92**	**11459.01**	**11611.93**	**2459.05**	**82.52**
NCUMA-3	**40**	**25.76**	**0.0222**	**25.75**	**0.0012**	**71.37**	**36.98**	**100.03**	**137.01**	**11428.78**	**11565.79**	**2436.96**	**82.60**
NCUMA-4	**42**	**26.5**	**0.0235**	**26.49**	**0.0011**	**73.77**	**46.43**	**91.41**	**137.84**	**11382.33**	**11520.17**	**2412.26**	**82.69**
NCUMA-5	**44**	**27.29**	**0.0248**	**27.28**	**0.0010**	**76.71**	**58.17**	**86.02**	**144.19**	**11330.49**	**11474.68**	**2388.21**	**82.77**

The maximum and minimum air cooling had given by 44 ˚C and 36 ˚C inlet air DBT (keeping water temperature constant). Table 5.73 shows 44 ˚C DBT air cool down water droplet up to 16.71 ˚C. The total exergy of air, exergy of water, and total

exergy of system decreased with increase the inlet air DBT temperature. The SLE of system increased because exergy destruction decreased with increase the initial air DBT.

5.21.4 Effect of variation in inlet Air Relative Humidity (NCUMH)

This study is based on he variation of inlet relative humidity from 20% to 40%. The other important persistent parameters of SCT are air DBT (40 ˚C), water droplet temperature (34 ˚C), multi droplet diameters (25.45 - 254.54 µm), and RLG (0.5). Table 5.74 shows exit air DBT, specific humidity, droplet temperature and thermal efficiency of SCT was increased with increasing the air relative humidity.

Table 5.74 Effect of variation in inlet air relative humidity (NCUMH)

1	2	3	4	5	6	7	8	9	10	11	12	13	14
Code	ϕ_{in} (%)	$T_{a,out}$ (˚C)	$\omega_{a,out}$ (kg_w/kg_a)	$T_{d,m,out}$ (˚C)	$m_{d,l}$ (kg/s)	η_{th} (%)	$X_{c,out}$ (W)	$X_{e,out}$ (W)	$X_{a,out}$ (W)	$X_{d,out}$ (W)	$X_{t,out}$ (W)	I_t (W)	η_{II} (%)
NCUMH-1	**20.00**	**25.76**	**0.0222**	**25.75**	**0.0012**	**71.37**	**36.98**	**100.03**	**137.01**	**11428.78**	**11565.79**	**2436.96**	**82.60**
NCUMH-2	**25.00**	**26.53**	**0.0233**	**26.52**	**0.0010**	**74.02**	**32.85**	**86.92**	**119.77**	**10567.58**	**9642.74**	**2404.45**	**80.04**
NCUMH-3	**30.00**	**27.31**	**0.0247**	**27.30**	**0.0008**	**77.66**	**27.76**	**61.36**	**89.12**	**9171.21**	**8076.80**	**2381.63**	**77.23**
NCUMH-4	**35.00**	**28.06**	**0.0263**	**28.05**	**0.0006**	**83.05**	**23.29**	**43.06**	**66.35**	**7988.92**	**6756.38**	**2431.46**	**73.54**
NCUMH-5	**40.00**	**28.78**	**0.0279**	**28.77**	**0.0004**	**91.55**	**19.35**	**36.86**	**56.21**	**6966.38**	**5615.65**	**2426.88**	**69.82**

Table 5.74 also shows 20% relative humidity air produced maximum cooling, i.e. up to 14.24 ˚C and 40% relative humidity air gave maximum thermal efficiency (91.55%) of SCT. Table 5.74 also shows total exergy of air, exergy of water, and SLE of SCT was decreased with increasing the relative humidity of the air. As relative humidity of air increased, the destruction in total exergy of the system relatively decreases because low relative humidity air absorbs more amount of water from droplets.

5.21.5 Effect of variation in inlet RLG (NCUML)

In this research variation of RLG was from 0.5 to 1.5 and additional constant important parameters are air DBT (40 ˚C), air relative humidity (20%), water droplet temperature (34 ˚C), and multi droplet diameters (25.45 - 254.54 µm). Table 5.75 shows as RLG increases exit air DBT, air specific humidity and droplet temperature increased because mass of water at inlet increased.

Table 5.75 Effect of variation in inlet RLG (NCUML)

1	2	3	4	5	6	7	8	9	10	11	12	13	14
Code	**RLG**$_{in}$	$T_{a,out}$ (˚C)	$\omega_{a,out}$ (kg_w/kg_a)	$T_{d,m,out}$ (˚C)	$m_{d,l}$ (kg/s)	η_{th} (%)	$X_{c,out}$ (W)	$X_{e,out}$ (W)	$X_{a,out}$ (W)	$X_{d,out}$ (W)	$X_{t,out}$ (W)	I_t (W)	η_{II} (%)
NCUML-1	**0.5**	**25.76**	**0.0222**	**25.75**	**0.0012**	**71.37**	**36.98**	**100.03**	**137.01**	**11428.78**	**11565.79**	**2436.96**	**82.60**
NCUML-2	**0.75**	**26.69**	**0.0236**	**26.68**	**0.0013**	**63.32**	**32.06**	**146.02**	**178.08**	**17286.59**	**17464.67**	**3539.45**	**83.15**
NCUML-3	**1**	**27.39**	**0.0247**	**27.38**	**0.0014**	**57.27**	**28.32**	**163.89**	**192.21**	**23186.79**	**23379.00**	**4626.51**	**83.48**
NCUML-4	**1.25**	**27.94**	**0.0255**	**27.93**	**0.0015**	**52.51**	**26.22**	**178.53**	**204.75**	**29091.92**	**29296.67**	**5710.20**	**83.69**
NCUML-5	**1.5**	**28.35**	**0.0262**	**28.34**	**0.0016**	**48.96**	**23.94**	**162.56**	**186.5**	**35046.95**	**35233.45**	**6774.80**	**83.87**

The maximum and minimum air DBT reduction was 14.24 ˚C and 11.65 ˚C which obtained at 0.5 and 1.5 RLG respectively. The range of SCT was decreased by increasing the RLG hence the thermal efficiency of SCT also decreased by increasing the RLG. The total exergy of air, exergy of water increased with increasing the RLG because exit air and water droplet temperature and mass of water increased with increases the RLG. As the amount of water in water to air mass flow ratio increased destruction in exergy of system along tower height increased because the amount of exergy release by water is more than the amount of exergy gain by air. The SLE of SCT increased with increase the RLG.

5.22 Three Dimensional Counter flow Mono Droplet SCT for Air Cooling Application

This study based on 3-D mono droplet counter flow CFD model to determine the effect of variation in inlet droplet diameters, water temperatures, air DBT, relative humidity of air and RLG on outlet parameters. Schematic diagram of 3-D counter flow SCT was shown in Figure 3.2. The mesh of 3-D counter flow SCT has shown in Figure 5.8. Initial conditions used for computer simulations are same as 2-D parallel flow mono droplets SCT used for air cooling application.

5.22.1 Effect of variation in initial droplets diameter (NCOCR)

This research shows the variation of water and air exit parameters by varying inlet droplet diameters from 200 - 1000 µm. The constant important inlet parameters used for this study are air DBT (40 ˚C), air relative humidity (20%), water temperature (34 ˚C), and RLG (0.5). Table 5.76 shows exit air DBT and water temperature increased and exit specific humidity, make up water required and thermal efficiency of SCT decreased with increase the droplet diameter because heat and mass transfer between air and water droplet decreases. The maximum and minimum water droplet temperature reduction is 13.00 ˚C and 02.49 ˚C which were obtained at 200 µm and 1000 µm respectively. The maximum SCT efficiency achieved with 200 µm droplet diameter and it was 68.43%. The total exergy of water and exergy of system increased with increases the droplet diameter. The SLE of SCT increased and exergy destruction of system was decreased with increasing the droplet diameters because heat and mass transfer between air and water decreases.

Table 5.76 Effect of variation in inlet droplet diameter (NCOCR)

1	2	3	4	5	6	7	8	9	10	11	12	13	14
Code	D_{in} (µm)	$T_{a,out}$ (˚C)	$\omega_{a,out}$ (kg_w/kg_a)	$T_{d,out}$ (˚C)	$m_{d,l}$ (kg/s)	η_{th} (%)	$X_{c,out}$ (W)	$X_{e,out}$ (W)	$X_{a,out}$ (W)	$X_{d,out}$ (W)	$X_{t,out}$ (W)	I_t (W)	η_{II} (%)
NCOCR-1	**200**	**26.1**	**0.0225**	**26.09**	**0.0013**	**68.43**	**36.28**	**100.46**	**136.74**	**11496.42**	**11633.16**	**2369.59**	**83.08**
NCOCR-2	**400**	**29.28**	**0.0217**	**27.71**	**0.0009**	**54.38**	**18.59**	**95.66**	**114.25**	**11568.126**	**11682.38**	**2320.37**	**83.43**
NCOCR-3	**600**	**34.47**	**0.0201**	**29.37**	**0.0006**	**40.07**	**5.42**	**50.87**	**56.29**	**11676.76**	**11733.05**	**2269.70**	**83.79**
NCOCR-4	**800**	**36.72**	**0.0182**	**30.33**	**0.0004**	**31.77**	**2.24**	**27.16**	**29.40**	**11756.146**	**11785.55**	**2217.20**	**84.17**
NCOCR-5	**1000**	**37.51**	**0.0173**	**30.87**	**0.0003**	**27.08**	**1.86**	**53.15**	**55.01**	**11784.02**	**11839.03**	**2163.72**	**84.55**

5.22.2 Effect of variation in inlet Water Temperature (NCOCD)

The effects of the variation of inlet water droplet temperature from 28 to 36 ˚C on exit parameters are given in Table 5.77. The additional significant persistent inlet constraints are air DBT (40 ˚C), air relative humidity (20%), water droplet diameters (25.45 - 254.54 µm), and RLG (0.5). Table 5.77 shows as inlet water temperature increase exit air DBT, air specific humidity, water temperature, and makeup water required increased. It also shows that when the temperature of inlet water is 28 ˚C, maximum cooling of air DBT was achieved (16.20 ˚C) as high temperature difference between water and air (keeping air temperature constant). The maximum SCT efficiency (75.54%) achieved by 28 ˚C inlet droplet temperature. As inlet water droplet temperature increases, the specific humidity of air increased as increase in the water temperature more water vapour is added in the air. Table 5.77 shows the thermal efficiency of SCT was deceased by increasing the water droplet temperature. Table 5.77 also shows that increase in inlet water temperature, more quantity of water vapour mixed in the air and increased total exergy of air. The exergy destruction of the system was increased and the SLE decreased by increasing the inlet water droplet temperature. The depicted destruction in total exergy of the system was more for

higher temperature droplet because it transfers water content into air faster than lower temperature droplets.

Table 5.77 Effect of variation in inlet water temperature (NCOCD)

1	2	3	4	5	6	7	8	9	10	11	12	13	14
Code	$T_{d,in}$ (˚C)	$T_{a,out}$ (˚C)	$\omega_{a,out}$ (kg_w/kg_a)	$T_{d,out}$ (˚C)	$m_{d,l}$ (kg/s)	η_{th} (%)	$X_{c,out}$ (W)	$X_{e,out}$ (W)	$X_{a,out}$ (W)	$X_{d,out}$ (W)	$X_{t,out}$ (W)	I_t (W)	η_{II} (%)
NCOCD-1	**28**	**23.8**	**0.0193**	**23.8**	**0.0010**	**75.54**	**50.52**	**60.44**	**110.96**	**11548.62**	**11659.58**	**2228.31**	**83.96**
NCOCD-2	**30**	**24.57**	**0.0205**	**24.57**	**0.0011**	**71.83**	**44.98**	**104.72**	**149.70**	**11499.54**	**11649.24**	**2270.58**	**83.69**
NCOCD-3	**32**	**25.35**	**0.0215**	**25.35**	**0.0012**	**69.56**	**40.02**	**121.97**	**161.99**	**11478.46**	**11640.45**	**2317.65**	**83.40**
NCOCD-4	**34**	**26.1**	**0.0225**	**26.09**	**0.0013**	**68.43**	**36.28**	**100.46**	**136.74**	**11496.42**	**11633.16**	**2369.60**	**83.08**
NCOCD-5	**36**	**26.84**	**0.0233**	**26.84**	**0.0014**	**67.55**	**33.67**	**115.74**	**149.41**	**11477.78**	**11627.19**	**2426.27**	**82.74**

5.22.3 Effect of variation in inlet air DBT (NCOCA)

This research is based on the variation of air DBT from 36 - 44 ˚C. The fixed inlet parameters taken for this study was air relative humidity (20%), water temperature (34 ˚C), droplet diameter (200 µm), and RLG (0.5). Table 5.78 shows exit air DBT, air specific humidity and droplet temperatures increased as inlet air DBT increases; it also shows 44 ˚C DBT air produce maximum cooling and it cool down water droplet up to 16.38 ˚C.

Table 5.78 Effect of variation in inlet air DBT (NCOCA)

1	2	3	4	5	6	7	8	9	10	11	12	13	14
Code	$T_{a,in}$ (˚C)	$T_{a,out}$ (˚C)	$\omega_{a,out}$ (kg_w/kg_a)	$T_{d,out}$ (˚C)	$m_{d,l}$ (kg/s)	η_{th} (%)	$X_{c,out}$ (W)	$X_{e,out}$ (W)	$X_{a,out}$ (W)	$X_{d,out}$ (W)	$X_{t,out}$ (W)	I_t (W)	η_{II} (%)
NCOCA-1	**36**	**24.68**	**0.0204**	**24.67**	**0.0015**	**65.57**	**24.87**	**172.91**	**197.78**	**11528.828**	**11726.61**	**2408.92**	**82.96**
NCOCA-2	**38**	**25.37**	**0.0211**	**25.36**	**0.0014**	**66.67**	**29.45**	**131.93**	**161.38**	**11518.328**	**11679.71**	**2391.27**	**83.01**
NCOCA-3	**40**	**26.1**	**0.0225**	**26.09**	**0.0013**	**68.43**	**36.28**	**100.46**	**136.74**	**11496.42**	**11633.16**	**2369.59**	**83.08**
NCOCA-4	**42**	**26.83**	**0.0237**	**26.82**	**0.0012**	**70.53**	**32.71**	**87.22**	**119.93**	**11467.378**	**11587.31**	**2345.12**	**83.17**
NCOCA-5	**44**	**27.62**	**0.0248**	**27.61**	**0.0011**	**72.95**	**46.42**	**65.78**	**112.20**	**11429.508**	**11541.71**	**2321.18**	**83.26**

Table 5.78 also represents that increase in inlet air DBT, thermal efficiency of SCT increased, and maximum thermal efficiency (72.95%) achieved at 44 ˚C. The total exergy of air, exergy of water, and exergy of system decreased with increased the inlet air DBT temperature. The SLE of system increased with increase the initial air DBT because exergy destruction decreased with increase the initial air DBT.

5.22.4 Effect of variation in inlet Air Relative Humidity (NCOCH)

This study was based on the deviation of inlet relative humidity from 20% to 40%. The persistent inlet parameters of this study was air DBT (36 ˚C), water droplet temperature (34 ˚C), droplet diameter (200 µm) and RLG (0.5). Table 5.79 shows 20% relative humidity air produced maximum cooling, i.e. up to 13.90 ˚C and 40% relative humidity air gave maximum efficiency (85.77%). Table 5.79 also shows as relative humidity of air increases total exergy of air, exergy of water, and SLE of SCT decreased. As relative humidity of air increases, the destruction in total exergy of

The system relatively decreased.

Table 5.79 Effect of variation in inlet air relative humidity (NCOCH)

1	2	3	4	5	6	7	8	9	10	11	12	13	14
Code	ϕ_{in} (%)	$T_{a,out}$ (˚C)	$\omega_{a,out}$ (kg_w/kg_a)	$T_{d,out}$ (˚C)	$m_{d,l}$ (kg/s)	η_{th} (%)	$X_{c,out}$ (W)	$X_{e,out}$ (W)	$X_{a,out}$ (W)	$X_{d,out}$ (W)	$X_{t,out}$ (W)	I_t (W)	η_{II} (%)
NCOCH-1	**20**	**26.10**	**0.0225**	**26.09**	**0.0013**	**68.43**	**36.28**	**100.46**	**136.74**	**11496.42**	**11633.16**	**2369.59**	**83.08**
NCOCH-2	**25**	**26.87**	**0.0232**	**26.86**	**0.0011**	**70.66**	**33.74**	**88.34**	**122.08**	**10423.85**	**9709.85**	**2337.34**	**80.60**
NCOCH-3	**30**	**27.64**	**0.0239**	**27.63**	**0.0009**	**73.84**	**29.76**	**62.52**	**92.28**	**9094.68**	**8143.54**	**2314.89**	**77.87**
NCOCH-4	**35**	**28.39**	**0.0258**	**28.38**	**0.0007**	**78.44**	**25.68**	**44.01**	**69.69**	**8086.94**	**6822.81**	**2365.03**	**74.26**
NCOCH-5	**40**	**29.11**	**0.0267**	**29.10**	**0.0005**	**85.77**	**23.17**	**29.39**	**52.56**	**7042.44**	**5681.71**	**2360.81**	**70.65**

5.22.5 Effect of variation in inlet RLG (NCOCL)

The Inlet RLG was varied from 0.5 to 1.5 in this research and its effects on various exit parameters are given in Table 5.80. The other important inlet parameters used for this study are air DBT (40 ˚C), air relative humidity (20%), water droplet temperature (34 ˚C), and multi droplet diameter (200 µm). Table 5.80 shows as RLG increases exit air DBT, air specific humidity and droplet temperature increased because mass of water at inlet increased with increase the RLG. The maximum and minimum air DBT reduction was 13.90 ˚C and 11.32 ˚C which obtained at 0.5 and 1.5 RLG respectively. The range of SCT was decreased by increasing the RLG hence the thermal efficiency of SCT also decreased by increasing the RLG. The total exergy of air, exergy of water was increased with increasing the RLG because exit air and water droplet temperature and mass of water were increased with increasing the RLG. As the amount of water in water to air mass flow ratio increased destruction in exergy of system along tower height increased because the amount of exergy release by water was more than the amount of exergy gain by air. The SLE of SCT increased with increase the RLG.

Table 5.80 Effect of variation in inlet RLG (NCOCL)

1	2	3	4	5	6	7	8	9	10	11	12	13	14
Code	**RLG_{in}**	**$T_{a,out}$ (˚C)**	**$\omega_{a,out}$ (kg_w/kg_a)**	**$T_{d,out}$ (˚C)**	**$m_{d,l}$ (kg/s)**	**η_{th} (%)**	**$X_{c,out}$ (W)**	**$X_{e,out}$ (W)**	**$X_{a,out}$ (W)**	**$X_{d,out}$ (W)**	**$X_{t,out}$ (W)**	**I_t (W)**	**η_{II} (%)**
NCOCL-1	**0.5**	**26.1**	**0.0225**	**26.09**	**0.0013**	**68.43**	**36.28**	**100.46**	**136.74**	**11496.42**	**11633.16**	**2369.59**	**83.08**
NCOCL-2	**0.75**	**27.03**	**0.0239**	**27.02**	**0.0014**	**60.38**	**26.35**	**157.38**	**183.73**	**17381.78**	**17565.51**	**3438.61**	**83.63**
NCOCL-3	**1**	**27.73**	**0.0250**	**27.72**	**0.0015**	**54.33**	**22.07**	**174.48**	**196.55**	**23316.60**	**23513.15**	**4492.36**	**83.96**
NCOCL-4	**1.25**	**28.27**	**0.0258**	**28.26**	**0.0016**	**49.65**	**18.94**	**180.66**	**199.60**	**29265.06**	**29464.66**	**5542.21**	**84.17**
NCOCL-5	**1.5**	**28.68**	**0.0265**	**28.67**	**0.0017**	**46.11**	**18.67**	**199.76**	**218.43**	**35216.51**	**35434.94**	**6573.31**	**84.35**

5.23 Three Dimensional Counter flow Multi Droplet SCT for Air Cooling Application

This study based on 3-D multi droplet counter flow CFD model to determine the effect of variation in inlet droplet diameters, water temperatures, air DBT, relative humidity of air and RLG on outlet parameters. Schematic diagram of 3-D counter flow SCT was shown in Figure 3.2. The mesh of 3-D counter flow SCT was shown in Figure 5.8. Initial conditions used for computer simulations are same as 2-D parallel flow multi droplets SCT used for air cooling application.

5.23.1 Effect of variation in initial droplets diameter (NCUCR)

This research based on the variation of inlet multi droplet diameter. The inlet constant parameters used in this research are air DBT (40 ˚C), air relative humidity (20%), water temperature (34 ˚C), and RLG (0.5). Table 5.81 shows as multi droplet diameter increase exit air DBT and water temperature increased and exit specific humidity, makeup water required and thermal efficiency of SCT decreased because heat and mass transfer between air and water droplet decreased. From the Table 5.81 it was also observed that 25.45 - 254.54 µm size water droplets produce maximum cooling (13.58 °C) and maximum efficiency (65.66%). The total exergy of air and exergy destruction decreased as inlet droplet diameter increases. The exergy of water, exergy of system and SLE was increased with increasing the droplet diameter because heat and mass transfer between air and water decreased.

Table 5.81 Effect of variation in inlet droplet diameter (NCUCR)

1	2	3	4	5	6	7	8	9	10	11	12	13	14
Code	D_{in} (μm)	$T_{a,out}$ (˚C)	$\omega_{a,out}$ (kg_w/kg_a)	$T_{d,m,out}$ (˚C)	$m_{d,l}$ (kg/s)	η_{th} (%)	$X_{c,out}$ (W)	$X_{e,out}$ (W)	$X_{a,out}$ (W)	$X_{d,out}$ (W)	$X_{t,out}$ (W)	I_t (W)	η_{II} (%)
NCUCR-1	**25.45-254.54**	**26.42**	**0.0228**	**26.41**	**0.0014**	**65.66**	**32.57**	**122.71**	**155.28**	**11545.42**	**11700.70**	**2302.05**	**83.56**
NCUCR-2	**50.90-509.09**	**29.60**	**0.0209**	**28.03**	**0.0010**	**51.61**	**18.94**	**72.02**	**90.96**	**11658.96**	**11749.92**	**2252.83**	**83.91**
NCUCR-3	**76.36-763.64**	**34.79**	**0.0160**	**29.68**	**0.0007**	**37.39**	**3.77**	**22.46**	**26.23**	**11774.36**	**11800.59**	**2202.16**	**84.27**
NCUCR-4	**101.81-1018.18**	**37.04**	**0.0142**	**30.64**	**0.0005**	**29.09**	**0.94**	**7.59**	**8.53**	**11844.56**	**11853.09**	**2149.66**	**84.65**
NCUCR-5	**127.27-1272.73**	**37.82**	**0.0131**	**31.18**	**0.0004**	**24.40**	**0.57**	**11.15**	**11.72**	**11894.85**	**11906.57**	**2096.18**	**85.03**

5.23.2 Effect of variation in inlet Water Temperature (NCUCD)

The research of this section is based on the variation of inlet water temperature from 28 - 36 ˚C. Table 5.82 shows deviations in outlet parameters at constant inlet air DBT (40 ˚C), air relative humidity (20 %), multi droplet diameter (25.45-254.54 μm) and RLG (0.5). Table 5.82 shows as inlet water temperature increase exit air DBT, air specific humidity, water temperature, and makeup water required increased. It also observed that when the temperature of inlet water was 28 ˚C, maximum cooling of air achieved (15.87 ˚C) as high temperature difference between water and air (keeping air temperature constant). The thermal efficiency of SCT was decreased with increasing the inlet water temperature. As inlet water droplet temperature increase, the specific humidity of air increased as due to increase in water temperature more water vapour was added to the air. Table 5.82 also shows that increase in inlet water temperature, more quantity of water vapour mixed in air and increased total exergy of air. The exergy destruction of system was increased and the SLE was decreased by increasing the inlet water droplet temperature. The depicted destruction in total exergy of the system was more for higher temperature droplet because it transfers water content into air faster than lower temperature droplets.

Table 5.82 Effect of variation in inlet water temperature (NCUCD)

1	2	3	4	5	6	7	8	9	10	11	12	13	14
Code	$T_{d,in}$ (˚C)	$T_{a,out}$ (˚C)	$\omega_{a,out}$ (kg_w/kg_a)	$T_{d,m,out}$ (˚C)	$m_{d,l}$ (kg/s)	η_{th} (%)	$X_{c,out}$ (W)	$X_{e,out}$ (W)	$X_{a,out}$ (W)	$X_{d,out}$ (W)	$X_{t,out}$ (W)	I_t (W)	η_{II} (%)
NCUCD-1	**28**	**24.13**	**0.0201**	**24.12**	**0.0011**	**69.78**	**47.75**	**75.84**	**123.59**	**11603.97**	**11727.56**	**2160.33**	**84.44**
NCUCD-2	**30**	**24.9**	**0.0206**	**24.89**	**0.0012**	**67.59**	**42.81**	**93.52**	**136.33**	**11580.64**	**11716.97**	**2202.86**	**84.17**
NCUCD-3	**32**	**25.67**	**0.0209**	**25.67**	**0.0013**	**66.21**	**39.45**	**108.07**	**147.52**	**11560.55**	**11708.07**	**2250.03**	**83.88**
NCUCD-4	**34**	**26.42**	**0.0228**	**26.41**	**0.0014**	**65.66**	**32.57**	**122.71**	**155.28**	**11545.42**	**11700.70**	**2302.06**	**83.56**
NCUCD-5	**36**	**27.16**	**0.0225**	**27.16**	**0.0015**	**65.19**	**33.22**	**106.08**	**139.3**	**11555.38**	**11694.68**	**2358.79**	**83.22**

5.23.3 Effect of variation in inlet air DBT (NCUCA)

Table 5.83 shows the effect of deviation in exit parameters of SCT at constant inlet air relative humidity (20%), water temperature (34 ˚C), multi droplet diameter (25.45-254.54 µm) and RLG (0.5) by varying the air DBT from 36 - 44 ˚C.

Table 5.83 Effect of variation in inlet air DBT (NCUCA)

1	2	3	4	5	6	7	8	9	10	11	12	13	14
Code	$T_{a,in}$ (˚C)	$T_{a,out}$ (˚C)	$\omega_{a,out}$ (kg_w/kg_a)	$T_{d,m,out}$ (˚C)	$m_{d,l}$ (kg/s)	η_{th} (%)	$X_{c,out}$ (W)	$X_{e,out}$ (W)	$X_{a,out}$ (W)	$X_{d,out}$ (W)	$X_{t,out}$ (W)	I_t (W)	η_{II} (%)
NCUCA-1	**36**	**25.02**	**0.0201**	**25.01**	**0.0016**	**63.18**	**9.45**	**158.78**	**168.23**	**11626.5279**	**11794.76**	**2340.77**	**83.44**
NCUCA-2	**38**	**25.7**	**0.0207**	**25.69**	**0.0015**	**64.12**	**20.14**	**136.17**	**156.31**	**11591.1779**	**11747.4879**	**2323.49**	**83.49**
NCUCA-3	**40**	**26.42**	**0.0228**	**26.41**	**0.0014**	**65.66**	**32.57**	**122.71**	**155.28**	**11545.42**	**11700.70**	**2302.05**	**83.56**
NCUCA-4	**42**	**27.15**	**0.0221**	**27.14**	**0.0013**	**67.39**	**33.65**	**111.44**	**145.09**	**11509.3579**	**11654.4479**	**2277.98**	**83.65**
NCUCA-5	**44**	**27.93**	**0.0229**	**27.92**	**0.0012**	**69.41**	**41.32**	**113.33**	**154.65**	**11454.0879**	**11608.7379**	**2254.15**	**83.74**

From Table 5.83 it was observed that exit air DBT, specific humidity and droplet temperatures increased relatively as inlet air DBT increases; it also shows 44 ˚C DBT air produce maximum cooling and it cool down water droplet up to 16.07 ˚C. Table 5.83 also represents that increase in inlet air DBT temperature, the thermal efficiency of SCT increased. The maximum thermal efficiency (69.41%) achieved by 44 ˚C inlet air DBT. The total exergy of air, exergy of water, and total exergy of the

system was decreased with increasing the inlet air DBT. The SLE of system was increased because exergy destruction decreased with increasing the initial air DBT.

5.23.4 Effect of variation in inlet Air Relative Humidity (NCUCH)

This study is based on the variation of inlet relative humidity from 20% to 40%, and other constant inlet parameters are air DBT (40 ˚C), water temperature (34 ˚C), multi droplet diameter (25.45-254.54 µm) and RLG (0.5). Table 5.84 shows exit air DBT, specific humidity, droplet temperature and thermal efficiency of SCT was increased with increasing the air relative humidity.

Table 5.84 Effect of variation in inlet air relative humidity (NCUCH)

1	2	3	4	5	6	7	8	9	10	11	12	13	14
Code	ϕ_{in} (%)	$T_{a,out}$ (˚C)	$\omega_{a,out}$ (kg_w/kg_a)	$T_{d,m,out}$ (˚C)	$m_{d,l}$ (kg/s)	η_{th} (%)	$X_{c,out}$ (W)	$X_{e,out}$ (W)	$X_{a,out}$ (W)	$X_{d,out}$ (W)	$X_{t,out}$ (W)	I_t (W)	η_{II} (%)
NCUCH-1	**20.00**	**26.42**	**0.0228**	**26.41**	**0.0014**	**65.66**	**32.57**	**122.71**	**155.28**	**11545.42**	**11700.70**	**2302.05**	**83.56**
NCUCH-2	**25.00**	**27.19**	**0.0235**	**27.18**	**0.0012**	**67.49**	**32.01**	**86.92**	**118.93**	**10506.78**	**9777.17**	**2270.02**	**81.16**
NCUCH-3	**30.00**	**27.95**	**0.0246**	**27.94**	**0.0010**	**70.25**	**28.03**	**61.36**	**89.39**	**9116.61**	**8210.65**	**2247.78**	**78.51**
NCUCH-4	**35.00**	**28.70**	**0.0263**	**28.69**	**0.0008**	**74.11**	**23.29**	**43.06**	**66.35**	**7969.39**	**6889.76**	**2218.08**	**74.99**
NCUCH-5	**40.00**	**29.42**	**0.0280**	**29.41**	**0.0006**	**80.34**	**19.02**	**39.56**	**58.58**	**6967.54**	**5748.50**	**2184.03**	**71.48**

Table 5.84 also shows 20% relative humidity air produce maximum cooling (13.58 ˚C), and 40% relative humidity air give maximum efficiency (80.34%). Table 5.84 also shows as relative humidity of air increased the change in total exergy of air, exergy of water, and second law efficiency of SCT was decreased. As relative humidity of air increase, the destruction in total exergy of system relatively decreased because low relative humidity air absorbs more amount of water from droplets.

5.23.5 Effect of variation in inlet RLG (NCUCL)

In this research inlet RLG was varied from 0.5 to 1.5, and persistent inlet parameters of SCT are air DBT (40 ˚C), air relative humidity (20%), Water temperature (34 ˚C), and multi droplet diameter (25.45-254.54 µm). Table 5.85 shows as RLG increases exit air DBT, air specific humidity, droplet temperature, and makeup water required increased as mass of water at inlet increased.

Table 5.85 Effect of variation in inlet RLG (NCUCL)

1	2	3	4	5	6	7	8	9	10	11	12	13	14
Code	**RLG**$_{in}$	$T_{a,out}$ (˚C)	$\omega_{a,out}$ (kg_w/kg_a)	$T_{d,m,out}$ (˚C)	$m_{d,l}$ (kg/s)	η_{th} (%)	$X_{c,out}$ (W)	$X_{e,out}$ (W)	$X_{a,out}$ (W)	$X_{d,out}$ (W)	$X_{t,out}$ (W)	I_t (W)	η_{II} (%)
NCUCL-1	**0.5**	**26.42**	**0.0228**	**26.41**	**0.0014**	**65.66**	**32.57**	**122.71**	**155.28**	**11545.42**	**11700.70**	**2302.05**	**83.56**
NCUCL-2	**0.75**	**27.35**	**0.0242**	**27.34**	**0.0015**	**57.61**	**32.3**	**146.04**	**178.34**	**17488.23**	**17666.57**	**3337.55**	**84.11**
NCUCL-3	**1**	**28.05**	**0.0253**	**28.04**	**0.0016**	**51.56**	**28.04**	**163.89**	**191.93**	**23455.64**	**23647.57**	**4357.94**	**84.44**
NCUCL-4	**1.25**	**28.58**	**0.0261**	**28.57**	**0.0017**	**46.97**	**25.34**	**178.53**	**203.87**	**29435.40**	**29639.27**	**5367.60**	**84.67**
NCUCL-5	**1.5**	**28.99**	**0.0268**	**28.98**	**0.0018**	**43.43**	**23.59**	**137.47**	**161.06**	**35475.38**	**35636.44**	**6371.81**	**84.83**

The maximum and minimum water droplet temperature reduction was 13.58 ˚C and 11.01 ˚C which obtained at 0.5 and 1.5 RLG respectively. The range of SCT was decreased by increasing the RLG hence the thermal efficiency of SCT also decreased by increasing the RLG. The total exergy of air, exergy of water was increased with increasing the RLG as exit air and water droplet temperature and mass of water increased with increases the RLG. As RLG increases destruction in exergy of system along tower height increased because the amount of exergy release by water was more than the amount of exergy gain by air. The SLE of SCT increased with increase the RLG.

5.24 Comparative Study of SCT with Change in Initial Droplet Diameter for Air Cooling Application

In this section the effects on exit parameters (i.e. air DBT, air specific humidity, thermal efficiency, SLE) due to variation in inlet droplet diameter of SCT, the exit parameter results were studied for parallel flow and counter flow configuration using 2-D MATLAB model and 3-D CFD model. The results were also compared for mono-droplet and multi-droplet diameter.

5.24.1 Variation in outlet air DBT with changes of initial droplets diameter

The variation of outlet air DBT with varying inlet droplet diameter for mono and multi droplet models for parallel and counter-flow configuration are shown in Figure 5.24. It was observed that the outlet air DBT increased with the increasing the inlet droplet diameter in all the cases of parallel flow and counter flow SCT. Figure 5.24 also shows parallel flow SCT predicted higher exit air DBT in comparison to counter flow SCT because heat and mass transfer in counter flow SCT was more than parallel flow SCT. Figure 5.24 also shows that parallel and counter multi droplet SCT predicted outlet air DBT higher than the mono droplet in both the cases of 2-D and 3-D. The multi droplet models were closer to the validation test as they described more realistic phenomena because mono droplet models considered more assumption compared to multi droplet models. The multi droplet 3-D CFD model predicted higher outlet temperature compared to multi droplet 2-D model of MATLAB, however 3-D CFD model with least error in the validation test as shown in the Figures 5.1 - 5.4. The minimum exit air DBT were obtained by parallel and counter flow

configurations were 27.47 ˚C and 25.41 ˚C, obtained by 200 µm droplet diameter MATLAB model.

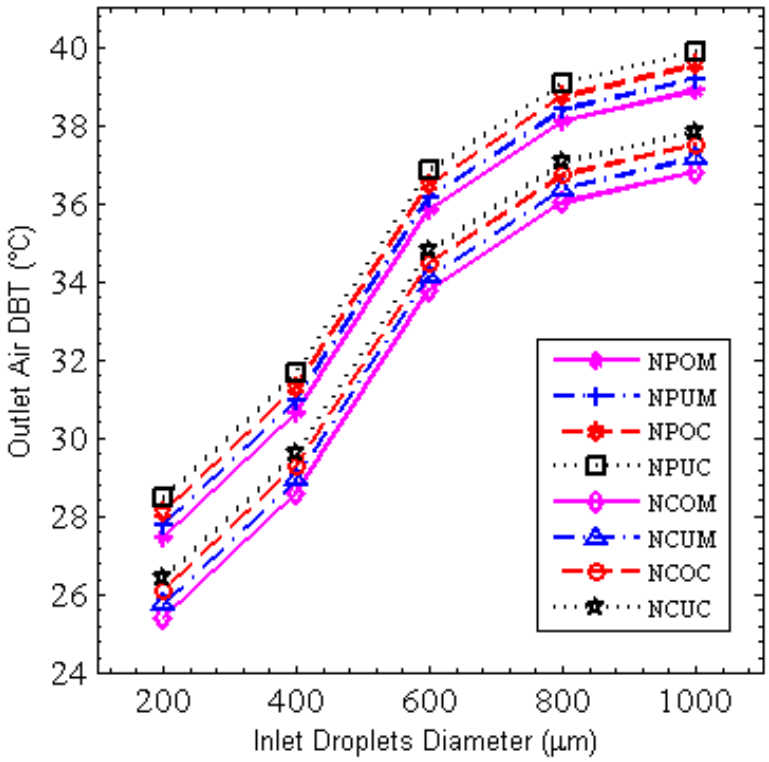

Figure 5.24 Outlet air DBT with variation in inlet droplet diameter

5.24.2 Variation in outlet air specific humidity with changes of initial droplets diameter

The variation of outlet specific humidity with varying inlet droplet diameter for mono and multi droplet models for parallel and counter-flow configuration is shown in Figure 5.25. It was observed that the outlet specific humidity had decreased with the increase the inlet droplet diameter in all the cases of parallel flow and counter flow SCT. The outlet air specific humidity for parallel flow cases was more than counter flow cases for same inlet droplet diameter. Figure 5.25 shows parallel flow SCT predicted higher exit specific humidity in comparison to counter flow SCT because parallel flow SCT has higher exit air DBT in comparison to counter flow

SCT. The Figure also shows that parallel and counter flow multi droplet shower cooling tower predicted outlet specific humidity higher than the mono droplet in both the cases of 2-D MATLAB and 3-D CFD models.

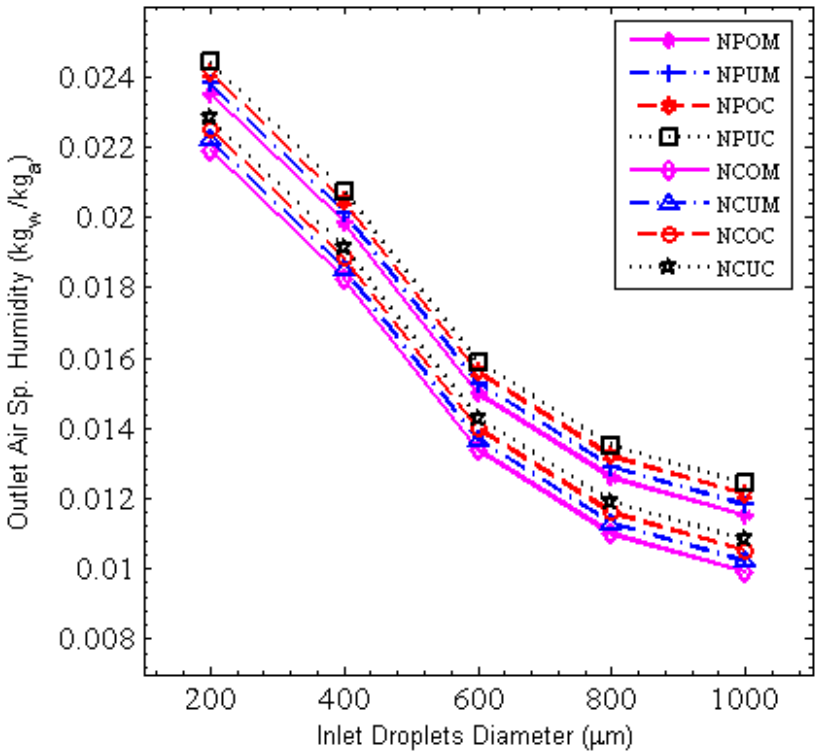

Figure 5.25 Outlet air specific humidity with variation in inlet droplet diameter

The multi droplet models were closer to the validation test as they described more accurate results because mono droplet models considered more assumption compared to multi droplet models. The multi droplet 3-D CFD model predicted higher specific humidity compared to multi droplet 2-D model of MATLAB, However 3-D CFD model with least error in the validation test as shown in Figures 5.1-5.4. The maximum exit air specific humidity obtained by parallel and counter flow configurations were 0.0244 kg_w/kg_a and 0.0228 kg_w/kg_a, obtained by 25.45 - 254.54 µm multi droplet diameter CFD models. The minimum exit air specific humidity obtained by parallel and counter flow configurations were 0.0115 kg_w/kg_a and 0.0099 kg_w/kg_a, obtained by 1000 µm droplet diameter MATLAB model.

5.24.3 Variation in thermal efficiency of SCT with change of initial droplets diameter

The variation of thermal efficiency of SCT with varying inlet droplet diameter for parallel and counter-flow configuration is shown in Figure 5.26.

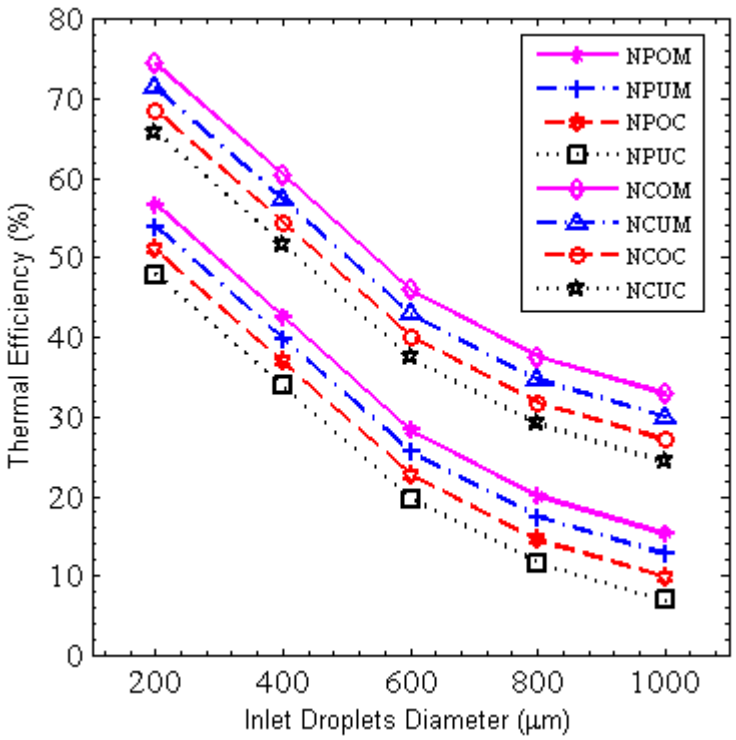

Figure 5.26 Thermal efficiency of SCT with variation in inlet droplet diameter

It was observed that thermal efficiency of SCT decreased with increase in the inlet droplet diameter in all the cases of parallel flow and counter flow models because heat and mass transfer between air and water droplet decreases with increase the droplet diameter. The thermal efficiency for parallel flow cases was lower than counter flow cases for same inlet droplet diameter. Figure 5.10 shows that parallel and counter flow multi droplet SCT predicted thermal efficiency lower than the mono droplet in both the cases of 2-D and 3-D. The multi droplet models were closer to the validation test as they described more accurate results because mono droplet models considered more assumption compared to multi droplet models. The multi droplet 3-

D CFD model predicted least thermal efficiency compared to multi droplet 2-D model of MATLAB, however 3-D CFD model with least error in the validation test as shown in Figures 5.1 - 5.4. The maximum thermal efficiency obtained by 3-D CFD model for parallel and counter flow configurations were 47.92% and 65.66% respectively.

5.24.4 Variation in SLE of SCT with change of initial droplets diameter

The variation of SLE of SCT with varying inlet droplet diameter for parallel and counter-flow configuration is shown in Figure 5.27. It observed that SLE of SCT was increased with the increasing the inlet droplet diameter in all the cases of parallel flow and counter flow models because total exergy of system increased with increase the droplet diameter. Figure 5.27 shows parallel flow SCT predicted higher SLE in comparison to counter flow SCT because heat and mass transfer in counter flow SCT was more than parallel flow SCT. Figure 5.27 also shows that parallel and counter multi droplet SCT predicted SLE higher than the mono droplet in both the cases of 2-D and 3-D. The overall minimum and maximum SLE attained by parallel flow configurations were 96.94% (by 200 µm droplet diameter MATLAB model) and 99.90% (by 127.27 - 1272.73 µm multi droplet diameter CFD model). The overall minimum and maximum SLE attains by counter flow configurations were 82.11% (by 200 µm droplet diameter MATLAB model) and 85.03% (by 127.27 - 1272.73 µm multi droplet diameters CFD model).

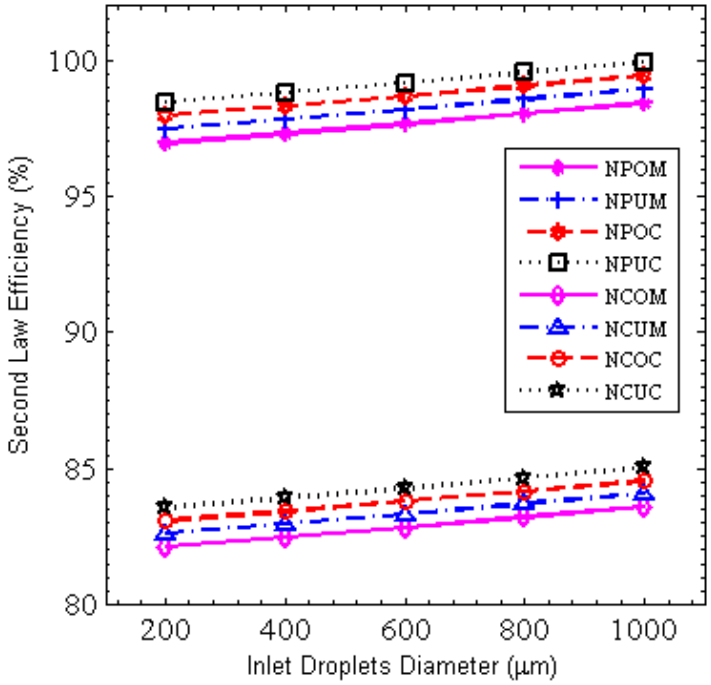

Figure 5.27 SLE of SCT with variation in inlet droplet diameter

5.25 Comparative Study of SCT with Change in Initial Water Temperature for Air Cooling Application

In this research the effects of inlet water temperatures from 28 - 36 ˚C on exit parameters (i.e. air DBT, specific humidity, thermal efficiency and SLE) were studied. The exit parameter results are obtained for parallel flow and counter flow configuration using 2-D MATLAB model and 3-D CFD model. These results also compared for the cases of mono-droplet and multi-droplet diameter.

5.25.1 Variation in outlet air DBT with changes of inlet water temperature

The variation of outlet air DBT with varying inlet water temperature from 28 - 36 ˚C for parallel and counter-flow configuration is shown in Figure 5.28.

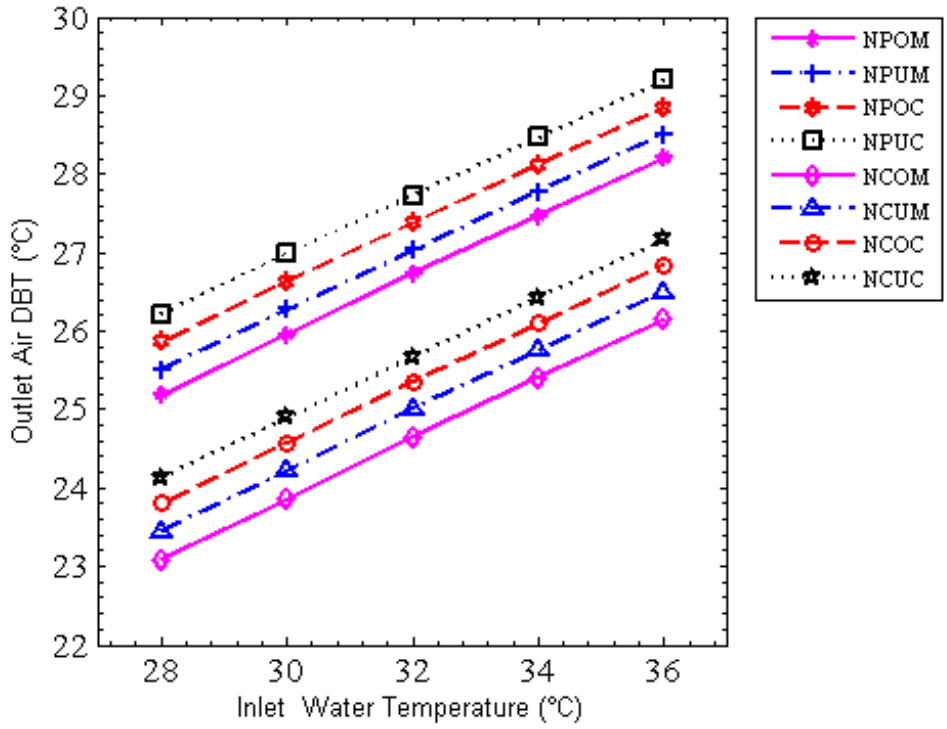

Figure 5.28 Outlet air DBT with variation in inlet water temperature

It observed that the outlet air DBT increased with increase the inlet water temperature for all the cases of parallel flow and counter flow SCT. The outlet air DBT for parallel flow cases was greater than counter flow cases for same inlet water temperature. Figure 5.28 shows parallel flow SCT predicted greater outlet air DBT in comparison to counter flow SCT because heat and mass transfer in parallel flow SCT was less than counter flow SCT. Figure 5.28 also shows that parallel and counter multi droplet SCT predicted outlet air temperature greater than the mono droplet in both the cases of 2-D MATLAB models and 3-D CFD models. The multi droplet

models were closer to the validation test as they described more accurate results because mono droplet models considered additional assumption compared to multi droplet models. The multi droplet 3-D CFD model expected higher outlet air DBT compared to multi droplet 2-D model of MATLAB, however 3-D CFD model has least error in the validation test. The overall minimum exit air DBT were obtained by parallel and counter flow configurations were 25.19 ˚C and 23.09 ˚C by 28 ˚C inlet water temperature mono droplet MATLAB model.

5.25.2 Variation in outlet air specific humidity with changes of inlet water temperature

The variation of outlet air specific humidity with varying inlet water temperature from 28 - 36 ˚C for parallel and counter flow configuration is shown in Figure 5.29. It is observed that the outlet specific humidity was increased with increasing the inlet water temperature for all the cases of parallel and counter flow SCT. Figure 5.29 shows parallel flow SCT models predicted higher exit specific humidity in comparison to counter flow SCT models because parallel flow SCT has higher exit air DBT in comparison to counter flow SCT. Figure 5.29 also shows that parallel and counter flow multi droplet SCT predicted outlet specific humidity higher than the mono droplet in both the cases of 2-D MATLAB and 3-D CFD models. The multi droplet models were closer to the validation test as they described more accurate results because mono droplet models considered more assumption compared to multi droplet models. The multi droplet 3-D CFD model predicted higher specific humidity compared to multi droplet 2-D model of MATLAB. The maximum exit air specific humidity obtained by parallel and counter flow configurations were 0.0255 kg_w/kg_a and 0.0239 kg_w/kg_a, obtained by multi droplet diameter CFD models. The minimum

exit air specific humidity obtained by parallel and counter flow configurations were 0.0205 kg_w/kg_a and 0.0189 kg_w/kg_a, obtained by mono droplet diameter MATLAB model.

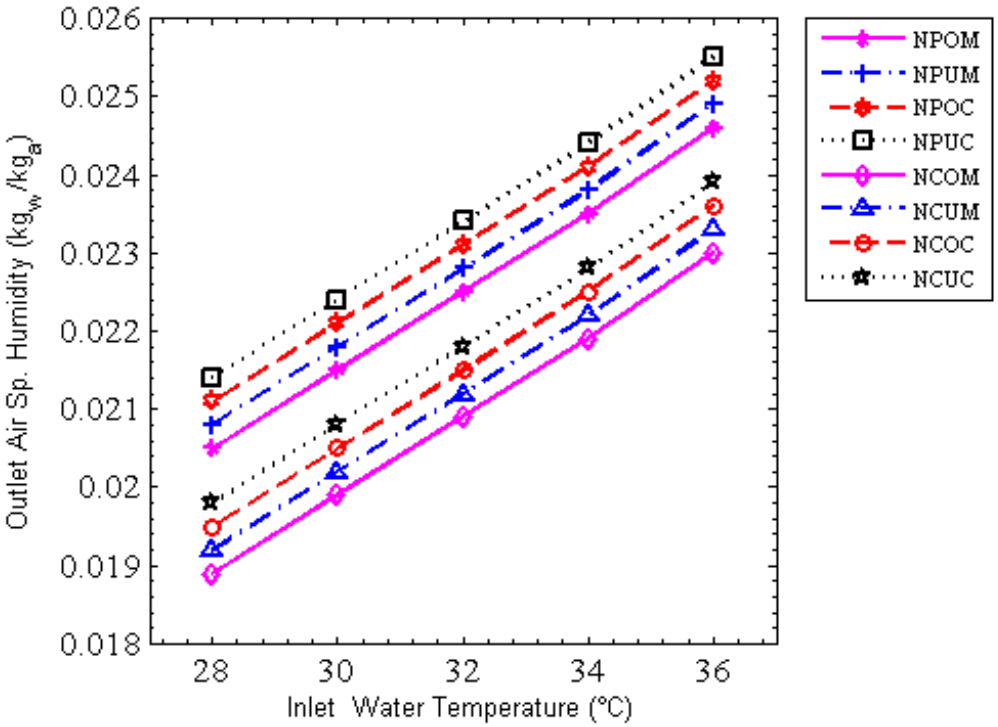

Figure 5.29 Outlet air specific humidity with variation in inlet droplet diameter

5.25.3 Variation in thermal efficiency of SCT with change of initial water temperature.

The variation of thermal efficiency of SCT by varying the inlet water temperature from 28 - 36 ˚C for parallel and counter flow configuration is shown in Figure 5.30. It was observed that thermal efficiency increased with the increased in the inlet water temperature for all the cases of parallel flow model and thermal efficiency decreased with the increased in the inlet water temperature for all cases of counter flow models. Figure 5.30 also shows that parallel and counter multi droplet SCT predicted thermal efficiency lesser than the mono droplet in both the cases of 2-

D and 3-D. The multi droplet models were closer to the validation test as they described more exact results as mono droplet models considered more assumption compared to multi droplet models. The multi droplet 3-D CFD model predicted least thermal efficiency compared to multi droplet 2-D model of MATLAB, however 3-D CFD model has least error in the validation test as shown in Figures 5.1 - 5.4. The overall maximum thermal efficiency obtained by 36 ˚C inlet water temperature parallel flow mono droplet MATLAB model was 57.52%. The overall maximum thermal efficiency obtained by 28 ˚C inlet water temperature counter flow mono droplet MATLAB model was 87.95%.

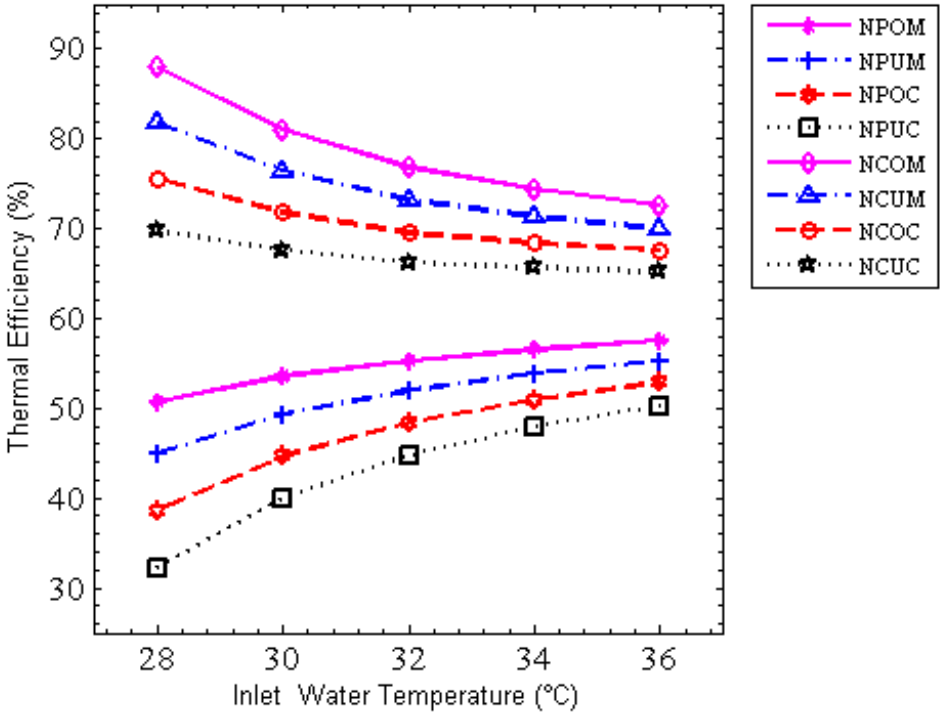

Figure 5.30 Thermal efficiency of SCT with variation in inlet water temperature

5.25.4 Variation in SLE of SCT with change of initial water temperature.

The variation of SLE of SCT with varying inlet water temperature from 28 - 36 ˚C for parallel and counter-flow configuration are shown in Figure 5.31. It was observed that SLE of SCT decreased with the increase in the inlet water temperature for all the cases of parallel flow and counter flow models because total system exergy destruction increased with increases the inlet water temperature. The maximum and minimum SLE obtains by 28 ˚C and 36 ˚C inlet water temperature respectively for all parallel flow and counter flow mono and multi droplet models. Figure 5.31 also shows parallel flow SCT predicted higher SLE in comparison to counter flow SCT because heat and mass transfer in counter flow SCT was more than parallel flow SCT. The Figure further shows that parallel and counter multi droplet SCT predicted SLE higher than the mono droplet in both the cases of 2-D and 3-D. The overall minimum and maximum SLE attained by parallel flow configurations were 96.55% (by 36 ˚C inlet water temperature mono droplet MATLAB model) and 99.46% (by 28 ˚C inlet water temperature multi droplet CFD model). The overall minimum and maximum SLE attains by counter flow configurations were 81.78% (by 36 ˚C inlet water temperature mono droplet MATLAB model) and 84.44% (by 28 ˚C inlet water temperature multi droplet CFD model).

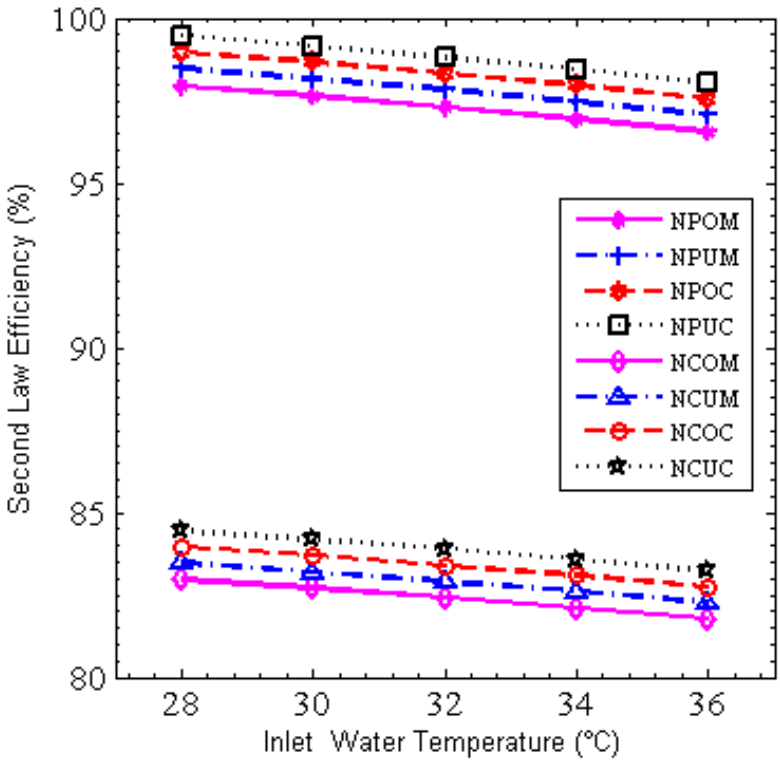

Figure 5.31 SLE of SCT with variation in inlet water temperature

5.26 Comparative Study of SCT with Change in Inlet air DBT for Air Cooling Application

In this section of research the effect of inlet air DBT from 36 - 44 ˚C on exit parameters (i.e. air DBT, air specific humidity, thermal efficiency and SLE) were studied. The exit parameter results are obtained for parallel flow and counter flow configuration using 2-D MATLAB model and 3-D CFD model. The exit parameter results were also compared for the cases of mono-droplet and multi-droplet.

5.26.1 Variation in outlet air temperature with changes of inlet air temperature

The variation of outlet air DBT with varied inlet air DBT from 36 - 44 ˚C for parallel and counter-flow configuration is shown in Figure 5.32. It was observed that the outlet air DBT increased with increasing the inlet air DBT for all the cases of parallel flow and counter flow SCT. Figure 5.32 shows parallel flow SCT predicted higher exit air temperature in comparison to counter flow SCT because heat and mass transfer in counter flow SCT was more than parallel flow SCT. Figure 5.32 also shows that parallel and counter multi droplet SCT predicted exit air temperature higher than the mono droplet in both the cases of 2-D and 3-D. The multi droplet models were closer to the validation test as they described more realistic phenomena because mono droplet models considered more assumption compared to multi droplet models. The multi droplet 3-D CFD model predicted higher outlet water temperature compared to multi droplet 2-D model of MATLAB, However 3-D CFD model with least error in the validation test as shown in the Figures 5.1 - 5.4. The overall minimum and maximum exit air DBT attains by parallel flow configurations was 26.08 ˚C (by 36 ˚C inlet air DBT mono droplet MATLAB model) and 29.94 ˚C (by 44 ˚C inlet air DBT multi droplet CFD model). The overall minimum and maximum exit air DBT attains by counter flow configurations are 23.98 ˚C (by 36 ˚C inlet air DBT mono droplet MATLAB model) and 27.93 ˚C (by 44 ˚C inlet air DBT multi droplet CFD model) respectively.

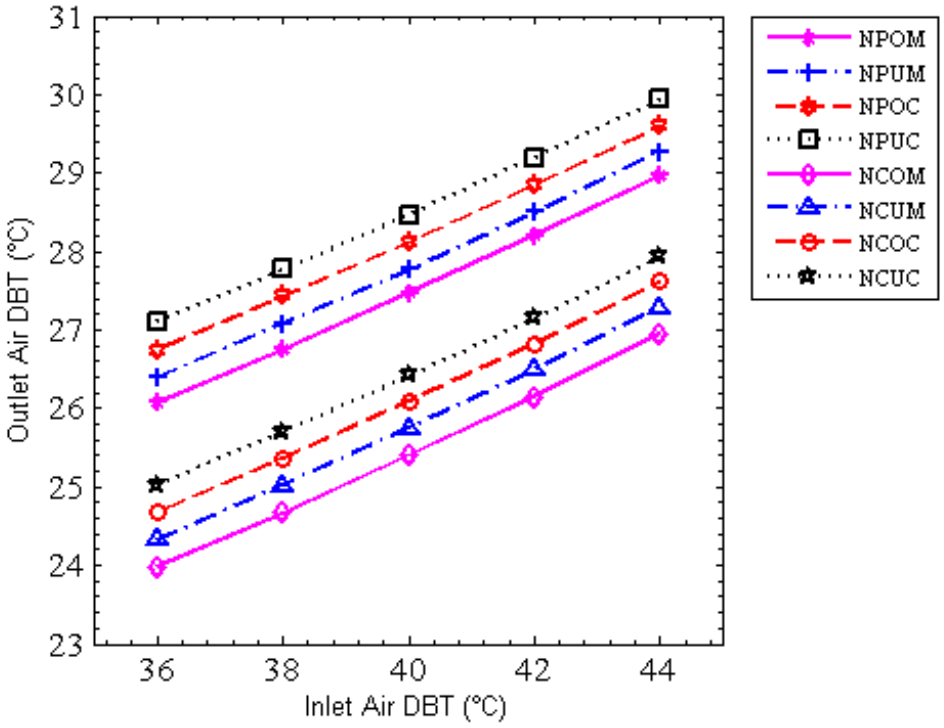

Figure 5.32 Outlet air DBT with variation in inlet air temperature

5.26.2 Variation in outlet air specific humidity with changes of inlet air temperature

The variation of outlet air specific humidity with varying inlet air DBT from 36 - 44 ˚C for parallel and counter-flow configuration are shown in Figure 5.33. It observed that the outlet specific humidity was increased with the increasing the inlet air DBT for all the cases of parallel flow and counter flow SCT. Figure 5.33 shows parallel flow SCT predicted higher exit specific humidity in comparison to counter flow SCT because parallel flow SCT has higher exit air DBT in comparison to counter flow SCT. Figure 5.33 also shows that parallel and counter flow multi droplet shower cooling tower predicted outlet specific humidity higher than the mono droplet in both the cases of 2-D MATLAB and 3-D CFD models. The multi droplet models were closer to the validation test as they described more accurate results because

mono droplet models considered more assumption compared to multi droplet models. The multi droplet 3-D CFD model predicted higher specific humidity compared to multi droplet 2-D model of MATLAB, However 3-D CFD model with least error in the validation test as shown in Figures 5.1-5.4. The overall maximum exit air specific humidity obtained by 40 ˚C multi droplet diameter CFD models of parallel and counter flow configurations were 0.0267 kg_w/kg_a and 0.0251 kg_w/kg_a. The minimum exit air specific humidity obtained by 40 ˚C droplet diameter MATLAB models of parallel and counter flow configurations were 0.0216 kg_w/kg_a and 0.0200 kg_w/kg_a.

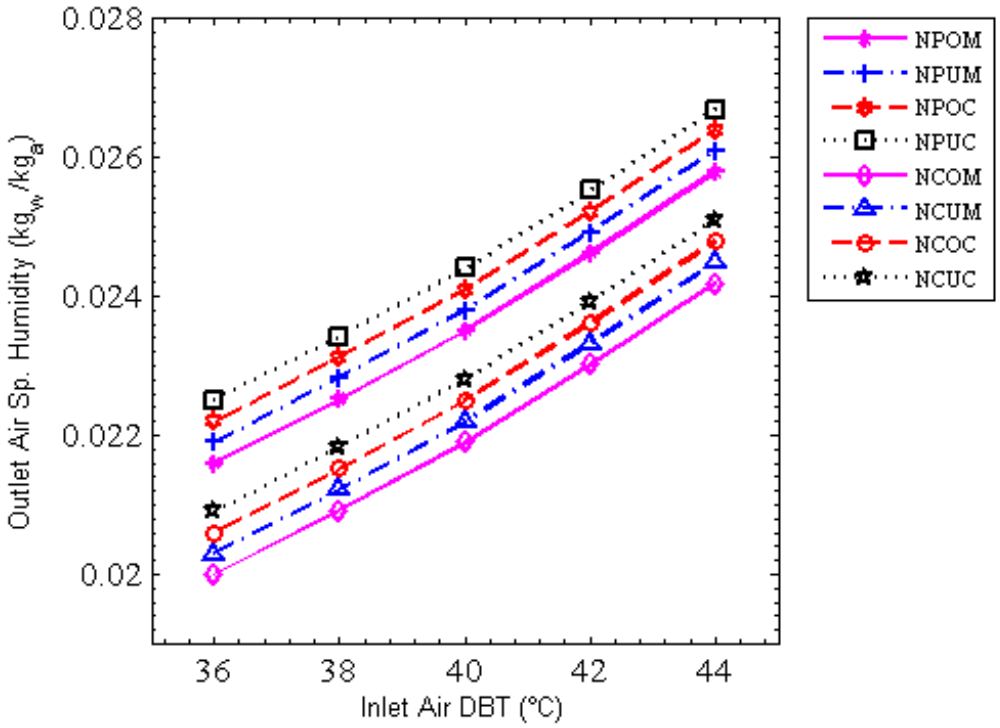

Figure 5.33 Outlet air specific humidity with variation in inlet droplet diameter

5.26.3 Variation in thermal efficiency of SCT with change of inlet air temperature.

The variation of thermal efficiency of SCT with varying the inlet air DBT from 36 - 44 ˚C for parallel and counter flow configuration are shown in Figure 5.34.

The thermal efficiency obtained from counter flow models was more than parallel flow models for same inlet air DBT because range (i.e. $T_{d,in} - T_{d,out}$) of SCT was more for counter flow models.

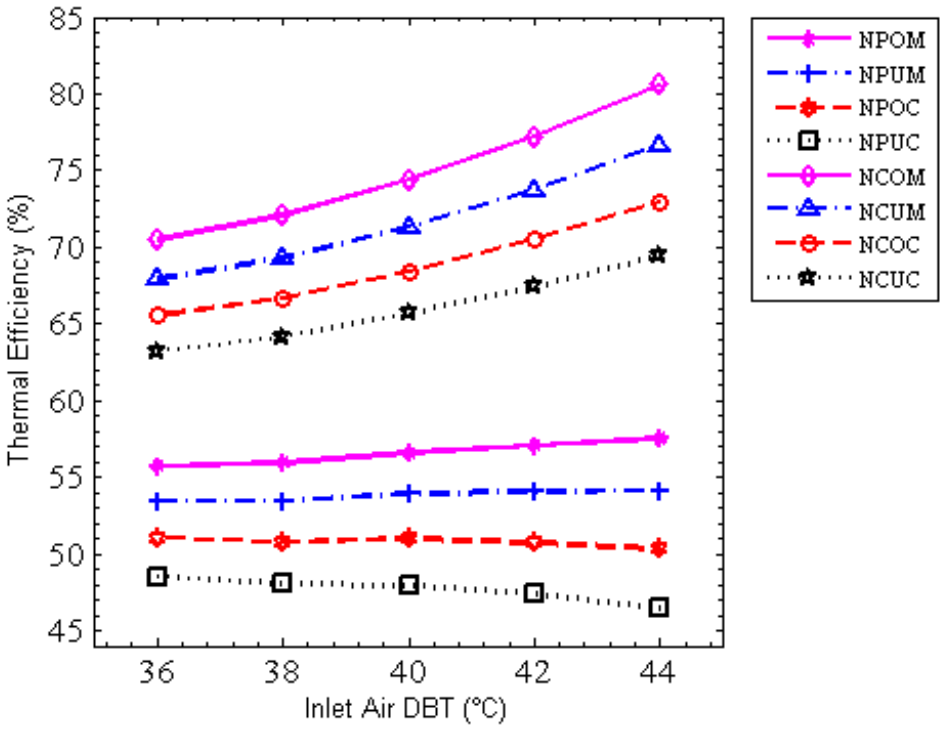

Figure 5.34 Thermal efficiency of SCT with variation in inlet air temperature

Figure 5.34 shows that parallel and counter multi droplet SCT predicted thermal efficiency lower than the mono droplet in both the cases of 2-D and 3-D. The multi droplet models were closer to the validation test as they described more accurate results because mono droplet models considered more assumption compared to multi droplet models. The multi droplet 3-D CFD model predicted least thermal efficiency compared to multi droplet 2-D model of MATLAB, However 3-D CFD model with least error in the validation test as shown in Figures 5.1 - 5.4. The overall maximum thermal efficiency obtained by 44 ˚C inlet water temperature parallel flow mono droplet MATLAB model was 57.53%. The overall maximum thermal efficiency

obtained by 44 ˚C inlet water temperature counter flow mono droplet MATLAB model was 80.59%.

5.26.4 Variation in SLE of SCT with change of inlet air temperature.

The variation of SLE of SCT with varying inlet air DBT from 36 - 44 ˚C for parallel and counter-flow configuration are shown in Figure 5.35.

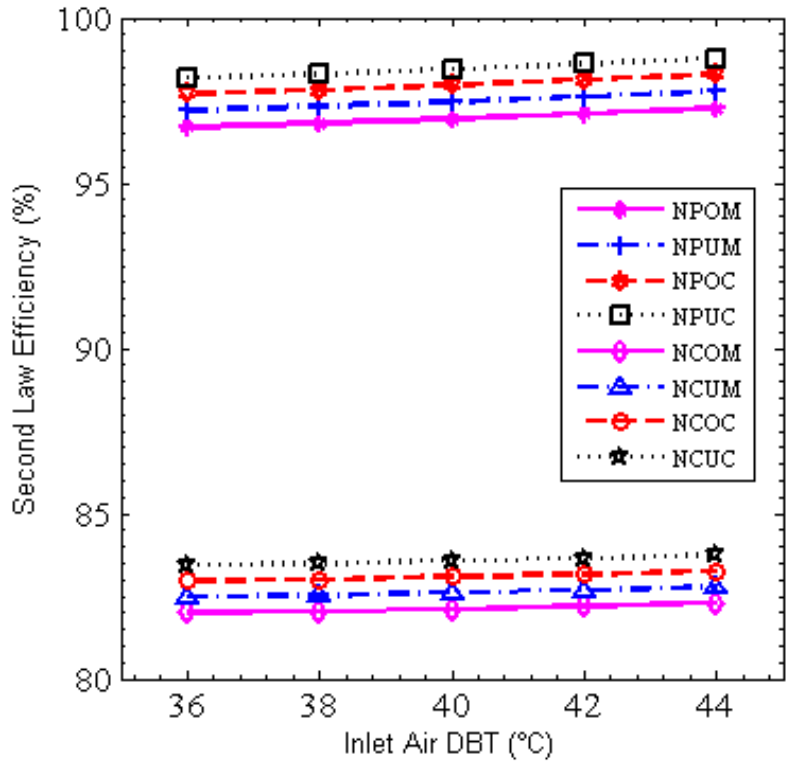

Figure 5.35 SLE of SCT with variation in inlet air temperature

It was observed that SLE of SCT was increased with the increasing the inlet air DBT for all the cases of parallel flow and counter flow models because total system exergy was decreased with increasing the inlet air DBT. Figure 5.35 shows parallel flow SCT predicted higher SLE in comparison to counter flow SCT because heat and mass transfer in counter flow SCT was more than parallel flow SCT. Figure 5.35 also shows that parallel and counter flow multi droplet SCT predicted SLE higher than the mono droplet in both the cases of 2-D and 3-D. The overall maximum

SLE attained by parallel flow and counter flow configurations were 98.75% and 83.74%, these SLE obtained by 44 ˚C multi droplet diameter CFD model. The overall minimum SLE attained by parallel flow and counter flow configurations were 96.70% and 81.99%, these SLE obtained by 36 ˚C mono droplet diameter MATLAB model.

5.27 Comparative Study of SCT with Change in Inlet Air Relative Humidity for Air Cooling Application

In order to study the effects of inlet air relative humidity from 20% to 40% on exit parameters (i.e. air DBT, air specific humidity, thermal efficiency and SLE). The exit parameter results was obtained for parallel flow and counter flow configuration using 2-D MATLAB model and 3-D CFD model. These exit parameter results was compared for the cases of mono-droplet and multi-droplet diameter.

5.27.1 Variation in outlet air temperature with changes of inlet air relative humidity

The variation of outlet air DBT with varying inlet air relative humidity from 20 - 40% for parallel flow and counter flow configuration is shown in Figure 5.36. It was observed that the outlet air temperature increased with the increasing the inlet air relative humidity for all the cases of parallel flow and counter flow SCT. Figure 5.36 shows the exit air DBT for parallel flow cases was greater than counter flow cases for same inlet air relative humidity because heat and mass transfer in counter flow SCT was higher than parallel flow SCT. Figure 5.36 also shows that parallel and counter multi droplet SCT predicted outlet air DBT higher than the mono droplet for both the cases of 2-D and 3-D. The multi droplet models were closer to the validation test

(Figure 5.1 - 5.4) as they described more accurate phenomena because mono droplet models considered more assumption compared to multi droplet models. The multi droplet 3-D CFD model predicted greater exit air DBT as compared to multi droplet 2-D model of MATLAB, however 3-D CFD model with least error in the validation test. The overall minimum exit air DBT attains by parallel and counter flow configurations was 27.47 ˚C and 25.41 ˚C respectively, these exit air DBT obtained by 20% relative humidity mono droplet MATLAB model. The overall maximum exit air DBT attains by parallel and counter flow configurations was 31.42 ˚C and 29.42 ˚C respectively, these exit air DBT obtained by 40% relative humidity multi droplet CFD model. The minimum temperature attains by parallel and counter flow 3-D CFD multi droplet model was 28.47 C and 26.42 C, these exit air DBT obtained by 20% relative humidity.

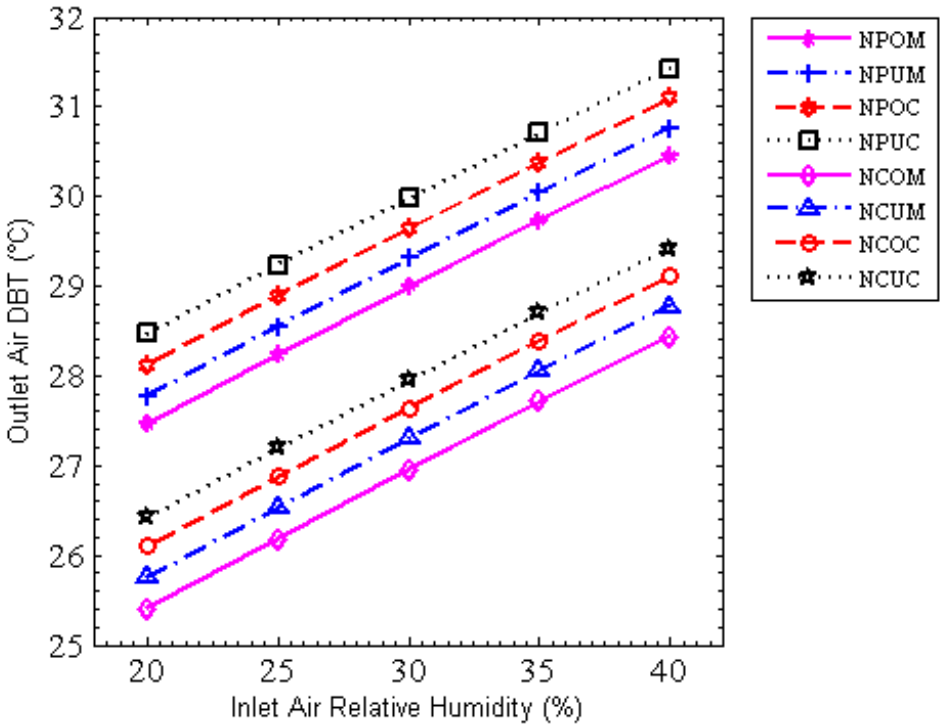

Figure 5.36 Outlet air DBT with variation in inlet air relative humidity

5.27.2 Variation in outlet air specific humidity with changes of inlet air relative humidity

The variation of exit air specific humidity with varying inlet air relative humidity from 20% to 40% for parallel flow and counter flow configuration is shown in Figure 5.37. It was observed that the outlet air specific humidity increased with the increasing the inlet air relative humidity for all the cases of parallel flow and counter flow SCT. Figure 5.37 also shows parallel flow SCT predicted higher exit specific humidity in comparison to counter flow SCT as parallel flow SCT has higher exit air DBT in comparison to counter flow SCT. Figure 5.37 also shows that parallel and counter flow multi droplet shower cooling tower predicted outlet specific humidity higher than the mono droplet in both the cases of 2-D MATLAB and 3-D CFD models. The multi droplet models were closer to the validation test (Figure 5.1 - 5.4) as they described more accurate results because mono droplet models considered more assumption compared to multi droplet models. The multi droplet 3-D CFD model predicted higher specific humidity compared to multi droplet 2-D model of MATLAB, However 3-D CFD model with least error in the validation. The overall maximum exit air specific humidity obtained by 40% relative humidity multi droplet diameter CFD model of parallel and counter flow configurations were 0.0291 kg_w/kg_a and 0.0275 kg_w/kg_a respectively. The minimum exit air specific humidity obtained by 20% relative humidity mono droplet diameter MATLAB model of parallel and counter flow configurations were 0.0235 kg_w/kg_a and 0.0219 kg_w/kg_a respectively.

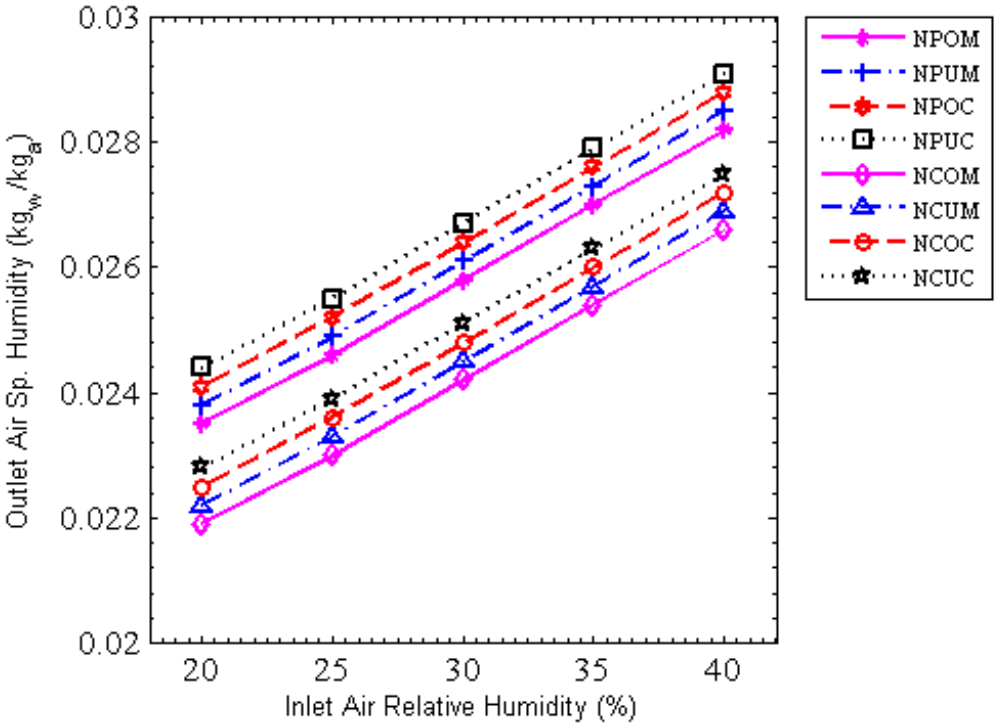

Figure 5.37 Outlet air specific humidity with variation in inlet droplet diameter

5.27.3 Variation in thermal efficiency of SCT with change of initial air relative humidity.

The variation in thermal efficiency of SCT with changes in inlet air specific humidity for parallel and counter flow configuration are shown in Figure 5.38. It was observed that thermal efficiency of SCT was increased with increasing the inlet air relative humidity for all the cases of parallel flow and counter flow models except multi droplet parallel flow CFD model due to error in results. The thermal efficiency obtained from counter flow models are more than parallel flow models for same inlet air relative humidity because evaporative heat transfer was increased with increasing the inlet air relative humidity.

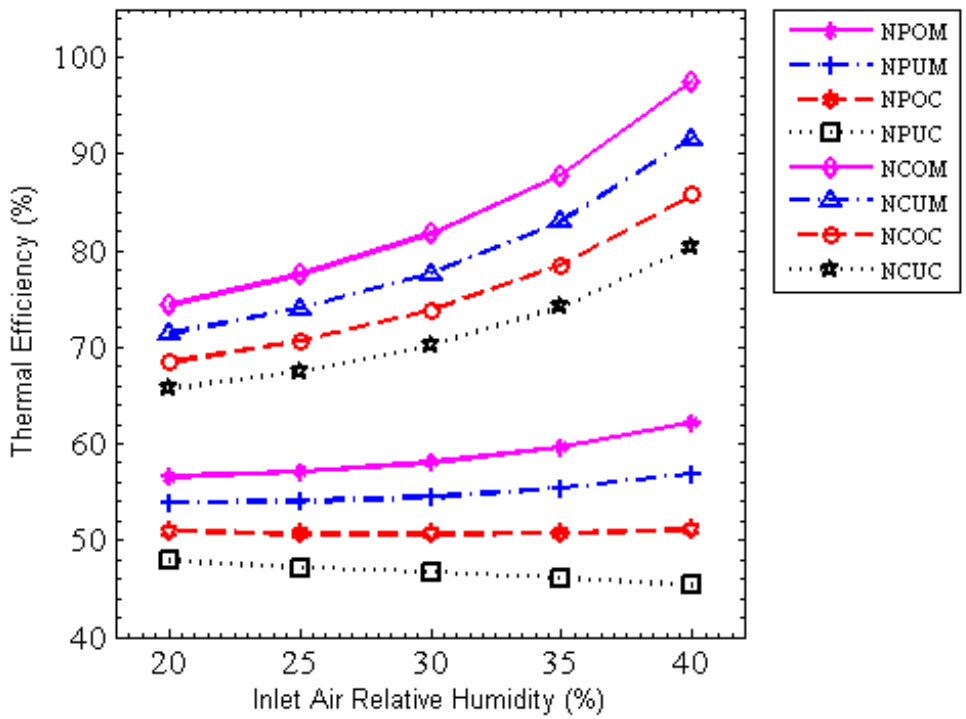

Figure 5.38 Thermal efficiency of SCT with variation in inlet air relative humidity

Figure 5.38 also shows that parallel and counter flow multi droplet SCT predicted thermal efficiency lower than the mono droplet in both the cases of 2-D and 3-D. The multi droplet models were closer to the validation test as they described more accurate results because mono droplet models considered more assumption compared to multi droplet models. The multi droplet 3-D CFD model predicted least thermal efficiency compared to multi droplet 2-D model of MATLAB. The overall maximum thermal efficiency obtained by 40% inlet relative humidity parallel and counter flow model were 62.13% and 97.50% respectively. The overall minimum thermal efficiency obtained by 20% relative humidity parallel and counter flow models were 47.92% and 65.66% respectively. The maximum efficiency achieved by counter flow 3-D CFD multi droplet model was 80.34%.

5.27.4 Variation in SLE of SCT with change of initial air relative humidity.

The variation of SLE of SCT with varying inlet air relative humidity for parallel and counter-flow configuration are shown in Figure 5.39.

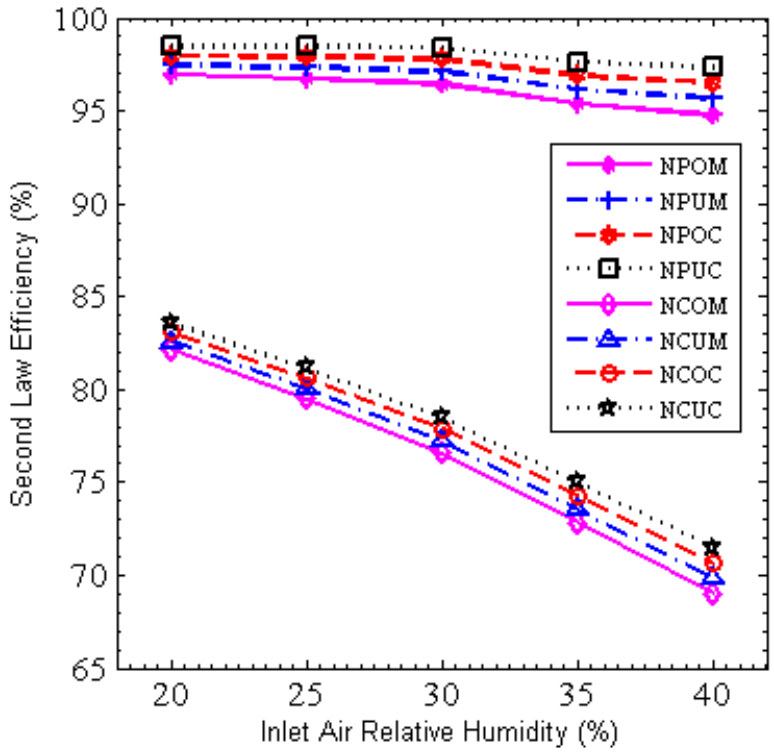

Figure 5.39 SLE of SCT with variation in inlet air relative humidity

It was observed that SLE of SCT was decreased with increasing the inlet air relative humidity for all the cases of parallel flow and counter flow models because total system exergy decreases with increases the inlet air relative humidity. Figure 5.39 shows parallel flow SCT predicted higher SLE in comparison to counter flow SCT for same inlet air relative humidity because heat and mass transfer in counter flow SCT was more than parallel flow SCT. Figure 5.39 also shows that parallel and counter multi droplet SCT predicted SLE higher than the mono droplet in both the cases of 2-D and 3-D. The maximum and minimum SLE obtained by 20% and 40%

initial air relative humidity respectively for parallel flow and counter flow models. The overall maximum SLE attained by parallel flow and counter flow configurations were 98.43% and 83.56%, these SLE obtained by 20% relative humidity multi droplet diameter CFD model. The overall minimum SLE attained by parallel flow and counter flow configurations were 94.76% and 69.00%, these SLE obtained by 40% relative humidity mono droplet diameter MATLAB model.

5.28 Comparative Study of SCT with Change in Inlet RLG for Air Cooling Application

Comparative study had performed in order to study the effects of inlet RLG from 0.5 to 1.5 on exit parameters (i.e. air DBT, air specific humidity, thermal efficiency and SLE). The exit parameter results are obtained for parallel flow and counter flow configuration using 2-D MATLAB model and 3-D CFD model. These exit parameter results are also compared for the cases of mono-droplet and multi-droplet diameters.

5.28.1 Variation in outlet air temperature with changes of inlet RLG.

The variation of outlet air DBT with varying inlet RLG from 0.5 to 1.5 for parallel and counter-flow configuration is shown in Figure 5.40. It was observed that the outlet air DBT increased with the increasing the inlet RLG for all the cases of parallel flow and counter flow SCT. The exit air DBT for parallel flow cases was greater than counter flow cases for same inlet RLG. Figure 5.40 shows counter flow model water droplet cool down faster because heat and mass transfer in counter flow

SCT was more than parallel flow SCT. Figure 5.40 also shows that parallel and counter multi droplet SCT predicted outlet air DBT higher than the mono droplet in both the cases of 2-D and 3-D. The multi droplet models were closer to the validation test as they described more realistic phenomena because mono droplet models considered more assumption compared to multi droplet models. The multi droplet 3-D CFD model predicted higher outlet temperature compared to multi droplet 2-D model of MATLAB, however 3-D CFD model with least error in the validation test as shown in the Figures 5.1 - 5.4. The overall minimum exit air DBT attained by 0.5 RLG mono droplet MATLAB model of parallel and counter flow configurations were 27.47 ˚C and 25.41 ˚C respectively. The minimum exit air DBT attained by multi droplet parallel and counter flow 3-D CFD model was 28.47 ˚C and 26.42 ˚C.

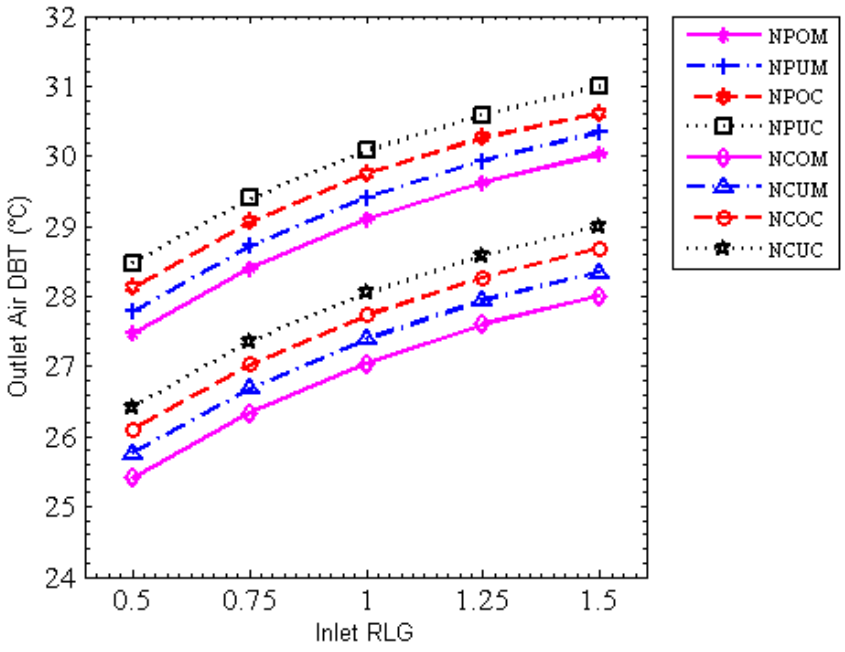

Figure 5.40 Outlet air DBT with changes of inlet RLG

5.28.2 Variation in outlet air specific humidity with changes of initial droplets diameter

The variation of exit air specific humidity with varying inlet RLG from 0.5 to 1.5 for parallel and counter flow configuration are shown in Figure 5.41.

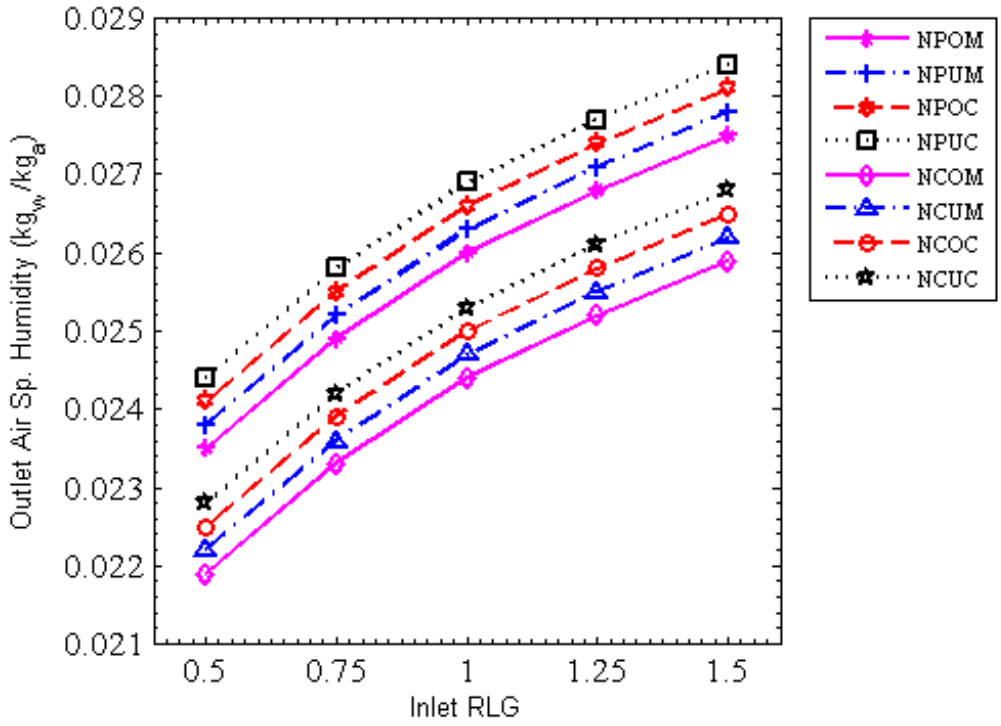

Figure 5.41 Outlet air specific humidity with variation in inlet droplet diameter

It was observed that the exit air specific humidity increased with the increasing the inlet RLG for all the cases of parallel flow and counter flow SCT. The exit air specific humidity for parallel flow cases are greater than counter flow cases for same inlet RLG. Figure 5.41 also shows that parallel and counter flow multi droplet SCT predicted higher outlet specific humidity than the mono droplet in both the cases of 2-D MATLAB and 3-D CFD models. The multi droplet models were closer to the validation test as they described more exact results because mono droplet models considered more assumption compared to multi droplet models. The multi

droplet 3-D CFD model predicted higher specific humidity compared to multi droplet 2-D model of MATLAB. The maximum exit air specific humidity obtained by parallel and counter flow configurations were 0.0284 kg_w/kg_a and 0.0268 kg_w/kg_a, these specific humidity obtained by multi droplet diameter CFD models respectively. The minimum exit air specific humidity obtained by parallel and counter flow configurations were 0.0235 kg_w/kg_a and 0.0219 kg_w/kg_a, these specific humidity obtained by mono droplet diameter MATLAB model respectively.

5.28.3 Variation in thermal efficiency of SCT with change of inlet RLG

The variation of thermal efficiency of SCT with varying inlet RLG from 0.5 to 1.5 for parallel and counter flow configuration are shown in Figure 5.42. It was observed that thermal efficiency of SCT decreased with the increasing the inlet RLG for all the cases of parallel flow and counter flow models. The thermal efficiency obtained from counter flow models was more than parallel flow models for same inlet RLG. Figure 5.42 also shows that parallel and counter multi droplet SCT predicted thermal efficiency lesser than the mono droplet in both the cases of 2-D and 3-D. The multi droplet models were closer to the validation test (Figure 5.1 - 5.4) as they described more accurate results because mono droplet models considered more assumption compared to multi droplet models. The multi droplet 3-D CFD model predicted least thermal efficiency compared to multi droplet 2-D model of MATLAB. The overall maximum thermal efficiency obtained by 0.5 RLG parallel and counter flow mono droplet MATLAB model was 56.57% and 74.39% respectively. The maximum efficiency obtained by parallel and counter flow 3-D CFD multi droplet model were 47.92% and 65.66% respectively.

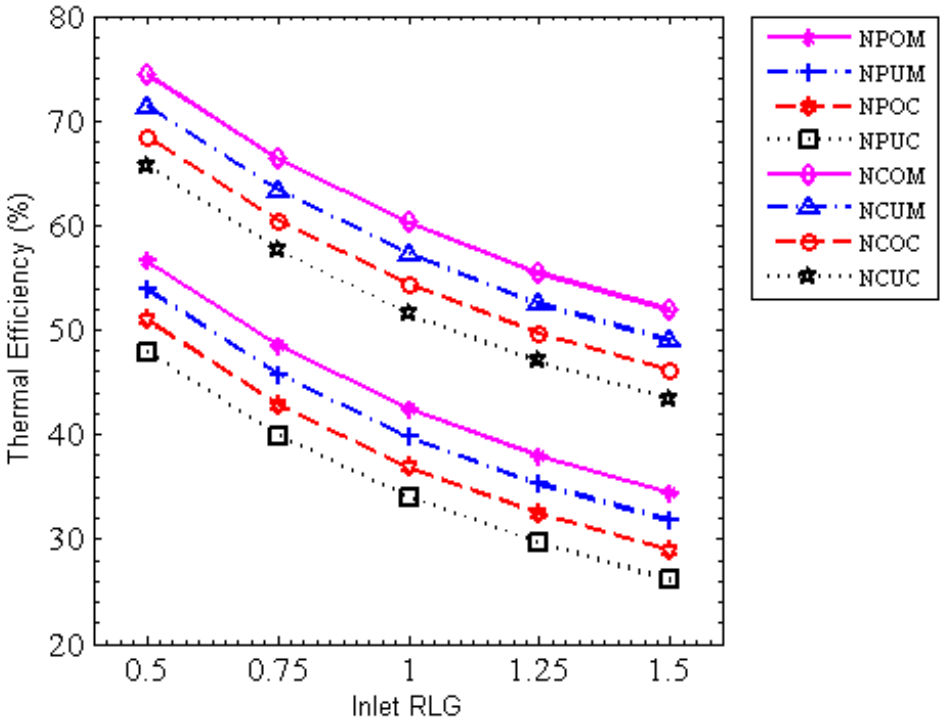

Figure 5.42 Thermal efficiency of SCT with variation in inlet RLG

5.28.4 Variation in SLE of SCT with change of inlet RLG.

The variation of the SLE of SCT with varying inlet RLG from 0.5 to 1.5 for parallel and counter flow configuration are shown in Figure 5.43. It was observed that the SLE of SCT increased with the increasing the inlet RLG for all the cases of parallel flow and counter flow models. The SLE for parallel flow cases was higher than counter flow cases for same inlet RLG. Figure 5.43 also shows parallel flow SCT predicted higher SLE in comparison to counter flow SCT because heat and mass transfer in counter flow SCT was more than parallel flow SCT. Figure 5.43 further shows that parallel and counter multi droplet SCT predicted SLE higher than the mono droplet in both the cases of 2-D and 3-D. The overall minimum and maximum SLE attained by parallel flow configurations were 96.94% (by 0.5 inlet RLG mono droplet MATLAB model) and 99.71% (by 1.5 RLG multi droplet CFD model)

respectively. The overall minimum and maximum SLE attains by counter flow configurations were 82.11% (by 0.5 inlet RLG mono droplet MATLAB model) and 84.83% (by 1.5 RLG multi droplet CFD model) respectively.

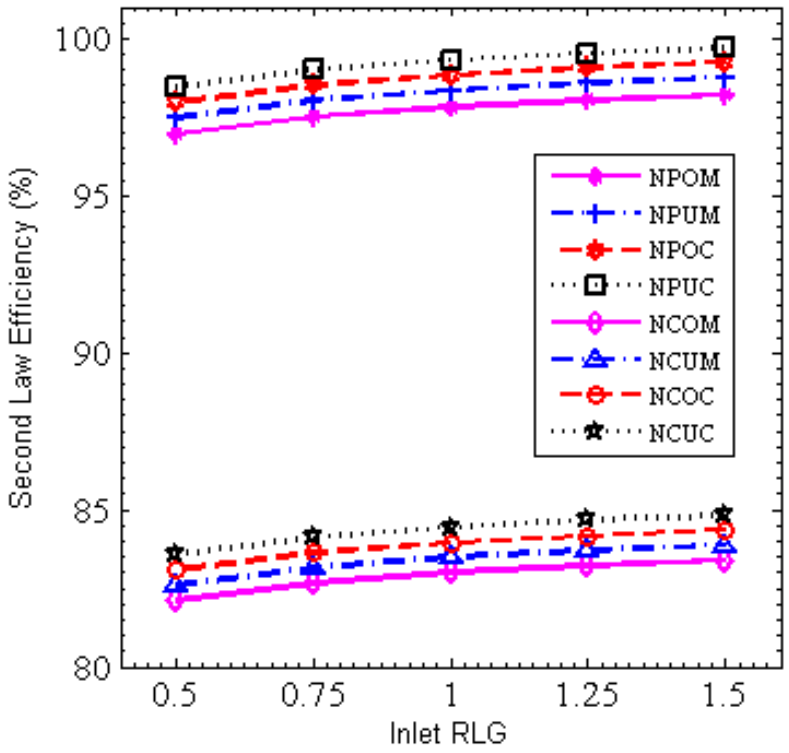

Figure 5.43 SLE of SCT with variation in inlet RLG

5.29 Optimization of Tower Height

5.29.1 Two dimensional multi droplet SCT with change of inlet air DBT for industrial application

Two dimensional parallel flow multi droplets SCT used for industrial application has been analysed for find its optimum height. Water at 56 ˚C is sprayed from the top of SCT and air is also admitted from the top. The temperature of air varied from 24 - 48 ˚C in the interval of 6 ˚C. When water sprayed from the top, it breaks into ten different diameters. Figure 5.44 shows trajectory of ten different

diameter droplets whose diameter varying from 31.8184 μm to 318.184 μm along tower height. Smaller size droplet covers longer path in comparison to large size droplets along the tower height. Figure 5.45 displays variation in temperature of ten different diameter water droplets (31.8184 - 318.184 μm) along tower height for 48 ˚C inlet air DBT. Smaller size droplet covers longer paths along the tower height, so retention time of smaller size droplet in SCT is greater as compared to larger size droplet. Water temperature drops due to evaporation of the outer layer of the droplet; outer layer takes the heat of evaporation from the inner part of the droplet. For the smaller size of water droplets direction of heat transfer reverse (air to water) along the SCT height, thus the temperature of smaller size water droplets start increasing after a certain distance along the height of SCT. Figure 5.46 denoted as inlet air DBT increases exit mean water droplet temperature relatively increases. Total system exergy is the sum of total air and water exergy. The total exergy of system reduces along the height due to irreversibility and due to water droplets and air interaction (Figure 5.47). Figure 5.48 shows the thermal efficiency of the cooling tower increases by increasing the inlet air DBT because as the air DBT increases its wet bulb temperature also increase. Second law efficiency at the exit of SCT increases with increase the inlet air DBT (Figure 5.49) because exit total exergy of the system relatively increases with increase the air DBT. Most importantly it is clear in all the results become asymptotic after tower height of 0.5 m. Similarly all mono and multi droplet 2-D and 3-D, parallel and counter flow SCT operated at different inlet parameters (i.e. droplet diameters, water temperature, air DBT, air specific humidity, and RLG) for industrial application also shows all performance parameters become asymptotic up to 0.5 m, so optimal performance of the SCT can be achieved at 0.5 m

height. So by reduce tower height up to 0.5 m initial investment and operational cost of SCT can be reduced.

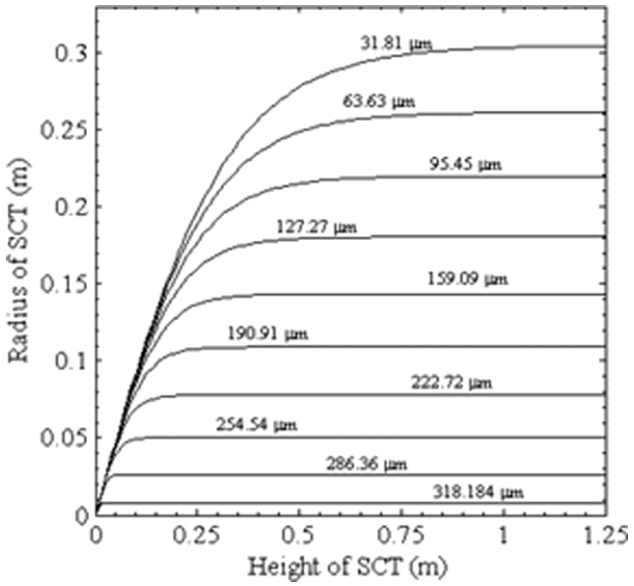

Figure 5.44 Trajectories of ten different diameters water droplets along tower height

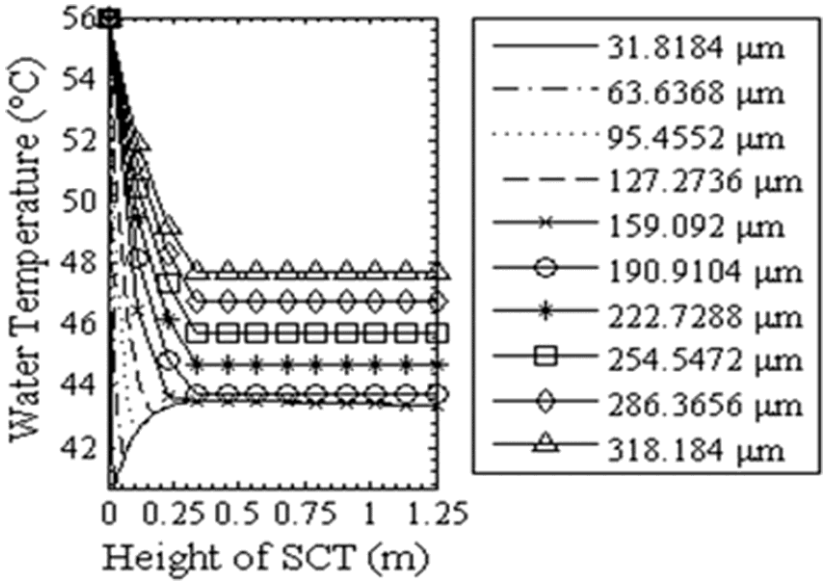

Figure 5.45 Ten different water droplets temperature along tower height

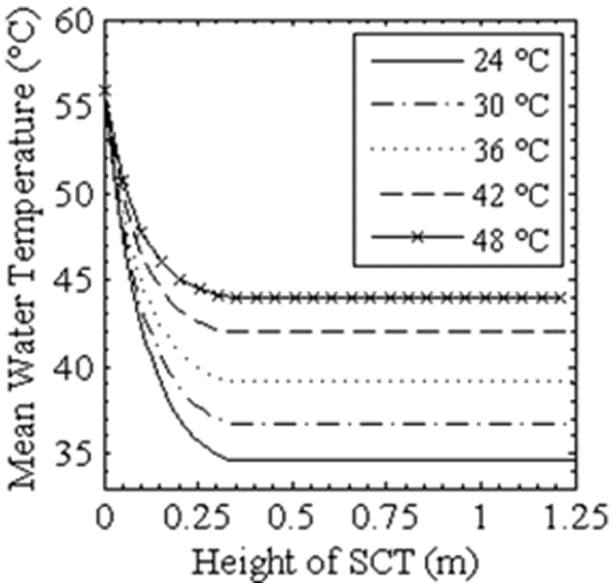

Figure 5.46 Mean water droplet temperature along the tower height

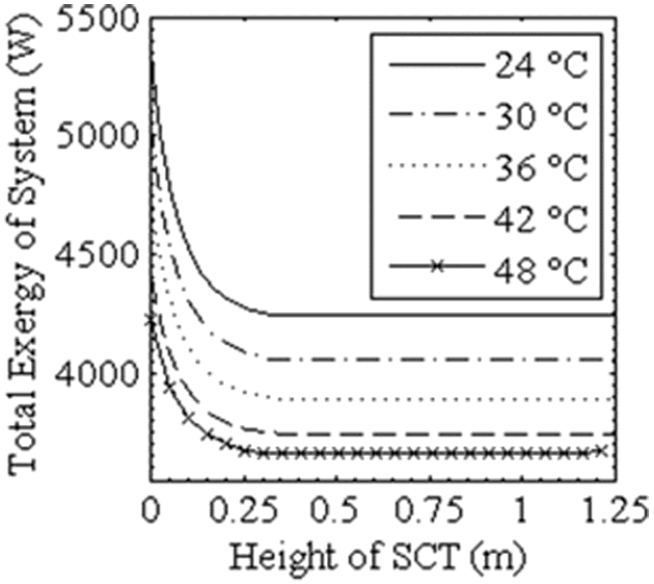

Figure 5.47 Total exergy of system along the tower height

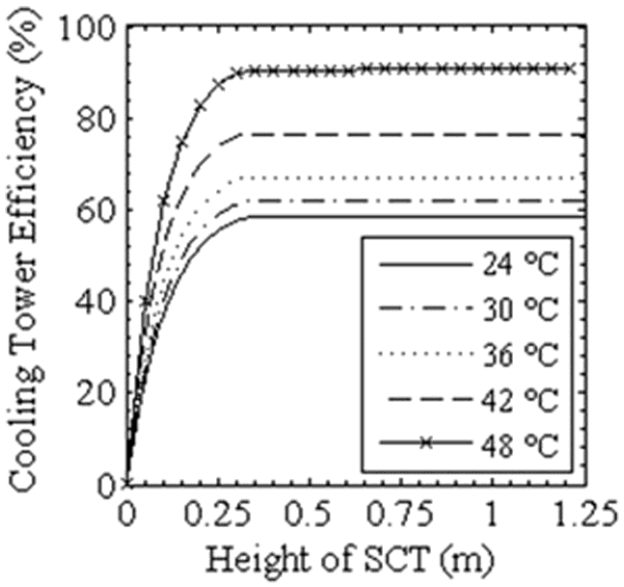

Figure 5.48 Thermal efficiency of SCT along the tower height

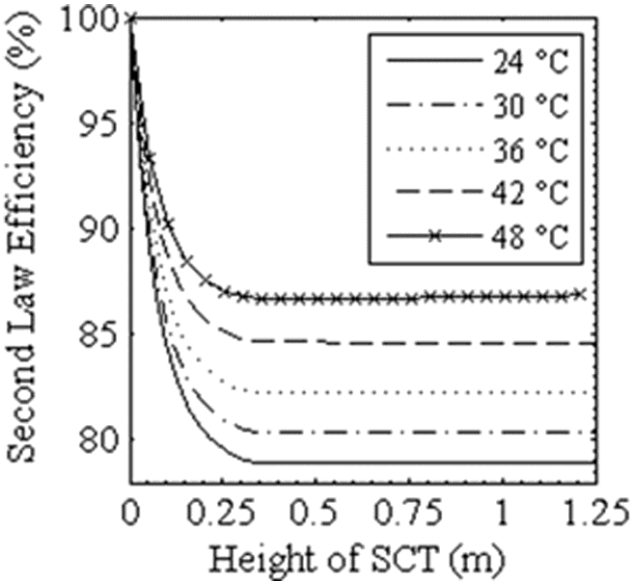

Figure 5.49 SLE of SCT along the tower height

5.29.2 Two dimensional multi droplet SCT with change of inlet water temperature for air cooling application

Two dimensional parallel flow multi droplets SCT has been analysed for find its optimum height. Figure 5.50 shows the trajectory of ten different diameter droplets

whose diameter varying from 25.45 µm to 254.54 µm along tower height. Smaller size droplet covers longer path in comparison to large size droplets along the tower height.

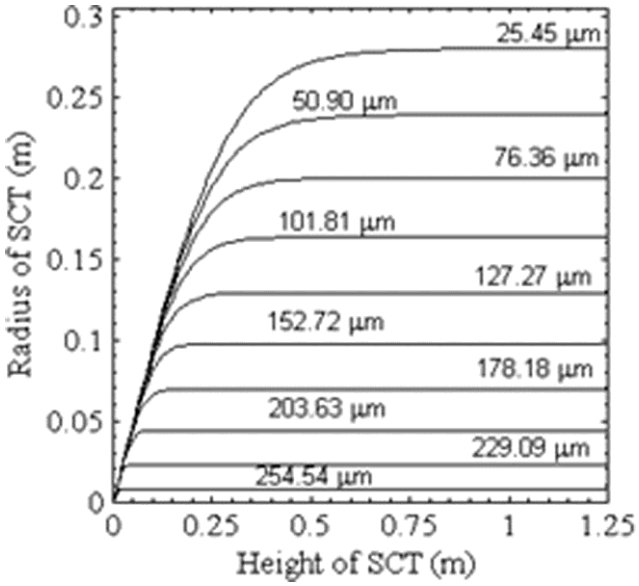

Figure 5.50 Variation in trajectory of different water droplets along the tower height

Figure 5.51 shows air DBT decreases along tower height, it also shows as the water inlet temperature increases from 28 ˚C to 36 ˚C exit air DBT increases. Figure 5.52 – Figure 5.55 as inlet water temperature increases air specific humidity, air convective exergy, air evaporative and thermal efficiency of SCT increases along tower height. Total exergy of the system is the sum of total exergy of air and water has destroyed continuously from top to bottom of SCT (Figure 5.56). Maximum exergy of the system is destructed at the top of the tower and decreases along its height. Figures 5.42 – 5.48 show that all performance parameters of SCT (i.e. air DBT, air specific humidity, air convective exergy, air evaporative exergy, cooling tower efficiency and exergy destruction) become asymptotic upto tower height of 0.5 m. Similarly all mono and multi droplet 2-D and 3-D, parallel and counter flow SCT operated at different inlet parameters (i.e. droplet diameters, water temperature, air

DBT, air specific humidity, and RLG) for air cooling application also shows all performance parameters become asymptotic up to 0.5 m, so optimal performance of the SCT can be achieved at 0.5 m height. So by reducing tower height up to 0.5 m initial investment and operational cost of SCT can be reduced.

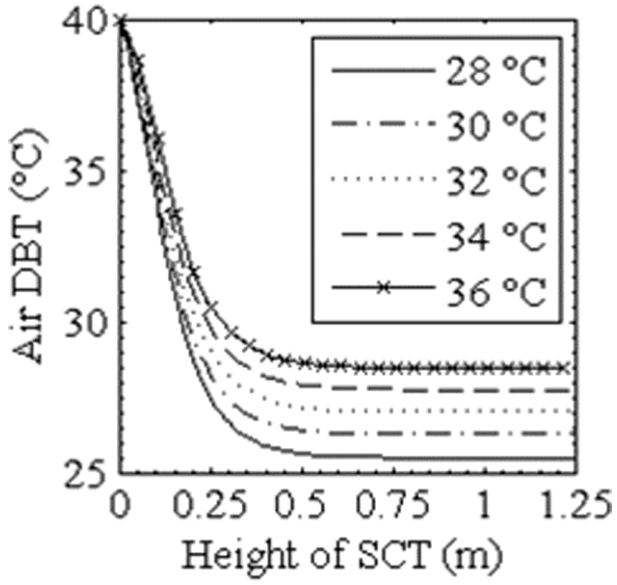

Figure 5.51 Variation in air DBT along the tower height

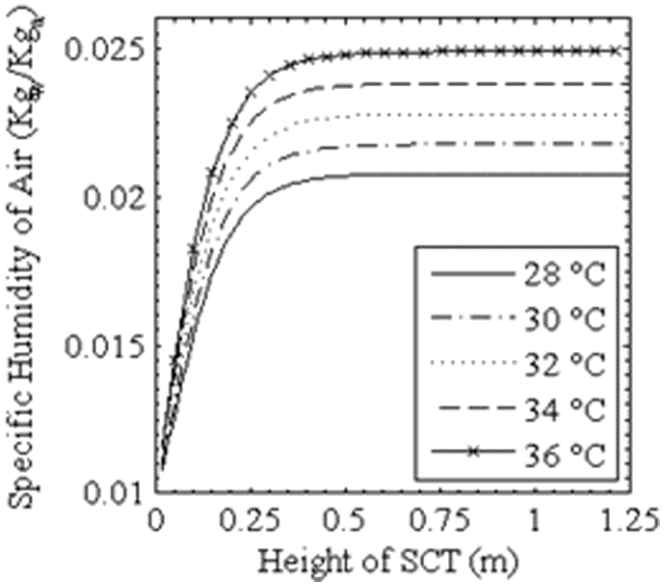

Figure 5.52 Variation in air specific humidity along the tower height

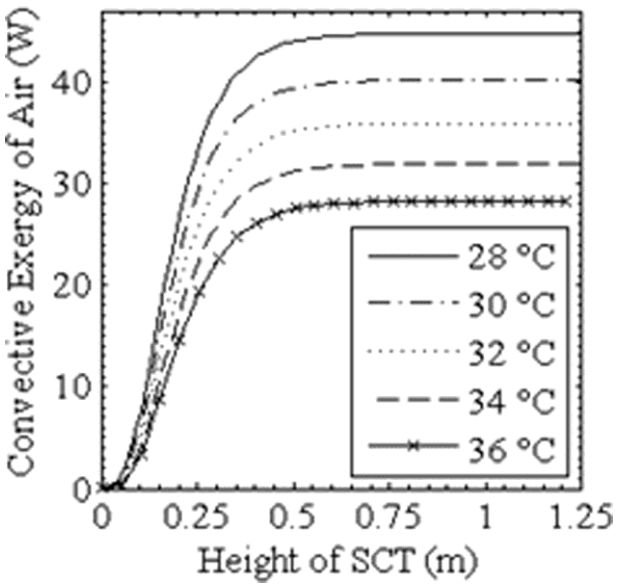

Figure 5.53 Variation in convective exergy of air along the tower height

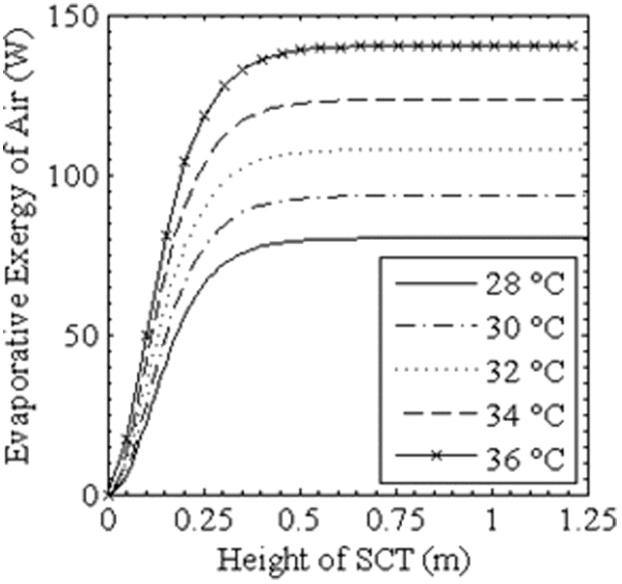

Figure 5.54 Variation in evaporative exergy of air along the tower height

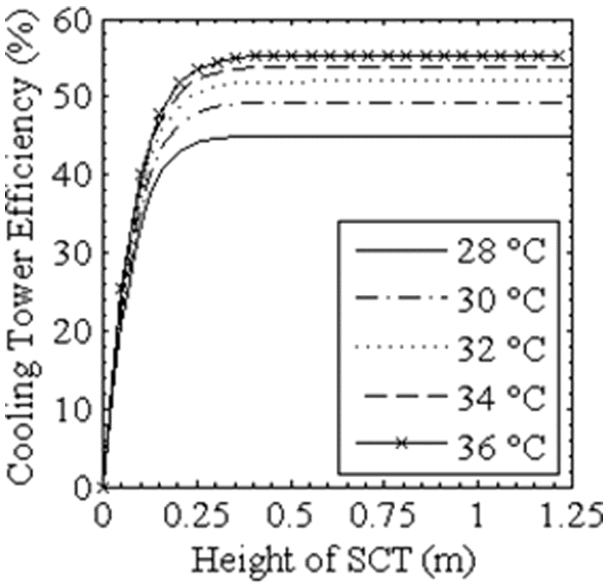

Figure 5.55 Variation in evaporative exergy of air along the tower height

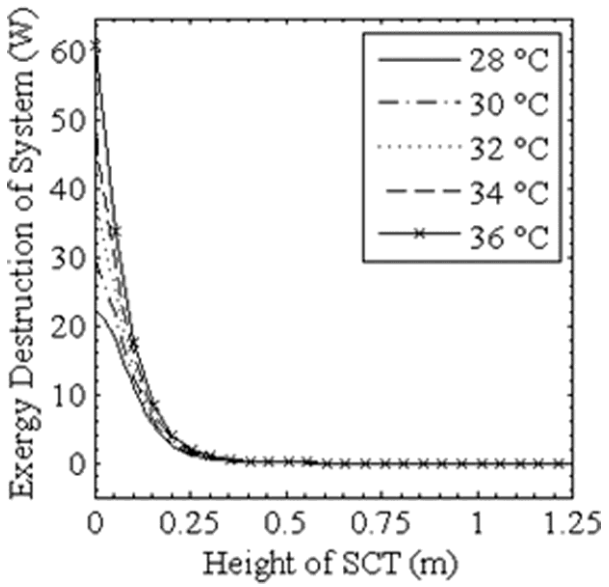

Figure 5.56 Variation in exergy destruction of system along the tower height

Chapter 6 CONCLUSIONS AND FUTURE SCOPE

6.1 Conclusions

The SCT operates without fill because of salt decomposition on the fill leads to deteriorate conventional cooling tower performance. The maintenance of SCT is also easy in comparison to the conventional cooling tower because it not uses fill. This study presents 2-D MATLAB and 3-D CFD models for energy and exergy analysis of mono and multi-diameter water droplets and air interaction along with the height of the forced draft parallel and counter flow SCT, to predict the exit condition of the water droplet and air for industrial application and air cooling application. In multi droplet diameters 2-D and 3-D models at the inlet of the tower, ten different diameters of water droplets simultaneously used at a given time for analysis and the distribution of the droplet diameter based on Rosin Rammler distribution. The exergy analysis of water droplet and air are considered to better understand the system. The eight types of each industrial and air cooling application cases were studied; their exit parameter results were compared and plotted. The parallel and counter flow multi droplet 3-D CFD model predicted more accurate results in compared to 2-D mono and multi droplet model and 3-D mono droplet model because 3-D CFD model represents least error in the validation test as shown in the figures 5.1 - 5.4.

6.1.1 The Major Finding of Industrial Application SCT

The major findings of SCT for industrial application:

(i) With increase in the inlet water droplet diameter in the SCT, exit water droplet temperature and SLE increase, and thermal efficiency of SCT decreases. Among all the SCT modelling, multi droplet model gives the maximum thermal efficiency and minimum exit water droplet temperature. The counter flow multi droplet SCT model is found to be 2 ˚C lower exit water droplet temperature and 10% higher thermal efficiency than the parallel flow SCT modelling.

(ii) The exit water droplet temperature and thermal efficiency of SCT increase with increase in the inlet air DBT (24 - 48 ˚C). The minimum exit water temperature is obtained by the counter flow multi droplet model compared to mono droplet model in all cases of SCT modelling.

(iii) As inlet air relative humidity increases (20 - 80%), the outlet water droplet temperature and thermal efficiency increase. In these cases again, the minimum exit water temperature and maximum thermal efficiency is given by counter flow multi droplet SCT model compared to parallel flow multi droplet SCT model.

(iv) With increase in the inlet RLG (0.5 - 2.0), the outlet water droplet temperature increases and thermal efficiency of SCT decreases. The minimum exit water temperature (37.83 ˚C) and the highest thermal efficiency (72.42%) were obtained by counter flow multi droplet SCT models.

(v) The SLE increases with increase in the inlet droplet diameter, air DBT and RLG in 2-D and 3-D, mono and multi droplet SCT. The tower SLE decreases with increase in the inlet water temperature and air relative humidity.

(vi) The total exergy of the system is controlled by exergy of water and air, but exergy of water is the main component present in the total exergy of the system.

(vii) The total exergy destruction of the system decreases with increase the inlet droplet diameter, air DBT and air relative humidity in 2-D and 3-D mono and multi droplet SCT. The tower exergy destruction increases with increase in the inlet water temperature and RLG.

(viii) The parameters of air and water become asymptotic up to 0.5 m height of the SCT so the optimum height of tower should be 0.5 m for same operating conditions. Thus, by reducing tower height investment cost can also be reduced.

6.1.2 The Major Finding of Air Cooling Application SCT

The major findings of SCT for air cooling application:

(i) The exit air specific humidity and thermal efficiency of SCT decrease with increase in the inlet water droplet diameter. The maximum thermal efficiency (65.66%) is achieved by counter flow multi droplet SCT models.

(ii) The outlet air DBT and SLE of tower increase with the increasing water droplet diameter. The minimum air DBT achieved in counter flow multi droplet SCT models was 26.42 ˚C.

(iii) With increase in the inlet water temperature (28 - 36 ˚C), the exit air DBT and specific humidity increase. The minimum air DBT (24.13 ˚C) was achieved by counter flow multi droplet SCT models. The maximum thermal efficiency

with varying in inlet water temperature for counter flow multi droplet model was 69.78%.

(iv) With increase in the inlet air DBT (36 - 44 ˚C), the exit air DBT and air specific humidity increases. Among all the cases of SCT modelling, the minimum outlet air DBT (25.02 ˚C) and the highest thermal efficiency (69.41%) were achieved in counter flow multi droplet models.

(v) With increase in the inlet air relative humidity (20 - 40%), the exit air specific humidity and air DBT increases. The minimum exit air DBT (26.42 ˚C) and maximum thermal efficiency (80.34%) were again achieved by counter flow multi droplet models compared to mono and parallel flow SCT models.

(vi) With increase in the inlet RLG (0.5 - 1.5), the exit air DBT and specific humidity increased, and thermal efficiency of SCT tower decreased. The lowest outlet air DBT (26.42 ˚C) and highest thermal efficiency (65.66%) were given by counter flow multi droplet models.

(vii) As the inlet droplet diameter, air DBT and RLG increased in 2-D and 3-D mono and multi droplet SCT the SLE of the tower also increased, and the SLE of tower decreased with increases the inlet water temperature and air relative humidity.

(viii) The air and water exergy variation have also been studied to explain the functioning of SCT. The total exergy of air controlled by its convective and evaporative exergy, and evaporative exergy of air is the main component present in the total exergy of air.

(ix) The 2-D and 3-D mono and multi droplet SCT exergy destruction increases with increase in the inlet water temperature and RLG and its exergy destruction of the system decreases with increase the inlet droplet diameter and air DBT.

(x) All the parameters of air and water become asymptotic up to 0.5 m SCT height so the best possible height of the SCT should be 0.5 m for the same operating conditions. Thus, initial and maintenance cost of SCT can be reduced by reducing the tower height.

6.2 Future Scope

The research indicates that there is considerable scope for further experimental and modelling work.

(i) The model is highly sensitive to multi droplet distribution. Future effort should be directed to analyse more categories of water droplet distribution, i.e. 25, 50 and 100 categories of droplets to predict the air and water exit conditions.

(ii) Different types of nozzles configuration can be used for study mono and multi droplet SCT.

REFERENCES

[1] Muangnoi, T., Asvapoositkul, W., & Hungspreugs, P. (2014). Performance characteristics of a downward spray water-jet cooling tower. *Applied Thermal Engineering*, *69*(1), 165-176.

[2] Terblanche, R., Reuter, H. C. R., & Kröger, D. G. (2009). Drop size distribution below different wet-cooling tower fills. *Applied Thermal Engineering*, *29*(8), 1552-1560.

[3] Nuyttens, D., Baetens, K., De Schampheleire, M., & Sonck, B. (2007). Effect of nozzle type, size and pressure on spray droplet characteristics. *Biosystems Engineering*, *97*(3), 333-345.

[4] Santangelo, P. E. (2010). Characterization of high-pressure water-mist sprays: Experimental analysis of droplet size and dispersion. *Experimental Thermal and Fluid Science*, *34*(8), 1353-1366.

[5] Santangelo, P. E., Ren, N., Tartarini, P., & Marshall, A. W. (2008). Spray characterization of high pressure water mist injectors: experimental and theoretical analysis. In *22nd European Conference on Liquid Atomization and Spray Systems-ILASS* (Vol. 2008).

[6] Santangelo, P. E., Tartarini, P., Pulvirenti, B., & Valdiserri, P. (2009). Discharge and dispersion in water-mist sprays: experimental and numerical analysis. In *11th triennial international conference on liquid atomization and spray systems-ICLASS* (Vol. 2009).

[7] Azzopardi, B. J. (1979). Measurement of drop sizes. *International Journal of Heat and Mass Transfer*, *22*(9), 1245-1279.

[8] Simmons, M. J., & Hanratty, T. J. (2001). Droplet size measurements in horizontal annular gas–liquid flow. *International journal of multiphase flow*, *27*(5), 861-883.

[9] Naphon, P. (2005). Study on the heat transfer characteristics of an evaporative cooling tower. *International communications in heat and mass transfer*, *32*(8), 1066-1074.

[10] Elsarrag, E. (2006). Experimental study and predictions of an induced draft ceramic tile packing cooling tower. *Energy Conversion and Management*, *47*(15), 2034-2043.

[11] Lemouari, M., Boumaza, M., & Kaabi, A. (2009). Experimental analysis of heat and mass transfer phenomena in a direct contact evaporative cooling tower. Energy conversion and management, 50(6), 1610-1617.

[12] Klimanek, A., & Białecki, R. A. (2009). Solution of heat and mass transfer in counter flow wet-cooling tower fills. International Communications in Heat and Mass Transfer, 36(6), 547-553.

[13] Qi, X., Liu, Z., & Li, D. (2007). Performance characteristics of a shower cooling tower. *Energy conversion and management*, *48*(1), 193-203.

[14] Qi, X., Liu, Z., & Li, D. (2008). Prediction of the performance of a shower cooling tower based on projection pursuit regression. *Applied Thermal Engineering*, *28*(8), 1031-1038.

[15] Yajima, S., & Givoni, B. (1997). Experimental performance of the shower cooling tower in Japan. *Renewable Energy*, *10*(2-3), 179-183.

[16] Givoni, B. (1997). Performance of the "shower" cooling tower in different climates. *Renewable energy*, *10*(2-3), 173-178.

[17] Pearlmutter, D., Erell, E., Etzion, Y., Meir, I. A., & Di, H. (1996). Refining the use of evaporation in an experimental down-draft cool tower. *Energy and buildings*, *23*(3), 191-197.

[18] Farnham, C., Nakao, M., Nishioka, M., Nabeshima, M., & Mizuno, T. (2011). Study of mist-cooling for semi-enclosed spaces in Osaka, Japan. *Procedia Environmental Sciences*, *4*, 228-238.

[19] Kachhwaha, S. S., Dhar, P. L., & Kale, S. R. (1998). Experimental studies and numerical simulation of evaporative cooling of air with a water spray—I. Horizontal parallel flow. *International Journal of Heat and Mass Transfer*, *41*(2), 447-464.

[20] Sureshkumar, R., Kale, S. R., & Dhar, P. L. (2008). Heat and mass transfer processes between a water spray and ambient air–I. Experimental data. *Applied Thermal Engineering*, *28*(5), 349-360.

[21] Sureshkumar, R., Dhar, P. L., & Kale, S. R. (2007). Effects of spray modeling on heat and mass transfer in air–water spray systems in parallel flow. *International communications in heat and mass transfer*, *34*(7), 878-886.

[22] Qureshi, B. A., & Zubair, S. M. (2006). A complete model of wet cooling towers with fouling in fills. *Applied Thermal Engineering*, *26*(16), 1982-1989.

[23] Cui, H., Li, N., Peng, J., Cheng, J., & Li, S. (2016). Study on the dynamic and thermal performances of a reversibly used cooling tower with upward spraying. *Energy*, *96*, 268-277.

[24] Bejan, A. (2006). Advanced Engineering Thermodynamic, *3 ed. John Wiley and Sons*, 204-224.

[25] Sirok, B., Blagojevic, B., Novak, M., Hocevar, M., & Jere, F. (2003). Energy and mass transfer phenomena in natural draft cooling towers. *Heat transfer engineering*, *24*(3), 66-75.

[26] Rotar, M., Širok, B., Drobnič, B., Novak, M., & Donevski, B. (2005). A numerical analysis of the local anomalies in a natural-draft cooling tower. *Heat transfer engineering*, *26*(9), 61-72.

[27] Blain, N., Belaud, A., & Miolane, M. (2016). Development and validation of a CFD model for numerical simulation of a large natural draft wet cooling tower. *Applied Thermal Engineering*, *105*, 953-960.

[28] Ma, H., Si, F., Kong, Y., Zhu, K., & Yan, W. (2015). A new theoretical method for predicating the part-load performance of natural draft dry cooling towers. *Applied Thermal Engineering*, *91*, 1106-1115.

[29] Nasrabadi, M., & Finn, D. P. (2014). Mathematical modeling of a low temperature low approach direct cooling tower for the provision of high temperature chilled water for conditioning of building spaces. *Applied Thermal Engineering*, *64*(1), 273-282.

[30] Sirena, J. A. (2013). Electrical-fluid dynamic performance of mechanical draft water cooling towers. *Applied Thermal Engineering*, *54*(1), 185-189.

[31] Jiang, J. J., Liu, X. H., & Jiang, Y. (2013). Experimental and numerical analysis of a cross-flow closed wet cooling tower. *Applied Thermal Engineering*, *61*(2), 678-689.

[32] Asvapoositkul, W., & Treeutok, S. (2012). A simplified method on thermal performance capacity evaluation of counter flow cooling tower. *Applied Thermal Engineering*, *38*, 160-167.

[33] Keshtkar, M. M. (2017). Performance analysis of a counter flow wet cooling tower and selection of optimum operative condition by MCDM-TOPSIS method. *Applied Thermal Engineering*, *114*, 776-784.

[34] Yang, X. L., Sun, F. Z., Kai, W. A. N. G., Shi, Y. T., & Wang, N. H. (2007). Numerical Simulation of Flow Fields in A Natural Draft Wet-Cooling Tower** Project supported by the Natural Science Foundation of Shandong Province (Grant No. Z2003F03). *Journal of Hydrodynamics, Ser. B*, *19*(6), 762-768.

[35] Singh, K., & Das, R. (2017). An improved constrained inverse optimization method for mechanical draft cooling towers. *Applied Thermal Engineering*, *114*, 573-582.

[36] Babinsky, E., & Sojka, P. E. (2002). Modeling drop size distributions. *Progress in energy and combustion science*, *28*(4), 303-329.

[37] Rosin, P. A. U. L. (1933). The laws governing the fineness of powdered coal. *J. Inst. Fuel.*, *7*, 29-36.

[38] Gonzalez-Tello, P., Camacho, F., Vicaria, J. M., & Gonzalez, P. A. (2008). A modified Nukiyama–Tanasawa distribution function and a Rosin–Rammler model for the particle-size-distribution analysis. *Powder Technology*, *186*(3), 278-281.

[39] Lefebvre, A.H. (1989). Atomization and Sprays Hemisphere Publishing Corporation, *New York*.

[40] Masters, K. (1991). Spray Drying Handbook, 5th ed., Longman Scientific and Technical, UK.

[41] Zunaid, M., Murtaza, M., & Kachhwaha, S.S. (2011). Performance analysis of down

draft parallel flow shower cooling tower, *Proceedings of the 21st National & 10th ISHMT-ASME Heat and Mass Transfer Conference,* IIT Madras, India, (2011).

[42] Zunaid, M., Murtaza, M., & Kachhwaha, S.S. (2013a). Theoretical study of a humidification-dehumidification desalination process using down draft parallel flow shower cooling tower, Indian Society For Technical Education (ISTE) Delhi Section Convention on "Technological Universities and Institutions in New Knowledge Age: *Future Perspectives and Action Plan, 5-6 September,* DTU, Delhi, India.

[43] Zunaid, M., Murtaza, M., & Kachhwaha, S.S. (2013b). Analysis of air and water spray interaction in downdraft parallel flow shower cooling tower, *Proceedings of the 22th National and 11th International ISHMT-ASME Heat and Mass Transfer Conference,* IIT Kharagpur, India.

[44] Zunaid, M., Murtaza, M., & Kachhwaha, S.S. (2013c). Exergy and performance analysis of parallel flow shower cooling tower, *International Conference Smart Technologies for Mechanical Engineering, 25-26 October,* DTU, Delhi, India.

[45] Murtaza, Q., Stokes, J., & Ardhaoui, M. (2012). Computational fluid dynamics analysis of the production of bio-thermal spray hydroxyapatite powders. *International Journal of Computational Materials Science and Surface Engineering*, *5*(1), 31-54.

[46] Fisenko, S. P., Petruchik, A. I., & Solodukhin, A. D. (2002). Evaporative cooling of water in a natural draft cooling tower. *International Journal of Heat and Mass Transfer*, *45*(23), 4683-4694.

[47] Muangnoi, T., Asvapoositkul, W., & Wongwises, S. (2007). An exergy analysis on the of a counter flow wet cooling tower. *applied thermal engineering*, *27*(5), 910-917.

[48] Qureshi, B. A., & Zubair, S. M. (2004). A comprehensive design and performance evaluation study of counter flow wet cooling towers. *International Journal of Refrigeration*, *27*(8), 914-923.

[49] Qureshi, B. A., & Zubair, S. M. (2003). Application of exergy analysis to various psychrometric processes. *International Journal of Energy Research*, *27*(12), 1079-1094.

[50] Gharagheizi, F., Hayati, R., & Fatemi, S. (2007). Experimental study on the performance of mechanical cooling tower with two types of film packing. *Energy conversion and management*, *48*(1), 277-280.

[51] Muangnoi, T., Asvapoositkul, W., & Wongwises, S. (2008). Effects of inlet relative humidity and inlet temperature on the performance of counter flow wet cooling tower based on exergy analysis. *Energy Conversion and Management*, *49*(10), 2795-2800.

[52] Osterle, F. (1991). On the analysis of counter-flow cooling towers. *International Journal of Heat and Mass Transfer*, *34*(4-5), 1313-1316.

[53] Fisenko, S. P., Brin, A. A., & Petruchik, A. I. (2004). Evaporative cooling of water in a mechanical draft cooling tower. *International Journal of Heat and Mass Transfer*, *47*(1), 165-177.

[54] Wang, W., Zhang, H., Liu, P., Li, Z., Lv, J., & Ni, W. (2017). The cooling performance of a natural draft dry cooling tower under crosswind and an enclosure approach to cooling efficiency enhancement. *Applied Energy*, *186*, 336-346.

[55] Reuter, H. C. R., & Kröger, D. G. (2011). Computational fluid dynamics analysis of cooling tower inlets. *Journal of Fluids Engineering*, *133*(8), 081104.

[56] Gan, G., Riffat, S. B., Shao, L., & Doherty, P. (2001). Application of CFD to closed-wet cooling towers. *Applied Thermal Engineering*, *21*(1), 79-92.

[57] Al-Waked, R., & Behnia, M. (2006). CFD simulation of wet cooling towers. *Applied Thermal Engineering*, *26*(4), 382-395.

[58] Williamson, N., Behnia, M., & Armfield, S. (2008). Comparison of a 2D axisymmetric CFD model of a natural draft wet cooling tower and a 1D model. *International journal of heat and mass transfer*, *51*(9), 2227-2236.

[59] Rubio-Castro, E., Serna-González, M., Ponce-Ortega, J. M., & Morales-Cabrera, M. A. (2011). Optimization of mechanical draft counter flow wet-cooling towers using a rigorous model. *Applied Thermal Engineering*, *31*(16), 3615-3628.

[60] Yoon, S. S., & Heister, S. D. (2004). A fully non-linear model for atomization of high-speed jets. *Engineering analysis with boundary elements*, *28*(4), 345-357.

[61] Halasz, B. (1999). Application of a general non-dimensional mathematical model to cooling towers. *International journal of thermal sciences*, *38*(1), 75-88.

[62] Stabat, P., & Marchio, D. (2004). Simplified model for indirect-contact evaporative cooling-tower behaviour. *Applied Energy*, *78*(4), 433-451.

[63] Qi, X., & Liu, Z. (2008a). Further investigation on the performance of a shower cooling tower. *Energy Conversion and Management*, *49*(4), 570-577.

[64] Qi, X., Liu, Z., & Li, D. (2008b). Numerical simulation of shower cooling tower based on artificial neural network. *Energy Conversion and Management*, *49*(4), 724-732.

[65] Kang, D., & Strand, R. K. (2013). Modeling of simultaneous heat and mass transfer within passive down-draft evaporative cooling (PDEC) towers with spray in FLUENT. *Energy and Buildings*, *62*, 196-209.

[66] Tan, K., & Deng, S. (2002). A method for evaluating the heat and mass transfer characteristics in a reversibly used water cooling tower (RUWCT) for heat recovery. *International Journal of Refrigeration*, *25*(5), 552-561.

[67] Tan, K., & Deng, S. (2003). A numerical analysis of heat and mass transfer inside a reversibly used water cooling tower. *Building and Environment*, *38*(1), 91-97.

[68] Zhang, Q., Wu, J., Zhang, G., Zhou, J., Guo, Y., & Shen, W. (2012). Calculations on performance characteristics of counter flow reversibly used cooling towers. *International journal of refrigeration*, *35*(2), 424-433.

[69] Rahmati, M., Alavi, S. R., & Tavakoli, M. R. (2016). Experimental investigation on performance enhancement of forced draft wet cooling towers with special emphasis on the role of stage numbers. *Energy Conversion and Management*, *126*, 971-981.

[70] Zamora, B., Kaisere, A. S., Kling, U., Lucas, M., & Ruíz, J. (2011). Uncertainty analysis in the numerical simulation of the air-water droplet motion through drift eliminators. *Journal of Fluids Engineering*, *133*(9), 094501.

[71] Milosavljevic, N., & Heikkilä, P. (2001). A comprehensive approach to cooling tower design. *Applied Thermal Engineering*, *21*(9), 899-915.

[72] Ardekani, M. A., Farhani, F., Mazidi, M., & Ranjbar, M. A. (2014). Study of degradation of dry cooling tower performance under wind conditions and method for tower efficiency enhancement (research note). *International Journal of Engineering-*

Transactions C: Aspects, *28*(3), 460.

[73] Kumar, N., & Pant, A. (2008). A computational approach to the flow of walter's liquid b′ through annulus of coaxial porous circular cylinders for high suction parameter (research note). *International Journal of Engineering-Transactions A: Basics*, *22*(2), 119.

[74] Heidarinejad, G., & Delfani, S. (2000). Direct numerical simulation of the wake flow behind a cylinder using random vortex method in medium to high Reynolds numbers. *International Journal of Engineering*, *13*(3), 33-50.

[75] Reuter, H. C. R. (2010). *Performance evaluation of natural draught cooling towers with anisotropic fills* (Doctoral dissertation, Stellenbosch: University of Stellenbosch).

[76] Viljoen, D. J. (2006). *Evaluation and performance prediction of cooling tower spray zones* (Doctoral dissertation, Stellenbosch: University of Stellenbosch).

[77] Williamson, N. J. (2008). Numerical modelling of heat and mass transfer and optimisation of a natural draft wet cooling tower (Doctoral dissertation, The school of Aerospace, Mechanical and Mechatronic Engineering: The University of Sydney).

[78] Hawlader, M. N. A., & Liu, B. M. (2002). Numerical study of the thermal–hydraulic performance of evaporative natural draft cooling towers. *Applied Thermal Engineering*, *22*(1), 41-59.

[79] Kasaeian, A. B., Mobarakeh, M. D., Golzari, S., & Akhlaghi, M. M. (2013). Energy and exergy analysis of air PV/T collector of forced convection with and without glass cover. *International Journal of Engineering-Transactions B: Applications*, *26*(8), 913.

[80] Kairouani, L., Hassairi, M., & Tarek, Z. (2004). Performance of cooling tower in south of Tunisia. *Building and environment*, *39*(3), 351-355.

[81] Qureshi, B. A., & Zubair, S. M. (2007). Second-law-based performance evaluation of cooling towers and evaporative heat exchangers. *International Journal of Thermal Sciences*, *46*(2), 188-198.

[82] Gharagheizi, F., Hayati, R., & Fatemi, S. (2007). Experimental study on the performance of mechanical cooling tower with two types of film packing. *Energy conversion and management*, *48*(1), 277-280.

[83] Hajidavalloo, E., Shakeri, R., & Mehrabian, M. A. (2010). Thermal performance of cross flow cooling towers in variable wet bulb temperature. *Energy Conversion and Management*, *51*(6), 1298-1303.

[84] Kloppers, J. C., & Kröger, D. G. (2005). Refinement of the transfer characteristic correlation of wet-cooling tower fills. *Heat transfer engineering*, *26*(4), 035-041.

[85] Chen, Q., Yang, K., Wang, M., Pan, N., & Guo, Z. Y. (2010). A new approach to analysis and optimization of evaporative cooling system I: Theory. *Energy*, *35*(6), 2448-2454.

[86] Chen, Q., Pan, N., & Guo, Z. Y. (2011). A new approach to analysis and optimization of evaporative cooling system II: Applications. *Energy*, *36*(5), 2890-2898.

[87] Lemouari, M., & Boumaza, M. (2010). Experimental investigation of the performance characteristics of a counter flow wet cooling tower. *International Journal of Thermal Sciences*, *49*(10), 2049-2056.

[88] Lucas, M., Ruiz, J., Martínez, P. J., Kaiser, A. S., Viedma, A., & Zamora, B. (2013). Experimental study on the performance of a mechanical cooling tower fitted with different types of water distribution systems and drift eliminators. *Applied Thermal Engineering*, *50*(1), 282-292.

[89] Qi, X., Liu, Y., & Liu, Z. (2013). Exergy based performance analysis of a shower cooling tower. *Strojniški vestnik-Journal of Mechanical Engineering*, *59*(4), 251-259.

[90] Belarbi, R., Ghiaus, C., & Allard, F. (2006). Modeling of water spray evaporation: Application to passive cooling of buildings. *Solar energy*, *80*(12), 1540-1552.

[91] Pearlmutter, D., Erell, E., & Etzion, Y. (2008). A multi-stage down-draft evaporative cool tower for semi-enclosed spaces: Experiments with a water spraying system. *Solar energy*, *82*(5), 430-440.

[92] Erell, E., Pearlmutter, D., & Etzion, Y. (2008). A multi-stage down-draft evaporative cool tower for semi-enclosed spaces: aerodynamic performance. *Solar Energy*, *82*(5), 420-429.

[93] Carew, P. J. (2006). Shower Tower, Miele Showroom, Johannesburg South Africa.

23rd Conference on Passive and Low Energy Architecture, Geneva, Switzerland, 6-8 September 2006.

[94] Ataei, A., Panjeshahi, M. H., & Gharaie, M. (2008). Performance evaluation of counter-flow wet cooling towers using exergetic analysis. *Transactions of the Canadian Society for Mechanical Engineering*, *32*(3-4), 499-512.

[95] Santos, J. C., Barros, G. D. T., Gurgel, J. M., & Marcondes, F. (2013). Energy and exergy analysis applied to the evaporative cooling process in air washers. *International*

Journal of Refrigeration, *36*(3), 1154-1161.

[96] Saffari, H., & Hosseinnia, S. M. (2009). Two-phase Euler-Lagrange CFD simulation of evaporative cooling in a Wind Tower. *Energy and Buildings*, *41*(9), 991-1000.

[97] Kachhwaha, S. S. (1995). Some studies on spray type evaporative cooling process, (Doctoral dissertation, India Institute of Technology, Delhi).

[98] Kachhwaha, S. S., Dhar, P. L., & Kale, S. R. (1998). Experimental studies and numerical simulation of evaporative cooling of air with a water sprayII. Horizontal counter flow. *International journal of heat and mass transfer*, *41*(2), 465-474.

[99] Marmouch, H., Orfi, J., & Nasrallah, S. B. (2010). Experimental study of the performance of a cooling tower used in a solar distiller. *Desalination*, *250*(1), 456-458.

[100] Singh, K., & Das, R. (2017). Simultaneous optimization of performance parameters and energy consumption in induced draft cooling towers. *Chemical Engineering Research and Design*, *123*, 1-13.

[101] Merkel, F. (1925). *Verdunstungskühlung*. VDI-Verlag.

[102] Zivi, S. M., & Brand, B. B. (1956). An analysis of the crossflow cooling tower. *Refrigeration Engineering*, *64*(8), 31-34.

[103] Jaber, H., & Webb, R. L. (1989). Design of cooling towers by the effectiveness-NTU method. *ASME J. Heat Transfer*, *111*(4), 837-843.

[104] Poppe, M., & Rögener, H. (1991). Berechnung von rückkühlwerken. *VDI Wärmeatlas*, *pp. Mi*.

[105] Kroger, D. G., & Kloppers, J. C. (2005a). Cooling tower performance evaluation: markel, poppe, and e-NTU methods of analysis. *ASME Journal of Engineering for Gas Turbines and Power*, *127*, 1-7.

[106] Kloppers, J. C., & Kroger, D. G. (2005b). The Lewis factor and its influence on the performance prediction of wet-cooling towers. *International Journal of Thermal Sciences*, *44*(9), 879-884.

[107] Kloppers, J. C., & Kröger, D. G. (2005c). A critical investigation into the heat and mass transfer analysis of counter flow wet-cooling towers. *International journal of heat and mass transfer*, *48*(3), 765-777.

[108] Mohiuddin, A. K. M., & Kant, K. (1996a). Knowledge base for the systematic design of wet cooling towers. Part I: Selection and tower characteristics. *International Journal of Refrigeration*, *19*(1), 43-51.

[109] Mohiuddin, A. K. M., & Kant, K. (1996b). Knowledge base for the systematic design of wet cooling towers. Part II: Fill and other design parameters. *International journal of refrigeration*, *19*(1), 52-60.

[110] Naik, B. K., Choudhary, V., Muthukumar, P., & Somayaji, C. (2017). Performance Assessment of a Counterflow Cooling Tower–Unique Approach. *Energy Procedia*, *109*, 243-252.

[111] Lucas, M., Martínez, P. J., & Viedma, A. (2009). Experimental study on the thermal performance of a mechanical cooling tower with different drift eliminators. *Energy Conversion and Management*, *50*(3), 490-497.

[112] Zubair, S. M. (2001). An improved design and rating analyses of counter flow wet

cooling towers. *Journal of Heat transfer*, *123*(4), 770-778.

[113] Khan, J. R., Yaqub, M., & Zubair, S. M. (2003). Performance characteristics of counter flow wet cooling towers. *energy conversion and management*, *44*(13), 2073-2091.

[114] Ghazani, M. A., Hashem-ol-Hosseini, A., & Emami, M. D. (2017). A comprehensive analysis of a laboratory scale counter flow wet cooling tower using the first and the second laws of thermodynamics. *Applied Thermal Engineering*, *125*, 1389-1401.

[115] Smrekar, J., Oman, J., & Širok, B. (2006). Improving the efficiency of natural draft cooling towers. *Energy Conversion and Management*, *47*(9), 1086-1100.

[116] Wang, L., & Li, N. (2011). Exergy transfer and parametric study of counter flow wet cooling towers. *applied thermal engineering*, *31*(5), 954-960.

[117] Ramkumar, R., & Ragupathy, A. (2011). Performance analysis of counter flow wet cooling tower. *International Journal of Air-Conditioning and Refrigeration*, *19*(02), 141-148.

[118] Qi, X., Liu, Y., Guo, Q., Yu, S., & Yu, J. (2016). Performance prediction of a shower cooling tower using wavelet neural network. *Applied Thermal Engineering*, *108*, 475-485.

[119] Cui, H., Li, N., Peng, J., Cheng, J., & Li, S. (2016). Study on the dynamic and thermal performances of a reversibly used cooling tower with upward spraying. *Energy*, *96*, 268-277.

[120] Mansour, M. K., & Hassab, M. A. (2014). Innovative correlation for calculating thermal performance of counter flow wet-cooling tower. *Energy*, *74*, 855-862.

[121] Al-Bassam, E., & Maheshwari, G. P. (2011). A new scheme for cooling tower water conservation in arid-zone countries. *Energy*, *36*(7), 3985-3991.

[122] Goudarzi, M. A. (2013). Proposing a new technique to enhance thermal performance and reduce structural design wind loads for natural drought cooling towers. *Energy*, *62*, 164-172.

[123] Lemouari, M., Boumaza, M., & Kaabi, A. (2011). Experimental investigation of the hydraulic characteristics of a counter flow wet cooling tower. *Energy*, *36*(10), 5815-5823.

[124] Asvapoositkul, W., & Kuansathan, M. (2014). Comparative evaluation of hybrid (dry/wet) cooling tower performance. *Applied Thermal Engineering*, *71*(1), 83-93.

[125] Jiang, J. J., Liu, X. H., & Jiang, Y. (2013). Experimental and numerical analysis of a cross-flow closed wet cooling tower. *Applied Thermal Engineering*, *61*(2), 678-689.

[126] Nasrabadi, M., & Finn, D. P. (2014). Performance analysis of a low approach low temperature direct cooling tower for high-temperature building cooling systems. Energy and Buildings, 84, 674-689.

[127] Hernandez-Calderon, O. M., Rubio-Castro, E., & Rios-Iribe, E. Y. (2014). Solving the heat and mass transfer equations for an evaporative cooling tower through an orthogonal collocation method. Computers & Chemical Engineering, 71, 24-38.

[128] Gao, M., Sun, F. Z., & Turan, A. (2014). Experimental study regarding the evolution of temperature profiles inside wet cooling tower under crosswind conditions. International Journal of Thermal Sciences, 86, 284-291.

[129] Zheng, W. Y., Zhu, D. S., Zhou, G. Y., Wu, J. F., & Shi, Y. Y. (2012). Thermal performance analysis of closed wet cooling towers under both unsaturated and supersaturated conditions. International journal of heat and mass transfer, 55(25), 7803-7811.

[130] Li, X., Xia, L., Gurgenci, H., & Guan, Z. (2017). Performance enhancement for the natural draft dry cooling tower under crosswind condition by optimizing the water distribution. *International Journal of Heat and Mass Transfer*, *107*, 271-280.

[131] Halasz, B. (1999). Application of a general non-dimensional mathematical model to cooling towers. *International journal of thermal sciences*, *38*(1), 75-88.

[132] Facao, J., & Oliveira, A. (2004). Heat and mass transfer correlations for the design of small indirect contact cooling towers. *Applied thermal engineering*, *24*(14), 1969-1978.

APPENDIX-A

Matlab code of 2-D mono droplet parallel flow SCT

```
%~~~~~~~~~~~~~~~~~~~~~~~~~~~~~~~~~~~~~~~~~~~~~~~~~~~~~~~~~~~~~~~~~~~~~~~~~~~~~~~~%
%File name: Downward parallel flow mono droplet SCT used for industrial application
%All units in SI
%~~~~~~~~~~~~~~~~~~~~~~~~~~~~~~~~~~~~~~~~~~~~~~~~~~~~~~~~~~~~~~~~~~~~~~~~~~~~~~~~%
input 'Starting phase I'
Dci=0.61; %Inlet dia. of cross section of SCT in meter
Dco=0.61; %Outlet dia. of cross section of SCT in meter
height=1.25; %Height of SCT in meter
L=height;
div=100; %Number of divisions over SCT height
 Tai=36+273.15;
Tdi=56+273.15;
Rhi=65; %Initial percentage relative humidity at inlet of SCT
Tambient=Tai;
AmbHum = Rhi;
 Di=250e-6;% initial dia. of water droplet in meter
Ui=10; %Magnitude of inlet droplet velocity in m/s
 Q=-400; %inlet air volume flow rate in m^3/hr, (1 cfm = 1.699 m3/h)
RLG=0.5; %Ratio of mdi/mai (water to air mass flow ratio, kg/kg) may be equal to [0.5, 1, 1.5, 2]
 Phi=45;  %Angle of projection of water droplet with horizontal in degrees
x=0.00; %Starting x co-ordinate of spray
 g=9.81; %Acceleration due to gravity (m/sec2)
  [fid,message] = fopen('Result.xls','w+');
fprintf(fid,'---------INITIAL INPUTS----------\n');
fprintf(fid,'Inlet dia of cross section of cooling tower (m), Dci = %6.6f\n',Dci);
fprintf(fid,'Outlet dia. of cross section of cooling tower (m), Dco = %6.6f\n',Dco);
fprintf(fid,'Height of draft in (m), height = %6.6f\n',height);
fprintf(fid,'Number of divisions over height, div = %6.6f\n',div);
fprintf(fid,'Droplet Dia to take into considderation (m), Di = %6.6f\n',Di);
fprintf(fid,'Ratio of mdi/ma, RLG = %6.6f\n',RLG);
fprintf(fid,'Inlet DBT of Air (C), Tai = %6.6f\n',Tai-273.15);
fprintf(fid,'Relative humidity at inlet in percentage, Rhi = %6.6f\n',Rhi);
```

```
fprintf(fid,'Inlet temp. of water in Kelvin, Tdi = %6.6f\n',Tdi-273.15);
fprintf(fid,'Magnitude of droplet velocity (m/s), U = %6.6f\n',Ui);
fprintf(fid,'Angle of projection of water droplet with horizontal (degrees), Phi = %6.6f\n',Phi);
fprintf(fid,'Starting x co-ordinate of spray, x = %6.6f\n',x);
fprintf(fid,'Inlet air supply rate in (m^3/hr), Q = %6.6f\n',Q);
fprintf(fid,'Acceleration due to gravity(m/sec2), g = %6.6f\n',g);
fclose(fid);

global  A Approach Approach_arr As AmbHum CC CC_arr Cd_v Const...
    CTE CTE_arr dD_max dsi ds dTa_max dTd_max dTwb_max...
    dmawp dmawp_arr Di D Dc Dci Dco dNdt div g...
    h havi hav hs hss hfg hfg0 hdi hd...
    height hm H Hai Hdi HTin HcngP_arr i k L Lef Lefs...
    mai ma md_arr mdi md Md md_loss md_loss_arr MTin mu ...
    Nusselt prand Pw Q Range Range_arr Rhi Rh dRh_max...
    Rho_ai Rho_a Re_v sn1 sn2 sn3 sn4 tmi tei Tambient...
    Tai Ta Ta_arr Tdi Td Twbi Twb ...
    ui u U Ux Uy v W Wds Wai Wa Wa0 Wsai Wsa ...
    Xd Xd_arr Xa_cond Xa_evap Xair zxc

sn1=0; %for generate the serial number.
sn2=0; %for generate the serial number.
sn3=0; %for generate the serial number.
i=0;
zxc=0;
 Ta=Tai;
Td=Tdi;
 %Calculate Initial Parameter Values to be given to SCT system
 Pw=Rho_w(Tdi); %Density of water in Kg/m3
THETA=Phi.*(pi./180); %Calculate angles in Radian.
Uxi=Ui.*cos(THETA) %Inlet horizontal component of Droplet velocity in m/s
Uyi=Ui.*sin(THETA)  %Inlet vertical component of Droplet velocity in m/s
Wsai = Wsair(Tai) %specific humidity of saturated air
Wai=(Rhi./100).*Wsai %Input specific Humidity of air in Kg/Kg of dry air
Wa0= (AmbHum./100).*Wsair(Tambient)
```

```
Rho_ai = Pa(Tai,Wai) %Density of air in Kg/m3
Ai=((pi./4).*Dci.^2) %Initial area of cross-section of cooling tower in m2
ui=Q./(Ai.*3600) %Initial air velocity at inlet in m/s
Const=Rho_ai.*Ai.*ui %mass flow rate of air in kg/s
Twbi = wbt(Tai,Wai)
mai=(Q./3600).*Rho_ai %Mass flow rate of moist air at inlet in Kg/s
ma=mai./(1+Wai) %mass of dry air
mdi=RLG.*mai  %Mass flow rate of water in Kg/s at inlet
 smawi=mai+mdi %Sum of mass flow rate of air and water at inlet of the SCT in Kg/s.
dNdt=(mdi.*6)./(Pw.*pi.*(Di.^3)) %Inlet total no. of droplets flow per second in SCT
hfg0=Hfgd(273.16) %Latent heat of water at 273.15 K in J/Kg.
W=((Uyi-ui).^2+Uxi.^2).^.5 %Relative velocity of droplet w.r.t. air in m/s
hai=Cpa(Tai).*(Tai) %specific enthalpy of dry air in moist air
hvi=Cpv(Tdi).*(Tdi)+hfg0 %specific enthalpy of water vapour in moist air
havi=hai+Wai.*hvi  %Inlet enthalpy of air vapor mixture
hdi=Cpd(Tdi).*(Tdi) %Inlet enthalpy of drop per Kg of water
MTin=ma.*(1+Wai)+mdi
Hai=ma.*havi %Air enthalpy at inlet
Hdi=mdi.*hdi %Water enthalpy at inlet
HTin=Hai+Hdi %Total enthalpy of air and water at inlet
H=height/(div-1)  %Calculate dy
t1=[Wai Wsai Rhi mai  mdi mai+mdi havi hdi Hai Hdi ui dNdt]
t1=t1';%Transpose matrix of t.
 %Open file for write initial values of Mass and Energy balance quantities of SCT
fid = fopen('Result.xls','a+');
fprintf(fid,'\n ~~~~~Mass and Energy input to SCT~~~~~');
fprintf(fid,'\n Wai \t Wsai \t Rhi \t mai \t mdi \t mai+mdi \t havi \t hdi \t Hai \t Hdi \t ui \t dNdt');
fprintf(fid,'\n %6.f \t %6.f \t %6.f \t %6.f \t %6.f \t %6.f \t %6.f \t %6.f \t %6.f \t %6.f \t
%6.f \t %6.f',t1);
fclose(fid);
 %Open file for write output values of Mass and Energy balance quantities of SCT
fid = fopen('Result.xls','a+');
fprintf(fid,'\n \n ~~~~~~~Mass and Energy balance of SCT and
Result_Intermediate_Values_of_Function~~~~~~~~~\n');
fprintf(fid,'sn1 \t z \t Ta \t Twb \t Td \t Rh \t Wa \t Wsa \t Wds \t ma \t ma.*(1+Wa) \t md \t md_loss \t
madWa \t dmw \t dmaw \t dmawp \t hav \t hd \t Hao \t Hwo \t Hin \t Hout \t dHToutHTin \t HcngP \t u
```

```
\t Dc \t Rho_a \t Pw \t h \t hm \t hs \t hfg \t v \t k \t mu \t Cpa(Ta) \t Cpv(Ta) \t Cpv(Td) \t Cpd(Td) \t
Lef \t Re_v \t  prand \t Cd_v \t Nusselt \t Approach \t Range \t CTE \t CC');
fclose(fid);
 Wa=Wai; D=Di; Ux=Uxi; Uy=Uyi; hav=havi; Td=Tdi;
% Linking input Matrix
M=[Wa D Ux Uy hav Td x];
M=M'  %Conjugate column input matrix
 options= odeset('Abstol',1e-6,'RelTol',1e-6,'Refine',1,'InitialStep',...
    H,'Maxstep',height); %This function fix tolerance of output parameters.
 [Z,Y]=ode45(@SCTsystem,[0:H:height],M,options);
 function [dydt]=SCTsystem(z,y)
 Wa=y(1); %specific humidity of air
D=y(2);   %droplet diameter (it varies with height of C.V)
Ux=y(3); %Inlet horizontal component of droplet velocity in m/s
Uy=y(4); %Inlet vertical component of droplet velocity in m/s
hav=y(5); %enthalpy of air vapor mixture
Td=y(6);  %temp. of water droplet in kelvin
x=y(7);  %Horizontal distance with z
 zxc=zxc+1;
i=i+1;
 % Supplementary equations for Calculating values at instantaneous steps
 dTd_max = Tdi-Td;
 Twb = wbt(Ta,Wa);
dTwb_max = Twbi-Twb;
 dD_max = Di-D;
 Dc=(z./L).*(Dco-Dci)+Dci;
Lef = Le(Wdrop(Td),Wa);  %Lewis factor for droplet and air interaction
Wsa = Wsair(Ta) %specific humidity of saturated air
ds = Wa./Wsa; %degree of saturation
Rh=(ds./(1-(1-ds).*(Psv(Ta)./101325))).*100;  %Calculate stepwise Relative humidity of Air
dRh_max = Rhi-Rh%;
Wds=Wdrop(Td)%; %sp. humidity of air at drop surface
Pw=Rho_w(Td)%;  %Density of Water
hfg0 = Hfgd(273.16);  %Latent heat of water at 273.15 K
%hv0=hfg0;
hs=Hsd(Td);  %Matrix of enthalpy of air mixture at the surface of droplet
```

```
 Ta=(hav-Wa.*hfg0)./(Cpa(Ta)+ Wa.*Cpv(Td))%;
hd=Cpd(Td).*Td; %enthalpy of drop
Rho_a = Pa(Ta,Wa);  %Density of air
A=(pi./4).*Dc.^2;  %Area of cross-section of cooling tower
u=ui.*(Rho_ai./Rho_a).*((Dci./Dc)^2);
W=((Uy-u).^2+Ux.^2).^.5;  %Relative velocity of droplet with air
hfg = hfg0 + Cpv(Td).*Td;  %Calculate stepwise Latent heat of vaporization
 v = KinVisc(Ta,Wa);  %Kinematic viscosity
k = ThermCond(Ta,Wa);  %Thermal Conductivity
 mu = v.*Rho_a;  %Dynamic viscosity of air
 Re_v=Re(W,D,v);  %Reynolds number for droplet air interaction
prand=Pr(mu,Cpa(Ta),k);  %Evaluate Prandtl No
Cd_v= Cd(Re_v);  %coefficient of Drag for droplet air interaction
Nusselt=Nu(Re_v,prand);  % Nusselt number for droplet air interaction
 h=Hc(Nusselt,D,k);  %Heat transfer coefficient for droplet air interaction
hm=h./((Cpa(Ta)+Wa.*Cpv(Ta)).*Lef);  %mass transfer coefficient for droplet air interaction
Cpav=Cpa(Ta)+Wa.*Cpv(Ta);%Average specific heat for air
N=dNdt./A;%Inlet total no. of droplets per second per unit cross sectional area of sct
As=pi.*D.^2; %Surface area of droplet m2
md=(Pw.*pi.*dNdt.*(D.^3-Di.^3)./6)+mdi;   %Row matrix of instantaneous mass flow rate of water
md_loss=mdi-md;
Approach=Td-Twbi;
Range=Tdi-Td;
CTE=((Tdi-Td).*100)./(Tdi-Twbi);  %Cooling tower efficiency
CC=md.*Cpd(Td).*(Tdi-Td);%Cooling capacity
 Md=md./dNdt;
 %-----Equations for mass balance and energy balance
sn1;
MTout=ma.*(1+Wa)+md;
madWa=abs(ma.*(Wa-Wai)); %diff in mass flow rate of air vapour mixture in SCT in Kg/s.
dmw=abs(md-mdi); %diff in mass flow rate of water in SCT in Kg/s.
dmaw=abs((madWa)-(dmw)); %Mass balance (diff in mass flow rate of air and water) in SCT in Kg/s.
dmawp=abs(((dmaw).*100)./(madWa)); %diff in percentage in mass flow rate of air and water in SCT.
 Hao=ma.*hav; %Air enthalpy at outlet
Hwo=md.*hd; %Water enthalpy at inlet
```

```
HTout=Hao+Hwo; %Total enthalpy of air and water at outlet

dHToutHTin=HTout-HTin;

HcngP=((HTout-HTin).*100)./HTin;

sn1=sn1+1;%for increment of serial number.

t2=[sn1 z Ta-273.15 Twb-273.15 Td-273.15 Rh Wa Wsa Wds ma ma.*(1+Wa) md md_loss madWa
dmw dmaw dmawp hav hd Hao Hwo HTin HTout dHToutHTin HcngP u Dc Rho_a Pw h hm hs hfg v
k mu Cpa(Ta) Cpv(Ta) Cpv(Td) Cpd(Td) Lef Re_v prand Cd_v Nusselt Approach Range CTE CC];

t2=t2';

fid = fopen('Result.xls','a+');

fprintf(fid,'\n %d \t %6.4f \t %6.4f \t %6.4f \t %6.4f \t %6.4f \t %6.4f \t %6.4f \t %6.4f \t %6.4f
\t %6.4f \t %6.4f \t %6.4f \t %6.4f \t %6.4f \t %6.4f \t %6.4f \t %6.4f \t %6.4f \t %6.4f
\t %6.4f \t %6.4f \t %6.4f \t %6.4f \t %6.4f \t %6.4f \t %6.4f \t %6.4f \t %6.4f \t %6.4f
\t %6.4f \t %6.4f \t %6.4f \t %6.4f \t %6.4f \t %6.4f \t %6.4f \t %6.4f \t %6.4f \t %6.4f
\t %6.4f \t %6.4f',t2);

fclose(fid);

    dydt=[

%Conservation of mass for air, dWa/dy

     ((md./ma).*(hm.*As.*(Wdrop(Td)-Wa))./(Md.*Uy)%;

     %Conservation of mass for water droplet, dD/dy

     (-2.*hm.*(Wdrop(Td)-Wa)./(Uy.*Pw))%;

     %Conservation of momentum for water droplet in x direction, dUx/dy

     (-3.* W.*Ux.*Rho_a.*Cd(Re_v)./(4.*Pw.*D.*Uy))-((3.*Ux./D).*(-2.*hm.*(Wdrop(Td)-Wa)./...

     (Uy.*Pw)))%;

%Conservation of momentum for water droplet in y direction, dUy/dy

     ((g.*(Pw-Rho_a)-(3.*Cd(Re_v).*Rho_a.*W.*(Uy-u)./(4.*D))).*/...

     (Pw.*Uy))-(3.*Uy./D).*(-2.*hm.*(Wdrop(Td)-Wa)./(Uy.*Pw))%;

%Conservation of energy for air, dhav/dy

     ((md/ma).*(6.*hm./(Pw.*Uy.*D)).*(Lef.*(hs - hav)+(1-Lef)...

     .*hfg.*(Wdrop(Td)- Wa)))%;

%Conservation of energy for water droplet, dTd/dy

     (- 6.*hm.*( Lef.*(hs - hav) + (1-Lef).*hfg.*(Wdrop(Td)- Wa))./...

     (Cpd(Td).*Pw.*D.*Uy))-((3.*Td./D).*(-2.*hm.*(Wdrop(Td)-Wa)./(Uy.*Pw)))%;

%Trajectory equation, dx/dy

     (Ux./Uy)%;

     ];

end

Wa_arr=Y(:,1); %Array of sp. humidity of air.
```

```
D_arr=Y(:,2);  %Array of drop dia. of water
Ux_arr=Y(:,3);
Uy_arr=Y(:,4);
hav_arr=Y(:,5);
Td_arr=Y(:,6);
x_arr=Y(:,7);
 W_arr=((Uy_arr-ui).^2+(Ux_arr).^2).^.5; %Array of relative velocity of air.
U_abs=((Uy_arr).^2+(Ux_arr).^2).^.5;
 md_arr=(Pw.*pi.*dNdt.*(D_arr.^3-Di.^3)./6)+mdi;
 %---makeup water required (mwr)
md_loss_arr=(mdi-md_arr);
mwr = md_loss_arr;
 Approach_arr=Td_arr-Twbi;
Range_arr=Tdi-Td_arr;
CTE_arr=((Tdi-Td_arr).*100)./(Tdi-Twbi);  %Cooling tower efficiency
CC_arr=md.*Cpd(Td_arr).*(Tdi-Td_arr);%Cooling capacity
 Ta=(hav-Wa.*hfg0)./(Cpa(Ta)+ Wa.*Cpv(Td))%;
 Ta_arr=(hav_arr-Wa_arr.*hfg0)./(Cpa(Ta)+ Wa_arr.*Cpv(Td_arr))%;%Calcuate stepwise air temp.
 Twb_arr = wbt(Ta_arr,Wa_arr);
 ds_arr=(Wa_arr./ Wsair(Ta_arr)); %degree of saturation
%Calcuate stepwise Relative humidity of Air
 Rh_arr=(ds_arr./(1-(1-ds_arr).*(Psv(Ta_arr)./101325))).*100;
%---Mass balance
 MTout_arr = ma.*(1+Wa_arr)+md_arr;
dMToutMTin_arr = MTout_arr - MTin;
dmawp_arr = (abs(MTout_arr - MTin).*100)./MTin;
%----Energy balance of SCT
hd_arr=Cpd(Td_arr).*Td_arr;
Hao_arr=ma.*hav_arr; %Air enthalpy at outlet
Hwo_arr=md_arr.*hd_arr; %Water enthalpy at inlet
HTout_arr=Hao_arr+Hwo_arr; %Total enthalpy of air and water at outlet
dHToutHTin_arr=HTout_arr-HTin;
HcngP_arr=(abs(HTout_arr-HTin).*100)./HTin;
 %------Exergy of water
Xd_arr = (md_arr).*((hf(Td_arr)-hg(Tambient))...
```

```
   - (Tambient.*(sf(Td_arr)-sg(Tambient))) - (461.*Tambient.*log(AmbHum./100)))

% Conductive exergy of air

 Xa_cond_arr = (ma).*(Cpa(Ta_arr).*(Ta_arr-Tambient)-
Tambient.*Cpa(Ta_arr).*log(Ta_arr./Tambient)...

   + Wa.*(Cpv(Ta_arr).*(Ta_arr-Tambient)- (Tambient.*Cpv(Ta_arr)).*log(Ta_arr./Tambient)));

% Evaporative exergy of air

Xa_evap_arr= ma.*( 287.*Tambient.*log((1+1.608.*Wa0)./(1+1.608.*Wa_arr))+ Wa_arr.*...

   (461.*Tambient.*log(((1+1.608.*Wa0).*Wa_arr)./((1+1.608.*Wa_arr).*Wa0))  )  );

%Total Air Exergy

Xair_arr   =(Xa_cond_arr+ Xa_evap_arr);

 if(Xair_arr <0)

   Xair_arr = -1.* Xair_arr; % Total Air Exergy

end

 Xtotal_arr = (Xd_arr + Xair_arr); % Total Exergy of System

 Xdestruct=Idestruction(Xtotal_arr);

NII=Xtotal_arr(end).*100./Xtotal_arr(1);

XdestructP = ((Xtotal_arr(1) - Xtotal_arr(end)).*100)./Xtotal_arr(1); %Percentage reduction in exergy

 %--> Write values in file

t6=[Z Xd_arr Xa_cond_arr Xa_evap_arr Xair_arr Xtotal_arr Xdestruct Xd_arr_s Xa_cond_arr_s
Xa_evap_arr_s Xair_arr_s Xtotal_arr_s Xdestruct_s];

t6=t6';

fid = fopen('Result.xls','a+');

fprintf(fid,'\n \n ~~~Exergy variation~~~~~~~~');

fprintf(fid,'\n Z \t Xd_arr \t Xa_cond_arr \t Xa_evap_arr \t Xair_arr \t Xtotal_arr \t Xdestruct \t
Xd_arr_s \t Xa_cond_arr_s \t Xa_evap_arr_s \t Xair_arr_s \t Xtotal_arr_s \t Xdestruct_s');

fprintf(fid,'\n %6.f \t %6.f \t %6.f \t %6.f \t %6.f \t %6.f \t %6.f \t %6.f \t %6.f \t
%6.f \t %6.f \t %6.f',t6);

fclose(fid);

t3=[Z Wa_arr D_arr Ux_arr Uy_arr hav_arr Ta_arr-273.15 Twb_arr-273.15 Td_arr-273.15 Rh_arr
md_loss_arr Ta_arr_s-273.15 Twb_arr_s-273.15 Td_arr_s-273.15 Rh_arr_s Wa_arr_s x_arr W_arr
U_abs dmawp_arr HcngP_arr Approach_arr Range_arr CTE_arr CC_arr];

 t3=t3';

fid = fopen('Result.xls','a+');

fprintf(fid,'\n \n ~~~~~~~~Results~~~~~~~~~~~~\n');

fprintf(fid,'z \t Wa_arr \t D_arr \t Ux_arr \t Uy_arr \t hav_arr \t  Ta_arr \t Twb_arr \t Td_arr \t Rh_arr \t
md_loss_arr \t Ta_arr_s \t Twb_arr_s \t Td_arr_s \t Rh_arr_s \t Wa_arr_s \t x_arr \t W_arr \t U_abs \t
dmawp_arr \t HcngP_arr  \t Approach_arr \t Range_arr \t CTE_arr \t CC_arr\n');
```

```
fprintf(fid,'%6.6f \t %6.6f \t %6.9f \t %6.6f \t %6.6f \t %6.6f \t %6.6f \t %6.6f \t %6.6f \t
%6.6f \t %6.6f \t %6.6f \t %6.6f \t %6.6f \t %6.6f \t %6.6f \t %6.6f \t %6.6f \t %6.6f \t %6.6f \t
%6.6f \t %6.6f \t %6.6f\n',t3);

fclose(fid);

 dTa_max = Tai-Ta;

 pmax = A.*ui.*dTa_max.*Cpa(Tai).*Rho_a; %maximum cooling power or cooling capacity

pmaxkw =pmax./1000; %maximum cooling power in KW

 mcc=[A ui Tai-273.15 Ta-273.15 dTa_max Tdi-273.15 Td-273.15 dTd_max Twbi-273.15 Twb-273.15
dTwb_max Rhi Rh dRh_max dD_max Cpa(Tai) Rho_a pmax pmaxkw Wai Wa Approach Range
CTE];

mcc = mcc';

fid = fopen('Result.xls','a+');

fprintf(fid,'\n ~~~~~~~~~~Results~~~~~~~~~~~~~~\n');

fprintf(fid,'A \t ui \t Tai \t Ta \t dTa_max \t Tdi \t Td \t dTd_max \t Twbi \t Twb \t dTwb_max \t Rhi \t
Rh \t dRh_max \t dD_max \t Cpa(Tai) \t Rho_a \t pmax \t pmaxkw \t Wai \t Wa \t Approach \t Range \t
CTE \n');

fprintf(fid,'%6.6f \t %6.6f \t %6.6f \t %6.6f \t %6.6f \t %6.6f \t %6.6f \t %6.6f \t %6.6f \t
%6.6f \t %6.6f \t %6.6f \t %6.6f \t %6.6f \t %6.6f \t %6.6f \t %6.6f \t %6.6f \t %6.6f \t %6.6f \t
%6.6f \t %6.6f \n',mcc);

fclose(fid);
```

APPENDIX-B

Matlab code of 2-D multi droplet parallel flow SCT

```
%~~~~~~~~~~~~~~~~~~~~~~~~~~~~~~~~~~~~~~~~~~~~~~~~~~~~~~~~~~~~~~~~~~~~~~~~~~~~~~~~%
%File name: Downward parallel flow multi droplet SCT used for industrial application
%All units in SI
%~~~~~~~~~~~~~~~~~~~~~~~~~~~~~~~~~~~~~~~~~~~~~~~~~~~~~~~~~~~~~~~~~~~~~~~~~~~~~~~~%
input 'Starting phase I'
Dc=0.61;% diameter of cross section of cooling tower in meters
height=1.25;
div=100;
%%%%if want to obtain drop dia. in order of 10e-6 then Dr is given below
Dr=31.8184e-6:31.8184e-6:318.184e-6;
Dm=180e-6;
uc=3.9342; %%%uniformity constant, constant describing the material uniformity
Ta=36.0+273.15;%Inlet Temperature of Air in Kelvin
Tai=Ta;
Tdi=56+273.15;%Inlet temp. of water in Kelvin
Td=Tdi;
Rh=65;%inlet Relative humidity in percentage
Rhi=Rh;
 Ui=20;%Magnitude of droplet velocity in m/s
U=Ui;
Phi=45;%Angle of projection of water droplet with horizontal in degrees
Q=400;%inlet air supply rate in m^3/hr.
RLG=0.5;%Ratio of the mass flow of air to water
x=0;%Starting x co-ordinate of spray
Pw=998.19;%Water density in kg/m3
Tambient=Tai; % Ambient Temperature in kelvin
AmbHum = Rhi; % Humidity of environment in percentage
  %Constant Parameters
g=9.81;%Acceleration due to gravity(m/sec2)
%Variable Initializing & Condition Implementers
Ta_arr=Ta;
Kwcheck=1;
```

```
[fid,message] = fopen('Result.xls','w+');
fprintf(fid,'---------INITIAL INPUTS----------\n');
fprintf(fid,'Dia of cooling tower (m), Dci = %6.6f\n',Dc);
fprintf(fid,'Height of cooling tower in (m), height = %6.6f\n',height);
fprintf(fid,'Number of divisions over height, div = %6.6f\n',div);
fprintf(fid,'Droplets Dia. to take into considderation (m), Dr = %6.9f\n',Dr);
fprintf(fid,'Mean Droplets Dia. (m), Dm = %6.6f\n',Dm);
fprintf(fid,'Value of, uc = %6.6f\n',uc);
fprintf(fid,'Ratio of mdi/ma, RLG = %6.6f\n',RLG);
fprintf(fid,'Inlet DBT of Air (C), Tai = %6.6f\n',Tai-273.15);
fprintf(fid,'Relative humidity at inlet in percentage, Rhi = %6.6f\n',Rhi);
fprintf(fid,'Inlet temp. of water in Kelvin, Tdi = %6.6f\n',Tdi-273.15);
fprintf(fid,'Magnitude of droplet velocity (m/s), Ui = %6.6f\n',Ui);
fprintf(fid,'Angle of projection of water droplet with horizontal (degrees), Phi = %6.6f\n',Phi);
fprintf(fid,'Starting x co-ordinate of spray, x = %6.6f\n',x);
fprintf(fid,'Inlet air supply rate in (m^3/hr), Q = %6.6f\n',Q);
fprintf(fid,'Acceleration due to gravity(m/sec2), g = %6.6f\n',g);
fprintf(fid,'Ambient Temperature (C), Tambient = %6.6f\n',Tambient);
fprintf(fid,'Ambient Relative humidity, AmbHum = %6.6f\n',AmbHum);
fprintf(fid,'Nullifying wall effect, Kwcheck = %6.6f\n',Kwcheck);
fclose(fid);
global A As AmbHum Cd_v Const dD_max dsi ds dTa_max...
    dTd_max dTwb_max dmawp dmawp_arr ...
    Di D Dc Dci Dco dNdt div g...
    h havi hav hs hss hfg hfg0 hdi hd...
    height hm H Hai Hdi HTin HTout i Kfr Kw Kwcheck k L Lef Lefs...
    mai ma main md_arr mdi md Mdi Md md_arr md_arr1 md_loss md_loss_arr...
    MTin MTout PMT_arr mu...
    Nusselt PHT PHT_arr PMT PMT_arr prand Pw Q Rhi Rh...
    dRh_max Rho_ai Rho_a Re_v...
    sn1 sn2 sn3 sn4 SCTcount SctMatrix SIZE SLE_arr summdi summd...
    sumHdi sumHdo tmi tei Tambient...
    Tai Ta Ta_arr Tdi Td Td_arr Tambient...
    Tdmean Tdmean_arr Thi Twbi Twb Xtotal ...
    ui u Ui Uxi Uyi U Ux Uy v W Wai Wa Wa0 Wds Wsai Wsa ...
```

```
    Xd Xd_arr Xa_cond Xa_evap Xair Xd Xa_cond...
    Xa_evap t zxc1 zxc2 zxc3 zxc4 zxc5 zxc6 abc1 abc2 abc3 abc4
  User_Input; %Loads the User variables
 abc1=0;
abc2=0;
abc3=0;
abc4=0;
sn1=0;
 %Calculates Parameters which will remain constant throughout the program
dropeqnsplver; %Computes and adds D=Droplet Dia, diff2(RR)=Probability function of Rosin Rammler distribution
Dr0=Dr0';
Kfr=  diff2(RR);
sum(Kfr)
Kfr=Kfr'
M=[Dr0 Kfr]%;%diameter & Probability distribution matrix
Di=M(:,1)%;%Stores Diameter matrix return from the function columnwise;
Di=Di'%;
Din=Di;%initial distribution of drop dia.
Kfr=M(:,2)%Stores Diameter Probability Distribution matrix returned from the function column wise;
Kfr=Kfr'
H=height/(div-1); %;%Calculate dz
 % Calcuate Initial Parameter Values to be given to SCT system
SIZE=size(Di',1)%;%Input Diameter matrix returns the no. of rows in Di'
Ui=Ui.*ones(size(Di))%;%Input Velocity matrix of drop same size as Di
THETA=(pi./180).*Phi%;%Calculate angles in Radian.
Uxi=Ui.*cos(THETA)%;%;%Inlet Horizontal Component of Droplet velocity
Uyi=Ui.*sin(THETA)%;%Inlet Vertical component of Droplet velocity
x=0.*ones(size(Ui))%;%Inlet displacement x matrix same size as Ud
t=0.*ones(size(Di))%; % Input retention time Matrix
Td=Tdi.*ones(size(Di))%;%Input temperature matrix same size as D
Tdmean =(sum(Kfr.*((Cpd(Td)).*Td))./Cpd((sum(Kfr.*Td)))%;
Tdmeani=Tdmean;
Wsai = Wsair(Tai)%specific humidity of saturated air
Wai=(Rhi./100).*Wsai%; %Input specific Humidity of air in Kg/Kg of dry air
Twbi = wbt(Tai,Wai)%;
```

```
Wa0= (AmbHum./100).*Ws(Tambient)%; % Ambient specific Humidity
hfg0=Hfgd(273.15)%;%Latent heat of water at 273.15K
A=AREA_sct(pi,Dc)%Area of cross-section of cooling tower in m2
u=Q./(A.*3600)%Air velocity in m/s
ui=u; %initial velocity of air
Rho_a=Pa(Tai,Wai); %Density of air in Kg/m3
Const=Rho_a.*A.*u;
 mai=(Q./3600).*Pa(Tai,Wai)%Massflow rate of moist air at inlet in Kg/s
main=mai
ma=mai./(1+Wai)%mass of dry air at inlet in Kg/s
mdi=mai.*RLG%;%massflow rate of water at inlet where RGL is ratio of mass flow of water to air
mdi=Kfr.*mdi%;%Inlet Water Mass flow matrix
summdi=sum(mdi); %Mass flow rate of water supplied through inlet in SCT in Kg/s.
MTin=mai+summdi;
 dNdt=mdi.*6./(Pw.*pi.*(Di.^3))%;%;%Inlet total no. of droplets per second
hai=Cpa(Tai).*(Tai)%; %specific enthalpy of dry air in moist air
hvi=Cpv(Tdmeani).*(Tdmeani)+hfg0%; %specific enthalpy of water vapour in moist air
havi=hai+Wai.*hvi%;  %Inlet enthalpy of air vapor mixture
Hai=ma.*havi%; %Air enthalpy at inlet
hdi=Cpd(Tdmeani).*(Tdmeani)%; %Inlet enthalpy of drop per Kg of water
Hdi=sum(mdi).*hdi%; %Water enthalpy at inlet
HTin=Hai+Hdi%;
 %Open file for write values of Mass balance quantities of SCT
fid = fopen('Result.xls','a+');
fprintf(fid,'\n \n ~~~~~~~INITIAL AIR AND WATER MASS FLOW RATE~~~~~~~ \n');
fprintf(fid,'Massflow rate of moist air at inlet in Kg/s, mai = %6.6f\n',mai);
fprintf(fid,'Massflow rate of dry air at inlet in Kg/s, ma = %6.6f\n',ma);
fprintf(fid,'Initially moisture present in air at inlet in Kg/Kg of dry air, Wai = %6.6f\n',Wai);
fprintf(fid,'Mass flow rate of individual water drop through inlet in SCT in Kg/s., mdi = %6.6f\n',mdi);
fprintf(fid,'Mass flow rate of total water drop through inlet in SCT in Kg/s., summdi =
%6.6f\n',summdi);
fprintf(fid,'Inlet total no. of droplets for a perticular dia. per second, dNdt = %6.6f\n',dNdt);
fclose(fid);
 %Open file for write values of energy balance quantities of SCT
fid = fopen('Result.xls','a+');
fprintf(fid,'\n \n ~~~~~~~~~~~INITIAL AIR AND WATER ENTHALPY~~~~~~~~ \n');
```

```
fprintf(fid,'Specific enthalpy of dry air at inlet in J/Kg, hai = %6.6f\n',hai);
fprintf(fid,'Specific enthalpy of air-vapur mixture at inlet in J/Kg, havi = %6.6f\n',havi);
fprintf(fid,'Enthalpy of air-vapur mixture at inlet in J/Kg, Hai = %6.6f\n',Hai);
fprintf(fid,'Specific enthalpy of water at inlet in J/Kg, hdi = %6.6f\n',hdi);
fprintf(fid,'Enthalpy of Water at inlet in J/Kg, Hdi = %6.6f\n',Hdi);
fprintf(fid,'Total enthalpy (air+water) at inlet in J/Kg, HTin = %6.6f\n',HTin);
fclose(fid);
 %Open file for write output values of Mass and Energy balance quantities of SCT
fid = fopen('Result.xls','a+');
fprintf(fid,'\n \n ~~~~~~MASS AND ENERGY BALANCE OF SCT AND
RESULT_INTERMEDIATE_VALUES_OF_FUNCTION~~~~~~~~~~\n');
fprintf(fid,'sn1 \t z \t Ta \t Twb \t Tdmean \t Rh \t Wa \t Wsa \t sum(Wds) \t ma \t ma.*(1+Wa) \t
sum(md) \t hav \t u \t Rho_a \t sum(h) \t sum(hm) \t sum(hs) \t sum(hfg) \t v \t k \t mu \t Cpa(Ta) \t
Cpv(Ta) \t Cpv(Tdmean) \t Cpd(Tdmean) \t sum(Lef) \t sum(Re_v) \t Prand \t sum(Cd_v) \t
sum(Nusselt)');
fclose(fid);
Uy=Uyi;
Ux=Uxi;
Wa=Wai;
hav=havi;
% Linking input Matrix
M=[Td Uy hav Wa Di Ux x t]%;
M=M'; %Here M is the input matrix consisting of one column
 options=odeset('Abstol',1e-6,'RelTol',1e-6,'Refine',4,'InitialStep',...
    H,'Maxstep',height);

[Z,Y]=ode45(@SCTsystem,[0:H:height],M,options);
function [dydt] = SCTsystem(z,y)

 y = y'  % row wise matrix
 abc1=abc1+1;
abc2=abc2+1;
abc3=abc3+1;
abc4=abc4+1;
 Td = y(1:SIZE) %water temperature row matrix
Uy = y((SIZE+1):(2*SIZE))%Row matrix of Vertical Component of droplet velocity
```

```
hav = y(2*SIZE+1) % Row matrix of air enthalpy.
Wa=y((2*SIZE+2)) %Row matrix of Specific Humidity
D=y((2*SIZE+3):(3*SIZE+2)) %Row matrix of droplet diameter
Ux=y((3*SIZE+3):(4*SIZE+2))%Row matrix of Horizontal Component of droplet Velocity
x=y((4*SIZE+3):(5*SIZE+2)) %Row matrix of Horizontal distance with z
t=y((5*SIZE+3):(6*SIZE+2))%;     %Row matrix of retention time with z
 As=pi.*D.^2%; %Surface area of droplet m2
Tdmean =(sum(Kfr.*((Cpd(Td)).*Td)))./Cpd((sum(Kfr.*Td)));
 %Tdmean =mean (Td);
Ta = (hav - Wa.*hfg0) ./ (Cpa(Ta) + Wa.*Cpv(Tdmean)); % Calculates Step wise Air temperature
ha=Cpa(Ta).*Ta; %specific enthalpy of dry air in moist air
hv=Cpv(Ta).*Ta+hfg0; %specific enthalpy of water vpour in moist air
hd=Cpd(Td).*(Td); %Inlet enthalpy of drop per Kg of water
Rho_a=Pa(Ta,Wa)%; %Density of air
u=Const./(Rho_a.*A); %Air velocity in SCT
W=((Uy-u).^2+Ux.^2).^.5 % Row matrix maginute of relative velocity of air w.r.t droplet
Cpav=Cpa(Ta)+Wa.*Cpv(Ta)%;%Average specific heat for air
hs=Hsd(Td) %Matrix of enthalpy of air mixture at the surface of droplet
hfg= hfg0 + Cpv(Td).*Td  %Calcuate stepwise Latent heat of vaporization
 % Air properties
v=KinVisc(Ta,Wa);% %Kinematic viscosity
k= ThermCond(Ta,Wa);% %Thermal Conductivity
mu= v.*Rho_a;%  %Dynamic viscosity of air
Prand=Pr(mu,Cpa(Ta),k);% %Evaluate Prandtl No
Wsa = Wsair(Ta);%
ds = Wa./Wsa;
Rh=(ds./(1-(1-ds).*(Psv(Ta)./101325))).*100;%
Wds=Wdrop(Td); %sp. humidity of air at drop surface
Wa=(Rh./100).*Wsa; %Input specific Humidity of air in Kg/Kg of dry air
Twb = wbt(Ta,Wa);
% Numbers for droplet air interaction
Lef=Le(Ws(Td),Wa);% %Row matrix Lewis factor for droplet air interaction
Re_v= Re(W,D,v);% %Row matrix of Reynold number for droplet air interaction
Cd_v= Cd(Re_v); %Row matrix of coefficient of Drag for droplet air interaction
Nusselt= Nu(Re_v, Prand); %Row matrix of Nusselt number for droplet air interaction
```

```
h=Hc(Nusselt, D, k); % Row matrix of Heat transfer coefficient for droplet air interaction
hm=h./((Cpa(Ta)+Wa.*Cpv(Ta)).*Lef); %Row matrix of mass transfer coefficient  for droplet
md=Pw.*pi.*dNdt.*(D.^3-Di.^3)./6 + mdi%;%Row matrix of instantaneous mass
Md=md./dNdt%;mass of single droplet
N=dNdt./A%; %Inlet total no. of droplets per second per unit cross...
%sectinal area of sct
sn1 %seriel no.
z %tower height
 %%Write output values of Mass and Energy balance quantities of SCT
sn1=sn1+1;
t2=[sn1 z Ta-273.15 Twb-273.15 Tdmean-273.15 Rh Wa Wsa sum(Wds) ma ma.*(1+Wa) sum(md)
hav u Rho_a sum(h) sum(hm) sum(hs) sum(hfg) v k mu Cpa(Ta) Cpv(Ta) Cpv(Tdmean) Cpd(Tdmean)
sum(Lef) sum(Re_v) Prand sum(Cd_v) sum(Nusselt)];
t2=t2';
fid = fopen('Result.xls','a+');
fprintf(fid,'\n %d \t %6.6f \t %6.6f \t %6.6f \t %6.6f \t %6.6f \t %6.6f \t %6.6f \t %6.6f \t %6.6f
\t %6.6f \t %6.6f \t %6.6f \t %6.6f \t %6.6f \t %6.6f \t %6.6f \t %6.6f \t %6.6f \t %6.6f \t %6.6f
\t %6.6f \t %6.6f \t %6.6f \t %6.6f \t %6.6f \t %6.6f \t %6.6f',t2);
fclose(fid);
 %Condition after drop strikes the wall
for i=1:SIZE
   if(x(i)>=Dc/2)
      n(i)=0%;
   else
      n(i)=1%;
   end
end
%This step provides for initial value
i=1
 %Conservation of Energy for water droplet
dTddz = n(i).*((-6.*hm(i).*( Lef(i).*(hs(i)- hav) + (1-...
   Lef(i)).*hfg(i).*(Ws(Td(i)) - Wa))./(Cpd(Td(i)).*Pw.*D(i).*Uy(i)))...
   -((3.*Td(i)./D(i)).*(-2.*hm(i).*(Ws(Td(i))-Wa)./(Uy(i).*Pw))))%;
 %Conservation of Momentum in y direction for water droplet
dUydz = n(i).*(((g.*(Pw-Rho_a)-(3.*Cd_v(i).*Rho_a.*W(i).*(Uy(i)-u)...
   ./(4.*D(i)))))./(Pw.*Uy(i)))-(3.*Uy(i)./D(i)).*(-2.*hm(i)...
```

```
   .*(Ws(Td(i))-Wa)./(Uy(i).*Pw)))%;
 %Conservation of energy for air droplet
dhavdz = n(i).*((md(i)./ma).*(6.*hm(i)./(Pw.*Uy(i).*D(i)))...
       .*(Lef(i).*(hs(i)-hav)+(1-Lef(i)).*hfg(i).*(Ws(Td(i))-Wa)))%;
 %Conservation of Mass for air
dWadz  = n(i).*(((md(i)./ma).*(hm(i).*As(i).*(Ws(Td(i))-Wa)))./...
   (Md(i).*Uy(i)))%;
 %Conservation of mass for water droplet
dDdz  =  n(i).*(-2.*hm(i).*(Ws(Td(i))-Wa)./(Uy(i).*Pw))%;
 % Conservation of Momentum in x direction for water droplet
dUxdz  = n(i).*((-3.* W(i).*Ux(i).*Rho_a.*Cd_v(i)./(4.*Pw.*D(i).*Uy(i)))...
   -((3.*Ux(i)./D(i)).*(-2.*hm(i).*(Ws(Td(i))-Wa)./(Uy(i).*Pw))))%;
 %Trajoctory equtation
dxdz = n(i).*(Ux(i)./Uy(i))%;
 %Retention time
dtdz  = n(i).*(1./Uy(i))%;
 %This step provides for concatenating the rest of the matrix
for i=2:SIZE
   %Conservation of Energy for water droplet
   dTddz =  [dTddz; n(i).*((-6.*hm(i).*( Lef(i).*(hs(i)- hav) + (1-...
      Lef(i)).*hfg(i).*(Ws(Td(i)) - Wa))./(Cpd(Td(i)).*Pw.*D(i).*Uy(i)))...
      -((3.*Td(i)./D(i)).*(-2.*hm(i).*(Ws(Td(i))-Wa)./(Uy(i).*Pw))))]%;
    %Conservation of Momentum in y direction for water droplet
   dUydz = [dUydz; n(i).*((g.*(Pw-Rho_a)-(3.*Cd_v(i).*Rho_a.*W(i)...
      .*(Uy(i)-u)./(4.*D(i)))./(Pw.*Uy(i)))-(3.*Uy(i)./D(i))...
      .*(-2.*hm(i).*(Ws(Td(i))-Wa)./(Uy(i).*Pw))]%;
    %Conservation of Energy for air
    dhavdz = dhavdz + n(i).*((md(i)./ma).*(6.*hm(i)./(Pw.*Uy(i).*D(i)))...
      .*(Lef(i).*(hs(i)-hav)+(1-Lef(i)).*hfg(i).*(Ws(Td(i))-Wa)))%;
   %Conservation of Mass for air
   dWadz =  dWadz +...
      n(i).*((md(i)./ma).*(hm(i).*As(i).*(Ws(Td(i))-Wa)))./(Md(i).*Uy(i))%;
    %Conservation of mass for water droplet
   dDdz =  [dDdz; n(i).*(-2.*hm(i).*(Ws(Td(i))-Wa)./(Uy(i).*Pw))]%;
    % Conservation of Momentum in x direction for water droplet
```

```
    dUxdz =  [dUxdz; n(i).*((-3.* W(i).*Ux(i).*Rho_a.*Cd_v(i)./(4.*Pw.*D(i)...
       .*Uy(i)))-((3.*Ux(i)./D(i)).*(-2.*hm(i).*(Ws(Td(i))-Wa)...
       ./(Uy(i).*Pw))))]%;
     %Trajoctory equtation
    dxdz = [dxdz; n(i).*(Ux(i)./Uy(i))]%;
      %Retention time
    dtdz  =[dtdz; n(i).*(1./Uy(i))]%;
end
 %Links the final matrix column wise
SctMatrix=[dTddz; dUydz; dhavdz; dWadz; dDdz; dUxdz; dxdz; dtdz];
%SctMatrix = real (SctMatrix);%For write real number only if result is
%complex number.
dydt=SctMatrix;
  %---------------------------------------------------------------
Td_arr=Y(:,1:SIZE);%Row matrix of water temp.
Uy_arr=Y(:,(SIZE+1):(2*SIZE));
hav_arr=Y(:,(2*SIZE+1));%Row matrix of air temp.
Wa_arr=Y(:,(2*SIZE+2));%Row matrix of specific humidity
D_arr=Y(:,(2*SIZE+3):(3*SIZE+2));%Row matrix of Droplet diameter
Ux_arr=Y(:,(3*SIZE+3):(4*SIZE+2));%Row matrix of Horizontal Component of droplet velocity
x_arr=Y(:,(4*SIZE+3):(5*SIZE+2));
t_arr=Y(:,(5*SIZE+3):(6*SIZE+2));
 W_arr=((Uy_arr-u).^2+(Ux_arr).^2).^.5; %Array of relative velocity of air.
U_abs=((Uy_arr).^2+(Ux_arr).^2).^.5;
 Tdmean =(sum(Kfr.*((Cpd(Td)).*Td))./Cpd((sum(Kfr.*Td)))
 zxc1=0;
for i=1:div
    zxc1=zxc1+1;
    Tdmean_arr(zxc1,:)=(sum(Kfr.*((Cpd(Td_arr(i,:))).*Td_arr(i,:)))./Cpd((sum(Kfr.*Td_arr(i,:))))
end
 zxc1a=0;
for i=1:div
    zxc1a=zxc1a+1;
    Ta_arr(zxc1a,:) =(hav_arr(i,:) - Wa_arr(i,:).*hfg0) ./ (Cpa(Ta) + Wa_arr(i,:).*Cpv(Tdmean_arr(i,:)))
end
```

```
 Twb_arr = wbt(Ta_arr,Wa_arr);
ds_arr=(Wa_arr./ Wsair(Ta_arr)) %degree of saturation
Rh_arr=(ds_arr./(1-(1-ds_arr).*(Psv(Ta_arr)./101325))).*100  %Calcuate stepwise Relative humidity of Air
 zxc2=0;
for i=1:div
    zxc2=zxc2+1;
    md_arr(zxc2,:) = Pw*pi*dNdt.*((D_arr(i,:).^3)./6);
end
 %-----Mass balance
zxc2A=0;
for i=1:div
    zxc2A=zxc2A+1;
    MTout_arr(zxc2A,:) = ma.*(1+Wa_arr(i,:))+ sum(md_arr(i,:))
end
zxc3=0;
for i=1:div
    zxc3=zxc3+1;
    dMT_arr (zxc3,:)= abs(MTout_arr(i,:) - MTin) %difference in matrix of total mass flow of air and water at outlet and inlet
end
 zxc4=0;
for i=1:div
    zxc4=zxc4+1;
    PdMT_arr (zxc4,:) = (abs(dMT_arr(i,:)).*100)./mean (MTin) %%percentage change matrix of total mass flow of air and water at outlet and inlet
end
 %------Energy balance of SCT
zxc6=0;
for i=1:div
    zxc6=zxc6+1;
    hao_arr (zxc6,:) = Cpa(Ta_arr(i,:)).*(Ta_arr(i,:))
end
 zxc6A=0;
for i=1:div
    zxc6A=zxc6A+1;
```

```
    hvo_arr (zxc6A,:) = (Cpv(Tdmean_arr(i,:)).*(Tdmean_arr(i,:)))+hfg0
end

zxc6B=0;
for i=1:div
    zxc6B=zxc6B+1;
    havo_arr (zxc6B,:) = hao_arr(i,:)+Wa_arr(i,:).*hvo_arr(i,:)
end
 zxc6C=0;
for i=1:div
    zxc6C=zxc6C+1;
    Hao_arr (zxc6C,:) = ma.*havo_arr(i,:)
end
zxc6D=0;
for i=1:div
    zxc6D=zxc6D+1;
    hdo_arr (zxc6D,:) = (Cpd(Tdmean_arr(i,:)).*(Tdmean_arr(i,:)))
end

zxc6E=0;
for i=1:div
    zxc6E=zxc6E+1;
    Hdo_arr (zxc6E,:) = sum(md_arr(i,:)).*hdo_arr(i,:)
end
 zxc7=0;
for i=1:div
    zxc7=zxc7+1;
    HTout_arr (zxc7,:) = Hao_arr(i,:)+Hdo_arr(i,:)
end
 zxc8=0;
for i=1:div
    zxc8=zxc8+1;
   dHT_arr (zxc8,:) =abs(HTout_arr(i,:)- HTin)
end
 zxc9=0;
```

```
for i=1:div
    zxc9=zxc9+1;
   PdHT_arr (zxc9,:) =(dHT_arr(i,:).*100)./HTin
end
zxc10=0;
for i=1:div
    zxc10=zxc10+1;
   Approach_arr (zxc10,:) =Tdmean_arr(i,:)-Twbi
end
 zxc11=0;
for i=1:div
    zxc11=zxc11+1;
   Range_arr (zxc11,:) =Tdi-Tdmean_arr(i,:)
end
%Cooling capacity
zxc11A=0;
for i=1:div
    zxc11A=zxc11A+1;
   CC_arr (zxc11A,:) =sum(md_arr(i,:)).*Cpd(Tdmean_arr(i,:)).*(Tdi-Tdmean_arr(i,:))
end
 %Cooling tower efficiency
zxc12=0;
for i=1:div
    zxc12=zxc12+1;
   CTE_arr (zxc12,:) = ((Tdi-Tdmean_arr(i,:)).*100)./(Tdi-Twbi)
end
 zxc12A=0;
for i=1:div
    zxc12A=zxc12A+1;
   md_loss_arr (zxc12A,:) = sum(mdi)-sum(md_arr(i,:))
end
 %for calculate last values
dTa_max=abs(Ta-Tai);
dTd_max=abs(Tdmean-Tdi);
```

```
dTwb_max=abs(Twb-Twbi);
dRh_max=abs(Rh-Rhi);
pmax = A.*ui.*dTa_max.*Cpa(Tai).*Rho_a;%maximum cooling power or cooling capacity
pmaxkw =pmax./1000;%maximum cooling power in KW
 %Exergy calculation
zxc14=0;
for i=1:div
   zxc14=zxc14+1;
   Xd_arr (zxc14,:) = sum(md_arr(i,:)).*((hf(Tdmean_arr(i,:))-hg(Tambient))...
   -(Tambient.*(sf(Tdmean_arr(i,:))-sg(Tambient))) - (461.*Tambient.*log(AmbHum./100)))
end
 Xa_cond_arr = (ma).*(Cpa(Ta_arr).*(Ta_arr-Tambient)-
Tambient.*Cpa(Ta_arr).*log(Ta_arr./Tambient)...
   + Wa_arr.*(Cpv(Ta_arr).*(Ta_arr-Tambient)- (Tambient.*Cpv(Ta_arr)).*log(Ta_arr./Tambient)))
Xa_evap_arr= ma.*( 287.*Tambient.*log((1+1.608.*Wa0)./(1+1.608.*Wa_arr))+ Wa_arr.*...
   (461.*Tambient.*log(((1+1.608.*Wa0).*Wa_arr)./((1+1.608.*Wa_arr).*Wa0))  )  )
Xair_arr   =(Xa_cond_arr+ Xa_evap_arr); %Total Air Exergy
 if(Xair_arr <0)
   Xair_arr = -1.* Xair_arr; % Total Air Exergy
end
 Xtotal_arr = Xd_arr + Xair_arr;
 SLE_arr = (Xtotal_arr*100)/Xtotal_arr(1,1);%second law efficiency
 Xdestruct=Idestruction(Xtotal_arr)
 zxc16=0;
for i=1:div
   zxc16=zxc16+1;
   NII (zxc16,:) = Xtotal_arr(div,:).*100./Xtotal_arr(1,:)
end
 zxc16A=0;
for i=1:div
   zxc16A=zxc16A+1;
   XdestructP (zxc16A,:) = ((Xtotal_arr(1,:) - Xtotal_arr(div,:)).*100)./Xtotal_arr(1,:)
end
 %Generate serial number
```

```
myvector=[1:div];

sno1_arr=myvector';

 %-> Write Exergy values in file

t6=[sno1_arr Z Xd_arr Xa_cond_arr Xa_evap_arr Xair_arr Xtotal_arr SLE_arr Xdestruct NII
XdestructP];

t6=t6';

fid = fopen('Result.xls','a+');

fprintf(fid,'\n \n ~~~EXERGY VARIATION ARRAY~~~~~~~~');

fprintf(fid,'\n sno1_arr \t Z \t Xd_arr \t Xa_cond_arr \t Xa_evap_arr \t Xair_arr \t Xtotal_arr \t SLE_arr
\t Xdestruct \t NII \t XdestructP');

fprintf(fid,'\n %d \t %6.6f \t %6.6f \t %6.6f \t %6.6f \t %6.6f \t %6.6f \t %6.6f \t %6.6f \t
%6.6f',t6);

fclose(fid);

 %-> Write values in file

arr1=[sno1_arr Z Ta_arr-273.15 Wa_arr Twb_arr-273.15 Rh_arr Tdmean_arr-273.15 Approach_arr
Range_arr CTE_arr CC_arr md_loss_arr hav_arr ds_arr MTout_arr dMT_arr PdMT_arr HTout_arr
dHT_arr PdHT_arr];

arr1=arr1';

fid = fopen('Result.xls','a+');

fprintf(fid,'\n \n~~~RESULT -> SINGLE COLUMN ARRAY~~~~~~~~~~\n');

fprintf(fid,'sno1_arr \t Z \t Ta_arr \t Wa_arr \t Twb_arr \t Rh_arr \t Tdmean_arr \t Approach_arr \t
Range_arr \t CTE_arr \t CC_arr \t md_loss_arr \t hav_arr \t ds_arr \t MTout_arr \t dMT_arr \t
PdMT_arr \t HTout_arr \t dHT_arr \t PdHT_arr \n');

fprintf(fid,'%d \t %6.6f \t %6.6f \t %6.6f \t %6.6f \t %6.6f \t %6.6f \t %6.6f \t %6.6f \t %6.6f \t
%6.6f \t %6.6f \t %6.6f \t %6.6f \t %6.6f \t %6.6f \t %6.6f \t %6.6f\n',arr1);

fclose(fid);

 %-> Write single values in file

 mcc=[A ui Tai-273.15 Ta-273.15 dTa_max Tdi-273.15 Tdmean-273.15 dTd_max Twbi-273.15 Twb-
273.15 dTwb_max Rhi Rh dRh_max Cpa(Tai) Rho_a pmax pmaxkw Wai Wa Approach_arr(div,:)
Range_arr(div,:) CTE_arr(div,:)];

mcc = mcc';

fid = fopen('Result.xls','a+');

fprintf(fid,'\n \n ~~~~~~~~~~RESULTS~~~~~~~~~~~~~~\n');

fprintf(fid,'A \t ui \t Tai \t Ta \t dTa_max \t Tdi \t Tdmean \t dTd_max \t Twbi \t Twb \t dTwb_max \t
Rhi \t Rh \t dRh_max \t Cpa(Tai) \t Rho_a \t pmax \t pmaxkw \t Wai \t Wa \t Approach \t Range \t CTE
\n');

fprintf(fid,'%6.6f \t %6.6f \t %6.6f \t %6.6f \t %6.6f \t %6.6f \t %6.6f \t %6.6f \t %6.6f \t
%6.6f \t %6.6f \t %6.6f \t %6.6f \t %6.6f \t %6.6f \t %6.6f \t %6.6f \t %6.6f \t %6.6f \t %6.6f \t
%6.6f \n',mcc);

fclose(fid);
```

```
fid = fopen('Result.xls','a+');

fprintf(fid,'\n \n~~~RESULT -> TRAJECTORY OF DROPLET ALONG SCT HEIGHT~~~\n');

fprintf(fid,'sno1_arr \t Z \t x_arr1 \t x_arr2 \t x_arr3 \t x_arr4 \t x_arr5 \t x_arr6 \t x_arr7 \t x_arr8 \t
x_arr9 \t x_arr10  \n');

fclose(fid);

 for i=1:div

arr1A=[sno1_arr(i,:) Z(i,:) x_arr(i,:)];

fid = fopen('Result.xls','a+');

fprintf(fid,'%d \t %6.6f \t %6.6f \t %6.6f \t %6.6f \t %6.6f \t %6.6f \t %6.6f \t %6.6f \t %6.6f \t
%6.6f \n',arr1A);

fclose(fid);

end

fid = fopen('Result.xls','a+');

fprintf(fid,'\n \n~~~RESULT -> WATER DROPLET TEMPERATURE ARRAY~~~~~~~~~~\n');

fprintf(fid,'sno1_arr \t Z \t Td_arr1 \t Td_arr2 \t Td_arr3 \t Td_arr4 \t Td_arr5 \t Td_arr6 \t Td_arr7 \t
Td_arr8 \t Td_arr9 \t Td_arr10  \n');

fclose(fid);

 for i=1:div

arr1A=[sno1_arr(i,:) Z(i,:) Td_arr(i,:)-273.15];

fid = fopen('Result.xls','a+');

fprintf(fid,'%d \t %6.6f \t %6.6f \t %6.6f \t %6.6f \t %6.6f \t %6.6f \t %6.6f \t %6.6f \t %6.6f \t
%6.6f \n',arr1A);

fclose(fid);

end

 fid = fopen('Result.xls','a+');

fprintf(fid,'\n \n~~~RESULT -> DIAMETER OF DROPLET~~~~~~~~~\n');

fprintf(fid,'sno1_arr \t Z \t D_arr1 \t D_arr2 \t D_arr3 \t D_arr4 \t D_arr5 \t D_arr6 \t D_arr7 \t D_arr8 \t
D_arr9 \t D_arr10  \n');

fclose(fid);

 for i=1:div

arr1A=[sno1_arr(i,:) Z(i,:) D_arr(i,:)];

fid = fopen('Result.xls','a+');

fprintf(fid,'%d \t %6.6f \t %6.6f \t %6.6f \t %6.6f \t %6.6f \t %6.6f \t %6.6f \t %6.6f \t %6.6f \t
%6.6f \n',arr1A);

fclose(fid);

end
```

```
 fid = fopen('Result.xls','a+');

fprintf(fid,'\n \n~~~RESULT -> MASS FLW RATE OF WATER~~~~~~~~\n');

fprintf(fid,'sno1_arr \t Z \t md_arr1 \t md_arr2 \t md_arr3 \t md_arr4 \t md_arr5 \t md_arr6 \t md_arr7 \t
md_arr8 \t md_arr9 \t md_arr10  \n');

fclose(fid);

 for i=1:div

arr1A=[sno1_arr(i,:) Z(i,:) md_arr(i,:)];

fid = fopen('Result.xls','a+');

fprintf(fid,'%d \t %6.6f \t %6.6f \t %6.6f \t %6.6f \t %6.6f \t %6.6f \t %6.6f \t %6.6f \t %6.6f \t
%6.6f \n',arr1A);

fclose(fid);

end

 fid = fopen('Result.xls','a+');

fprintf(fid,'\n \n~~~RESULT -> VELOCITY OF DROPLET IN X DIRECTION (ALONG TOWER
WIDTH)~~~~~~~~\n');

fprintf(fid,'sno1_arr \t Z \t Ux_arr1 \t Ux_arr2 \t Ux_arr3 \t Ux_arr4 \t Ux_arr5 \t Ux_arr6 \t Ux_arr7 \t
Ux_arr8 \t Ux_arr9 \t Ux_arr10  \n');

fclose(fid);

 for i=1:div

arr1A=[sno1_arr(i,:) Z(i,:) Ux_arr(i,:)];

fid = fopen('Result.xls','a+');

fprintf(fid,'%d \t %6.6f \t %6.6f \t %6.6f \t %6.6f \t %6.6f \t %6.6f \t %6.6f \t %6.6f \t %6.6f \t
%6.6f \n',arr1A);

fclose(fid);

end

 fid = fopen('Result.xls','a+');

fprintf(fid,'\n \n~~~RESULT -> VELOCITY OF DROPLET IN Y DIRECTION (ALONG TOWER
HEIGHT)~~~~~~~~\n');

fprintf(fid,'sno1_arr \t Z \t Uy_arr1 \t Uy_arr2 \t Uy_arr3 \t Uy_arr4 \t Uy_arr5 \t Uy_arr6 \t Uy_arr7 \t
Uy_arr8 \t Uy_arr9 \t Uy_arr10  \n');

fclose(fid);

 for i=1:div

arr1A=[sno1_arr(i,:) Z(i,:) Uy_arr(i,:)];

fid = fopen('Result.xls','a+');

fprintf(fid,'%d \t %6.6f \t %6.6f \t %6.6f \t %6.6f \t %6.6f \t %6.6f \t %6.6f \t %6.6f \t %6.6f \t
%6.6f \n',arr1A);

fclose(fid);

end
```

```
 fid = fopen('Result.xls','a+');

fprintf(fid,'\n \n~~~RESULT -> RETANTION TIME~~~~~~~~~~~~~\n');

fprintf(fid,'sno1_arr \t Z \t t_arr1 \t t_arr2 \t t_arr3 \t t_arr4 \t t_arr5 \t t_arr6 \t t_arr7 \t t_arr8 \t t_arr9 \t t_arr10  \n');

fclose(fid);

 for i=1:div

arr1A=[sno1_arr(i,:) Z(i,:) t_arr(i,:)];

fid = fopen('Result.xls','a+');

fprintf(fid,'%d \t %6.6f \t %6.6f \t %6.6f \t %6.6f \t %6.6f \t %6.6f \t %6.6f \t %6.6f \t %6.6f \t %6.6f \n',arr1A);

fclose(fid);

end
```

List of Publications based on the research work

Papers Published in International Journals

(i) Zunaid, M., Murtaza, Q. and Gautam, S., "Energy and performance analysis of multi droplets shower cooling tower at different inlet water temperature for air cooling application". Applied Thermal Engineering, 121, 1070-1079, DOI: 10.1016/j.applthermaleng.2017.04.157, Elsevier.

(ii) Zunaid, M., Murtaza, Q. and Gautam, S., "Energy and Second Law of Thermodynamics Analysis of Shower Cooling Tower with Variation in Inlet Air Temperature". International Journal of Engineering (IJE) Transactions A, 30(7), 1090-1097, DOI: 10.5829/idosi.ije.2017.30.07a.19.

Paper under review

(i) Zunaid, M., Murtaza, Q. and Gautam, S., "Energy and Exergy Analysis of Multi Droplet Shower Cooling Tower with Variation in Water to Air Mass Flow Ratio". Journal of Engineering Science and Technology, Malaysia.

Papers published in international/ national conference proceedings

(i) Zunaid, M., Murtaza, Q. and Kachhwaha, S.S., "Performance analysis of down draft parallel flow shower cooling tower", Proceedings of the 21st National & 10^{th} ISHMT-ASME Heat and Mass Transfer Conference, IIT Madras, India, (2011).

(ii) Zunaid, M., Murtaza, Q. and Kachhwaha, S.S., "Analysis of air and water spray interaction in downdraft parallel flow shower cooling tower", Proceedings of the 22th National and 11th International ISHMT-ASME Heat and Mass Transfer Conference, IIT Kharagpur, India, (2013).

(iii) Zunaid, M., Murtaza, Q., Samsher and Kachhwaha, S.S., "Exergy and Performance Analysis of Parallel Flow Shower Cooling Tower", International Conference Smart Technologies for Mechanical Engineering, 25-26 October (2013), DTU, Delhi, India.

(iv) Zunaid, M., Murtaza, Q., Samsher and Kachhwaha, S.S., "Theoretical Study of a Humidification-Dehumidification Desalination Process Using Down Draft Parallel Flow Shower Cooling Tower", Indian Society For Technical Education (ISTE) Delhi Section Convention on "Technological Universities and Institutions in New Knowledge Age: Future Perspectives and Action Plan, 5-6 September, (2013), DTU, Delhi, India.

Biographical profile of researcher

Mohammad Zunaid is currently working as Assistant Professor in the Department of Mechanical Engineering, Delhi Technological University (Formerly Delhi College of Engineering). He received his Bachelor's and Master's Degree in Mechanical Engineering from Aligarh Muslim University, Aligarh, India. He has published more than twenty research papers in international/national journals and conferences. He has worked as Computational Fluid Dynamics Engineer in Zeus Numerix Pvt. Ltd. Mumbai, India, and Finite Element Analysis Engineer in Manufacturing Design Solutions Gurgaon, India. Also he has more than ten years of teaching experience.